12-2022

Old-Growth Forest Dynamics After Fire and Drought in the Sierra Nevada, California, USA

Kendall M.L. Becker
Utah State University

Follow this and additional works at: https://digitalcommons.usu.edu/etd

Part of the Environmental Sciences Commons

OLD-GROWTH FOREST DYNAMICS AFTER FIRE AND DROUGHT

IN THE SIERRA NEVADA, CALIFORNIA, USA

by

Kendall M.L. Becker

A dissertation submitted in partial fulfillment
of the requirements for the degree

of

DOCTOR OF PHILOSOPHY

in

Ecology

Approved:

_____   _____
James A. Lutz, Ph.D.   Andrew Kulmatiski, Ph.D.
Major Professor   Committee Member

_____   _____
Larissa L. Yocom, Ph.D.   Janneke HilleRisLambers, Ph.D.
Committee Member   Committee Member

_____   _____
R. Justin DeRose, Ph.D.   D. Richard Cutler, Ph.D.
Committee Member   Vice Provost of Graduate Studies

UTAH STATE UNIVERSITY
Logan, Utah

2022

ABSTRACT

Old-growth Forest Dynamics after Fire and Drought

in the Sierra Nevada, California, USA

by

Kendall M.L. Becker, Doctor of Philosophy

Utah State University, 2022

Major Professor: Dr. James A. Lutz
Department: Wildland Resources

Understanding forest ecosystems is important because forests cover approximately one-third of Earth's land area, store half of Earth's carbon, shelter half of Earth's species, and absorb a quarter of new anthropogenic carbon emissions, slowing climate change. This dissertation provides insight into future forest habitat, fuels, species composition, and structure by investigating what happens to snags, seedlings, and trees in an old-growth forest after a low- to moderate-severity fire.

Chapter II explores how low- to moderate-severity fire changes snag fall dynamics. Predicting how long snags will remain standing after fire is essential for managing habitat, understanding chemical cycling in forests, and modeling forest succession and fuels. Pre-fire snags—which tend to be preferred habitat because they include more large-diameter snags in advanced stages of decay—were at least twice as likely to fall as new snags within 3–5 years after fire. Pre-existing snags were most likely to persist five years

after fire if they were > 50 cm in diameter, > 20 m tall, and charred on the bole to heights above 3.7 m.

Chapter III examines the effects of disturbance severity and microclimate on post-fire seedlings to compare the regeneration niches of co-occurring tree species. Available seed, lower substrate burn severity, higher neighborhood disturbance severity, and earlier snowmelt during the germination year gave *Pinus lambertiana* seedlings an advantage over *Abies concolor* seedlings, suggesting that lower-severity fire could naturally shift species composition toward *Pinus* species, which are more resistant to fire and drought.

Chapter IV studies the effects of lower-severity fire on carbon allocation to tree boles by analyzing the tree-ring widths of seven mixed-conifer species throughout the Sierra Nevada. Post-fire growth patterns often did not differ more than one standard deviation from growth fluctuations at adjacent unburned plots, suggesting that reintroducing lower-severity fire will not adversely affect the capacity of surviving trees to attain pre-fire rates of carbon accumulation within five years after fire.

Chapter V focuses on recruitment of large-diameter trees after fire, analyzing how local post-fire mortality within tree neighborhoods impacts post-fire radial growth of surviving trees. Cause of mortality influenced the relationship between neighborhood change and the growth of surviving trees in species-specific ways, suggesting that species differences in cause of mortality could affect the species composition of future large-diameter tree populations.

These findings demonstrate that low- to moderate-severity fire can promote *Pinus* seedlings and trees, exemplifying the concept that ecosystems shift toward species composition and structure that maximize resilience to challenging climate and

disturbance regimes. This research was possible because of the existence of a long-term, spatially explicit, observational old-growth forest dataset with annual resolution.

(246 pages)

PUBLIC ABSTRACT

Old-growth Forest Dynamics after Fire and Drought

in the Sierra Nevada, California, USA

Kendall M.L. Becker

Understanding forest ecosystems is important because forests cover approximately one-third of Earth's land area, store half of Earth's carbon, shelter half of Earth's species, and absorb a quarter of new anthropogenic carbon emissions, slowing climate change. This dissertation provides insight into future forest habitat, fuels, species composition, and structure by investigating what happens to snags, seedlings, and trees in an old-growth forest after a low- to moderate-severity fire.

Chapter II explores how low- to moderate-severity fire changes snag fall rates. Predicting how long snags will remain standing after fire is essential for managing habitat, understanding chemical cycling in forests, and modeling forest succession and fuels. Pre-fire snags—which tend to be preferred habitat because they include more large-diameter snags in advanced stages of decay—were at least twice as likely to fall as new snags within 3–5 years after fire. Pre-existing snags were most likely to persist five years after fire if they were > 50 cm in diameter, > 20 m tall, and charred on the trunk to heights above 3.7 m.
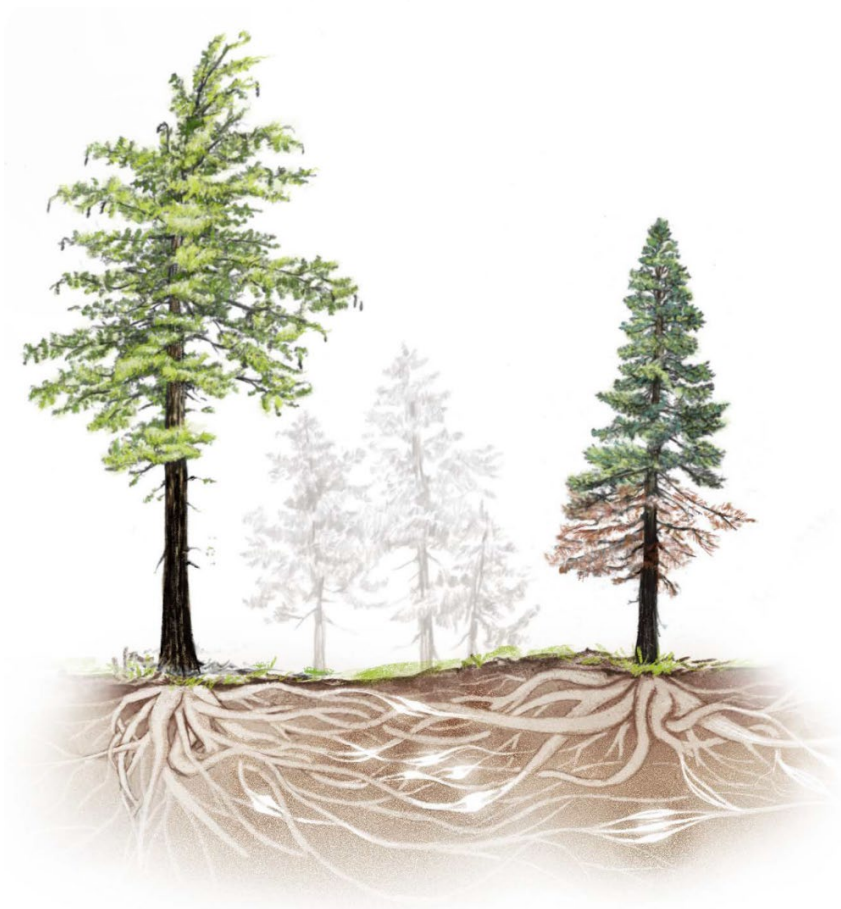
Chapter III examines the effects of fire severity and microclimate on conifer regeneration after fire. Available seed, lower burn severity on the forest floor, more fire-caused tree mortality, and earlier snowmelt during the germination year gave *Pinus lambertiana* seedlings an advantage over *Abies concolor* seedlings, suggesting that

lower-severity fire could naturally shift forest species composition toward *Pinus* species, which are more resistant to fire and drought.

Chapter IV investigates the effects of lower-severity fire on tree growth by analyzing the tree-ring widths of seven mixed-conifer species throughout the Sierra Nevada. Post-fire growth patterns were not substantially different from growth fluctuations at adjacent unburned plots, suggesting that reintroducing lower-severity fire to forests where fire has been excluded over the last century will not prevent surviving trees from attaining pre-fire growth rates within five years after fire.

Chapter V focuses on recruitment of large-diameter trees after fire, analyzing how local post-fire mortality within tree neighborhoods impacts post-fire radial growth of surviving trees. Cause of mortality influenced the relationship between neighborhood change and the growth of surviving trees, and this relationship was different for *A. concolor* compared to *P. lambertiana*, suggesting that species differences in cause of mortality could affect the species composition of future large-diameter tree populations.

These findings demonstrate that low- to moderate-severity fire can promote *Pinus* seedlings and trees, exemplifying the concept that ecosystems shift toward species composition and structure that maximize resilience to challenging climate and disturbance regimes. This research was possible because of the existence of a long-term, spatially explicit, observational old-growth forest dataset with annual resolution.

Artwork by Marissa Devey

ACKNOWLEDGMENTS

CONTENTS

LIST OF TABLES

LIST OF FIGURES

CHAPTER I

INTRODUCTION

Forests cover approximately one-third of Earth's land area, store about half of Earth's carbon, shelter about half of Earth's species, and absorb about 25% of new anthropogenic carbon emissions, slowing climate change (Davies et al., 2021; Keenan and Williams, 2018). Forests are also places of mystery and transcendence (Williams and Harvey, 2001). Current advancements in our knowledge of how forest ecosystems function coincide with an era of unprecedented change, driven by rapid global warming from anthropogenic carbon emissions (Pörtner et al., 2022; "We must get a grip on forest science — before it's too late," 2022).

Climate change affects forest composition, structure, and existence by altering the frequency, severity, and extent of forest disturbances (Seidl et al., 2017). For example, in the western United States, over the last three decades, annual area burned has increased more than six-fold, from less than 90,000 ha burned in 1985 to over 580,000 ha burned in 2017 (Parks and Abatzoglou, 2020). Area burned at high severity parallels this trend, representing about one-third of the total area burned each year (Miller et al., 2009; Parks and Abatzoglou, 2020). The increase in area burned at high severity has garnered well deserved attention due to observed threats of soil erosion (Certini, 2005), carbon stock reduction, and vegetation type conversion following failed natural conifer regeneration (Kemp et al., 2016; Stevens-Rumann et al., 2018; Stewart et al., 2021; Tepley et al., 2017; Young et al., 2019). However, recent estimates (2017) show that two-thirds of the annual area burned experiences low- or moderate-severity fire, not high-severity fire (Parks and Abatzoglou, 2020). Areas burned at low or moderate severity are more likely

to continue to support forest vegetation due to the survival of parent trees (Shive et al., 2018; Stewart et al., 2021; Urza and Sibold, 2017) and aboveground climate buffering (Baumeister and Callaway, 2006; Dobrowski et al., 2015; Young et al., 2019) from the retention of trees, snags, and logs. Understanding how forests respond to climate and environmental factors after low- and moderate-severity fire is vital to estimating successional trajectories where forests are more likely to persist.

Overview

This dissertation aims to improve understanding of how forests change over time after compound disturbances that include drought and low- to moderate-severity fire. One way to study forest change is through demographic analysis of the population components. This dissertation includes chapters on three demographic groups—snags, seedlings, and trees—that are located in the Yosemite Forest Dynamics Plot (YFDP), a 25.6-ha permanent plot in an old-growth stand of *Abies concolor–Pinus lambertiana* (white fir–sugar pine) forest in Yosemite National Park, California, USA (Lutz et al., 2012). Within the YFDP, all trees ≥ 1 cm diameter at breast height (DBH) have been tagged, mapped, and annually monitored since 2010, allowing us to explore questions about how and why forests change through time (Lutz, 2015).

Within the last decade, the YFDP has experienced two major disturbances. A drought of historic severity impacted the region from 2012 through 2015 (Belmecheri et al., 2016). In the middle of this drought, from August 17, 2013 through October 23, 2013, the Rim Fire burned 104,131 ha, and the YFDP was included in the fire footprint (Stavros et al., 2016). As the Rim Fire burned toward the YFDP, Yosemite managers ignited an unmanaged backing fire on August 31, 2013, which entered the study area at

approximately 1:30 a.m. on September 1 (Jeronimo et al., 2020). Fire severity within the YFDP, as inferred from Landsat-derived scenes, was largely low and moderate (Blomdahl et al., 2019). The fire reduced aboveground live shrub biomass from 3,490 to 269 kg ha^{-1} (Lutz et al., 2017) and consumed 79% of total surface fuel (Cansler et al., 2019). Only 4.9% of the plot surface was manually delineated as unburned in patches ≥ 1 m^2 (Blomdahl et al., 2019).

This dissertation analyzes the effects of climate, fire, and tree neighborhood on 1) the longevity of pre-existing and fire-generated snags (Chapter II), 2) the survival of conifer seedlings that germinated after fire (Chapter III), and 3) the radial growth of surviving trees (Chapters IV and V).

Fire regime

Ecosystem structure and function through time are closely linked to disturbance regime (Johnstone et al., 2016). Disturbance type, frequency, severity, spatial pattern, and seasonality exert selection pressure on vegetation, resulting in plant communities that 1) are adapted to characteristic disturbance patterns and 2) influence the behavior and effects of disturbance by defining the template upon which those processes act (Agee, 1993; Johnstone et al., 2016; van Wagtendonk et al., 2020). In the western United States, fire is a key process that continues to exemplify the feedbacks between disturbance and vegetation (Sugihara et al., 2006). Understanding the historical relationship between fire and vegetation and observing how contemporary changes to the fire regime have changed vegetation are preliminary to forming realistic expectations of future patterns of disturbance and vegetation for areas within the western United States (Dale et al., 2001) and specifically within the Sierra Nevada (van Wagtendonk and Lutz, 2007).

Here I describe the historical and contemporary fire regimes, and the presumed effects on vegetation, that characterize a 500-year-old *Abies concolor–Pinus lambertiana* (white fir–sugar pine) mixed-conifer forest in Yosemite National Park (Yosemite). I discuss how future disturbances are likely to affect ecosystem structure and function, with respect to habitat provision by snags, species composition as reflected by regeneration patterns, and the implications of the future vegetation and disturbance regime on carbon cycling. I identify gaps in knowledge of historical and contemporary fire regimes and acknowledge sources of uncertainty surrounding predictions of future regimes. Finally, I place the study area, the Yosemite Forest Dynamics Plot (YFDP; (Lutz et al., 2012), within its larger geographic context and suggest an appropriate scope of inference for the findings that will be presented in this dissertation.

Fire regimes are comprehensively typified by seven attributes—type (e.g., crown vs. surface), intensity (i.e., energy released), severity (i.e., ecological impact), size, spatial pattern (i.e., patchiness), frequency, and seasonality—only some of which can be quantified for historical regimes. Correlations among some of these factors allow inferences to be drawn about historical regimes from records that can, depending on the resolution of the reconstruction method, provide information about fire occurrence, frequency, and seasonality. For example, areas historically subjected to frequent fire are often presumed to have experienced low-intensity and low-severity surface fires due to shorter intervals between events, which constrained the amount of fuel that could accumulate (Parks et al., 2015; Scholl and Taylor, 2010).

Prehistoric fire in the Sierra Nevada bioregion has been documented throughout the last 16,000 years using charcoal layers in lake sediment cores and throughout the last

3,000 years in fire-scarred trees (Swetnam, 1993; van Wagtendonk and Fites-Kaufman, 2006). Extractions from Swamp Lake in Yosemite National Park show that concentrations of charcoal and pollen from the current mixed-conifer species increased approximately 10,400 years ago as the area gradually deglaciated (Smith and Anderson, 1992; van Wagtendonk and Fites-Kaufman, 2006). Historical reconstructions based on fire-scarred trees provide more detailed information about fire return intervals but primarily represent lower-severity events that scarred but did not kill trees in areas where trees have survived other agents of mortality (North et al., 2007; Swetnam, 1993; Taylor et al., 2014). Despite these limitations, numerous studies have used tree-ring records to reconstruct fire histories for the last several centuries at the stand and forest level (Beaty and Taylor, 2008, 2007; North et al., 2007; Taylor et al., 2014; Van de Water and North, 2010). Van de Water and Safford (2011) synthesized 38 studies and reported the following fire return interval summary statistics for dry mixed-conifer forests, the broad category relevant to the YFDP (Fites-Kaufman et al., 2007; Lutz et al., 2012): mean—11 yr; median—9 yr; mean-minimum—5 yr; mean-maximum—50 yr.

Barth et al. (2015) reconstructed fire history within the YFDP and reported a mean fire return interval of 29.5 years based on cross-sections from 10 *Pinus lambertiana* (sugar pine) and 2 *Calocedrus decurrens* (incense-cedar) specimens located within or adjacent to the plot. This estimate is best interpreted as a "maximum" value due to potential undersampling. The last widespread fire occurred in 1900, though evidence of spot fires in 1916, 1926, and 1947 was also detected. Fires typically occurred in the late summer following the onset of dormancy. Tree survival of fires suggests that the historical regime was characterized by low-intensity, low-severity surface fires. The

small sample size of fire-scarred individuals (12) and small size of the YFDP (25.6 ha) precluded assessment of fire size and spatial pattern.

Scholl and Taylor (2010) used 209 cross-sections to reconstruct the fire history of a 2,125-ha mixed-conifer forest in Big Oak Flat, an area approximately 5 km from the YFDP with a more southern aspect and an abundance of *Pinus ponderosa* (ponderosa pine), which is hardly present in the YFDP. From 286 fire events, 79.8% of which occurred in latewood or after dormancy, Scholl and Taylor (2010) identified a mean fire return interval of 12.4 years. Fire severity was inferred by using dendrochronological techniques to assign trees to 20-year age classes: High fire frequency and representation of multiple age classes at each plot suggested that low-severity fire was the norm. Eighty-one percent of fires intersected with the study area boundary, again hindering estimates of fire size (Scholl and Taylor, 2010).

The recent fire regime of the YFDP and surrounding area has been characterized by fire suppression management policies that began when Yosemite National Park was established in 1890 and continued when the National Park Service assumed control in 1916 (van Wagtendonk, 2007). The practices of the United States government differed considerably from the Native American management that preceded Euro-American settlement. Native Americans had augmented the natural fire regime by igniting additional fires to remove brush, maintain meadows, improve browse for deer, stimulate production of weaving materials, and reduce fuels (Anderson and Moratto, 1996). Despite proponents within the new government—including Roy Headley, Robert Marshall, and Aldo Leopold—who advocated for allowing fires to burn in remote areas, aggressive fire suppression was implemented throughout the Sierra Nevada, including in

National Parks, until 1968, when the National Park Service first officially recognized fire as an ecological process (van Wagtendonk, 2007).

Yosemite began its "Natural Fire Management" approach in 1972, initially allowing wildland fire use above 2,440 m and starting a prescribed burning program (van Wagtendonk, 2007). The Forest Service followed suit in 1974, with a mix of wildland fire use and prescribed fire (Debruin, 1974). Nonetheless, fire suppression remains a dominant management practice by all jurisdictions in every instance when fires could threaten human structures or expand beyond what fire fighter personnel could contain (Miller et al., 2012; van Wagtendonk and Fites-Kaufman, 2006).

Between 1984 and 2009, 148 fires > 40 ha burned in Yosemite, with an annual average of 4,144 ha burned (Lutz et al., 2011). Some areas, such as the 16,209-ha Illilouette Creek basin that experienced 157 fires between 1973 and 2011 (van Wagtendonk et al., 2012), are regarded as largely restored due to multiple overlapping fires. More productive areas, however, have increased in tree density and accumulated ladder fuels, heightening the risk that fire reintroduction could result in high-severity crown fire (Barth et al., 2015; Kane et al., 2015; Van de Water and North, 2011). Fire suppression in these areas continues to enable shade-tolerant *Abies concolor* (white fir) and *Calocedrus decurrens* (incense-cedar) to fill in lower montane forests in the Sierra Nevada (North et al., 2005; Parsons and DeBenedetti, 1979; Vankat and Major, 1978). Thus, the increase in tree density over the past century does not just represent a structural shift but also a change in species composition. The shade-tolerance, generalist nature, and high regeneration rates of these species create a positive feedback that reinforces their greater abundance, counter to restoration objectives (Becker and Lutz, 2016; Collins et

al., 2011; Webster and Halpern, 2010).

The increase in fuels, driven primarily by fire suppression, combines with contemporary climate to produce today's fire regime. Increases in area burned, fire size, and fire severity have been documented throughout the western United States in recent decades, and studies have correlated these phenomena with reduced winter snowpack, lag effects of wetter years followed by drought, and extreme fire weather (Littell et al., 2009; Lutz et al., 2009; Stavros et al., 2014; Westerling et al., 2006). Projected reductions in snowpack and warmer temperatures suggest that more large, severe events are likely to occur in the immediate future (Walton et al., 2017). The type of vegetation that interacts with fire in the long term, however, will reflect the combination of these fire-prone years as well as wetter years that promote plant establishment and growth (North et al., 2005; van Wagtendonk et al., 2020); vegetation changes that result as plants establish after fire and respond to a shifted climate envelope may ultimately temper the immediate effects of climate on fire size and severity (Lutz et al., 2010; Seidl et al., 2017). California is home to many fire- and drought-adapted species, including numerous shrub species that already occupy the montane forest understory (Fites-Kaufman et al., 2007; Lutz et al., 2017; van Wagtendonk and Fites-Kaufman, 2006). If high fire severity reduces tree cover, these other life forms may become more prominent and shift the fire regime toward that of lower elevation chaparral systems (Lauvaux et al., 2016; Nagel and Taylor, 2005).

The YFDP was materially affected by the increase in megafires in 2013, when managers ignited the area near the plot in advance of the Rim Fire (Larson et al., 2016; Stavros et al., 2016). The plot burned at low and moderate severity (Blomdahl et al., 2019), likely a result of the fire burning downhill and at night, as opposed to during peak

high temperature and low humidity conditions. The YFDP provides an opportunity to track vegetation development following low- and moderate-severity fire and to observe the behavior and effects of subsequent disturbances on that template (Lutz et al., 2018).

Fire directly affects forest structure and function by consuming snags and logs, killing trees, and re-initiating stand development (Franklin et al., 2002; Hood et al., 2010; Knapp et al., 2005; Zald et al., 2008). Thus, increased fire severity and area burned will have immediate effects on these forest components. Snags provide structural habitat for numerous species of birds and small mammals to nest, rest, roost, and forage (Brown et al., 2003; Harmon et al., 1986; Rabe et al., 1998). Bark beetles and woodborers occupy snags during multiple life cycle phases and are an important food source for woodpeckers and other bird species (Raphael and White, 1984). Snags also represent large, slowly decomposing pools of carbon and nutrients (Cousins et al., 2015) that contribute to slow-paced chemical cycling (Harmon et al., 1986). Fire may partially or completely consume snags, particularly those in more advanced stages of decay, which tend to be of larger diameter, more rare, and more valuable as habitat (Hyde et al., 2011; Innes et al., 2006; Meyer et al., 2005; Raphael and White, 1984; Stephens and Moghaddas, 2005). Snag recruitment through fire-induced tree mortality, however, is unlikely to replace large-diameter debris. The thicker bark of large-diameter trees confers resistance to cambial heating, making large individuals less susceptible to death by fire (Brando et al., 2012; van Mantgem and Schwartz, 2003; VanderWeide and Hartnett, 2011). Thus, low-severity fires may consume large, decayed individuals that provide preferred habitat (Meyer et al., 2005; Raphael and White, 1984), while recruiting numerous small snags that provide less preferred habitat for a shorter period (Raphael and Morrison, 1987). Conversely, an

increase in moderate- and high-severity fire could improve habitat in the short-term by recruiting larger-diameter snags while supplies last (Collins et al., 2011).

The species composition of post-fire regeneration will affect forest structure and function in the longer term. Dendrochronological studies in the Sierra Nevada indicate that recruitment was historically episodic, possibly reflecting similarly episodic mast years and low-severity fire events (Beaty and Taylor, 2007; North et al., 2005; Scholl and Taylor, 2010). North et al. (2005), however, found that regeneration patterns were species specific. *Abies concolor* and *C. decurrens* recruited continuously, while *Pinus lambertiana* (sugar pine) recruitment often resulted from the combination of a fire event that exposed mineral soil and higher precipitation in the years following. Thus, *Pinus* species may be at a disadvantage in contemporary post-fire environments if warmer temperatures and reduced snowpack preclude their successful recruitment. Moreover, seed inputs from *A. concolor* and *C. decurrens* may continually exceed historical levels where individuals that established since the onset of fire suppression have attained large, fire-resistant size (Becker and Lutz, 2016). If high fire severity does not remove conifer seed sources, shade-tolerant species, rather than *Pinus* species, may dominate future forests, meaning that frequent fire will continue to be necessary to prevent ladder fuels from accumulating. In contrast, if conifer seed sources are depleted, fire- and drought-adapted chaparral species may drive a vegetation type conversion.

Assuming that higher-severity fire does reduce tree cover, snow dynamics and carbon storage capacity will be affected (Krofcheck et al., 2017; Wiechmann et al., 2015). In warmer forests where the mean winter temperature is > -1° C, lower tree cover is associated with longer snow retention, due to less longwave radiation from tree boles

(Lundquist et al., 2013; Teich et al., 2022). This could potentially dampen the effect of temperature increases on extending the fire season in some areas (Westerling et al., 2006). Less tree cover would, however, also reduce aboveground carbon stores. With more carbon occupying the atmosphere and acting as a greenhouse gas, global temperatures would increase more rapidly, potentially overriding the effect of lower tree cover on snow retention and further extending the fire season (Walton et al., 2017).

Gaps in historical knowledge of fire regimes weaken our ability to accurately predict the effects of current fire regimes and yet, in many instances, are unavoidable. Dendrochronological studies estimate fire size, frequency, and seasonality for a subset of events: surface fires of low severity where trees survived. Historical fire intensity and severity are typically inferred from fire frequency (Scholl and Taylor, 2010), but the fine-scale spatial patterns of these regime attributes remain unknown. This is because there is no evidence of trees that may have existed but died and decomposed in the decades prior to data collection (North et al., 2007; Taylor et al., 2014). Not knowing whether these trees existed or not impairs our ability to estimate the fine-scale patchiness of fire severity because we cannot distinguish between areas where no trees were and potential patches of high-severity fire (or mortality by other agents). This, in turn, weakens our ability to assess the degree to which the fine-scale severity of current fires might resemble or differ from historical events. Moreover, tree survival is only one facet of fire severity. Other ecological impacts on soils, snags, and logs from historical fires are completely undescribed. These knowledge gaps lead to uncertainty surrounding the long-term effects of contemporary fires. Yet even a complete understanding of historical effects may be irrelevant because today's vegetation, climate, and fire regimes are so changed

(Johnstone et al., 2016).

Large areas of continuous forest in the Sierra Nevada—that have responded to fire suppression with considerable increases in tree density—now constitute novel ecosystems. Whether mechanical treatments and multiple fires can reduce the risk of high-severity fire in these systems—and whether unsupervised, low-severity fire regimes would even be tenable given the proximity of the wildland-urban interface—remains to be seen (North et al., 2015, 2007).

This dissertation uses data from the YFDP, a study area where geographic breadth has been sacrificed in favor of annual data points and depth of study (Lutz, 2015; Lutz et al., 2018). Findings from the YFDP could directly inform the management of old-growth, fire-suppressed dry mixed-conifer forests that experience low- to moderate-severity fire. In the Sierra Nevada fire-suppressed, dry mixed-conifer forests are widespread, but old-growth stands are more likely confined to National Park reserves (Fites-Kaufman et al., 2007). Prescribed burns that can be set during periods of moderate weather, making low- to moderate-severity outcomes more likely, are also more prevalent within National Parks (Miller et al., 2012). The direct management gains from the YFDP may thus pertain to a small, but rare and highly valued, category of forest stands.

References

Agee, J.K., 1993. Fire ecology of Pacific Northwest forests. Island Press, Washington, D.C.

Anderson, M.K., Moratto, M.J., 1996. Native American land-use practices and ecological impacts.

Barth, M.A.F., Larson, A.J., Lutz, J.A., 2015. A forest reconstruction model to assess changes to Sierra Nevada mixed-conifer forest during the fire suppression era. For. Ecol. Manage. 354, 104–118. https://doi.org/10.1016/j.foreco.2015.06.030

Baumeister, D., Callaway, R.M., 2006. Facilitation by Pinus flexilis during succession: A hierarchy of mechanisms benefits other plant species. Ecology 87, 1816–1830. https://doi.org/10.1890/0012-9658(2006)87[1816:FBPFDS]2.0.CO;2

Beaty, R.M., Taylor, A.H., 2008. Fire history and the structure and dynamics of a mixed conifer forest landscape in the northern Sierra Nevada, Lake Tahoe Basin, California, USA. For. Ecol. Manage. 255, 707–719. https://doi.org/10.1016/j.foreco.2007.09.044

Beaty, R.M., Taylor, A.H., 2007. Fire disturbance and forest structure in old-growth mixed conifer forests in the northern Sierra Nevada, California. J. Veg. Sci. 18, 879–890. https://doi.org/10.1658/1100-9233(2007)18[879:FDAFSI]2.0.CO;2

Becker, K.M.L., Lutz, J.A., 2016. Can low-severity fire reverse compositional change in montane forests of the Sierra Nevada, California, USA? Ecosphere 7, 1–22. https://doi.org/10.1002/ecs2.1484

Belmecheri, S., Babst, F., Wahl, E.R., Stahle, D.W., Trouet, V., 2016. Multi-century evaluation of Sierra Nevada snowpack. Nat. Clim. Chang. 6, 2–3. https://doi.org/10.1038/nclimate2809

Blomdahl, E.M., Kolden, C.A., Meddens, A.J.H., Lutz, J.A., 2019. The importance of small fire refugia in the central Sierra Nevada, California, USA. For. Ecol. Manage. 432, 1041–1052. https://doi.org/10.1016/j.foreco.2018.10.038

Brando, P.M., Nepstad, D.C., Balch, J.K., Bolker, B., Christman, M.C., Coe, M., Putz, F.E., 2012. Fire-induced tree mortality in a neotropical forest: The roles of bark traits, tree size, wood density and fire behavior. Glob. Chang. Biol. 18, 630–641. https://doi.org/10.1111/j.1365-2486.2011.02533.x

Brown, J.K., Reinhardt, E.D., Kramer, K.A., 2003. Coarse woody debris: managing benefits and fire hazard in the recovering forest. USDA For. Serv. Gen. Tech. Rep. 105, 1–16.

Cansler, C.A., Swanson, M.E., Furniss, T.J., Larson, A.J., Lutz, J.A., 2019. Fuel dynamics after reintroduced fire in an old-growth Sierra Nevada mixed-conifer forest. Fire Ecol. 15. https://doi.org/10.1186/s42408-019-0035-y

Certini, G., 2005. Effects of fire on properties of forest soils: A review. Oecologia 143, 1–10. https://doi.org/10.1007/s00442-004-1788-8

Collins, B.M., Everett, R.G., Stephens, S.L., 2011. Impacts of fire exclusion and recent managed fire on forest structure in old growth Sierra Nevada mixed-conifer forests. Ecosphere 2, 1–14. https://doi.org/10.1890/ES11-00026.1

Cousins, S.J.M., Battles, J.J., Sanders, J.E., York, R.A., 2015. Decay patterns and carbon density of standing dead trees in California mixed conifer forests. For. Ecol.

Manage. 353, 136–147. https://doi.org/10.1016/j.foreco.2015.05.030

Dale, V.H., Joyce, L.A., McNulty, S., Neilson, R.P., Ayres, M.P., Flannigan, M.D., Hanson, P.J., Irland, L.C., Ariel, E., Peterson, C.J., Simberloff, D., Swanson, F.J., Stocks, B.J., Wotton, B.M., Dale, V.H., Joyce, L.A., Mcnulty, S., Ronald, P., Matthew, P., Simberloff, D., Swanson, F.J., Stocks, B.J., Wotton, B.M., 2001. Climate change and forest disturbances. Bioscience 51, 723–734.

Davies, S.J., Abiem, I., Abu Salim, K., Aguilar, S., Allen, D., Alonso, A., Anderson-Teixeira, K., Andrade, A., Arellano, G., Ashton, P.S., Baker, P.J., Baker, M.E., Baltzer, J.L., Basset, Y., Bissiengou, P., Bohlman, S., Bourg, N.A., Brockelman, W.Y., Bunyavejchewin, S., Burslem, D.F.R.P., Cao, M., Cárdenas, D., Chang, L.W., Chang-Yang, C.H., Chao, K.J., Chao, W.C., Chapman, H., Chen, Y.Y., Chisholm, R.A., Chu, C., Chuyong, G., Clay, K., Comita, L.S., Condit, R., Cordell, S., Dattaraja, H.S., de Oliveira, A.A., den Ouden, J., Detto, M., Dick, C., Du, X., Duque, Á., Ediriweera, S., Ellis, E.C., Obiang, N.L.E., Esufali, S., Ewango, C.E.N., Fernando, E.S., Filip, J., Fischer, G.A., Foster, R., Giambelluca, T., Giardina, C., Gilbert, G.S., Gonzalez-Akre, E., Gunatilleke, I.A.U.N., Gunatilleke, C.V.S., Hao, Z., Hau, B.C.H., He, F., Ni, H., Howe, R.W., Hubbell, S.P., Huth, A., Inman-Narahari, F., Itoh, A., Janík, D., Jansen, P.A., Jiang, M., Johnson, D.J., Jones, F.A., Kanzaki, M., Kenfack, D., Kiratiprayoon, S., Král, K., Krizel, L., Lao, S., Larson, A.J., Li, Y., Li, X., Litton, C.M., Liu, Y., Liu, S., Lum, S.K.Y., Luskin, M.S., Lutz, J.A., Luu, H.T., Ma, K., Makana, J.R., Malhi, Y., Martin, A., McCarthy, C., McMahon, S.M., McShea, W.J., Memiaghe, H., Mi, X., Mitre, D., Mohamad, M., Monks, L., Muller-Landau, H.C., Musili, P.M., Myers, J.A., Nathalang, A., Ngo, K.M., Norden, N., Novotny, V., O'Brien, M.J., Orwig, D., Ostertag, R., Papathanassiou, K., Parker, G.G., Pérez, R., Perfecto, I., Phillips, R.P., Pongpattananurak, N., Pretzsch, H., Ren, H., Reynolds, G., Rodriguez, L.J., Russo, S.E., Sack, L., Sang, W., Shue, J., Singh, A., Song, G.Z.M., Sukumar, R., Sun, I.F., Suresh, H.S., Swenson, N.G., Tan, S., Thomas, S.C., Thomas, D., Thompson, J., Turner, B.L., Uowolo, A., Uriarte, M., Valencia, R., Vandermeer, J., Vicentini, A., Visser, M., Vrska, T., Wang, Xugao, Wang, Xihua, Weiblen, G.D., Whitfeld, T.J.S., Wolf, A., Wright, S.J., Xu, H., Yao, T.L., Yap, S.L., Ye, W., Yu, M., Zhang, M., Zhu, D., Zhu, L., Zimmerman, J.K., Zuleta, D., 2021. ForestGEO: Understanding forest diversity and dynamics through a global observatory network. Biol. Conserv. 253. https://doi.org/10.1016/j.biocon.2020.108907

Debruin, H.W., 1974. From fire control to fire management, a major policy change in the Forest Service, in: Proceedings of the Tall Timbers Fire Ecology Conference. pp. 11–17.

Dobrowski, S.Z., Swanson, A.K., Abatzoglou, J.T., Holden, Z.A., Safford, H.D., Schwartz, M.K., Gavin, D.G., 2015. Forest structure and species traits mediate projected recruitment declines in western US tree species. Glob. Ecol. Biogeogr. 1–11.

Fites-Kaufman, J., Rundel, P., Stephenson, N., Weixelman, D.A., 2007. Montane and subalpine vegetation of the Sierra Nevada and Cascade ranges, in: Terrestrial Vegetation of California. pp. 456–501.

Franklin, J.F., Spies, T.A., Pelt, R. V., Carey, A.B., Thornburgh, D.A., Berg, D.R., Lindenmayer, D.B., Harmon, M.E., Keeton, W.S., Shaw, D.C., Bible, K., Chen, J., 2002. Disturbances and structural development of natural forest ecosystems with silvicultural implications, using Douglas-fir forests as an example. For. Ecol. Manage. 155, 399–423. https://doi.org/10.1016/S0378-1127(01)00575-8

Harmon, M.E., Franklin, J.F., Swanson, F.J., Sollins, P., Gregory, S. V., Lattin, J.D., Anderson, N.H., Cline, S.P., Aumen, N.G., Sedell, J.R., Lienkaemper, G.W., Cromack, K.J., Cummins, K.W., 1986. Ecology of coarse woody debris in temperate ecosystems. Adv. Ecol. Res. 15, 133–302.

Hood, S.M., Smith, S.L., Cluck, D.R., 2010. Predicting mortality for five California conifers following wildfire. For. Ecol. Manage. 260, 750–762. https://doi.org/10.1016/j.foreco.2010.05.033

Hyde, J.C., Smith, A.M.S., Ottmar, R.D., Alvarado, E.C., Morgan, P., 2011. The combustion of sound and rotten coarse woody debris: a review. Int. J. Wildl. Fire 20, 163–174. https://doi.org/10.1029/2010WR009341.Citation

Innes, J.C., North, M.P., Williamson, N., 2006. Effect of thinning and prescribed fire restoration treatments on woody debris and snag dynamics in a Sierran old-growth, mixed-conifer forest. Can. J. For. Res. 36, 3183–3193. https://doi.org/10.1139/X06-184

Jeronimo, S.M.A., Lutz, J.A., R. Kane, V., Larson, A.J., Franklin, J.F., 2020. Burn weather and three-dimensional fuel structure determine post-fire tree mortality. Landsc. Ecol. 35, 859–878. https://doi.org/10.1007/s10980-020-00983-0

Johnstone, J.F., Allen, C.D., Franklin, J.F., Frelich, L.E., Harvey, B.J., Higuera, P.E., Mack, M.C., Meentemeyer, R.K., Metz, M.R., Perry, G.L.W., Schoennagel, T., Turner, M.G., 2016. Changing disturbance regimes, ecological memory, and forest resilience. Front. Ecol. 14, 369–378. https://doi.org/10.1017/CBO9781107415324.004

Kane, V.R., Lutz, J.A., Cansler, C.A., Povak, N.A., Churchill, D.J., Smith, D.F., Kane, J.T., North, M.P., 2015. Water balance and topography predict fire and forest structure patterns. For. Ecol. Manage. 338, 1–13. https://doi.org/10.1016/j.foreco.2014.10.038

Keenan, T.F., Williams, C.A., 2018. The terrestrial carbon sink. Annu. Rev. Environ. Resour. 43, 219–243. https://doi.org/10.1146/annurev-environ-102017-030204

Kemp, K.B., Higuera, P.E., Morgan, P., 2016. Fire legacies impact conifer regeneration

across environmental gradients in the U.S. northern Rockies. Landsc. Ecol. 31, 619–636. https://doi.org/10.1007/s10980-015-0268-3

Knapp, E.E., Keeley, J.E., Ballenger, E.A., Brennan, T.J., 2005. Fuel reduction and coarse woody debris dynamics with early season and late season prescribed fire in a Sierra Nevada mixed conifer forest. For. Ecol. Manage. 208, 383–397. https://doi.org/10.1016/j.foreco.2005.01.016

Krofcheck, D.K., Hurteau, M.D., Scheller, R.M., Loudermilk, E.L., 2017. Restoring surface fire stabilizes forest carbon under extreme fire weather in the Sierra Nevada. Ecosphere 8, 1–18. https://doi.org/10.1002/ecs2.1663

Larson, A.J., Cansler, C.A., Cowdery, S.G., Hiebert, S., Furniss, T.J., Swanson, M.E., Lutz, J.A., 2016. Post-fire morel (Morchella) mushroom abundance, spatial structure, and harvest sustainability. For. Ecol. Manage. 377, 16–25. https://doi.org/10.1016/j.foreco.2016.06.038

Lauvaux, C.A., Skinner, C.N., Taylor, A.H., 2016. High severity fire and mixed conifer forest-chaparral dynamics in the southern Cascade Range, USA. For. Ecol. Manage. 363, 74–85. https://doi.org/10.1016/j.foreco.2015.12.016

Littell, J.S., Mckenzie, D., Peterson, D.L., Westerling, A.L., 2009. Climate and wildfire area burned in western U.S. ecoprovinces, 1916-2003. Ecol. Appl. 19, 1003–1021. https://doi.org/10.1890/07-1183.1

Lundquist, J.D., Dickerson-Lange, S.E., Lutz, J.A., Cristea, N.C., 2013. Lower forest density enhances snow retention in regions with warmer winters: A global framework developed from plot-scale observations and modeling. Water Resour. Res. 49, 6356–6370. https://doi.org/10.1002/wrcr.20504

Lutz, J.A., 2015. The evolution of long-term data for forestry: large temperate research plots in an era of global change. Northwest Sci. 89, 255–269. https://doi.org/10.3955/046.089.0306

Lutz, J.A., Furniss, T.J., Germain, S.J., Becker, K.M.L., Blomdahl, E.M., Jeronimo, S.M.A., Cansler, C.A., Freund, J.A., Swanson, M.E., Larson, A.J., 2017. Shrub communities, spatial patterns, and shrub-mediated tree mortality following reintroduced fire in Yosemite National Park, California, USA. Fire Ecol. 13, 104–126. https://doi.org/10.4996/fireecology.1301ppp

Lutz, J.A., Key, C.H., Kolden, C.A., Kane, J.T., van Wagtendonk, J.W., 2011. Fire frequency, area burned, and severity: A quantitative approach to defining a normal fire year. Fire Ecol. 7, 51–65. https://doi.org/10.4996/fireecology.0702051

Lutz, J.A., Larson, A.J., Swanson, M.E., 2018. Advancing fire science with large forest plots and a long-term multidisciplinary approach. Fire 1, 1–7. https://doi.org/10.3390/fire1010005

Lutz, J.A., Larson, A.J., Swanson, M.E., Freund, J.A., 2012. Ecological importance of large-diameter trees in a temperate mixed-conifer forest. PLoS One 7, e36131. https://doi.org/10.1371/journal.pone.0036131

Lutz, J.A., van Wagtendonk, J.W., Franklin, J.F., 2010. Climatic water deficit, tree species ranges, and climate change in Yosemite National Park. J. Biogeogr. 37, 936–950. https://doi.org/10.1111/j.1365-2699.2009.02268.x

Lutz, J.A., van Wagtendonk, J.W., Thode, A.E., Miller, J.D., Franklin, J.F., 2009. Climate, lightning ignitions, and fire severity in Yosemite National Park, California, USA. Int. J. Wildl. Fire 18, 765–774. https://doi.org/10.1071/WF08117

Meyer, M.D., Kelt, D.A., North, M.P., 2005. Nest trees of Northern flying squirrels in the Sierra Nevada. J. Mammal. 86, 275–280. https://doi.org/10.1644/BEH-110.1

Miller, J.D., Collins, B.M., Lutz, J.A., Stephens, S.L., van Wagtendonk, J.W., Yasuda, D.A., 2012. Differences in wildfires among ecoregions and land management agencies in the Sierra Nevada region, California, USA. Ecosphere 3, 1–20.

Miller, J.D., Safford, H.D., Crimmins, M., Thode, A.E., 2009. Quantitative evidence for increasing forest fire severity in the Sierra Nevada and southern Cascade Mountains, California and Nevada, USA. Ecosystems 12, 16–32. https://doi.org/10.1007/s10021-008-9201-9

Nagel, T.A., Taylor, A.H., 2005. Fire and Persistence of Montane Chaparral in Mixed Conifer Forest Landscapes in the northern Sierra Nevada, Lake Tahoe Basin, Calififonia, USA. J. Torrey Bot. Soc. 132, 442–457.

North, M., Brough, A., Long, J., Collins, B., Bowden, P., Yasuda, D., Miller, J., Sugihara, N., 2015. Constraints on mechanized treatment significantly limit mechanical fuels reduction extent in the Sierra Nevada. J. For. 113, 40–48. https://doi.org/10.5849/jof.14-058

North, M., Hurteau, M., Fiegener, R., Barbour, M., 2005. Influence of fire and El Niño on tree recruitment varies by species in Sierran mixed conifer. For. Sci. 51, 187–197.

North, M., Innes, J., Zald, H., 2007. Comparison of thinning and prescribed fire restoration treatments to Sierran mixed-conifer historic conditions. Can. J. For. Res. 37, 331–342. https://doi.org/10.1139/X06-236

Parks, S.A., Abatzoglou, J.T., 2020. Warmer and drier fire seasons contribute to increases in area burned at high severity in western US forests from 1985 to 2017. Geophys. Res. Lett. 47, 1–10. https://doi.org/10.1029/2020GL089858

Parks, S.A., Holsinger, L.M., Miller, C., 2015. Wildland fire as a self-regulating mechanism: the role of previous burns and weather in limiting fire progression. Ecol. Appl. 25, 1478–1492.

Parsons, D.J., DeBenedetti, S.H., 1979. Impact of fire suppression on a mixed-conifer forest. For. Ecol. Manage. 2, 21–33. https://doi.org/10.1016/0378-1127(79)90034-3

Pörtner, H.-O., Roberts, D.C., Tignor, M., Poloczanska, E.S., Mintenbeck, K., Alegría, A., M. Craig, S. Langsdorf, S. Löschke, V. Möller, A. Okem, B.R., 2022. Climate change 2022: Impacts, adaptation, and vulnerability.

Rabe, M.J., Morrell, T.E., Green, H., deVos Jr., J.C., Miller, C.R., 1998. Characteristics of ponderosa pine snag roosts used by reproductive bats in northern Arizona. J. Wildl. Manage. 62, 612–621. https://doi.org/10.2307/3802337

Raphael, M.G., Morrison, M.L., 1987. Decay and dynamics of snags in the Sierra Nevada, California. For. Sci. 33, 774–783.

Raphael, M.G., White, M., 1984. Use of snags by cavity-nesting birds in the Sierra Nevada. Wildl. Monogr. 86, 3–66.

Scholl, A.E., Taylor, A.H., 2010. Fire regimes, forest change, and self-organization in an old-growth mixed-conifer forest, Yosemite National Park, USA. Ecol. Appl. 20, 362–380. https://doi.org/10.1890/08-2324.1

Seidl, R., Thom, D., Kautz, M., Martin-Benito, D., Peltoniemi, M., Vacchiano, G., Wild, J., Ascoli, D., Petr, M., Honkaniemi, J., Lexer, M.J., Trotsiuk, V., Mairota, P., Svoboda, M., Fabrika, M., Nagel, T.A., Reyer, C.P.O., 2017. Forest disturbances under climate change. Nat. Clim. Chang. 7, 395.

Shive, K.L., Preisler, H.K., Welch, K.R., Safford, H.D., Butz, R.J., O'Hara, K.L., Stephens, S.L., 2018. From the stand scale to the landscape scale: predicting the spatial patterns of forest regeneration after disturbance. Ecol. Appl. 28, 1626–1639. https://doi.org/10.1002/eap.1756

Smith, S.J., Anderson, S.R., 1992. Late Wisconsin paleoecologic record from Swamp Lake, Yosemite National Park, California. Quat. Res. 102, 91–102.

Stavros, E.N., Abatzoglou, J., Larkin, N.K., Mckenzie, D., E Ashley Steel, 2014. Climate and very large wildland fires in the contiguous western USA. Int. J. Wildl. Fire 23, 899–914.

Stavros, N.E., Tane, Z., Kane, V.R., Veraverbeke, S., Mcgaughey, R.J., Lutz, J.A., Ramirez, C., Schimel, D., 2016. Unprecedented remote sensing data over King and Rim megafires in the Sierra Nevada Mountains of California. Ecology 97, 3334. https://doi.org/10.1002/ecy.1577

Stephens, S.L., Moghaddas, J.J., 2005. Fuel treatment effects on snags and coarse woody debris in a Sierra Nevada mixed conifer forest. For. Ecol. Manage. 214, 53–64. https://doi.org/10.1016/j.foreco.2005.03.055

Stevens-Rumann, C.S., Kemp, K.B., Higuera, P.E., Harvey, B.J., Rother, M.T., Donato, D.C., Morgan, P., Veblen, T.T., 2018. Evidence for declining forest resilience to wildfires under climate change. Ecol. Lett. 21, 243–252. https://doi.org/10.1111/ele.12889

Stewart, J.A.E., van Mantgem, P.J., Young, D.J.N., Shive, K.L., Preisler, H.K., Das, A.J., Stephenson, N.L., Keeley, J.E., Safford, H.D., Wright, M.C., Welch, K.R., Thorne, J.H., 2021. Effects of postfire climate and seed availability on postfire conifer regeneration. Ecol. Appl. 31, 1–14. https://doi.org/10.1002/eap.2280

Sugihara, N.G., van Wagtendonk, J.W., Fites-Kaufman, J., 2006. Fire as an ecological process, in: Sugihara, N.G., Van Wagtendonk, J.W., Shaffer, K.E., Fites-kaufman, J., Thode, A.E. (Eds.), Fire in California's Ecosystems. University of California Press, Berkeley, pp. 58–74.

Swetnam, T.W., 1993. Fire history and climate change in giant sequoia groves. Science (80-.). 262, 885–889.

Taylor, A.H., Vandervlugt, A.M., Maxwell, R.S., Beaty, R.M., Airey, C., Skinner, C.N., 2014. Changes in forest structure, fuels and potential fire behaviour since 1873 in the Lake Tahoe Basin, USA. Appl. Veg. Sci. 17, 17–31. https://doi.org/10.1111/avsc.12049

Teich, M., Becker, K.M.L., Raleigh, M.S., Lutz, J.A., 2022. Large-diameter trees affect snow duration in post-fire old-growth forests. Ecohydrology 15. https://doi.org/10.1002/eco.2414

Tepley, A.J., Thompson, J.R., Epstein, H.E., Anderson-Teixeira, K.J., 2017. Vulnerability to forest loss through altered postfire recovery dynamics in a warming climate in the Klamath Mountains. Glob. Chang. Biol. 23, 4117–4132. https://doi.org/10.1111/gcb.13704

Urza, A.K., Sibold, J.S., 2017. Climate and seed availability initiate alternate post-fire trajectories in a lower subalpine forest. J. Veg. Sci. 28, 43–56. https://doi.org/10.1111/jvs.12465

Van de Water, K., North, M., 2011. Stand structure, fuel loads, and fire behavior in riparian and upland forests, Sierra Nevada Mountains, USA; a comparison of current and reconstructed conditions. For. Ecol. Manage. 262, 215–228. https://doi.org/10.1016/j.foreco.2011.03.026

Van de Water, K.M., North, M., 2010. Fire history of coniferous riparian forests in the Sierra Nevada. For. Ecol. Manage. 260, 384–395. https://doi.org/10.1016/j.foreco.2010.04.032

Van de Water, K.M., Safford, H.D., 2011. A summary of fire frequency estimates for California vegetation before Euro-American settlement. Fire Ecol. 7, 26–58.

https://doi.org/10.4996/fireecology.0703026

van Mantgem, P.J., Schwartz, M., 2003. Bark heat resistance of small trees in Californian mixed conifer forests: testing some model assumptions. For. Ecol. Manage. 178, 341–352. https://doi.org/10.1016/S0378-1127(02)00554-6

van Wagtendonk, J.W., 2007. The history and evolution of wildland fire use. Fire Ecol. 3, 3–17. https://doi.org/10.4996/fireecology.0302003

van Wagtendonk, J.W., Fites-Kaufman, J.A., 2006. Sierra Nevada bioregion, in: Fire in California's Ecosystems. pp. 264–294.

van Wagtendonk, J.W., Lutz, J.A., 2007. Fire regime attributes of wildland fires in Yosemite National Park, USA. Fire Ecol. 3, 34–52. https://doi.org/10.4996/fireecology.0302034

van Wagtendonk, J.W., Moore, P.E., Yee, J.L., Lutz, J.A., 2020. The distribution of woody species in relation to climate and fire in Yosemite National Park, California, USA. Fire Ecol. 16, 1–23. https://doi.org/10.1186/s42408-020-00079-9

van Wagtendonk, J.W., van Wagtendonk, K.A., Thode, A.E., 2012. Factors associated with the severity of intersecting fires in Yosemite National Park, California, USA. Fire Ecol. 8, 11–31. https://doi.org/10.4996/fireecology.0801011

VanderWeide, B.L., Hartnett, D.C., 2011. Fire resistance of tree species explains historical gallery forest community composition. For. Ecol. Manage. 261, 1530–1538. https://doi.org/10.1016/j.foreco.2011.01.044

Vankat, J.L., Major, J., 1978. Vegetation changes in Sequoia National Park, California. J. Biogeogr. 5, 377–402.

Walton, D.B., Hall, A., Berg, N., Schwartz, M., Sun, F., 2017. Incorporating snow albedo feedback into downscaled temperature and snow cover projections for California's Sierra Nevada. J. Clim. 1417–1438. https://doi.org/10.1175/JCLI-D-16-0168.1

We must get a grip on forest science — before it's too late, 2022. Nature 608, 449.

Webster, K.M., Halpern, C.B., 2010. Long-term vegetation responses to reintroduction and repeated use of fire in mixed-conifer forests of the Sierra Nevada. Ecosphere 1, art9. https://doi.org/10.1890/ES10-00018.1

Westerling, A.L., Hidalgo, H.G., Cayan, D.R., Swetnam, T.W., 2006. Warming and earlier spring increase western U.S. forest wildfire activity. Science (80-.). 313, 940–943. https://doi.org/10.1126/science.1128834

Wiechmann, M.L., Hurteau, M.D., North, M.P., Koch, G.W., Jerabkova, L., 2015. The carbon balance of reducing wildfire risk and restoring process: An analysis of 10-

year post-treatment carbon dynamics in a mixed-conifer forest. Clim. Chang. 132, 709–719. https://doi.org/10.1007/s10584-015-1450-y

Williams, K., Harvey, D., 2001. Transcendent experience in forest environments. J. Environ. Psychol. 21, 249–260. https://doi.org/10.1006/jevp.2001.0204

Young, D.J.N., Werner, C.M., Welch, K.R., Young, T.P., Safford, H.D., Latimer, A.M., 2019. Post-fire forest regeneration shows limited climate tracking and potential for drought-induced type conversion. Ecology 100, 1–13. https://doi.org/10.1002/ecy.2571

Zald, H.S.J., Gray, A.N., North, M., Kern, R.A., 2008. Initial tree regeneration responses to fire and thinning treatments in a Sierra Nevada mixed-conifer forest, USA. For. Ecol. Manage. 256, 168–179. https://doi.org/10.1016/j.foreco.2008.04.022

CHAPTER II

PREDICTING SNAG FALL IN AN OLD-GROWTH FOREST AFTER FIRE

Abstract

Snags, standing dead trees, are becoming more abundant in forests as tree mortality rates continue to increase due to fire, drought, and bark beetles. Snags provide habitat for birds and small mammals, and when they fall to the ground, the resulting logs provide additional wildlife habitat and affect nutrient cycling, fuel loads, and fire behavior. Predicting how long snags will remain standing after fire is essential for managing habitat, understanding chemical cycling in forests, and modeling forest succession and fuels. Few studies, however, have quantified how fire changes snag fall dynamics. We compared post-fire fall rates of snags that existed pre-fire (n = 2,013) and snags created during or after fire (n = 8,222), using three years of pre-fire and five years of post-fire data from an annually monitored, 25.6-ha spatially explicit plot that burned at low to moderate severity in the California Rim Fire of 2013. We used random forest models to 1) identify predictors of post-fire snag fall for pre-existing and new snags, and 2) assess the influence of spatial neighborhood and local fire severity on snag fall after fire. Fall rates of pre-existing snags increased three years after fire. Five years after fire, pre-existing snags were twice as likely to fall as new snags. Pre-existing snags were most likely to persist five years after fire if they were > 50 cm in diameter, > 20 m tall, and charred on the bole above 3.7 m. New snags were also more likely to persist five years after fire if they were > 20 m tall. Spatial neighborhood (e.g., tree density) and local fire severity (e.g., fire-caused crown injury) within 15 m of each snag barely improved predictions of post-fire snag fall. Land managers should expect fall rates of pre-existing

snags to exceed fall rates of new snags within five years after fire, an important habitat consideration because pre-existing snags represent a wider range of size and decay classes.

Introduction

Snags—standing dead trees—and logs perform vital functions in forest ecosystems. Snags contribute to gradual chemical cycling while providing habitat for numerous species of birds and mammals (Harmon et al., 1986; Meyer et al., 2005; Rabe et al., 1998; Raphael and White, 1984; Thomas, 1979). When snags fragment or fall, the resulting logs provide denning habitat, protect movement pathways, and accelerate soil development by cycling carbon and nutrients at a faster rate than snags (Bull and Heater, 2000; Butts and McComb, 2000; Cousins et al., 2015; Harmon et al., 1986; Ucitel et al., 2003). Intersecting or stacked logs (sensu Lutz et al., 2021; their Figure 8) can spread fire, potentially killing vegetation and altering soil characteristics (Knapp, 2015; Monsanto and Agee, 2008). As tree mortality rates continue to increase in response to drought, bark beetles, and fire (Allen et al., 2010; van Mantgem et al., 2009), snags will become more abundant, and understanding post-fire snag dynamics will become more central to managing habitat and modeling fuels and fire behavior.

Snag longevity depends on snag attributes, including bole and crown architecture, wood strength, and resistance to decay (Dunn and Bailey, 2012). Large-diameter snags commonly persist longer than small-diameter snags (Grayson et al., 2019; Morrison and Raphael, 1993; Ritchie et al., 2013), as do shorter snags, particularly those with broken tops (Dahms 1949, Morrison and Raphael 1993, Everett et al. 1999, Chambers and Mast 2005, Russell et al. 2006, but see Grayson et al. 2019). Species differ in wood strength

and susceptibility to decay. *Abies* snags typically persist longer than *Pinus* snags, potentially due to faster heartwood decay in *Abies* and higher bole breakage rates; in such cases, the standing portion of the snag persists longer because it is shorter and less susceptible to windthrow (Das et al., 2016; Morrison and Raphael, 1993; Russell et al., 2006). In contrast, stems with root rot (e.g., *Heterobasidion annosum*, *Armillaria* spp.) are prone to structural weakness at the base, which may increase their chance of falling, even if the bole is not highly decayed (Cousins et al., 2015; Harmon et al., 1986).

Studies of snag longevity have previously focused on two snag populations, trees killed by fire (Grayson et al., 2019) and trees killed by other causes (Conner et al., 2005; Ganey et al., 2021; Garber et al., 2005; Keen, 1929; Mitchell and Preisler, 1998; Runkle, 2013; Russell and Weiskittel, 2012). However, little is known about snags that existed before fire and remain standing after fire. The ecological importance of this pre-existing snag population is expanding as more forest burns each year (Parks and Abatzoglou, 2020). Pre-existing snags may have recruited gradually, from different causes of death, and are likely to represent a range of size and decay classes, especially in old forests (Conner et al., 2005). When a stand-level mortality event results in a pulse of new snags, pre-existing snags can function as lifeboats for species, meeting size and decay class requirements that the new cohort of snags may not provide for years or decades (Franklin et al., 2000).

The attributes of pre-existing snags determine how species use them but also how long they remain standing after fire. When the attributes of pre-existing snags differ from fire-killed snags, we expect snag fall rates to vary between these populations, but the direction of these changes is unclear: pre-existing snags may include larger individuals

that are less likely to burn through at the base but are more likely to fall due to advanced decay (Garber et al., 2005; Keen, 1929; Russell and Weiskittel, 2012); in contrast, fire-killed trees may be smaller and therefore fall sooner (Gaines et al., 1958; Grayson et al., 2019; Innes et al., 2006). Local fire behavior should also alter snag dynamics by consuming stems at the base and increasing resistance to decay through charring, but whether the sum of these effects increases or decreases snag longevity is unknown. As both pre-existing and fire-killed snags become more abundant in forests, improved understanding of snag longevity after fire is needed to manage habitat and parameterize fuel models.

We monitored 39,026 spatially explicit stems before and after a low- to moderate-severity fire to compare annual fall rates of pre-existing snags and snags created in or after the fire. Specifically, we 1) identify important predictors of post-fire snag fall for pre-existing and new snags, and 2) determine if spatial neighborhood or local fire severity improves predictions of snag fall. We expected higher local fire severity to increase consumption at the stem base, making it more likely for both pre-existing and new snags to fall after fire.

Methods

Study area

The Yosemite Forest Dynamics Plot (YFDP; 37.77°N, 119.92°W) is a 25.6-ha study area in an unlogged, old-growth *Abies concolor–Pinus lambertiana* forest in Yosemite National Park (Lutz, 2015; Lutz et al., 2012; Figure 2.1). Elevation within the YFDP ranges from 1774 m to 1911 m. Between 1981 and 2010 the modeled mean January

temperature range was -0.5 °C to 9.7 °C, and the mean July temperature range was 14.2

°C to 28.1 °C; mean annual precipitation was 1068 mm with the majority falling as snow

(Prism Climate Group 2016). Principal tree species ordered by pre-fire live tree

abundance include *Abies concolor* [Gord. & Glend.] Lindl. ex Hildebr. (white fir), *Pinus*

lambertiana Douglas (sugar pine), *Cornus nuttallii* Audubon ex Torr. & A. Gray (Pacific

dogwood), *Calocedrus decurrens* [Torr.] Florin (incense-cedar), and *Quercus kelloggii*

Newberry (California black oak) (Table 2.1).

Vegetation communities in the Sierra Nevada are strongly influenced by the presence

and absence of fire (van Wagtendonk et al., 2020). The historical (pre-European

settlement) fire regime of the YFDP was characterized by low- to moderate-severity

surface fires and a mean fire return interval of approximately 30 yr (Barth et al., 2015),

slightly longer than mean values for other lower montane mixed-conifer forests in the

central Sierra Nevada (Scholl and Taylor, 2010). Although lightning-ignited spot fires

have occurred within the YFDP over the past century, the area has been largely fire-

excluded since the last widespread event in 1900 (Barth et al., 2015; Scholl and Taylor,

2010), leading to high tree density (Barth et al., 2015; Lutz et al., 2012) and surface fuel

accumulation (Gabrielson et al. 2012, Lutz et al. 2014, Cansler et al. 2019).

On September 1st and 2nd, 2013, the YFDP burned in a fire set by Park managers to

control the spread of the Rim Fire (Furniss et al., 2020b; Stavros et al., 2016). Fire

severity within the YFDP as inferred from Landsat-derived scenes was largely low and

moderate (Blomdahl et al., 2019). Both severity and spatial pattern were consistent with

other fires in Yosemite since the mid-1970s (van Wagtendonk and Lutz, 2007). The fire

reduced aboveground live shrub biomass from 3,490 to 269 kg ha^{-1} (Lutz et al., 2017a)

and consumed 79% of total surface fuel loading, which had an average value of 192.0 Mg ha^{-1} before the fire (Cansler et al., 2019).

Data collection

The YFDP was installed in 2009 and 2010 following the protocols of the Smithsonian Forest Global Observatory (ForestGEO; Davies et al., 2021). The 25.6-ha area (800 m × 320 m) was subdivided into 20 m × 20 m cells, and field crews surveyed in the corners of each cell with total stations (Lutz et al. 2012). Trees ≥ 1 cm diameter at breast height (DBH) and snags ≥ 10 cm DBH were tagged and mapped relative to the surveyed corners; DBH and species of each tagged stem were recorded. Snag height was measured with laser rangefinders (Impulse Rangefinder model 200, Laser Tech, Centennial, CO, USA), top diameter and percent of stem still standing were estimated, and each snag was assigned to one of five decay classes (1, least decayed; 5, most decayed) (Maser and Trappe, 1984).

In annual demographic surveys that began in 2011 (Lutz, 2015), field technicians documented recruitment (i.e., trees that had newly attained ≥ 1 cm DBH), tree mortality, and tree and snag fall (i.e., stem uprooted or snapped below DBH). These records associated each tagged individual with an annual status of live tree, snag, or log. Field crews recorded the DBH, height, top diameter, and percent of stem still standing for each new mortality. Logs ≥ 50 cm in diameter and ≥ 1 m long were mapped relative to stems and grid corners; length, short- and long-end diameter, and decay class were recorded.

In May 2014, following the Rim Fire, field crews reassessed decay class and re-measured DBH, height, and top diameter of all snags documented before the fire. Stems were recorded as consumed if stem height was reduced to below DBH and no piece of

bole ≥ 1 m long was found nearby. Percent crown injury was recorded for every tree that had been alive in 2013 (Varner et al., 2021). Maximum bole scorch height was recorded for all stems. Logs ≥ 50 cm in diameter and ≥ 1 m long were re-mapped and re-measured. If any piece of re-mapped log moved during the fire, this was noted. Unburned areas ≥ 1 m^2 were mapped relative to stems and grid corners (Blomdahl et al., 2019).

Snag abundance, volume, biomass, and carbon content

We used DBH, height, and top diameter measurements to calculate annual snag density, basal area, volume, biomass, and carbon (C) content by species, diameter class, and decay class for pre-fire and post-fire snag populations. We estimated snag volume as the sum of two conical frustums (i.e., decapitated cones), from the base of the stem to DBH, and from DBH to the tip or break point of the bole. For conifers, we used species-specific equations from Wensel and Krumland (1983) to model the inside-of-bark diameter at the stem base, and specific-specific equations from Biging (1984) to model the inside-of-bark diameter at the top of the stem if the stem was broken. We used species-specific equations from Zeibig-Kichas et al. (2016) to model bark thickness at DBH. If the stem was broken, we used species-specific equations from Wensel and Olson (1995) to model bark thickness at the base of the stem and at the top of the stem. For hardwoods, we used DBH to represent outside-of-bark basal diameter.

We estimated pre-fire and post-fire snag biomass by multiplying snag volume by species- and decay-class–specific density values from Cousins et al. (2015) or Harmon et al. (2008). Values from Cousins et al. (2015) were used whenever possible because they were based on wood samples from standing snags, whereas values from Harmon et al. (2008) were based on standing snags and logs combined. We estimated pre-fire and post-

fire snag C content by multiplying snag biomass by species- and decay-class–specific C concentration values from Cousins et al. (2015). When specific C concentration values were not available, we used 0.5 (Lutz et al., 2017b; Thomas and Martin, 2012).

Snag status transitions

We determined annual recruitment, persistence, fall, and consumption rates of snags by associating each stem with an annual transition status for 2011 through 2018: tree to snag, snag to snag, snag to log, or snag to consumed. We grouped snags as small ($1 \leq DBH < 10$ cm), medium ($10 \leq DBH < 60$ cm), or large ($DBH \geq 60$ cm) and low decay (class 1), moderate decay (class 2 or 3), or advanced decay (class 4 or 5). We chose these diameter classes to be consistent with other studies (Furniss et al., 2020b; Lutz et al., 2018a; Michel et al., 2014) and because snags < 10 cm DBH were not inventoried when the YFDP was established. For each snag diameter class, we calculated the probability of a stem undergoing each type of transition in each year (Figures A.1–A.11). Snags could transition between decay classes only in 2014, when decay class was reassessed.

Snag attributes

We characterized each snag by fixed, pre-fire, and post-fire attributes (Table A.6). Fixed snag attributes included species, years between fire and death (for just post-fire snags), and topography. Slope, aspect, topographic position, terrain ruggedness, and roughness were calculated in R using the terrain function in the raster package (Hijmans, 2020). A 1-m digital elevation model was aggregated to 10 m × 10 m cells. Topographic metrics were calculated for each cell based on the cell and the surrounding eight, 10 m ×

10 m cells, and these values were assigned to the snags within the central cell. Pre-fire snag attributes included pre-fire DBH, height, and decay class. Post-fire snag attributes included post-fire DBH, height, decay class, bole scorch, crown injury (for just post-fire snags), and whether the snag was located in an unburned patch ≥ 1 m^2 (Blomdahl et al., 2019).

Neighborhood metrics

We used forest inventory data from 2013 to characterize the pre-fire spatial neighborhood around each snag in two ways. First, we calculated snag isolation, represented by the distance from each snag to the nearest tree, snag, or piece of log. We considered snag isolation because it is a less labor-intensive way to summarize neighborhood. Second, we calculated tree, snag, and log density metrics in five annuli with radii of 0–3, 3–6, 6–9, 9–12, and 12–15 m, expanding out from each snag (Table A.6). We considered five neighborhood sizes by including metrics from successive annuli. Our purpose was to identify a threshold radius beyond which neighborhood no longer influences snag persistence after fire.

For annulus metrics based primarily on live trees (i.e., live tree density, density of new mortalities, density of newly fallen stems, and log density), we calculated density by five diameter classes. We defined these classes by identifying DBH thresholds associated with an 80% (10 cm), 60% (15 cm), 40% (21 cm), and 20% (28 cm) fire-year mortality rate. We used DBH thresholds based on fire effects rather than arbitrary diameter classes so the neighborhood metrics would relate more directly to local fire severity, not just forest structure. For annulus metrics based on snags, we calculated density of small, medium, and large snags (see *Snag status transitions*).

To characterize local fire severity around each snag, we calculated the same metrics using forest inventory data from 2014, and added metrics for consumed trees, snags, and logs (Table 2.2; Table A.6). Logs ($\geq$ 50 cm in diameter and $\geq$ 1 m long) that had been present before the fire were spatially adjusted back to their pre-fire location if they had moved. We determined log consumption by subtracting the post-fire volume and biomass from the pre-fire volume and biomass within each 1-m^2 area. We represented the influence of log consumption on snag fall by estimating the total fire radiative energy (FRE) reaching each focal snag from logs within 15 m that had been consumed (Appendix A: Methods: Equation 2.1).

To represent the influence of neighborhood crown injury on snag fall, we developed equations using basal area and percent crown injury as a proxy for volume of crown injured within each neighborhood annulus (Appendix A: Methods: Equations 2.2–2.4). Lastly, we represented the influence of neighborhood bole scorch on snag fall by developing a metric where bole scorch of stems within 15 m of the focal snag was weighted by distance from the focal snag according to the inverse-square law (Appendix A: Methods: Equation 2.5).

Model framework

This study was designed to identify important predictors of snag fall for two snag populations, snags that existed before the fire (pre-fire snags) and snags that died in or after the fire (post-fire snags). For each snag population, the response variable was binary: 0 if the snag remained standing five years after the fire, and 1 if the snag fell within five years after the fire. We created one set of models based on pre-fire predictors and another based on post-fire predictors (Table 2.2). Our purpose was to 1) produce

results relevant to managers who only have access to pre-fire or post-fire data, and 2) identify which fire effects most improve snag fall predictions. For each set of models, we compared the predictive power of snag attributes, different types of neighborhood metrics, and different neighborhood sizes by running random forest models with unique subsets of predictors. We compared 14 models predicting the fall of pre-fire snags, and 13 models predicting the fall of post-fire snags. Because neighborhood metrics extended to 15 m from each snag, only snags that were within 15 m of the plot boundary were included as focal snags.

Variable selection

For each model, we used the Boruta function (Kursa and Rudnicki, 2020, 2010) to determine which variables were confirmed to influence snag fall. The Boruta function determines whether a variable is confirmed by 1) randomly permuting all predictors to create a set of "shadow" predictors, 2) running random forest on the combined set of predictors and "shadow" predictors, and 3) calculating variable importance. This process is repeated, creating a distribution of importance values for each predictor variable and a distribution of the importance values of the most important "shadow" predictor in each run. Predictor variables with median importance values that exceed the median importance value associated with the most important "shadow" predictor in each run are confirmed as important variables. We removed variables that were not confirmed from future analyses.

Next, we removed selected remaining variables to avoid collinearity among predictors because the importance values generated by random forest are not meaningful if the predictor variables are highly correlated. The importance function in random forest

determines the importance of a predictor variable by calculating the out-of-bag error for each tree (i.e., the mean prediction error of samples not included in each tree), permuting the predictor variable of interest in the out-of-bag samples, recalculating the out-of-bag error for each tree, calculating the difference between the two out-of-bag error rates for each tree, averaging the differences, and normalizing the value by dividing by the standard deviation of the differences. During this process, only one predictor variable is permuted at a time. If that permuted variable is highly correlated with another variable, the out-of-bag error rates may not change very much—despite permuting the variable—because the out-of-bag samples could still be categorized similarly by the highly correlated variable that was not permuted. Therefore, we removed selected predictor variables to avoid correlations at or above three thresholds: $r = 0.7$, $r = 0.5$, and $r = 0.3$ (Table A.7). We compared random forest models using predictor variables selected at these three thresholds to determine how sensitive our model results were to arbitrary thresholds (Figures A.12, A.13, and A.14).

For each model, we selected predictors to remove by identifying all variables that correlated with other variables at or above the specified threshold (e.g., $r = 0.7$). We identified the pair of variables with the highest correlation. Then we kept the variable in the pair that had higher correlations with other variables and removed all the variables it correlated with. This process was repeated until no pairs of variables correlated with each other at or above the specified threshold.

Random forest models

We used the randomForest function (Cutler et al., 2007; Liaw and Wiener, 2018) to determine which variables were important predictors of a whether a snag fell within five

years after the fire (1) or not (0). We computed model accuracy using 10-fold cross validation. We calculated sensitivity (percent of outcomes correctly classified as fallen), specificity (percent of outcomes correctly classified as persisting), and PCC (percent of outcomes correctly classified, a weighted average of sensitivity and specificity). We repeated this procedure 15 times on each model using different seeds to ensure that our results were robust.

For each snag population (i.e., pre-fire snags or new post-fire snags) and predictor set (i.e., pre-fire or post-fire attributes and neighborhood metrics), we used best performance in the lowest performing metric (e.g., specificity or sensitivity) to identify the most predictive collinearity threshold and the most predictive model within that group (Figures A.12 and A.13). We chose this method because there was little variation in PCC values among the models, and we wanted to identify the model that performed best at what the models in each group did worst (Appendix A: Methods: random forest models).

For each of the selected models, we averaged variable importance values across runs with different seeds to determine mean importance of each predictor variable. We report the five most important variables in each model (Tables 2.3 and 2.4) and include complete variable importance results in Table A.7.

Partial dependence plots

For the models selected as "best," we used the partialPlot function in the pdp package (Greenwell, 2018) to visualize the relationships between snag fall and each of the nine most important, continuous predictor variables. We inspected the partial dependence plots and used values from the literature and natural breaks in the data to demarcate threshold values. We subset the snag fall data according to these thresholds and ran the

partialPlot function to depict interactions between snag fall and the three most important post-fire predictor variables. All analyses were conducted in R version 4.0.2 (R Core Team, 2020).

Results

Fall rates of pre-fire snags

In 2009 and 2010, there were 2,282 medium and 436 large snags, together representing 7.2% of total inventoried stems (n_{stems} = 37,546; Figure 2.2; Tables A.1–A.3). During the pre-fire period from 2011 to 2013, recruitment rates (100 × new snags/snags of previous year) of medium and large snags ranged from 9.5% to 21.8% and exceeded fall rates (100 × newly fallen snags/snags of previous year), which ranged from 0.0 to 4.4%. Pre-fire snags were more likely to persist through the fire year if they had a larger DBH and were less decayed. In the fire, 45.7% of small, 17.8% of medium, and no large pre-fire snags of low decay were consumed. Snag fall rate in the fire year was highest for small snags (8.3%) and lower for medium (4.4%) and large (4.8%) snags.

Patterns of pre-fire snag fall during the post-fire period from 2014 to 2018 exceeded pre-fire fall rates and varied by diameter class and decay class (Figure 2.2; Tables A.1–A.3). Small snags had the highest fall rate of the three diameter classes one year after the fire (29.7%), and these rates remained high throughout the study period (23.5–33.3%), meaning that although the number of pre-fire snags still standing was reduced each year, a similar proportion of those snags fell annually. In contrast, the fall rate of medium snags decreased one year after fire (1.5%) and then increased over the next three years, from 7.1% to 25.3% to 40.9%. As the number of medium pre-fire snags decreased during

the post-fire period, a higher proportion of those snags fell each year. Large snags of advanced decay were more likely to fall than less decayed snags, but this difference was not apparent until four years after fire. Fall rates for large snags were low (0.0–2.3%) for the first three years after fire. This changed in 2018, when 12.0–18.2% of large snags of advanced decay fell, compared with only 3.1% of large snags of low decay.

Fall rates of post-fire snags

In the fire year, 15,925 small, 5,472 medium, and 44 large snags were recruited, reflecting fire-year mortality rates of 77.6%, 44.6%, and 3.2% for the three size classes (Figure 2.2; Tables A.4 and A.5). Abundance of small snags remained high for one year after the fire and then decreased when fall rates (12.5–33.2%) far exceeded recruitment rates (0.5–0.7%). Abundance of medium snags increased for two years post-fire, then decreased, but biomass continued to increase through 2017, indicating that, within the medium size class, smaller snags were falling as larger snags were recruited. Abundance of large snags increased substantially three years after the fire and represented 75.3% of the snag biomass in 2018.

Snag fall model comparisons

For the four categories of random forest models (2 snag populations × 2 predictor sets), the most predictive models were associated with higher collinearity thresholds, r = 0.7 and r = 0.5 (Figure 2.3). Among these selected models, median PCC ranged from 68% to 75%. Median sensitivity (i.e., correctly classified fallen) and specificity (i.e., correctly classified persisting) ranged from 57% to 80% (Figure 2.3). Random forest models of pre-fire snags were best at predicting snag fall, the more common outcome in

that population, whereas models of post-fire snags were better at predicting snag persistence, the more common outcome in that population. When the post-fire snag dataset was balanced, models were better at predicting snag fall than snag persistence (Figure A.14).

Models based on post-fire predictors had higher PCC by about 2% than models based on pre-fire predictors (Figure 2.3). PCC increased by about 1% when any type of neighborhood predictor was included. When considering just the "best" model in each panel, no single neighborhood size was optimal. Neighborhood sizes of the "best" models ranged from a 3-m to a 15-m radius.

Important predictors of snag fall

For pre-fire snags, DBH and snag height were the most important predictors of snag fall after fire (Table 2.3, Table A.7, Figures A.19 and A.20). When pre-fire predictor variables were considered, species was the third most important variable, followed by two neighborhood metrics that represented the presence of medium and large trees within 3 m. Among post-fire predictors, bole scorch was the third most important predictor, followed by the neighborhood metric of crown injury to stems within 3 m; snag class was the fifth most important predictor.

For snags created in or after the fire, species and years between fire and tree death were important predictors of snag fall (Table 2.4). When pre-fire variables were considered, size- and decay-class–related snag attributes were not included, and topographic position index, slope, and aspect were more important than pre-fire neighborhood variables (Table A.7). In models based on post-fire predictors, snag attributes were included, and snag height ranked just below species in importance.

DBH was likely important as well but was removed prior to running the model due to high correlation with height (r = 0.87, Table A.7). No neighborhood metrics were among the top five most important predictors for models of newly dead post-fire snags.

Interactions of important variables

Fall rate of subpopulations of pre-fire snags ranged from 0.22 to 0.64 (Figure 2.4). Fall rate was most sensitive to DBH. As DBH increased up to 50 cm, fall rate decreased, then stabilized. Among larger snags (> 50 cm DBH), higher bole scorch (≥ 3.7 m) decreased the probability of falling. Taller snags (> 16 m) were also less likely to fall.

Fall rate of subpopulations of post-fire snags ≥ 10 cm DBH ranged from 0.19 to 0.48 (Figure 2.5). Fall rate decreased as post-fire snag height increased up to 20 m, at which point fall rate stabilized. At all heights, fall rate was higher for trees that died within one year of the fire and lower for trees that died two or more years after the fire. Fall rate was barely higher for *P. lambertiana* compared to *A. concolor*, and this difference was only observed among snags that died two or more years after the fire.

Discussion

This study is the first to report fall rates of pre-fire snags before and after fire and to compare fall rates of pre-fire and newly dead post-fire snags. Fall rates of pre-fire snags increased after low- to moderate-severity fire. By three years after fire, pre-fire snags were more than twice as likely to fall as newly dead post-fire snags (Figure 2.2). These results are consistent with current understanding of how snag size, decay class, and fire interact. For a given size class, pre-fire snags would be more decayed than newly dead snags, making pre-fire snags more likely to fall (Garber et al., 2005; Russell and

Weiskittel, 2012). Pre-fire snags are also more likely to be consumed at the base during fire than fire-killed snags due to lower water content (Campbell et al., 2007) and absent, thinner, or loose bark. Managers should expect low- and moderate-severity fire to reduce populations of large, decayed snags through consumption and accelerated snag fall, decreasing post-fire habitat quality and increasing subsequent fuel loads (Lutz et al., 2020). Although the loss of pre-fire snags during and after fire may be dwarfed by recruitment from delayed mortality of large trees (Tables A.1 and A.4), the new snag recruits will require time to reach the moderate and advanced decay classes that characterize preferred vertebrate habitat (Raphael and White, 1984; Thomas, 1979). Longer-term studies are needed to determine how the different fall rates of pre-existing and newly dead post-fire snags affect the availability of snags of different size and decay classes through time.

Snag attributes

Previous research has shown that snag attributes, topography, and neighborhood metrics can improve predictions of snag fall (Chambers and Mast, 2005; Everett et al., 1999; Grayson et al., 2019; Russell et al., 2006). Our models found that predictor variables in these categories were important, but the order of importance differed between pre-fire and newly dead post-fire snags. Snag attributes—such as species, DBH, height, decay class, and bole scorch height—were better predictors of snag fall than topography, pre-fire spatial neighborhood, and local fire severity.

Species was moderately important for pre-fire snags but was the most important predictor for newly dead post-fire snags (Tables 2.3 and 2.4). For post-fire snags that died 2–4 years after fire, fall rates tended to be slightly higher for *P. lambertiana* than *A.*

concolor (Figure 2.5). This result is consistent with previous snag research showing that *Pinus* spp. fall sooner than *Abies* spp. (Dunn and Bailey, 2012; Morrison and Raphael, 1993; Ritchie et al., 2013), and a species-specific comparison by Grayson et al. (2019), showing that *P. lambertiana* fell sooner than *A. concolor* during the first 10 years after death. The small difference in fall rates between *P. lambertiana* and *A. concolor* that we observed is also supported by a species-specific result from Bagne et al. (2008), who found that *P. lambertiana* and *A. concolor* snags were equally likely to fall one year after prescribed fire.

For pre-fire snags, DBH supplanted species as the most important predictor variable (Figure 2.4). Fall rates for pre-fire snags dropped sharply as DBH increased to 50 cm, but beyond this DBH threshold, fall rates stabilized at lower values (i.e., 0.2–0.4). Because our study took place in an old-growth forest with a substantial population of large-diameter trees, the 50 cm DBH threshold at which fall rates stabilized is meaningful: 392 pre-fire snags (19.5%) had a pre-fire DBH ≥ 50 cm, and 326 pre-fire snags (16.2%) had a post-fire DBH ≥ 50 cm. The low fall rates for pre-fire snags > 50 cm DBH support work by Grayson et al. (2019), who found that post-fire snags ≥ 50 cm DBH were likely to persist for 10 years after death.

Numerous studies of post-fire snags have found that fall rate decreases with larger DBH (Chambers and Mast, 2005; Dahms, 1949; Dunn and Bailey, 2012; Everett et al., 1999; Grayson et al., 2019; Lyon, 1977; Morrison and Raphael, 1993; Ritchie et al., 2013; Russell et al., 2006). This was clearly supported in our study as well, with only 28.2% of medium and large post-fire snags falling compared to 59.5% of small post-fire snags (Figure 2.2). In fact, the difference in fall rates between these two size classes was

greater than the difference between pre-fire and post-fire snags of the same size class—only 51.2% of medium and large pre-fire snags fell within the five-year study period. Despite the obvious influence of DBH on the fall rates of post-fire snags, DBH was not included as a predictor in the final models because it was highly correlated with post-fire snag height (Table A.7).

Snag height was an important predictor for pre-fire and newly dead post-fire snags (Figures 2.4 and 2.5). For both populations, fall rates decreased as height increased, until fall rate stabilized at lower values (i.e., 0.4) for snags taller than 20 m (Figures A.19, A.20, and A.22). These results differ from several studies that found shorter snags were less likely to fall (Chambers and Mast, 2005; Dahms, 1949; Morrison and Raphael, 1993; Russell et al., 2006). In the case of Dahms (1949) and Morrison and Raphael (1993), this difference could be attributed to the 11- to 15-year period between when the fire occurred and when snag monitoring began. However, Chambers and Mast (2005) and Russell et al. (2006) conducted studies within a similar time frame to ours. Another explanation could be the different species studied (only Morrison and Raphael [1993] included *A. concolor*) and the apparent tendency of the species in our study to break below 1.37 m (Grayson et al. 2019). Grayson et al. (2019) included both *A. concolor* and *P. lambertiana* and, similar to our result, found that taller snags were less likely to fall by 10 years after death.

Years between fire and death was an important predictor of snag fall for newly dead post-fire snags. Trees that survived two or more years after fire had a lower chance of falling within five years of the fire (Figure 2.5). This result is explained by the higher mortality rates for larger-diameter trees three and four years after fire (Jeronimo et al., 2020); these snags would have been less likely to fall because of their larger DBH and

lower degree of decay. However, our results differ from Grayson et al. (2019), who show that years between fire and death did not affect snag persistence for *A. concolor* and *P. lambertiana*. We attribute this inconsistency to the different time scales of our studies. Our analysis was limited to five years post-fire, so snags that died three years after the fire only had two years in which to fall, whereas Grayson et al. (2019) monitored snags for 10 years after death.

Bole scorch height was an important predictor of snag fall for pre-fire and post-fire snags. Fall rates were generally lower for pre-fire snags with bole scorch ≥ 3.7 m tall, if DBH was > 50 cm. Charring of pre-fire snags likely retards colonization by decay fungi, and this apparently increased snag persistence more than consumption at the snag base reduced it. A similar relationship between bole scorch height and snag fall held true for newly dead post-fire snags. Fall rate decreased as bole scorch increased to the height of 7 m (Figure A.22). Higher bole scorch on newly killed trees may reduce palatability for bark beetles (e.g., *Dendroctonus ponderosae*, *Scolytus ventralis*), potentially slowing the entrance of decay fungi carried by colonizing beetles and cavity excavators (Farris et al., 2004; Harrington, 1996). When removing bark on new mortalities in the field, we typically found galleries beneath uncharred bark, but not under charred bark, suggesting that stems with extensive bole scorch provide less substrate for insect and subsequent fungal infestation.

Topographic variables were more important for predicting fall of post-fire snags than pre-fire snags, but the magnitude of the effect was low (Table 2.5, Table A.7). For post-fire snags, fall rates were slightly higher on convex terrain, perhaps due to increased wind exposure (Figures A.21 and A.22). These results differ from a study by Everett et al.

(1999), which found that snags were less likely to fall on convex terrain. Few other studies have found relationships between topographic variables and snag fall. Russell et al. (2006) considered slope and aspect as potential predictors of snag fall, but neither variable was included in the best models. Similarly, Dunn and Bailey (2012) found no relationship between slope or aspect and snag fall.

Neighborhood variables

Neighborhood metrics barely improved predictions of snag fall, similar to other studies that have found no relationship between neighborhood and snag fall (Dunn and Bailey, 2012; Grayson et al., 2019; Ritchie et al., 2013). We had expected higher local fire severity to increase fall rates due to greater consumption at the snag base. Instead we found that charring from bole scorch made snags less likely to fall and that including neighborhood metrics only improved model PCCs by 1% (Figures 2.3 and 2.4). Although the magnitude of the effect was low, pre-fire snags were slightly less likely to fall (< 8% change) if medium or large live trees were present within 3 m (Table 2.4, Figure A.19), consistent with results from Chambers and Mast (2005) and Russell et al. (2006). The presence of larger neighbors might extend snag longevity by protecting the focal snag from windthrow. Our prevailing message, however, is that the relationship between neighborhood and snag fall was weak. We assessed the importance of neighborhood more directly than any prior study because we used spatially explicit measurements—not remote sensing (Russell et al., 2006), stand-level treatments (Ritchie et al., 2013), or non-spatially explicit stand metrics (Chambers and Mast, 2005; Dunn and Bailey, 2012; Grayson et al., 2019). The trivial 1% improvement in PCC associated with neighborhood

predictors makes clear that managers should focus on species, diameter, height, bole scorch height, and decay class rather than neighborhood if the goal is to predict snag fall.

Conclusions

Predicting how long snags will remain standing after fire is important for managing habitat, understanding chemical cycling in forests, and modeling forest succession and fuels. In our study, pre-fire snags were at least twice as likely to fall as new snags within 3–5 years after fire. For pre-existing snags, diameter, height, and bole scorch height were better predictors of snag fall after fire than spatial neighborhood or local fire severity metrics. Pre-existing snags were most likely to persist five years after fire if they were > 50 cm in diameter, > 20 m tall, and charred on the bole above 3.7 m. When anticipating habitat availability and fuels, managers should expect fall rates of pre-existing snags to initially exceed fall rates of new snags.

References

Allen, C.D., Macalady, A.K., Chenchouni, H., Bachelet, D., McDowell, N., Vennetier, M., Kitzberger, T., Rigling, A., Breshears, D.D., Hogg, E.H. (Ted), Gonzalez, P., Fensham, R., Zhang, Z., Castro, J., Demidova, N., Lim, J.H., Allard, G., Running, S.W., Semerci, A., Cobb, N., 2010. A global overview of drought and heat-induced tree mortality reveals emerging climate change risks for forests. For. Ecol. Manage. 259, 660–684. https://doi.org/10.1016/j.foreco.2009.09.001

Bagne, K.E., Purcell, K.L., Rotenberry, J.T., 2008. Prescribed fire, snag population dynamics, and avian nest site selection. For. Ecol. Manage. 255, 99–105. https://doi.org/10.1016/j.foreco.2007.08.024

Barth, M.A.F., Larson, A.J., Lutz, J.A., 2015. A forest reconstruction model to assess changes to Sierra Nevada mixed-conifer forest during the fire suppression era. For. Ecol. Manage. 354, 104–118. https://doi.org/10.1016/j.foreco.2015.06.030

Biging, G.S., 1984. Taper equations for second-growth mixed conifers of northern California. For. Sci. 30, 1103–1117.

Blomdahl, E.M., Kolden, C.A., Meddens, A.J.H., Lutz, J.A., 2019. The importance of small fire refugia in the central Sierra Nevada, California, USA. For. Ecol. Manage. 432, 1041–1052. https://doi.org/10.1016/j.foreco.2018.10.038

Bull, E.L., Heater, T.W., 2000. Resting and denning sites of American martens in Northeastern Oregon. Northwest Sci. 74, 179–185. https://doi.org/http://hdl.handle.net/2376/1018

Butts, S.R., McComb, W.C., 2000. Associations of forest-floor vertebrates with coarse woody debris in managed forests of western Oregon. J. Wildl. Manage. 64, 95–104.

Campbell, J., Donato, D., Azuma, D., Law, B., 2007. Pyrogenic carbon emission from a large wildfire in Oregon, United States. J. Geophys. Res. 112, 1–11.

Cansler, C.A., Swanson, M.E., Furniss, T.J., Larson, A.J., Lutz, J.A., 2019. Fuel dynamics after reintroduced fire in an old-growth Sierra Nevada mixed-conifer forest. Fire Ecol. 15. https://doi.org/10.1186/s42408-019-0035-y

Chambers, C.L., Mast, J.N., 2005. Ponderosa pine snag dynamics and cavity excavation following wildfire in northern Arizona. For. Ecol. Manage. 216, 227–240. https://doi.org/10.1016/j.foreco.2005.05.033

Conner, R.N., Saenz, D., Conner, R.N., Saenz, D., 2005. The longevity of large pine snags in eastern Texas. Wildl. Soc. Bull. 33, 700–705.

Cousins, S.J.M., Battles, J.J., Sanders, J.E., York, R.A., 2015. Decay patterns and carbon density of standing dead trees in California mixed conifer forests. For. Ecol. Manage. 353, 136–147. https://doi.org/10.1016/j.foreco.2015.05.030

Cutler, R.D., Edwards, T.H., Beard, K.H., Cutler, A., Hess, K.T., Gibson, J., Lawler, J.J., 2007. Random forests for classification in ecology. Ecology 88, 2783–2792. https://doi.org/10.1890/07-0539.1

Dahms, W., 1949. How long do ponderosa pine snags stand? Portland, OR.

Das, A.J., Stephenson, N.L., Davis, K.P., 2016. Why do trees die? Characterizing the drivers of background tree mortality. Ecology 97, 2616–2627. https://doi.org/10.1002/ecy.1497

Davies, S.J., Abiem, I., Abu Salim, K., Aguilar, S., Allen, D., Alonso, A., Anderson-Teixeira, K., Andrade, A., Arellano, G., Ashton, P.S., Baker, P.J., Baker, M.E., Baltzer, J.L., Basset, Y., Bissiengou, P., Bohlman, S., Bourg, N.A., Brockelman, W.Y., Bunyavejchewin, S., Burslem, D.F.R.P., Cao, M., Cárdenas, D., Chang, L.W., Chang-Yang, C.H., Chao, K.J., Chao, W.C., Chapman, H., Chen, Y.Y., Chisholm, R.A., Chu, C., Chuyong, G., Clay, K., Comita, L.S., Condit, R., Cordell, S., Dattaraja, H.S., de Oliveira, A.A., den Ouden, J., Detto, M., Dick, C., Du, X.,

Duque, Á., Ediriweera, S., Ellis, E.C., Obiang, N.L.E., Esufali, S., Ewango, C.E.N., Fernando, E.S., Filip, J., Fischer, G.A., Foster, R., Giambelluca, T., Giardina, C., Gilbert, G.S., Gonzalez-Akre, E., Gunatilleke, I.A.U.N., Gunatilleke, C.V.S., Hao, Z., Hau, B.C.H., He, F., Ni, H., Howe, R.W., Hubbell, S.P., Huth, A., Inman-Narahari, F., Itoh, A., Janík, D., Jansen, P.A., Jiang, M., Johnson, D.J., Jones, F.A., Kanzaki, M., Kenfack, D., Kiratiprayoon, S., Král, K., Krizel, L., Lao, S., Larson, A.J., Li, Y., Li, X., Litton, C.M., Liu, Y., Liu, S., Lum, S.K.Y., Luskin, M.S., Lutz, J.A., Luu, H.T., Ma, K., Makana, J.R., Malhi, Y., Martin, A., McCarthy, C., McMahon, S.M., McShea, W.J., Memiaghe, H., Mi, X., Mitre, D., Mohamad, M., Monks, L., Muller-Landau, H.C., Musili, P.M., Myers, J.A., Nathalang, A., Ngo, K.M., Norden, N., Novotny, V., O'Brien, M.J., Orwig, D., Ostertag, R., Papathanassiou, K., Parker, G.G., Pérez, R., Perfecto, I., Phillips, R.P., Pongpattananurak, N., Pretzsch, H., Ren, H., Reynolds, G., Rodriguez, L.J., Russo, S.E., Sack, L., Sang, W., Shue, J., Singh, A., Song, G.Z.M., Sukumar, R., Sun, I.F., Suresh, H.S., Swenson, N.G., Tan, S., Thomas, S.C., Thomas, D., Thompson, J., Turner, B.L., Uowolo, A., Uriarte, M., Valencia, R., Vandermeer, J., Vicentini, A., Visser, M., Vrska, T., Wang, Xugao, Wang, Xihua, Weiblen, G.D., Whitfeld, T.J.S., Wolf, A., Wright, S.J., Xu, H., Yao, T.L., Yap, S.L., Ye, W., Yu, M., Zhang, M., Zhu, D., Zhu, L., Zimmerman, J.K., Zuleta, D., 2021. ForestGEO: Understanding forest diversity and dynamics through a global observatory network. Biol. Conserv. 253. https://doi.org/10.1016/j.biocon.2020.108907

Dunn, C.J., Bailey, J.D., 2012. Temporal dynamics and decay of coarse wood in early seral habitats of dry-mixed conifer forests in Oregon's Eastern Cascades. For. Ecol. Manage. 276, 71–81. https://doi.org/10.1016/j.foreco.2012.03.013

Everett, R., Lehmkuhl, J., Schellhaas, R., Ohlson, P., Keenum, D., Riesterer, H., Spurbeck, D., 1999. Snag dynamics in a chronosequence of 26 wildfires on the east slope of the Cascade Range in Washington State, USA. Int. J. Wildl. Fire 9, 223–234. https://doi.org/10.1071/wf00011

Farris, K.L., Huss, M.J., Zack, S., 2004. The role of foraging woodpeckers in the decomposition of ponderosa pine snags. Condor 106, 50–59.

Franklin, J.F., Lindenmayer, D., MacMahon, J.A., Mckee, A., Magnuson, J., Perry, D.A., Waide, R., Foster, D., 2000. Threads of continuity. Conserv. Biol. Pract. 1, 8–16. https://doi.org/10.1111/j.1526-4629.2000.tb00155.x

Furniss, T.J., Larson, A.J., Kane, V.R., Lutz, J.A., 2020. Wildfire and drought moderate the spatial elements of tree mortality. Ecosphere 11. https://doi.org/10.1002/ecs2.3214

Gabrielson, A.T., Larson, A.J., Lutz, J.A., Reardon, J.J., 2012. Biomass and burning characteristics of sugar pine cones. Fire Ecol. 8, 58–70. https://doi.org/10.4996/fireecology.0803058

Gaines, E.M., Kallander, H.R., Wagner, J.A., 1958. Controlled burning in southwestern ponderosa pine: results from the Ble Mountain Plots, Fort Apache Indian Reservation. J. For. 56, 323–327.

Ganey, J.L., Iniguez, J.M., Vojta, S.C., Iniguez, A.R., 2021. Twenty years of drought - mediated change in snag populations in mixed - conifer and ponderosa pine forests in Northern Arizona.

Garber, S.M., Brown, J.P., Wilson, D.S., Maguire, D. a, Heath, L.S., 2005. Snag longevity under alternative silvicultural regimes in mixed-species forests of central Maine. Can. J. For. Res. 35, 787–796. https://doi.org/10.1139/x05-021

Grayson, L.M., Cluck, D.R., Hood, S.M., 2019. Persistence of fire-killed conifer snags in California, USA. Fire Ecol. 15, 1–14. https://doi.org/10.1186/s42408-018-0007-7

Greenwell, B., 2018. pdp: partial dependence plots. CRAN Repos. version 0.7.0.

Harmon, M.E., Franklin, J.F., Swanson, F.J., Sollins, P., Gregory, S. V., Lattin, J.D., Anderson, N.H., Cline, S.P., Aumen, N.G., Sedell, J.R., Lienkaemper, G.W., Cromack, K.J., Cummins, K.W., 1986. Ecology of coarse woody debris in temperate ecosystems. Adv. Ecol. Res. 15, 133–302.

Harmon, M.E., Woodall, C.W., Fasth, B., Sexton, J., 2008. Woody detritus density and density reduction factors for tree species in the United States: a synthesis. USDA Gen. Tech. Rep. NRS-29. USDA For. Serv. North. Res. Stn. 84.

Harrington, M.G., 1996. Fall rates of prescribed fire-killed ponderosa pine. Res. Pap. INT-RP-489 Ogden, UT:, 1–7. https://doi.org/10.4135/9781483340333.n89

Hijmans, R.J., 2020. Raster: geographic data analysis and modeling. CRAN Repos. version 3.3-13.

Innes, J.C., North, M.P., Williamson, N., 2006. Effect of thinning and prescribed fire restoration treatments on woody debris and snag dynamics in a Sierran old-growth, mixed-conifer forest. Can. J. For. Res. 36, 3183–3193. https://doi.org/10.1139/X06-184

Jeronimo, S.M.A., Lutz, J.A., R. Kane, V., Larson, A.J., Franklin, J.F., 2020. Burn weather and three-dimensional fuel structure determine post-fire tree mortality. Landsc. Ecol. 35, 859–878. https://doi.org/10.1007/s10980-020-00983-0

Keen, F.P., 1929. How soon do yellow pine snags fall? J. For. 27, 735–737.

Knapp, E.E., 2015. Long-term dead wood changes in a Sierra Nevada mixed conifer forest: Habitat and fire hazard implications. For. Ecol. Manage. 339, 87–95. https://doi.org/10.1016/j.foreco.2014.12.008

Kursa, M.B., Rudnicki, W.R., 2020. Boruta: wrapper algorithm for all relevant feature selection. CRAN Repos. version 7.00.

Kursa, M.B., Rudnicki, W.R., 2010. Feature selection with the boruta package. J. Stat. Softw. 36, 1–13. https://doi.org/10.18637/jss.v036.i11

Liaw, A., Wiener, M., 2018. Briemain and Cutler's random forests for classification and regression. version 4.6-14. https://doi.org/10.1023/A

Lutz, J.A., 2015. The evolution of long-term data for forestry: large temperate research plots in an era of global change. Northwest Sci. 89, 255–269. https://doi.org/10.3955/046.089.0306

Lutz, J.A., Furniss, T.J., Germain, S.J., Becker, K.M.L., Blomdahl, E.M., Jeronimo, S.M.A., Cansler, C.A., Freund, J.A., Swanson, M.E., Larson, A.J., 2017a. Shrub communities, spatial patterns, and shrub-mediated tree mortality following reintroduced fire in Yosemite National Park, California, USA. Fire Ecol. 13, 104–126. https://doi.org/10.4996/fireecology.1301ppp

Lutz, J.A., Furniss, T.J., Johnson, D.J., Davies, S.J., Allen, D., Alonso, A., Anderson-Teixeira, K.J., Andrade, A., Baltzer, J., Becker, K.M.L., Blomdahl, E.M., Bourg, N.A., Bunyavejchewin, S., Burslem, D.F.R.P., Cansler, C.A., Cao, K., Cao, M., Cárdenas, D., Chang, L.W., Chao, K.J., Chao, W.C., Chiang, J.M., Chu, C., Chuyong, G.B., Clay, K., Condit, R., Cordell, S., Dattaraja, H.S., Duque, A., Ewango, C.E.N., Fischer, G.A., Fletcher, C., Freund, J.A., Giardina, C., Germain, S.J., Gilbert, G.S., Hao, Z., Hart, T., Hau, B.C.H., He, F., Hector, A., Howe, R.W., Hsieh, C.F., Hu, Y.H., Hubbell, S.P., Inman-Narahari, F.M., Itoh, A., Janík, D., Kassim, A.R., Kenfack, D., Korte, L., Král, K., Larson, A.J., Li, Y. De, Lin, Y., Liu, S., Lum, S., Ma, K., Makana, J.R., Malhi, Y., McMahon, S.M., McShea, W.J., Memiaghe, H.R., Mi, X., Morecroft, M., Musili, P.M., Myers, J.A., Novotny, V., de Oliveira, A., Ong, P., Orwig, D.A., Ostertag, R., Parker, G.G., Patankar, R., Phillips, R.P., Reynolds, G., Sack, L., Song, G.Z.M., Su, S.H., Sukumar, R., Sun, I.F., Suresh, H.S., Swanson, M.E., Tan, S., Thomas, D.W., Thompson, J., Uriarte, M., Valencia, R., Vicentini, A., Vrška, T., Wang, X., Weiblen, G.D., Wolf, A., Wu, S.H., Xu, H., Yamakura, T., Yap, S., Zimmerman, J.K., 2018. Global importance of large-diameter trees. Glob. Ecol. Biogeogr. 27, 849–864. https://doi.org/10.1111/geb.12747

Lutz, J.A., Larson, A.J., Swanson, M.E., Freund, J.A., 2012. Ecological importance of large-diameter trees in a temperate mixed-conifer forest. PLoS One 7, e36131. https://doi.org/10.1371/journal.pone.0036131

Lutz, J.A., Matchett, J.R., Tarnay, L.W., Smith, D.F., Becker, K.M.L., Furniss, T.J., Brooks, M.L., 2017b. Fire and the distribution and uncertainty of carbon sequestered as aboveground tree biomass in Yosemite and Sequoia & Kings Canyon National

Parks. Land 6, 1–24. https://doi.org/10.3390/land6010010

Lutz, J.A., Schwindt, K.A., Furniss, T.J., Freund, J.A., Swanson, M.E., Hogan, K.I., Kenagy, G.E., Larson, A.J., 2014. Community composition and allometry of *Leucothoe davisiae*, *Cornus sericea*, and *Chrysolepis sempervirens*. Can. J. For. Res. 44, 1–7. https://doi.org/10.1139/cjfr-2013-0524

Lutz, J.A., Struckman, S., Furniss, T.J., Birch, J.D., Yocom, L.L., McAvoy, D.J., 2021. Large-diameter trees, snags, and deadwood in southern Utah, USA. Ecol. Process. 10. https://doi.org/10.1186/s13717-020-00275-0

Lutz, J.A., Struckman, S., Furniss, T.J., Cansler, C.A., Germain, S.J., Yocom, L.L., McAvoy, D.J., Kolden, C.A., Smith, A.M.S., Swanson, M.E., Larson, A.J., 2020. Large-diameter trees dominate snag and surface biomass following reintroduced fire. Ecol. Process. 9. https://doi.org/10.1186/s13717-020-00243-8

Lyon, L.J., 1977. Attrition of lodgepole pine snags on the Sleeping Child Burn, Montana, USDA Forest Service Research Note INT-219. Ogden, UT.

Maser, C., Trappe, J., 1984. The seen and unseen world of the fallen tree, USDA Forest Service, Pacific Northwest Forest and Range Experiment Station, General Technical Report PNW-164. https://doi.org/10.1017/CBO9781107415324.004

Meyer, M.D., Kelt, D.A., North, M.P., 2005. Nest trees of Northern flying squirrels in the Sierra Nevada. J. Mammal. 86, 275–280. https://doi.org/10.1644/BEH-110.1

Michel, L.A., Peppe, D.J., Lutz, J.A., Driese, S.G., Dunsworth, H.M., Harcourt-Smith, W.E.H., Horner, W.H., Lehmann, T., Nightingale, S., McNulty, K.P., 2014. Remnants of an ancient forest provide ecological context for Early Miocene fossil apes. Nat. Commun. 5, 1–9. https://doi.org/10.1038/ncomms4236

Mitchell, R.G., Preisler, H.K., 1998. Fall rate of lodgepole pine killed by the mountain pine beetle in central Oregon. West. J. Appl. For. 13, 23–26. https://doi.org/10.1093/wjaf/13.1.23

Monsanto, P.G., Agee, J.K., 2008. Long-term post-wildfire dynamics of coarse woody debris after salvage logging and implications for soil heating in dry forests of the eastern Cascades, Washington. For. Ecol. Manage. 255, 3952–3961. https://doi.org/10.1016/j.foreco.2008.03.048

Morrison, M.L., Raphael, M.G., 1993. Modeling the Dynamics of Snags. Ecol. Appl. 3, 322–330.

Parks, S.A., Abatzoglou, J.T., 2020. Warmer and drier fire seasons contribute to increases in area burned at high severity in western US forests from 1985 to 2017. Geophys. Res. Lett. 47, 1–10. https://doi.org/10.1029/2020GL089858

PRISM Climate Group, 2016. PRISM 800-m Climate Normals (1981-2010).

R Core Team, 2020. R: a language and environment for statistical computing.

Rabe, M.J., Morrell, T.E., Green, H., deVos Jr., J.C., Miller, C.R., 1998. Characteristics of ponderosa pine snag roosts used by reproductive bats in northern Arizona. J. Wildl. Manage. 62, 612–621. https://doi.org/10.2307/3802337

Raphael, M.G., White, M., 1984. Use of snags by cavity-nesting birds in the Sierra Nevada. Wildl. Monogr. 86, 3–66.

Ritchie, M.W., Knapp, E.E., Skinner, C.N., 2013. Snag longevity and surface fuel accumulation following post-fire logging in a ponderosa pine dominated forest. For. Ecol. Manage. 287, 113–122. https://doi.org/10.1016/j.foreco.2012.09.001

Runkle, J.R., 2013. Thirty-two years of change in an old-growth Ohio beech-maple forest. Ecology 94, 1165–1175. https://doi.org/10.1890/11-2199.1

Russell, M.B., Weiskittel, a R., 2012. Assessing and modeling snag survival and decay dynamics for the primary species in the Acadian forest of Maine, USA. For. Ecol. Manage. 284, 230–240. https://doi.org/http://dx.doi.org/10.1016/j.foreco.2012.08.004

Russell, R.E., Saab, V. a., Dudley, J.G., Rotella, J.J., 2006. Snag longevity in relation to wildfire and postfire salvage logging. For. Ecol. Manage. 232, 179–187. https://doi.org/10.1016/j.foreco.2006.05.068

Scholl, A.E., Taylor, A.H., 2010. Fire regimes, forest change, and self-organization in an old-growth mixed-conifer forest, Yosemite National Park, USA. Ecol. Appl. 20, 362–380. https://doi.org/10.1890/08-2324.1

Stavros, N.E., Tane, Z., Kane, V.R., Veraverbeke, S., Mcgaughey, R.J., Lutz, J.A., Ramirez, C., Schimel, D., 2016. Unprecedented remote sensing data over King and Rim megafires in the Sierra Nevada Mountains of California. Ecology 97, 3334. https://doi.org/10.1002/ecy.1577

Thomas, J.W., 1979. Wildlife habitats in managed forests: the Blue Mountains of Oregon and Washington, Agriculture Handbook No. 553. Washington, D.C., USA. https://doi.org/10.2307/3898589

Thomas, S.C., Martin, A.R., 2012. Carbon content of tree tissues: a synthesis. Forests 3, 332–352. https://doi.org/10.3390/f3020332

Ucitel, D., Christian, D.P., Graham, J.M., 2003. Vole use of coarse woody debris and implications for habitat and fuel management. J. Wildl. Manage. 67, 65–72.

van Mantgem, P.J., Stephenson, N.L., Byrne, J.C., Daniels, L.D., Franklin, J.F., Fulé, P.Z., Harmon, M.E., Larson, A.J., Smith, J.M., Taylor, A.H., Veblen, T.T., 2009. Widespread increase of tree mortality rates in the western United States. Science (80-.). 323, 521–524. https://doi.org/10.1126/science.1165000

van Wagtendonk, J.W., Lutz, J.A., 2007. Fire regime attributes of wildland fires in Yosemite National Park, USA. Fire Ecol. 3, 34–52. https://doi.org/10.4996/fireecology.0302034

van Wagtendonk, J.W., Moore, P.E., Yee, J.L., Lutz, J.A., 2020. The distribution of woody species in relation to climate and fire in Yosemite National Park, California, USA. Fire Ecol. 16. https://doi.org/10.1186/s42408-020-00079-9

Varner, J.M., Hood, S.M., Aubrey, D.P., Yedinak, K., Hiers, J.K., Jolly, W.M., Shearman, T.M., McDaniel, J.K., O'Brien, J.J., Rowell, E.M., 2021. Tree crown injury from wildland fires: causes, measurement and ecological and physiological consequences. New Phytol. 231, 1676–1685. https://doi.org/10.1111/nph.17539

Wensel, L.C., Krumland, B., 1983. Volume and taper relationships for redwood, Douglas fir, and other conifers in California's north coast. Division of Agricultural Sciences Bulletin 1907, University of California.

Wensel, L.C., Olson, C.M., 1995. Tree taper model volume equations. Hilgardia 62, 67.

Zeibig-Kichas, N.E., Ardis, C.W., Berrill, J.-P., King, J.P., 2016. Bark thickness equations for mixed-conifer forest type in Klamath and Sierra Nevada Mountains of California. Int. J. For. Res. 2016, 1–10. https://doi.org/10.1155/2016/1864039

Tables

Table 2.1. Abundance, density, and basal area of five species of snags in the Yosemite Forest Dynamics Plot. Pre-fire snags include snags inventoried at plot establishment in 2009 and 2010 and trees that died after plot establishment and before the fire in September of 2013. Post-fire snags include trees that died in or up to five years after the fire (i.e., 2014–2018).

Snag population	Snag abundance	Density (snags ha^{-1})	Basal area (m^2 ha^{-1})
Pre-fire snags DBH ≥ 10 cm			
Abies concolor	1,467	57.3	7.242
Pinus lambertiana	399	15.6	7.180
Quercus kelloggii	108	4.2	0.144
Calocedrus decurrens	36	1.4	0.465
Cornus nuttallii	3	0.1	0.002
Total	2,013	78.6	15.033
Post-fire snags DBH ≥ 10 cm			
Abies concolor	6,202	242.3	11.476
Pinus lambertiana	1,162	45.4	11.462
Quercus kelloggii	387	15.1	0.502
Calocedrus decurrens	282	11	0.907
Cornus nuttallii	189	7.4	0.100
Total	8,222	321.2	24.447
Post-fire snags 1 ≤ DBH < 10 cm			
Abies concolor	10,759	420.3	0.996
Pinus lambertiana	1,777	69.4	0.143
Quercus kelloggii	1,411	55.1	0.073
Calocedrus decurrens	601	23.5	0.053
Cornus nuttallii	232	9.1	0.020
Total	14,780	577.4	1.285

Table 2.2. Descriptions of 14 sets of predictor variables for binary random forest models of post-fire snag fall for pre-fire and newly dead post-fire snag populations. Each row represents a set of predictor variables. See Table A.6 for descriptions of the variables in each predictor variable category. [†]Models of the post-fire snag population did not include pre-fire snag attributes. [§]The model based just on fixed snag attributes was not included in the analysis.

| | | Categories of predictors in each model | | | | | | | Scale | | | | |
| | | Snag attributes | | | Snag neighborhood metrics | | | | Neighborhood annuli (m) | | | | |
Predictor set	Fixed	Pre-fire	Post-fire	Pre-fire isolation	Pre-fire annuli	Post-fire fixed	Post-fire isolation	Post-fire annuli	0–3	3–6	6–9	9–12	12–15
Post-fire 0–15 m	×		×			×		×	×	×	×	×	×
0–12 m	×		×			×		×	×	×	×	×	
0–9 m	×		×			×		×	×	×	×		
0–6 m	×		×			×		×	×	×			
0–3 m	×		×			×		×	×				
Isolation	×		×			×	×						
Attributes	×		×										
Pre-fire 0–15 m	×	×[†]			×				×	×	×	×	×
0–12 m	×	×[†]			×				×	×	×	×	
0–9 m	×	×[†]			×				×	×	×		
0–6 m	×	×[†]			×				×	×			
0–3 m	×	×[†]			×				×				
Isolation	×	×[†]		×									
Attributes	×	×[†§]											

Table 2.3. Mean variable importance (MI) across 15 model runs for the five most important variables in the most predictive models of the post-fire fall of pre-fire snags ≥ 10 cm DBH. **Snag attributes** are in bold blue text. Neighborhood attributes are in plain text. Model letters correspond to Figure 2.3.

Predictor set	Population: pre-fire medium and large snags	
	Variable	Mean
	Model A: Neighborhood: 0–3 m Collinearity threshold: r = 0.7	
Post-fire	**Post-fire DBH**	67.1
	Post-fire snag height	38.1
	Bole scorch	21.2
	Distance-weighted crown injury in 0–3 m circle	14.2
	Post-fire decay class	14.0
	Model B Neighborhood: 0–15 m Collinearity threshold: r = 0.7	
Pre-fire	**Pre-fire DBH**	64.4
	Pre-fire snag height	27.5
	Species	10.8
	Pre-fire density of live trees ≥ 28 cm DBH in 0–3 m	10.3
	Pre-fire basal area of live trees in 0–3 m circle	8.8

Table 2.4. Mean variable importance (MI) across 15 model runs for the five most important variables in the most predictive models of the post-fire fall of newly dead post-fire snags ≥ 10 cm DBH. **Snag attributes** are in bold blue text. Model letters correspond to Figure 2.3.

Predictor set	Snag population: post-fire DBH ≥ 10 cm	
	Variable	Mean importance
	Model C: Neighborhood: 0–6 m Collinearity threshold: r =	
Post-fire	**Species**	61.5
	Post-fire snag height	55.7
	Years between fire and death	32.0
	Bole scorch	27.9
	Topographic position	23.6
	Model D: Neighborhood: 0–3 m Collinearity threshold: r =	
Pre-fire	**Species**	81.6
	Years between fire and death	58.3
	Topographic position	46.6
	Slope	41.1
	Aspect	38.7

Figures
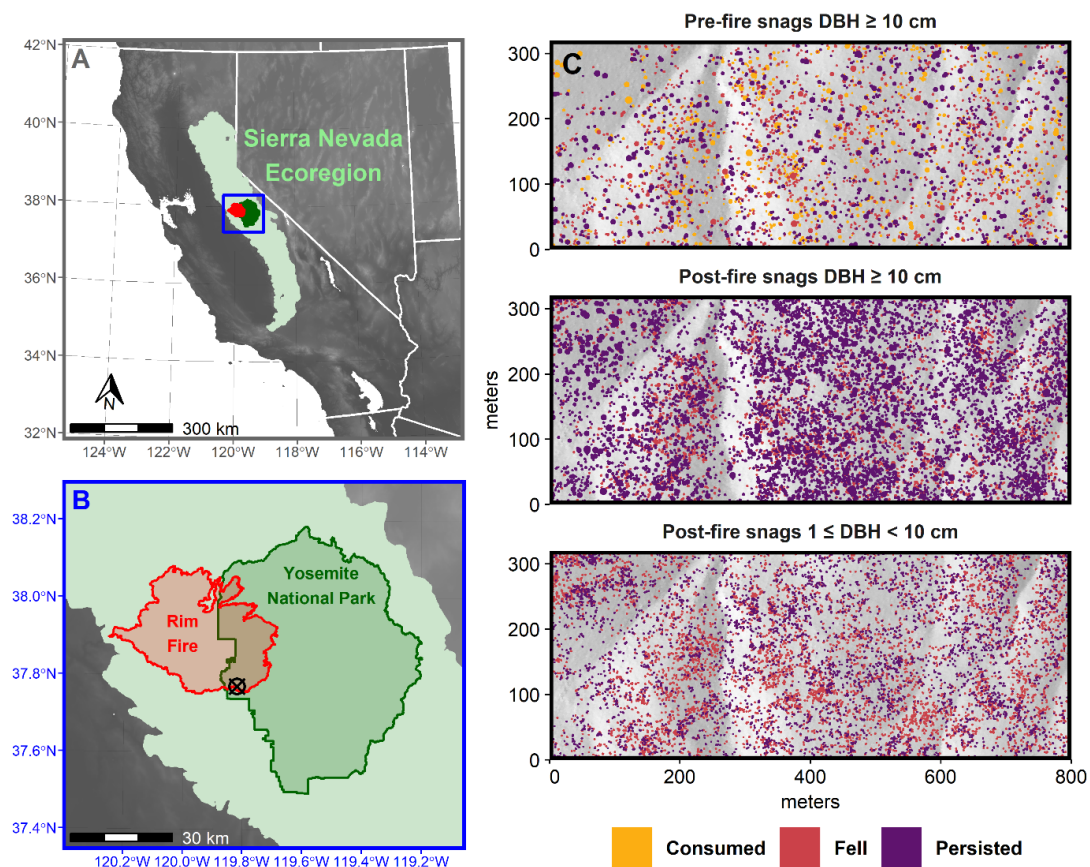
Figure 2.1. The Yosemite Forest Dynamics Plot (YFDP) is a 25.6-ha permanent study area in an old-growth *Abies concolor–Pinus lambertiana* forest in Yosemite National Park in the central Sierra Nevada, California, USA. The YFDP was installed in 2009 and 2010 and burned at low to moderate severity in the 2013 Rim Fire. Stems maps (C) show snag outcomes in 2018 for snags that existed before the fire (pre-fire) and snags that were created in or after the fire (post-fire). Stem diameters appear four times larger than their measured size. Only the top panel includes consumed snags because trees that were consumed in the fire never became snags.
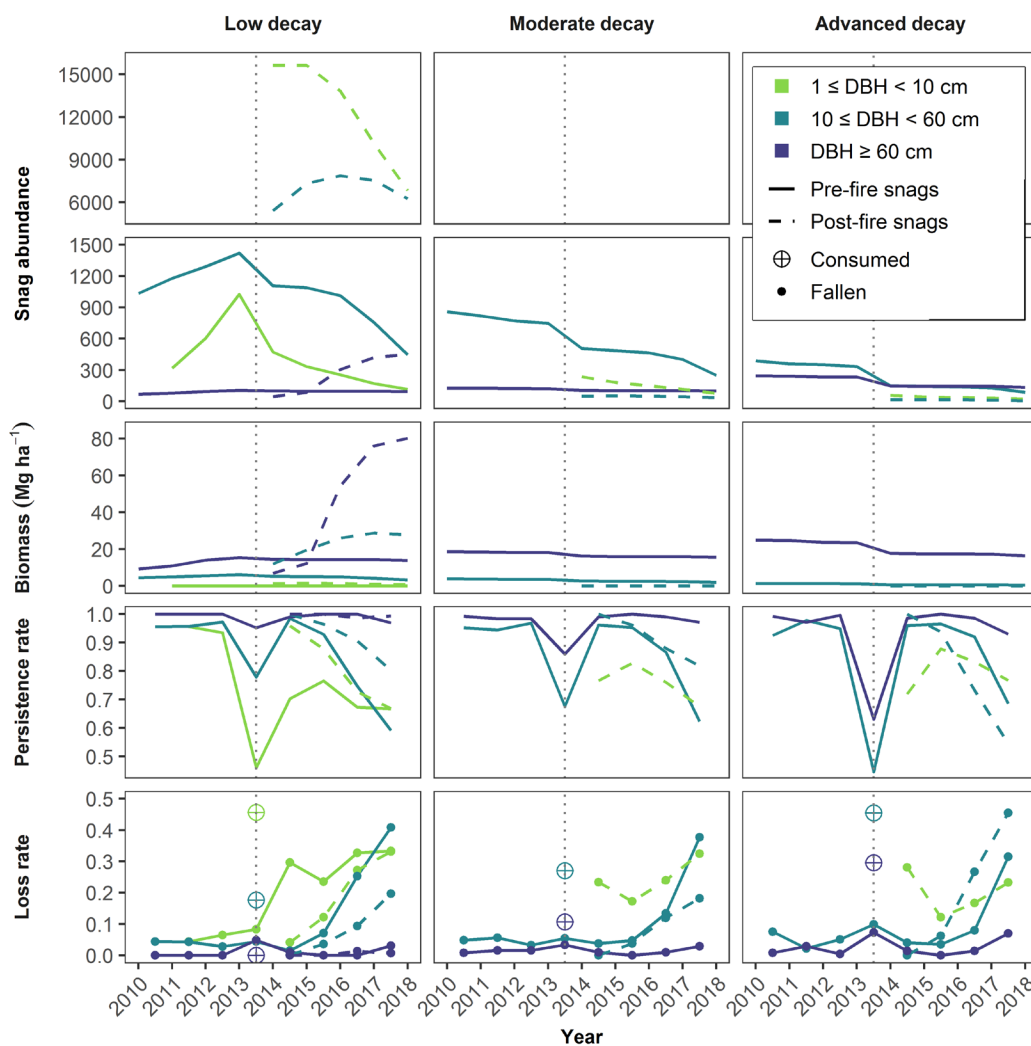
Figure 2.2. Snag dynamics in the Yosemite Forest Dynamics Plot from 2011 to 2018. Note the different y-axis scales for snag abundance. Snag persistence and loss rates were calculated as annual changes in the snag population between summer field seasons. The vertical dotted line represents the Rim Fire in the fall of 2013. In the fire year, snag loss is split into snag consumption and snag fall. All snags $1 \leq DBH < 10$ cm died after 2010. Low Decay: decay class 1; Moderate Decay: decay class 2 or 3; Advanced Decay: decay class 4 or 5.
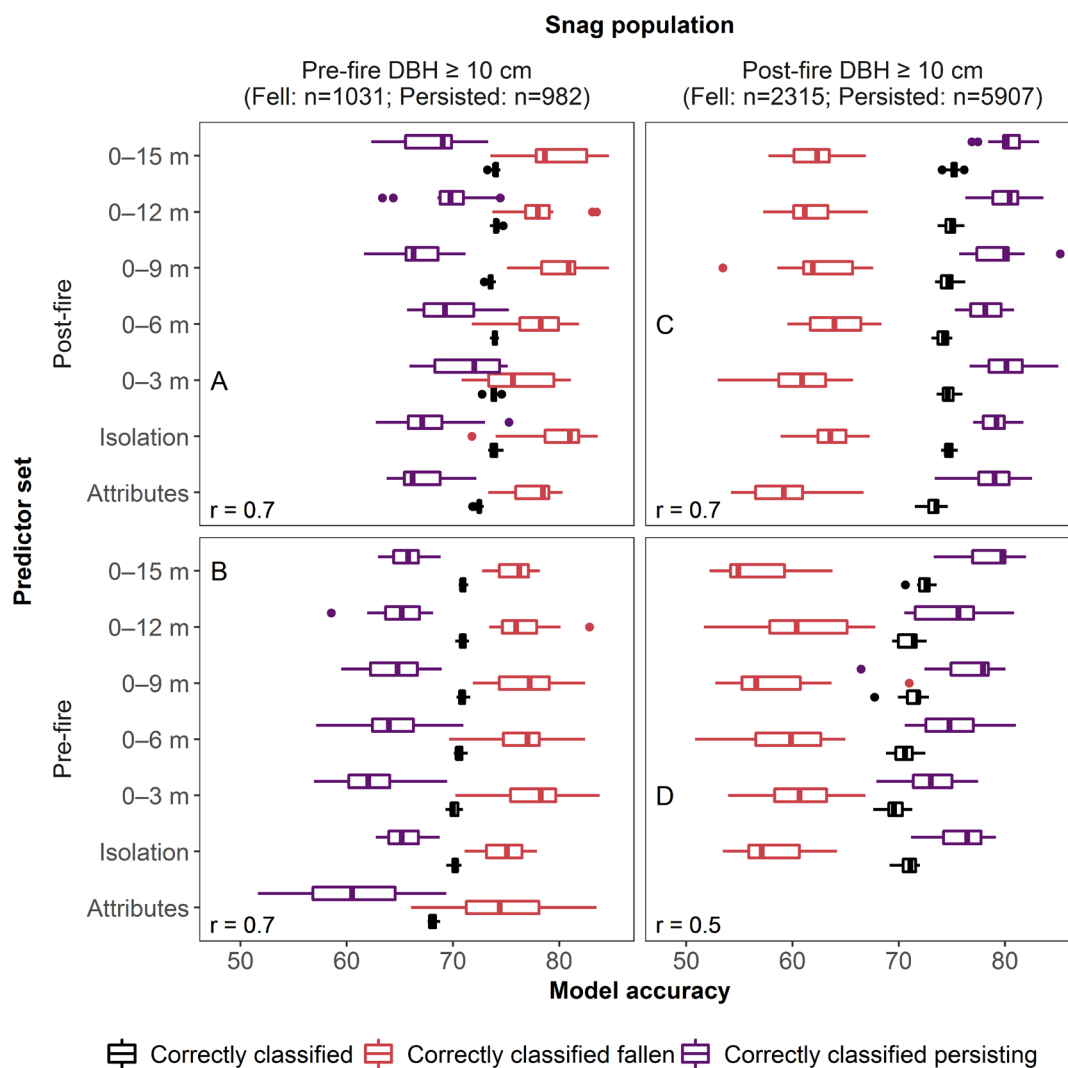
Figure 2.3. Accuracy metrics for selected random forest models of snag fall within five years after fire for snags that existed before the fire (pre-fire) and snags that died in or after the fire (post-fire). Panel rows indicate whether the models were constrained to pre-fire or post-fire predictor variables. Within each panel, up to seven models occupy seven rows (see Table 2.2); the accuracy of each model is represented by the three boxplots that occupy that row. The boxplots represent the distribution of the model accuracy from 15 random forest analyses, each run with a different seed. Letters A, B, C, and D denote the models with the best performance in the lowest performing model accuracy metric for each snag population and predictor variable set. r-values in the lower-left corner of each panel indicate the collinearity threshold used to select the predictor variables in that panel (See *2.3.7 Random forest models*).
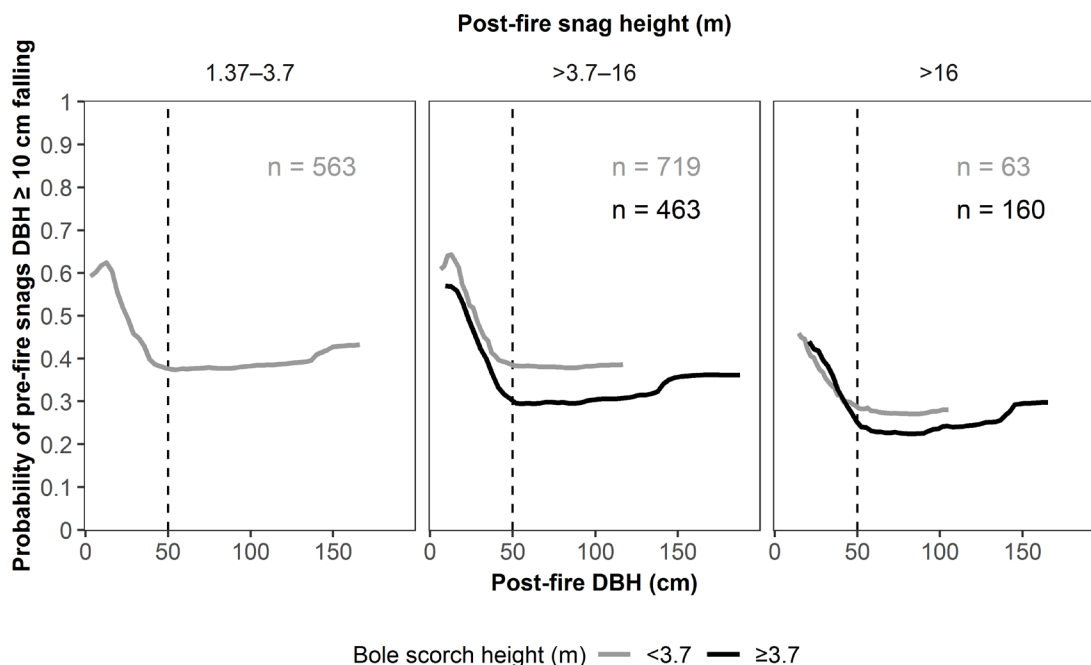
Figure 2.4. Multivariate partial dependence plots for the best model (Figure 2.3A) that used post-fire variables to predict the fall of pre-fire snags ≥ 10 cm DBH. Data were subset based on important variables for that model: pre-fire snag height and bole scorch. Threshold values for pre-fire snag height were based on bird use snag height thresholds (Raphael and White 1984, their Table 11) (Figure A.20). Threshold values for bole scorch were based on where the individual partial dependence plot for bole scorch passed from snags being more likely to fall to being more likely to persist (Figure A.20). Black and gray lines represent mean partial dependence values from 15 model runs. The dashed line at DBH = 50 cm indicates where fall rates start to plateau.
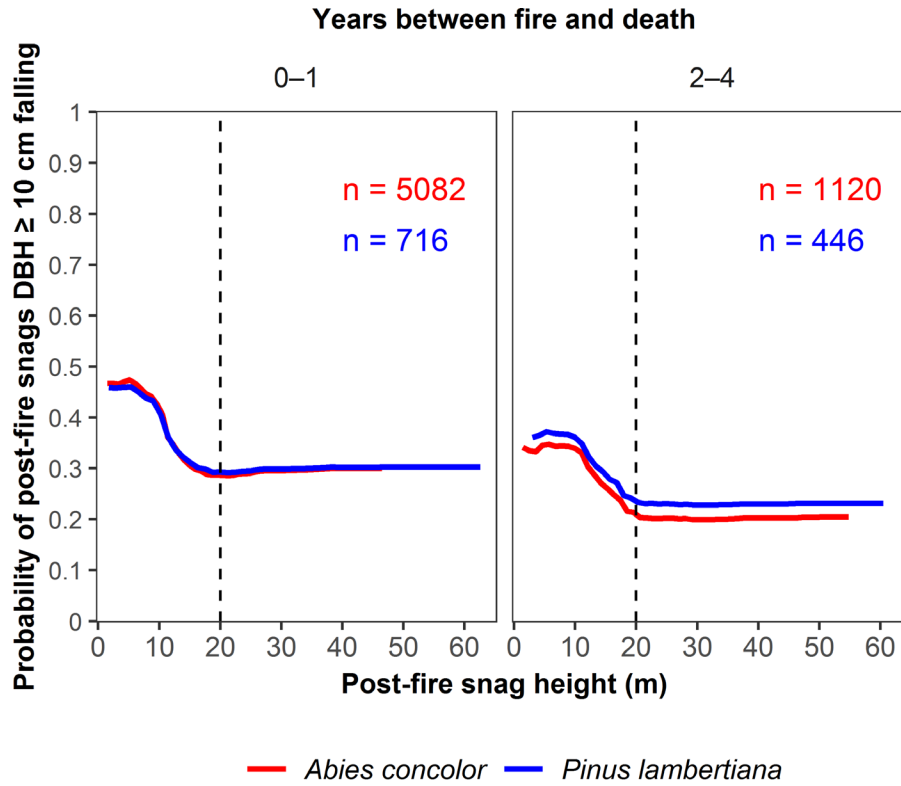
Figure 2.5. Multivariate partial dependence plots for the best model (Figure 2.3C) that used just post-fire variables to predict the fall of post-fire snags ≥ 10 cm DBH. Data were subset based on important variables for that model: species and years between fire and tree death. Lines represent mean partial dependence values from 15 model runs. The dashed line at height = 20 m indicates where fall rates start to plateau.

CHAPTER III

DIFFERENCES IN REGENERATION NICHE MEDIATE HOW DISTURBANCE
SEVERITY AND MICROCLIMATE AFFECT FOREST SPECIES COMPOSITION

Abstract

Climate change is altering forest composition through species-specific responses to fire and drought. Future forest composition will depend on how the different regeneration niches of co-occurring species align with current environmental conditions, especially after fire, which can promote germination by exposing mineral soil. Few studies, however, have examined the effects of disturbance severity and microclimate on post-fire regeneration to define and compare the regeneration niches of co-occurring tree species. We used seven years of annual demography and microenvironment data to examine how disturbance severity, snow duration, and temperature extremes affect the survival of naturally germinated seedlings of *Abies concolor* (white fir) and *Pinus lambertiana* (sugar pine) after a low- to moderate-severity fire. We defined disturbance severity at the microsite level, based on characteristics of the substrate, and at the neighborhood level, based on tree mortality. Both disturbance severity and snow duration had species-specific effects on seedling survival, but these differed by life stage. During the germination year, later snow disappearance was associated with a 0.6 increase in survival probability for *A. concolor* but hardly affected *P. lambertiana*; in contrast, higher neighborhood disturbance severity increased survival of both species. After the germination year, higher substrate burn severity was associated with a 0.8 increase in survival probability for *A. concolor* but hardly affected *P. lambertiana*; higher neighborhood disturbance severity and later snow disappearance increased annual survival of both species, but

maximum summer temperature had minimal effect. Overall, available seed, higher

substrate burn severity, higher neighborhood disturbance severity, and later snow

disappearance promoted natural regeneration. However, lower substrate burn severity

and earlier snow disappearance in the germination year disadvantaged *A. concolor*

seedlings, increasing the relative abundance of *P. lambertiana* seedlings compared to the

local tree population. Our results indicate that natural post-fire compositional shifts

toward drought-tolerant *Pinus* species—and away from less drought-tolerant *Abies*

species—are possible in the Sierra Nevada, with potential benefits for forest persistence

under climate change. Broadly, we show that species differences in regeneration niches

shape how disturbance severity and microclimate affect forest species composition.

Introduction

Climate change is altering forest composition through species-specific responses to

fire and drought (Allen et al., 2010; Halofsky et al., 2020). Fire and drought can change

forest composition through differential mortality of trees, reflecting differences in species

tolerances (Agee, 1993; Breshears et al., 2005; Voelker et al., 2018), and through

differential success of seedlings, reflecting differences in species regeneration

requirements (Bell et al., 2014; Dobrowski et al., 2015; Grubb, 1977). Forest persistence

under climate change will depend at least partially on successful tree seedling recruitment

and the ability of those species assemblages to adapt to future fire and climate regimes

(Dobrowski et al., 2015; Halofsky et al., 2020).

Understanding how disturbance and climate affect regeneration processes is key to

predicting species range shifts, which are occurring in response to climate change and

will define the extent and composition of future forests (Bell et al., 2014; Dobrowski et

al., 2015; Harsch et al., 2009). The regeneration niche encompasses seed production, seed dispersal, germination, establishment, and growth until maturity (Grubb, 1977). When the requirements of a regeneration niche are met within and beyond range limits, species may expand their range or continue to occupy areas within their current range, affecting the competition and facilitation experienced by existing and incoming species (Dobrowski et al., 2015; Kroiss and Hille Ris Lambers, 2015). Climate change influences range shift dynamics by increasing the frequency, extent, and magnitude of large-scale disturbances, which affect multiple components of the regeneration niche: seed availability via parent tree abundance, germination via substrate quality, and survival and growth via competition and facilitation from existing vegetation (Breshears et al., 2005; Donato et al., 2016; Grubb, 1977; A. L. Smith et al., 2016).

Previous research has investigated how post-fire conditions and varying microclimate overlap with regeneration niches. High-severity fire can have negative effects on recruitment by killing vegetation, which reduces seed availability, climate buffering, and belowground facilitation (Baumeister and Callaway, 2006; Dobrowski et al., 2015; Dove and Hart, 2017; Song et al., 2015; Stevens-Rumann et al., 2018; Teste et al., 2009; Young et al., 2019). High temperatures can create a hydrophobic soil layer that increases runoff (Certini, 2005), and lack of shade can accelerate snowmelt and evaporative loss (Teich et al., 2022). Higher-severity fire, however, can also positively affect recruitment by improving access to mineral soil (Gray et al., 2005; Moghaddas et al., 2008; Zald et al., 2008), increasing nitrogen and phosphorous availability for up to three years (Adkins et al., 2020; Nave et al., 2011), and reducing competition for light, water, and nutrients (A. L. Smith et al., 2016). Greater mean annual precipitation increases seedling survival (A.

L. Smith et al., 2016; Stewart et al., 2021; Young et al., 2019), but longer snow duration can have positive or negative effects, depending on the species (Kroiss and Hille Ris Lambers, 2015). Despite the demonstrated effects of disturbance severity and climate on recruitment, few studies have examined the relative importance of disturbance severity and annual microclimate—factors likely to be affected by climate change—on the recruitment of co-occurring species (Pörtner et al., 2022; Stewart et al., 2021; Young et al., 2019).

The mixed-conifer forests of the Sierra Nevada, California, USA, provide an opportunity to ask how disturbance severity and microclimate affect conifer recruitment in species-specific ways. In this ecosystem, large areas of mixed-conifer forests burn at low and moderate severity (Parks and Abatzoglou, 2020), priming forests to support post-fire regeneration by not killing parent trees (Shive et al., 2018; Stewart et al., 2021; Urza and Sibold, 2017) and exposing mineral soil (Gray et al., 2005; Moghaddas et al., 2008; Zald et al., 2008). Years of higher seed availability due to masting often differ among species and may not follow fire events or precede favorable climate conditions, suggesting that both chance and species' environmental tolerances will affect future composition (Davis et al., 2019; Fowells and Schubert, 1956; Kroiss and Hille Ris Lambers, 2015). Recent research, however, has focused on the initial bottleneck—lack of seed dispersal, especially into large high-severity patches—while overlooking microsite dynamics in areas where natural germination has occurred and differential mortality may shift species composition (Shive et al., 2018; Young et al., 2019). Moreover, most studies have taken a landscape-level approach, identifying relationships between seedling survival and remotely sensed fire severity and climate variables, which propagate

considerable uncertainty about actual tree survival (Furniss et al., 2020a), do not account for the effects of delayed tree mortality, and rely on inferences about what directly influences seedling survival at the microsite level (Dobrowski, 2011; Stewart et al., 2021).

We combined statistical modeling with a seven-year dataset of post-fire seedling demography to investigate whether and how fire will alter the composition of mixed-conifer forests in the Sierra Nevada. Specifically, we asked: 1) Does disturbance severity at the microsite or neighborhood scale have species-specific effects on regeneration? and 2) Do these effects differ by seedling stage (i.e., germination year vs. second-year and older)? We also 3) investigated how the influence of disturbance severity on regeneration compared to the influence of microsite snow duration and high temperature extremes, characteristics that are projected to decrease and increase, respectively, with climate change (Pörtner et al., 2022).

Higher fire intensity increases nutrient availability (Adkins et al., 2020; Certini, 2005), so we expected greater seedling survival on sites with higher substrate burn severity. Given that our study area experienced a low- to moderate-severity fire and many parent trees survived, we expected that post-fire tree mortality at the neighborhood level would have species-specific effects on seedling survival by releasing seedlings with different tolerances from competition for light and water. We expected that this effect would be most pronounced during the germination year because seedlings are most vulnerable when young (Fowells and Schubert, 1951) and because these years overlapped with a severe drought, meaning that water would be a limiting factor (Belmecheri et al., 2016). During the germination year, we anticipated that longer snow duration would have

species-specific effects on seedling survival, but we did not have strong expectations for how the magnitude of this effect would compare with disturbance severity or high temperature extremes. After the germination year, however, we expected that disturbance severity would have stronger species-specific effects on survival than microclimate because this later period did not coincide with anomalous climate years, making it less likely that water or temperature would have been limiting factors.

Methods

Study area

This study was conducted in the Yosemite Forest Dynamics Plot (YFDP; 37.77°N, 119.92°W), a 25.6-ha study area in an unlogged, old-growth (oldest trees >500 yr) *Abies concolor–Pinus lambertiana* (white fir–sugar pine) forest in Yosemite National Park (Lutz et al., 2012; Figure 3.1). The YFDP ranges in elevation from 1774 m to 1911 m. Between 1981 and 2010 the modeled mean January temperature ranged from -0.5 °C to 9.7 °C, and the mean July temperature ranged from 14.2 °C to 28.1 °C; mean annual precipitation was 1068 mm with the majority falling as snow (Prism Climate Group, 2016). Approximately 85% of the YFDP has metasedimentary soils of the Clarklodge-Ultic complex (water-holding capacity of 160 mm in the top 150 cm of soil), and 15% of the plot has Humic Dystroxerepts-Typic Haploxerults-Inceptic soils of the Haploxeralfs complex (water-holding capacity 70 mm in the top 150 cm of soil; Lutz et al., 2012). Six soil pits dug around the YFDP perimeter characterized soil texture in the top 150 cm as sandy loam most often, followed by loam and sandy clay loam. Principal tree species ordered by abundance are *Abies concolor* (white fir), *Pinus lambertiana* (sugar pine),

Cornus nuttallii (Pacific dogwood), *Calocedrus decurrens* (incense-cedar), and *Quercus kelloggii* (California black oak).

Prior to European settlement, the YFDP experienced low- to moderate-severity surface fires with a mean fire return interval of 30 yr (Barth et al., 2015). Although lightning-ignited spot fires have occurred within the YFDP since 1900, the area has been largely fire-excluded since the last widespread event in 1900 (Barth et al., 2015; Scholl and Taylor, 2010), leading to high tree density (Figure B.6; Barth et al., 2015; Lutz et al., 2012) and surface fuel accumulation (Gabrielson et al., 2012, Lutz et al., 2014, Cansler et al., 2019).

On September 1st and 2nd, 2013, the YFDP burned in an unmanaged backfire set by Yosemite managers to control the spread of the Rim Fire (Jeronimo et al., 2020; Stavros et al., 2016), which occurred during the second year of a four-year drought of historic severity (Belmecheri et al., 2016; Furniss et al., 2020b). Fire severity within the YFDP, as inferred from Landsat-derived scenes, was largely low and moderate (Blomdahl et al., 2019), consistent in both severity and spatial heterogeneity with recent fires in Yosemite (van Wagtendonk and Lutz, 2007). The fire reduced aboveground live shrub biomass from 3,490 to 269 kg ha^{-1} (Lutz et al., 2017a) and consumed 79% of total surface fuel (Cansler et al., 2019). Only 4.9% of the plot surface was manually delineated as unburned in patches ≥ 1 m^2 (Blomdahl et al., 2019).

Study species

Abies concolor and *P. lambertiana* are masting conifer species that do not seed-bank. Larger seed crops are produced every 3–9 years by *A. concolor* and every 3–5 years by *P. lambertiana* (Fowells and Schubert, 1956). Dominant *A. concolor* (30–90 cm DBH) and

P. lambertiana (> 50 cm DBH) produce the majority of seed. *Abies concolor* seeds are smaller than *P. lambertiana* seeds but can be more abundant and disperse distances up to two times tree height, increasing the chance of germination at a favorable microsite (Fowells and Schubert, 1956; Zald et al., 2008). *Pinus lambertiana* invest in larger, energy-rich seeds, with a smaller wing, leading to shorter wind dispersal distances of 30–50 m, but caching by birds and small mammals can expand dispersal extent (Fowells and Schubert, 1951).

Both *A. concolor* and *P. lambertiana* are moderately fire resistant when mature, due to thick bark, elevated crowns, and needles of moderate flammability (de Magalhães and Schwilk, 2012; Furniss et al., 2020b; Minore, 1979). As juveniles, however, *A. concolor* may be more susceptible to fire-caused mortality than *P. lambertiana* (van Wagtendonk, 1983). At maturity, *A. concolor* are more shade tolerant and less drought tolerant than *P. lambertiana* (Minore, 1979; Niinemets and Valladares, 2006), but, as seedlings, these differences between species can disappear (Kern, 1996; Oliver and Dolph, 1992) or, in the case of drought tolerance, even be reversed (Kern, 1996). Therefore, mature forests with a greater *P. lambertiana* component may be more resistant to drought, but the conditions required during regeneration to produce that composition are less certain.

Seedling data collection

We installed 63, 1-m^2 seedling quadrats on a grid throughout the YFDP in 2014 (62 quadrats) and 2015 (1 quadrat) to document conifer regeneration (Figure 3.1). Seedling quadrats were mapped to surveyed grid corners in the YFDP (Lutz et al., 2012) based on slope-corrected distance and azimuth.

Seedling species, age, and height were documented once in July 2014, twice in 2015–2018, and once in 2019 and 2020. In 2014 and 2015, when signs of fire were still detectable, the substrates around each seedling were identified as burned or unburned. Only 1.7% of seedlings did not germinate on burned substrate, so substrate burn status was not analyzed further. Percent cover by substrate (e.g., bare ground, litter, cobble) and the immediate substrate of each seedling (e.g., bare ground, litter, moss) were recorded at each census. Most seedlings (95.5%) germinated in litter, and 81.1% of those germinated in ≤ 1 cm of litter. The remaining seedlings (4.5%) germinated on bare ground. Percent of understory cover by species was recorded in each quadrat, starting in 2015, but was not strongly related to seedling survival.

Disturbance severity metrics

During seedling quadrat installation, we recorded the percentage of area burned within each quadrat and assessed the burn severity of that portion using the burn severity coding matrix for forest substrates in the Fire Monitoring Handbook (USDI National Park Service, 2003). For each quadrat, we calculated percent burned × burn severity to generate substrate burn severity.

We used annual maps of all trees ≥ 1 cm DBH in the YFDP (Lutz et al., 2012) to calculate neighborhood-level, tree-mortality–based disturbance severity metrics for the area around each seedling quadrat. Because fire damage contributed to tree mortality from 2014 through 2020 (Furniss et al., 2020b; Jeronimo et al., 2020), we calculated disturbance severity for each post-fire year (2014–2020) based on cumulative post-fire tree mortalities. Disturbance severity was represented as the ratio of crowding of trees that died after the fire to crowding of pre-fire live trees. To quantify crowding, we

applied a distance-diminished, diameter-weighted crowding (C) index to trees within a specified radius of each seedling quadrat (Equation 3.1).

$$C_i = \sum_{j=1}^{n} \frac{DBH_j}{1+Distance_{ij}} \qquad (3.1)$$

This crowding index summarizes spatial pattern and diameter information in a single metric that accounts for 1) the diminished influence of neighbor tree j when it is farther from seedling quadrat i and 2) the increased influence of larger-diameter neighbor trees. By applying this index separately to trees that died after the fire and trees that were alive before the fire, and then assessing a ratio (i.e., $C_{i,post-fire}/C_{i,pre-fire}$), we consider spatial pattern and tree size, while using the concept of mortality rate to control for differences in neighborhood density. We calculated annual cumulative disturbance severity metrics for circular neighborhoods with radii of 10, 20, 30, and 40 m.

Microclimate metrics

Each seedling quadrat was outfitted with a HOBO temperature and light sensor to detect days of snow cover, time of snowmelt, and minimum and maximum daily temperature during summer and winter. During the summers of 2015–2018, HOBOs logged data every hour; during the winters of 2015 (i.e., Fall 2014–Spring 2015) and 2016, HOBOs logged data every two hours; and during the winters of 2017–2020 and the summers of 2019 and 2020, HOBOs logged data every three hours.

Snow duration and temperature metrics were derived from HOBO data loggers following the methods of Raleigh et al. (2013) and Teich et al. (2022) (Figure B.2). Damped diurnal variations indicated snow presence and were used to determine the Julian date of the last snow disappearance, the Julian date of snow disappearance after

the longest period of continuous snow cover, the number of days of longest continuous snow cover, and the total number of days of snow cover.

To determine whether high temperatures during periods of increasing water deficit impacted seedling survival, we calculated a rolling mean of maximum daily temperatures for periods of 1, 3, 5, and 7 days for June–August (summer) and September (fall). We used the highest mean value for each time period and season to represent high temperatures experienced at each seedling quadrat.

Modeling seedling survival

Disturbance severity. We used generalized linear mixed-effects models to examine whether disturbance severity has species-specific effects on seedling survival. Our response variable denoted whether a seedling that germinated in 2014 or 2015 survived until 2020 or not. We represented disturbance severity at two scales, microsite-level substrate burn severity and neighborhood-level disturbance severity. We investigated species-specific effects of disturbance severity by considering two interaction terms: species × substrate burn severity and species × neighborhood disturbance severity. We performed model selection (Table B.3) and present the model with the lowest AIC (Equation 3.2):

$$\log[-log(1 - P_{ij})] = \alpha_0 + u_j + \beta_1 Species_i + \beta_2 Substrate.burn.severity_j$$

$$+ \beta_3 Neighborhood.disturbance.severity_j$$

$$+ \beta_4 Species_i Substrate.burn.severity_j \tag{3.2}$$

P_{ij} is the probability of seedling i in quadrat j dying by 2020. α_0 is an intercept term. u_j is the random intercept term for quadrat j, which adjusts the α_0 intercept value to

account for quadrat differences. $\beta_{1...4}$ are estimated parameters for each explanatory variable. We compared the AIC values for models with disturbance severity metrics based on 1) different neighborhood sizes (radii 10, 20, 30, or 40 m), and 2) successive post-fire years (2014–2020), and selected the neighborhood size and post-fire year associated with the lowest AIC (30 m; 2015).

Disturbance severity by life stage. To determine whether the species-specific effects of disturbance severity on seedling survival differed by life stage, we fit Equation 3.2 using different response variables: survival at the end of the germination year, or survival after the germination year until 2020.

Disturbance severity vs. microclimate. To compare the species-specific influences of disturbance severity and microclimate on seedling survival during different life stages, we fit separate generalized linear mixed-effects models to predict seedling survival during the germination year and after the germination year. Models of survival during the germination year were limited to seedlings that germinated in 2015 because we did not have microclimate data for the seedling quadrat locations before we installed them in 2014. To model survival after the germination year, we conducted a repeated-measures analysis where the response variable was annualized survival for each seedling.

To examine species-specific effects of disturbance severity and annual microclimate, we included interaction terms for species crossed with substrate burn severity, annual cumulative neighborhood disturbance severity, snow duration preceding the most recent growing season, and maximum temperature during the most recent growing season. We compared the AIC values of models that used each of the four snow duration metrics and each of the maximum temperature metrics. Final snow disappearance date and one-day

summer maximum temperature were associated with the lowest AIC (Table B.2).

For models of first-year survival, we performed model selection (Table B.4) and
present the model with the lowest AIC (Equation 3.3):

$$\log[-\log(1 - P_{ij})] = \alpha_0 + u_j + \beta_1 Species_i$$

$$+\beta_2 Neighborhood.disturbance.severity_j$$

$$+ \beta_3 Snow.duration_j + \beta_4 Species_i Snow.duration_j \tag{3.3}$$

P_{ij} is the probability of seedling i in quadrat j dying by 2016 (i.e., during the
germination year). α_0 is an intercept term, u_j is the random intercept term for quadrat j,
and $\beta_{1...4}$ are estimated parameters.

For models of annual survival after the germination year, we performed model
selection (Table B.4) and present the model with the lowest AIC (Equation 3.4):

$$\log[-\log(1 - P_{ij})] = \alpha_0 + u_j + \beta_0 Seedling.age_i + \beta_1 Species_i$$

$$+ \beta_2 Substrate.burn.severity_j + \beta_3 Neighborhood.disturbance.severity_j$$

$$+ \beta_4 Snow.duration_j + \beta_5 Summer.max.temp_j$$

$$+ \beta_6 Species_i Substrate.burn.severity_j + \beta_7 Species_i Summer.max.temp_j \tag{3.4}$$

P_{ij} is the probability of seedling i in quadrat j dying in a given year. α_0 is an intercept
term, u_j is the random intercept term for quadrat j, and $\beta_{0...7}$ are estimated parameters.

Model settings. For each model, we fit a binomial regression model to our Bernoulli-
distributed response variable and used a complementary log-log link function because it
does not assume that seedling deaths occurred exactly when our annual sampling scheme
detected them (Allison, 2010). All numeric variables were standardized, so estimated
coefficients represent the relative importance of the predictors. All models were fit in R

using the "glmer" function in the "lmer4" package, version 1.1.29 (R Core Team, 2020).

We used the "vif" function in the "car" package, version 3.1.0, to assess variable inflation

factors of the predictors in each model. All values were < 3, indicating low

multicollinearity among predictors (Figures B.3–B.5).

Results

Seedling demography

During the seven years following a low- to moderate-severity fire, we observed 590

A. concolor and 188 *P. lambertiana* seedlings germinate in the 63, 1-m^2 seedling

quadrats (Figure 3.2). Most seedlings (93.8%) germinated one or two years after fire

(Table B.1). Seedling survival rates differed by life stage. First-year survival rates were

lower for *A. concolor* (43.2%) than for *P. lambertiana* (61.5%), but trends were similar

for both species after the first year (Figure 3.2). Higher survival of *P. lambertiana* during

the germination year shifted seedling composition by increasing the proportion of *P.

lambertiana*. Considering just the seedlings that germinated in 2014 or 2015, *P.

lambertiana* represented 23.8% of the germinants but 32.9% of the surviving seedlings in

2020.

Disturbance severity affects seedling survival

Substrate burn severity had species-specific effects on seedling survival from

germination in 2014 or 2015 through 2020 (Figure 3.3 [Both stages combined], Table

B.6). Substrate burn severity was positively related to seedling survival for both species

but had a much stronger positive effect on *A. concolor* seedlings. Neighborhood

disturbance severity was also positively related to seedling survival but did not have

species-specific effects.

Disturbance severity effects differ by life stage

The effects of disturbance severity on seedling survival differed by life stage (Figure 3.3, Table B.6). During the germination year, higher neighborhood disturbance severity was associated with greater seedling survival and had similar effects on both species, while substrate burn severity had no significant effect. After the germination year, substrate burn severity had a strong positive effect on *A. concolor* survival but a weak and slightly negative effect on *P. lambertiana* survival. Neighborhood disturbance severity two years after fire did not significantly affect survival of seedlings after the germination year and through 2020.

Disturbance severity and microclimate effects on annual survival differ by life stage

During the germination year, snow disappearance date had species-specific effects on seedling survival, but neighborhood disturbance severity did not (Figure 3.4, Tables B.4 and B.7). Later snow disappearance and higher neighborhood disturbance severity were associated with greater survival of *A. concolor* seedlings, and the magnitude of these effects was similar (Table B.7). In contrast, survival of *P. lambertiana* seedlings was positively related to neighborhood disturbance severity but only weakly related to snow disappearance date.

After the germination year, substrate burn severity had species-specific effects on annual seedling survival, but neighborhood disturbance severity and snow disappearance date did not (Figure 3.5, Tables B.5 and B.7). Higher substrate burn severity, higher neighborhood disturbance severity, and later snow disappearance were associated with

greater annual survival of *A. concolor* seedlings, and the magnitude of these effects was similar. In contrast, annual survival of *P. lambertiana* seedlings was positively related to higher neighborhood disturbance severity and later snow disappearance date but only weakly (and negatively) related to higher substrate burn severity. When snow disappearance date was below the median value, it had more effect on seedling survival, indicating that our study included instances when snow duration was a limiting factor and instances when it was not (Figure B.4). Maximum summer temperature had minimal effect on survival of either species.

Discussion

Overall, our results suggest that fire can alter the composition of mixed-conifer forests in the Sierra Nevada by increasing *P. lambertiana* recruitment and decreasing *A. concolor* recruitment relative to tree populations (Figure 3.6). Microsite factors that may themselves be altered by climate change (i.e., neighborhood disturbance severity, substrate burn severity, and snow duration) had significant and sometimes differential effects on the recruitment of these species, suggesting that compositional shifts will be difficult to predict.

Disturbance severity affects seedling composition

Disturbance severity is likely to influence the occurrence and direction of compositional shifts through effects on seedling survival that are sometimes species specific. For example, after the germination year, the species-specific effects of substrate burn severity on seedling survival maintained the compositional changes that resulted from differential mortality during the germination year. We suggest that substrate burn

severity became important after the germination year because higher burn severity can extend changes to soil characteristics (Adkins et al., 2020). Soil heating decreases fungal biomass, including mycorrhizal associates, but increases available nitrogen and phosphorous as well as the abundance of coliotrophic bacteria, which are associated with faster decomposition (Adkins et al., 2020; Dove and Hart, 2017). Our results indicate that *A. concolor* seedlings benefited from the prolonged effects of soil heating more than *P. lambertiana* seedlings, perhaps because *A. concolor* establish from a smaller seed (Fowells and Schubert, 1956).

In contrast, the non-species–specific effects of higher neighborhood disturbance severity indirectly set the stage for compositional change by increasing survival of both species, thereby maintaining a seedling population that could be acted upon by other factors. We propose several reasons neighborhood disturbance severity had positive effects on seedling survival. Because our metric for neighborhood disturbance severity was based on tree mortality, DBH, and proximity to seedling quadrats, higher values would indicate death of larger and/or nearby trees, which would immediately liberate water resources while still providing shade, at least in the short term. Water and shade may have been especially important to the seedlings in our first-year survival models because they germinated during the last two years of a severe four-year drought (Belmecheri et al., 2016). After the germination year, annual cumulative neighborhood disturbance severity continued to positively affect seedling survival (Tables B.6 and B.7). Gradual needle deposition from newly dead trees eventually reduces shade and accelerates snowmelt, reversing the initial benefits to seedlings from nearby tree mortality (Teich et al., 2022). Moreover, larger trees ($\geq$ 60 cm DBH) died three and four

years post-fire (Jeronimo et al., 2020). These trees would have had greater effects on resource availability (Lutz et al., 2012; Teich et al., 2022), and their delayed mortality was not strongly spatially correlated with immediate mortality of smaller trees (< 60 cm DBH; Furniss et al., 2020). Therefore, neighborhood disturbance severity was initially important when water and shade would have most benefited germinants, and these positive effects persisted as delayed morality of larger trees continued to mediate resource availability.

Microclimate affects seedling composition

Our models of first-year survival demonstrate that snow duration prior to germination can determine the direction of compositional change (Figure 3.4, Table B.7). Earlier snow disappearance in the spring of 2015 reduced the survival of *A. concolor* seedlings that germinated in 2015, while barely affecting *P. lambertiana* seedlings (Figure 3.4). Given that earlier snowmelt could decrease soil moisture during germination, our results suggest that *A. concolor* seedlings benefit more from moist soils during germination than *P. lambertiana* seedlings. This difference between species may have been especially detectable in our study because 2015 coincided with the fourth year of a severe drought (Belmecheri et al., 2016). In the YFDP, considerable mortality of large-diameter trees ($\geq$ 60 cm DBH) in 2016 further suggests that water was severely limiting (Furniss et al., 2020b; Jeronimo et al., 2020). As earlier snowmelt becomes more frequent with climate change (Pörtner et al., 2022), seedling composition may shift toward more drought-tolerant species, especially when drought coincides with the germination year.

However, our results also indicate that snow duration only drives compositional change when water is limiting (see also Germain and Lutz, 2020), since snow duration

did not have species-specific effects on seedling survival after the germination year. This could be for several reasons: 1) after 2015, the last germination year in this study, the 2012–2015 drought was over and water was no longer limiting, 2) mortality of large-diameter trees after 2015 reduced competition for water, or 3) only seedlings that were less sensitive to water limitation had survived. Overall, the positive relationship between water availability and post-fire seedling survival is consistent with other studies (Davis et al., 2019; Shive et al., 2018; Stewart et al., 2021; Urza and Sibold, 2017; Welch et al., 2016; Young et al., 2019).

Relative influence of seed rain, disturbance severity, and microclimate on seedling composition

The relative importance of species identity, disturbance severity, and snow duration on seedling survival indicates that stochastic processes (e.g., seed rain composition, fire) and climate change will make predicting compositional change difficult. During the germination year, species identity was the most important predictor of seedling survival, followed by neighborhood disturbance severity and then snow duration (Table B.7). The importance of species identity over other factors highlights the fundamental role of seed rain composition in creating opportunities for compositional shifts. After the germination year, species identity remained most important for *P. lambertiana*, while substrate burn severity became most important for *A. concolor*. Snow duration was still the second most important predictor of survival for both species. Thus, in chronological order, compositional change will first be constrained by seed rain composition, then by snow duration during the germination year, and later by substrate burn severity. Ordered by magnitude, compositional change will first be constrained by seed rain composition, then

substrate burn severity (acting after the germination year), and then by snow duration during the germination year. Whether natural compositional shifts occur therefore depends on the coincident timing of fire (which exposes mineral soil) and seed availability, the burn severity of the substrates where the seeds of different species land, and the timing of snowmelt at those germination sites.

Study limitations and future directions

A strength of this study was that it annually tracked seedlings *in situ* following a low- to moderate-severity fire that occurred during a severe drought (Belmecheri et al., 2016), which may mimic future conditions under climate change (Marshall et al., 2019; Pörtner et al., 2022). However, the study design also limited our scope of inference. For example, climate inferences are constrained by the weather that occurred between 2014 and 2020, and this was superimposed on lockstep advancements in seedling age and time since fire, potentially confounding the effects of annual climate, seedling age, and other post-fire changes, such as delayed tree mortality and rebounding microbe populations, on seedling survival (Adkins et al., 2020; Furniss et al., 2020b). We were also only able to model survival of two seedling cohorts, and germination year was highly correlated with species (phi coefficient = 0.84; Figure 3.2). To verify that the effects we attribute to species were not confounded with germination cohort, we ran all models with cohort in place of species as a predictor. In every model, when germination cohort replaced species, the estimated parameter value was closer to zero, the *p*-value associated with the parameter was the same or larger, and the AIC for the model was larger. These metrics demonstrate that species was more predictive of seedling survival than germination cohort. However, we hope that future *in situ* seedling studies have even representation of multiple species

in multiple germination cohorts to better isolate the effects of species from the effects of seedling age and time since fire.

Deeper understanding of the effects of microclimate on first-year seedlings that germinate after fire is still needed. We encourage future researchers to deploy temperature and light data loggers immediately after low- and moderate-severity fires, and to track soil moisture and nutrients throughout the first growing season, to better describe the relationship between mortality during the germination year and species-specific responses to environmental conditions that may alter under climate change.

Implications and conclusions

This study demonstrates that species-specific responses to post-fire conditions can shift seedling species composition, which could lead to changes in future overstory composition. Our results are relevant to forest managers in the Sierra Nevada because we show that natural post-fire conditions can favor *P. lambertiana* seedlings while disadvantaging *A. concolor* seedlings. In the mixed-conifer forests of the Sierra Nevada, a century of fire suppression has allowed many shade-tolerant *A. concolor* to reach maturity and populate lower strata of the canopy with ladder fuels (Figure B.6; Becker and Lutz, 2016; Kilgore and Briggs, 1972). We show that available seed, lower substrate burn severity, higher neighborhood disturbance severity, and earlier snowmelt during the germination year can naturally shift the composition of these forests away from dominance by *A. concolor*. Natural processes may therefore support and bolster fire use, thinning, and post-fire planting programs that aim to increase forest resilience under climate change by retaining *Pinus* species. Broadly, our results show that species differences in regeneration niches will mediate how disturbance severity and

microclimate influence future forest species composition.

References

Adkins, J., Docherty, K.M., Gutknecht, J.L.M., Miesel, J.R., 2020. How do soil microbial communities respond to fire in the intermediate term? Investigating direct and indirect effects associated with fire occurrence and burn severity. Sci. Total Environ. 745. https://doi.org/10.1016/j.scitotenv.2020.140957

Agee, J.K., 1993. Fire ecology of Pacific Northwest forests. Island Press, Washington, D.C.

Allen, C.D., Macalady, A.K., Chenchouni, H., Bachelet, D., McDowell, N., Vennetier, M., Kitzberger, T., Rigling, A., Breshears, D.D., Hogg, E.H. (Ted), Gonzalez, P., Fensham, R., Zhang, Z., Castro, J., Demidova, N., Lim, J.H., Allard, G., Running, S.W., Semerci, A., Cobb, N., 2010. A global overview of drought and heat-induced tree mortality reveals emerging climate change risks for forests. For. Ecol. Manage. 259, 660–684. https://doi.org/10.1016/j.foreco.2009.09.001

Allison, P.D., 2010. Survival analysis using SAS: a practical guide, Second. ed. SAS Institute.

Barth, M.A.F., Larson, A.J., Lutz, J.A., 2015. A forest reconstruction model to assess changes to Sierra Nevada mixed-conifer forest during the fire suppression era. For. Ecol. Manage. 354, 104–118. https://doi.org/10.1016/j.foreco.2015.06.030

Baumeister, D., Callaway, R.M., 2006. Facilitation by Pinus flexilis during succession: A hierarchy of mechanisms benefits other plant species. Ecology 87, 1816–1830. https://doi.org/10.1890/0012-9658(2006)87[1816:FBPFDS]2.0.CO;2

Becker, K.M.L., Lutz, J.A., 2016. Can low-severity fire reverse compositional change in montane forests of the Sierra Nevada, California, USA? Ecosphere 7, 1–22. https://doi.org/10.1002/ecs2.1484

Bell, D.M., Bradford, J.B., Lauenroth, W.K., 2014. Early indicators of change: Divergent climate envelopes between tree life stages imply range shifts in the western United States. Glob. Ecol. Biogeogr. 23, 168–180. https://doi.org/10.1111/geb.12109

Belmecheri, S., Babst, F., Wahl, E.R., Stahle, D.W., Trouet, V., 2016. Multi-century evaluation of Sierra Nevada snowpack. Nat. Clim. Chang. 6, 2–3. https://doi.org/10.1038/nclimate2809

Blomdahl, E.M., Kolden, C.A., Meddens, A.J.H., Lutz, J.A., 2019. The importance of small fire refugia in the central Sierra Nevada, California, USA. For. Ecol. Manage. 432, 1041–1052. https://doi.org/10.1016/j.foreco.2018.10.038

Breshears, D.D., Cobb, N.S., Rich, P.M., Price, K.P., Allen, C.D., Balice, R.G., Romme, W.H., Kastens, J.H., Floyd, M.L., Belnap, J., Anderson, J.J., Myers, O.B., Meyer, C.W., 2005. Regional vegetation die-off in response to global-change-type drought. Proc. Natl. Acad. Sci. U. S. A. 102, 15144–15148. https://doi.org/10.1073/pnas.0505734102

Cansler, C.A., Swanson, M.E., Furniss, T.J., Larson, A.J., Lutz, J.A., 2019. Fuel dynamics after reintroduced fire in an old-growth Sierra Nevada mixed-conifer forest. Fire Ecol. 15. https://doi.org/10.1186/s42408-019-0035-y

Certini, G., 2005. Effects of fire on properties of forest soils: A review. Oecologia 143, 1–10. https://doi.org/10.1007/s00442-004-1788-8

Davis, K.T., Dobrowski, S.Z., Higuera, P.E., Holden, Z.A., Veblen, T.T., Rother, M.T., Parks, S.A., Sala, A., Maneta, M.P., 2019. Wildfires and climate change push low-elevation forests across a critical climate threshold for tree regeneration. Proc. Natl. Acad. Sci. U. S. A. 116, 6193–6198. https://doi.org/10.1073/pnas.1815107116

de Magalhães, R.M., Schwilk, D.W., 2012. Leaf traits and litter flammability: evidence for non-additive mixture effects in a temperate forest. J. Ecol. 100, 1–11. https://doi.org/10.1111/j.1365-2745.2012.01987.x

Dobrowski, S.Z., 2011. A climatic basis for microrefugia: the influence of terrain on climate. Glob. Chang. Biol. 17, 1022–1035. https://doi.org/10.1111/j.1365-2486.2010.02263.x

Dobrowski, S.Z., Swanson, A.K., Abatzoglou, J.T., Holden, Z.A., Safford, H.D., Schwartz, M.K., Gavin, D.G., 2015. Forest structure and species traits mediate projected recruitment declines in western US tree species. Glob. Ecol. Biogeogr. 1–11.

Donato, D.C., Harvey, B.J., Turner, M.G., 2016. Regeneration of montane forests 24 years afer the 1988 Yellowstone fires: A fire-catalyzed shif in lower treelines? Ecosphere 7, 1–16. https://doi.org/10.1002/ecs2.1410/supinfo

Dove, N.C., Hart, S.C., 2017. Fire reduces fungal species richness and in situ mycorrhizal colonization: a meta-analysis. Fire Ecol. 13, 37–65. https://doi.org/10.4996/fireecology.130237746

Fowells, H., Schubert, G., 1951. Natural reproduction in certain cutover pine-fir stands of California. J. For. 49, 192–196. https://doi.org/10.1093/jof/49.3.192

Fowells, H.A., Schubert, G.H., 1956. Seed crops of forest trees in the pine region of California. USDA Tech. Bull. 1150, 1–48.

Furniss, T.J., Kane, V.R., Larson, A.J., Lutz, J.A., 2020a. Detecting tree mortality with Landsat-derived spectral indices: Improving ecological accuracy by examining

uncertainty. Remote Sens. Environ. 237, 111497.
https://doi.org/10.1016/j.rse.2019.111497

Furniss, T.J., Larson, A.J., Kane, V.R., Lutz, J.A., 2020b. Wildfire and drought moderate the spatial elements of tree mortality. Ecosphere 11.
https://doi.org/10.1002/ecs2.3214

Gabrielson, A.T., Larson, A.J., Lutz, J.A., Reardon, J.J., 2012. Biomass and burning characteristics of sugar pine cones. Fire Ecol. 8, 58–70.
https://doi.org/10.4996/fireecology.0803058

Germain, S.J., Lutz, J.A., 2020. Climate extremes may be more important than climate means when predicting species range shifts. Clim. Change 163, 579–598.
https://doi.org/10.1007/s10584-020-02868-2

Gray, A.N., Zald, H.S.J., Kern, R.A., North, M., 2005. Stand conditions associated with tree regeneration in Sierran mixed-conifer forests. For. Sci. 51, 198–210.

Grubb, P.J., 1977. The maintenance of species-richness in plant communities: the importance of the regeneration niche. Biol. Rev. 52, 107–145.

Halofsky, J.E., Peterson, D.L., Harvey, B.J., 2020. Changing wildfire, changing forests: the effects of climate change on fire regimes and vegetation in the Pacific Northwest, USA. Fire Ecol. 16. https://doi.org/10.1186/s42408-019-0062-8

Harsch, M.A., Hulme, P.E., McGlone, M.S., Duncan, R.P., 2009. Are treelines advancing? A global meta-analysis of treeline response to climate warming. Ecol. Lett. 12, 1040–1049. https://doi.org/10.1111/j.1461-0248.2009.01355.x

Jeronimo, S.M.A., Lutz, J.A., R. Kane, V., Larson, A.J., Franklin, J.F., 2020. Burn weather and three-dimensional fuel structure determine post-fire tree mortality. Landsc. Ecol. 35, 859–878. https://doi.org/10.1007/s10980-020-00983-0

Kern, R.A., 1996. A comparative field study of growth and survival of Sierran conifer seedlings. Duke University.

Kilgore, B.M., Briggs, G.S., 1972. Restoring fire to high elevation forests in California. J. For. 70, 266–271.

Kolden, C.A., Lutz, J.A., Key, C.H., Kane, J.T., van Wagtendonk, J.W., 2012. Mapped versus actual burned area within wildfire perimeters: characterizing the unburned. For. Ecol. Manage. 286, 38–47. https://doi.org/10.1016/j.foreco.2012.08.020

Kroiss, S.J., Hille Ris Lambers, J., 2015. Recruitment limitation of long-lived conifers: implications for climate change responses. Ecology 96, 1286–1297.

Lutz, J.A., Furniss, T.J., Germain, S.J., Becker, K.M.L., Blomdahl, E.M., Jeronimo,

S.M.A., Cansler, C.A., Freund, J.A., Swanson, M.E., Larson, A.J., 2017. Shrub communities, spatial patterns, and shrub-mediated tree mortality following reintroduced fire in Yosemite National Park, California, USA. Fire Ecol. 13, 104–126. https://doi.org/10.4996/fireecology.1301ppp

Lutz, J.A., Larson, A.J., Swanson, M.E., Freund, J.A., 2012. Ecological importance of large-diameter trees in a temperate mixed-conifer forest. PLoS One 7, e36131. https://doi.org/10.1371/journal.pone.0036131

Lutz, J.A., Schwindt, K.A., Furniss, T.J., Freund, J.A., Swanson, M.E., Hogan, K.I., Kenagy, G.E., Larson, A.J., 2014. Community composition and allometry of *Leucothoe davisiae*, *Cornus sericea*, and *Chrysolepis sempervirens*. Can. J. For. Res. 44, 1–7. https://doi.org/10.1139/cjfr-2013-0524

Marshall, A.M., Abatzoglou, J.T., Link, T.E., Tennant, C.J., 2019. Projected changes in interannual variability of peak snowpack amount and timing in the western United States. Geophys. Res. Lett. 46, 8882–8892. https://doi.org/10.1029/2019GL083770

Minore, D., 1979. Comparative autecological characteristics of northwestern tree species: a literature review. Pacific Northwest Forest and Range Experiment Station.

Moghaddas, J.J., York, R.A., Stephens, S.L., 2008. Initial response of conifer and California black oak seedlings following fuel reduction activities in a Sierra Nevada mixed conifer forest. For. Ecol. Manage. 255, 3141–3150. https://doi.org/10.1016/j.foreco.2007.11.009

Nave, L.E., Vance, E.D., Swanston, C.W., Curtis, P.S., 2011. Fire effects on temperate forest soil C and N storage. Ecol. Appl. 21, 1189–1201. https://doi.org/10.1890/10-0660.1

Niinemets, Ü., Valladares, F., 2006. Tolerance to shade, drought, and waterlogging of temperate northern hemisphere trees and shrubs. Ecol. Monogr. 76, 521–547. https://doi.org/10.1890/0012-9615(2006)076[0521:TTSDAW]2.0.CO;2

Oliver, W.W., Dolph, K., 1992. Mixed-conifer seedling growth varies in response to overstory release. For. Ecol. Manage. 48, 179–183. https://doi.org/10.1016/0378-1127(92)90130-2

Parks, S.A., Abatzoglou, J.T., 2020. Warmer and drier fire seasons contribute to increases in area burned at high severity in western US forests from 1985 to 2017. Geophys. Res. Lett. 47, 1–10. https://doi.org/10.1029/2020GL089858

Pörtner, H.-O., Roberts, D.C., Tignor, M., Poloczanska, E.S., Mintenbeck, K., Alegría, A., M. Craig, S. Langsdorf, S. Löschke, V. Möller, A. Okem, B.R., 2022. Climate change 2022: Impacts, adaptation, and vulnerability.

PRISM Climate Group, 2016. PRISM 800-m Climate Normals (1981-2010).

Raleigh, M.S., Rittger, K., Moore, C.E., Henn, B., Lutz, J.A., Lundquist, J.D., 2013. Ground-based testing of MODIS fractional snow cover in subalpine meadows and forests of the Sierra Nevada. Remote Sens. Environ. 128, 44–57. https://doi.org/10.1016/j.rse.2012.09.016

Scholl, A.E., Taylor, A.H., 2010. Fire regimes, forest change, and self-organization in an old-growth mixed-conifer forest, Yosemite National Park, USA. Ecol. Appl. 20, 362–380. https://doi.org/10.1890/08-2324.1

Shive, K.L., Preisler, H.K., Welch, K.R., Safford, H.D., Butz, R.J., O'Hara, K.L., Stephens, S.L., 2018. From the stand scale to the landscape scale: predicting the spatial patterns of forest regeneration after disturbance. Ecol. Appl. 28, 1626–1639. https://doi.org/10.1002/eap.1756

Smith, A.L., Blanchard, W., Blair, D.P., Mcburney, L., Banks, S.C., Driscoll, D.A., Lindenmayer, D.B., 2016. The dynamic regeneration niche of a forest following a rare disturbance event. Divers. Distrib. 22, 457–467. https://doi.org/10.1111/ddi.12414

Song, Y.Y., Simard, S.W., Carroll, A., Mohn, W.W., Zeng, R. Sen, 2015. Defoliation of interior Douglas-fir elicits carbon transfer and stress signalling to ponderosa pine neighbors through ectomycorrhizal networks. Sci. Rep. 5, 1–9. https://doi.org/10.1038/srep08495

Stavros, N.E., Tane, Z., Kane, V.R., Veraverbeke, S., Mcgaughey, R.J., Lutz, J.A., Ramirez, C., Schimel, D., 2016. Unprecedented remote sensing data over King and Rim megafires in the Sierra Nevada Mountains of California. Ecology 97, 3334. https://doi.org/10.1002/ecy.1577

Stevens-Rumann, C.S., Kemp, K.B., Higuera, P.E., Harvey, B.J., Rother, M.T., Donato, D.C., Morgan, P., Veblen, T.T., 2018. Evidence for declining forest resilience to wildfires under climate change. Ecol. Lett. 21, 243–252. https://doi.org/10.1111/ele.12889

Stewart, J.A.E., van Mantgem, P.J., Young, D.J.N., Shive, K.L., Preisler, H.K., Das, A.J., Stephenson, N.L., Keeley, J.E., Safford, H.D., Wright, M.C., Welch, K.R., Thorne, J.H., 2021. Effects of postfire climate and seed availability on postfire conifer regeneration. Ecol. Appl. 31, 1–14. https://doi.org/10.1002/eap.2280

Teich, M., Becker, K.M.L., Raleigh, M.S., Lutz, J.A., 2022. Large-diameter trees affect snow duration in post-fire old-growth forests. Ecohydrology 15. https://doi.org/10.1002/eco.2414

Teste, F.P., Simard, S.W., Durall, D.M., Guy, R.D., Jones, M.D., Schoonmaker, A.L., 2009. Access to mycorrhizal networks and roots of trees: Importance for seedling survival and resource transfer. Ecology 90, 2808–2822. https://doi.org/10.1890/08-1884.1

Urza, A.K., Sibold, J.S., 2017. Climate and seed availability initiate alternate post-fire trajectories in a lower subalpine forest. J. Veg. Sci. 28, 43–56. https://doi.org/10.1111/jvs.12465

USDI National Park Service, 2003. Fire monitoring handbook. Fire Management Program Center, National Interagency Fire Center, Boise, ID.

van Mantgem, P.J., Schwartz, M., 2003. Bark heat resistance of small trees in Californian mixed conifer forests: testing some model assumptions. For. Ecol. Manage. 178, 341–352. https://doi.org/10.1016/S0378-1127(02)00554-6

van Wagtendonk, J.W., 1983. Prescribed fire effects on forest understory mortality, in: Proceedings of the 7th Conference on Fire and Forest Meteorology. American Meteorological Society, Boston, pp. 136–138.

van Wagtendonk, J.W., Lutz, J.A., 2007. Fire regime attributes of wildland fires in Yosemite National Park, USA. Fire Ecol. 3, 34–52. https://doi.org/10.4996/fireecology.0302034

Voelker, S.L., DeRose, R.J., Bekker, M.F., Sriladda, C., Leksungnoen, N., Kjelgren, R.K., 2018. Anisohydric water use behavior links growing season evaporative demand to ring-width increment in conifers from summer-dry environments. Trees - Struct. Funct. 32, 735–749. https://doi.org/10.1007/s00468-018-1668-1

Welch, K.R., Safford, H.D., Young, T.P., 2016. Predicting conifer establishment post wildfire in mixed conifer forests of the North American Mediterranean-climate zone. Ecosphere 7. https://doi.org/10.1002/ecs2.1609

Young, D.J.N., Werner, C.M., Welch, K.R., Young, T.P., Safford, H.D., Latimer, A.M., 2019. Post-fire forest regeneration shows limited climate tracking and potential for drought-induced type conversion. Ecology 100, 1–13. https://doi.org/10.1002/ecy.2571

Zald, H.S.J., Gray, A.N., North, M., Kern, R.A., 2008. Initial tree regeneration responses to fire and thinning treatments in a Sierra Nevada mixed-conifer forest, USA. For. Ecol. Manage. 256, 168–179. https://doi.org/10.1016/j.foreco.2008.04.022
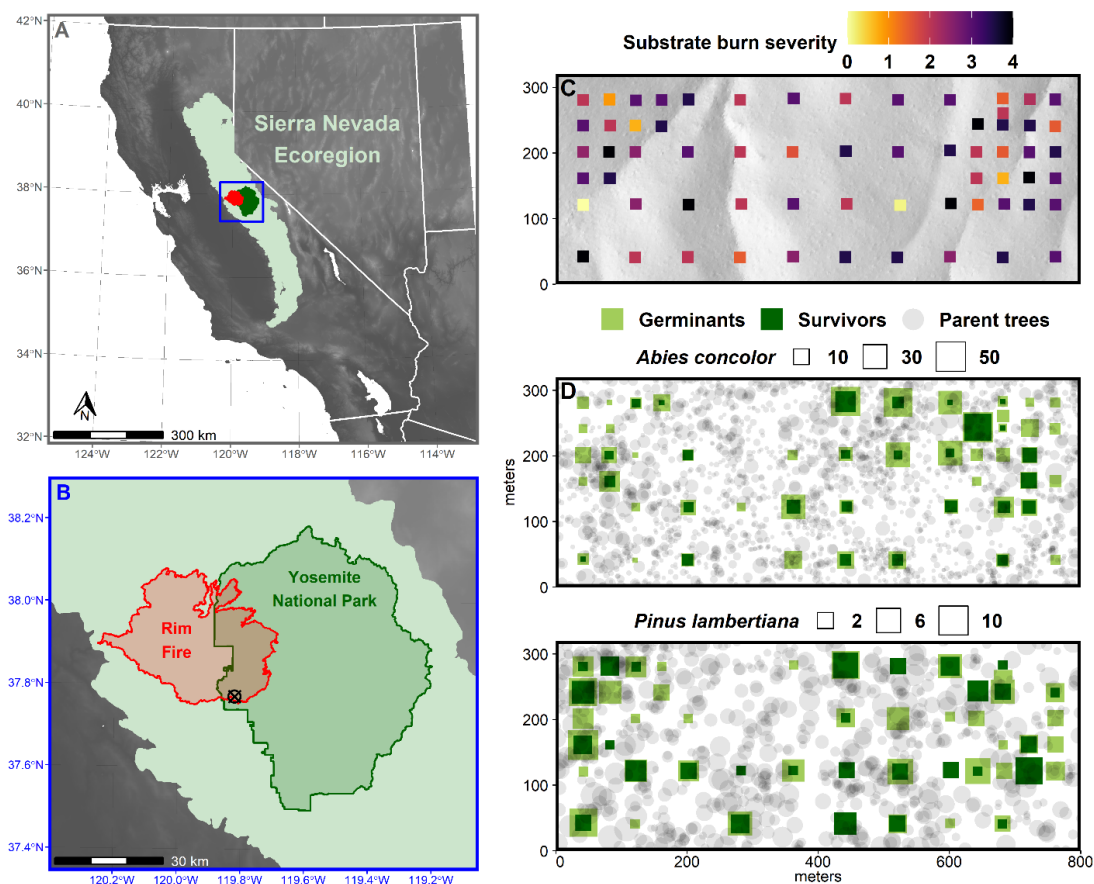
Figures

Figure 3.1. The Yosemite Forest Dynamics Plot (YFDP) is a 25.6-ha permanent study area in an old-growth *Abies concolor–Pinus lambertiana* forest in Yosemite National Park in the central Sierra Nevada, California, USA (A). The YFDP burned at low to moderate severity in the 2013 Rim Fire (B), after which 1-m^2 seedling quadrats and adjacent seed traps were installed at 63 locations (C). Sampling density was higher in areas with a southern aspect (northwest corner) or high abundance of *Quercus kelloggii* (northeast corner). Only seedlings that germinated in 2014 or 2015 are included as germinants and survivors (D). Survivor seedlings were alive in 2020. Trees that were alive in 2014 with ≥ 30 cm DBH for *A. concolor* and ≥ 50 cm DBH for *P. lambertiana* are depicted as parent trees. Stem diameters appear 20 times larger than their measured size.
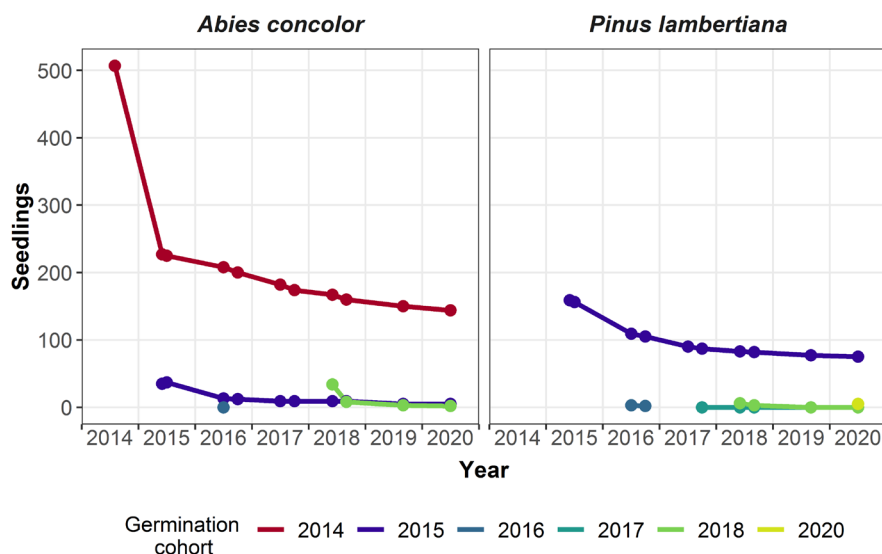
Figure 3.2. Seedling abundance by germination cohort in 63, 1-m^2 quadrats in the Yosemite Forest Dynamics Plot, which burned at low to moderate severity in the fall of 2013. Seedling inventories began in 2014. See Figure B.1 to compare seedling abundance in unburned patches.
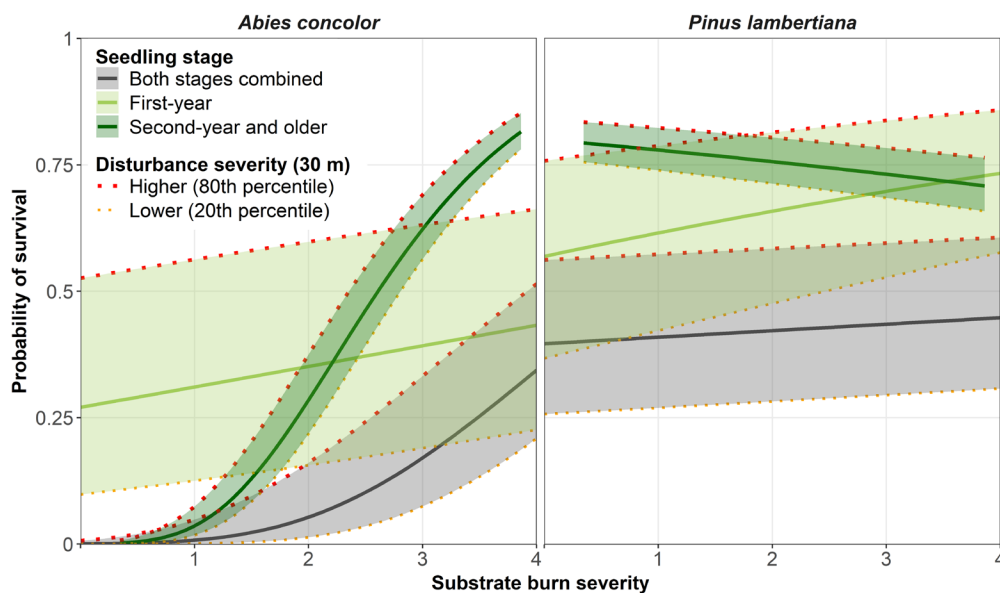
Figure 3.3. Modeled survival of *A. concolor* and *P. lambertiana* seedlings that germinated in 2014 or 2015 after a low- to moderate-severity fire in the fall of 2013. To compare the influence of disturbance severity on survival during different life stages, we fit three models (Table B.6): 1) seedling survival from germination until 2020 (Both stages combined), 2) seedling survival during the germination year (First-year), and 3) seedling survival after the germination year until 2020 (Second-year and older). Solid lines represent the 50th percentile of neighborhood disturbance severity, which was based on tree mortality within the first two years after the fire.
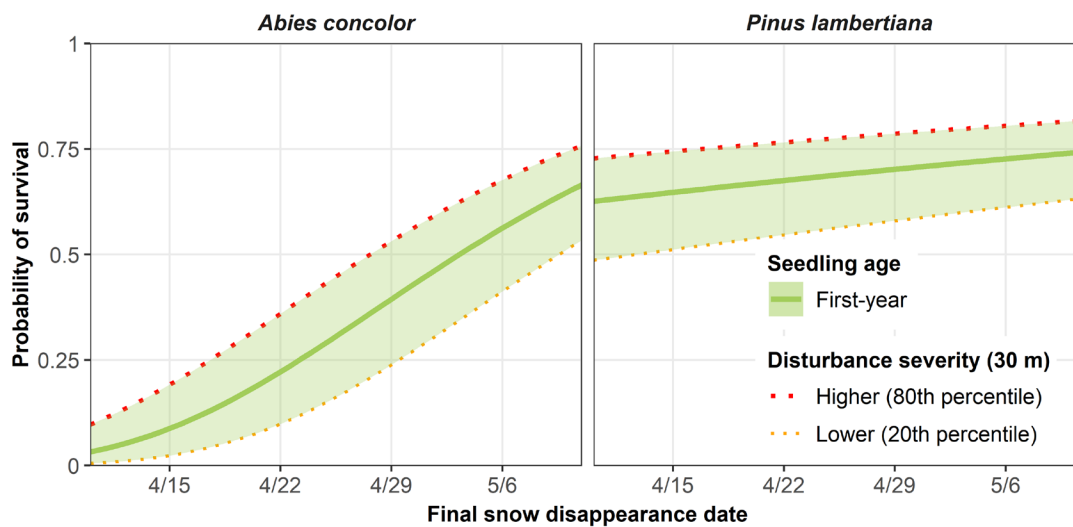
Figure 3.4. Modeled survival of *A. concolor* and *P. lambertiana* seedlings that germinated in 2015 after a low- to moderate-severity fire in the fall of 2013. We compared the influence of disturbance severity and snow duration on first-year survival (Table B.7). Solid lines represent the 50th percentile of neighborhood disturbance severity, which was based on tree mortality within the first two years after the fire.
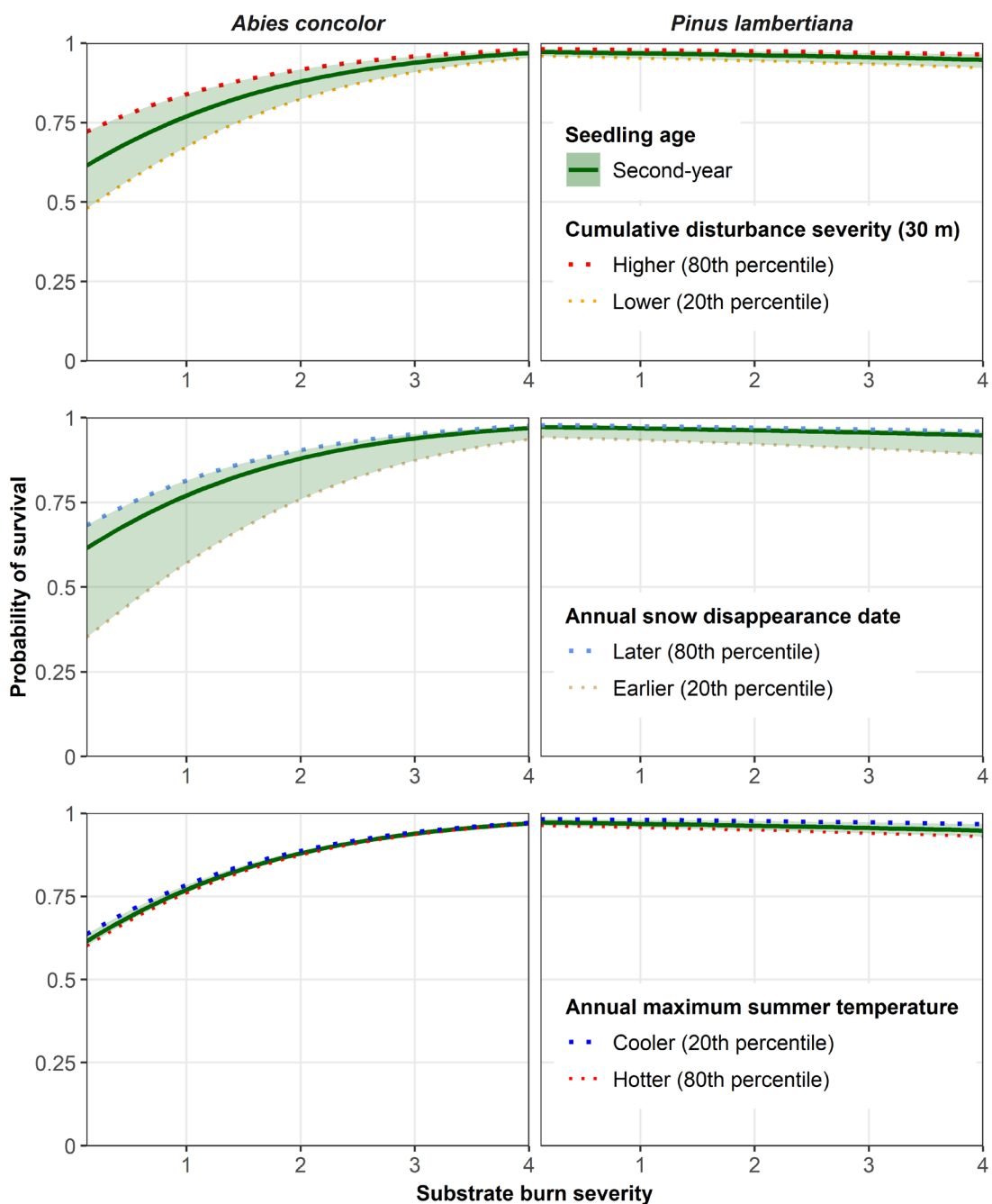
Figure 3.5. Modeled annual survival of second-year *A. concolor* and *P. lambertiana* seedlings that germinated in 2014 or 2015 after a fire in the fall of 2013. We compared the effects of disturbance severity, snow duration, and summer maximum temperature on annualized seedling survival (Table B.7). Solid lines represent the 50th percentile of the variable identified in each legend. Variables not depicted were set to 50th percentile values.
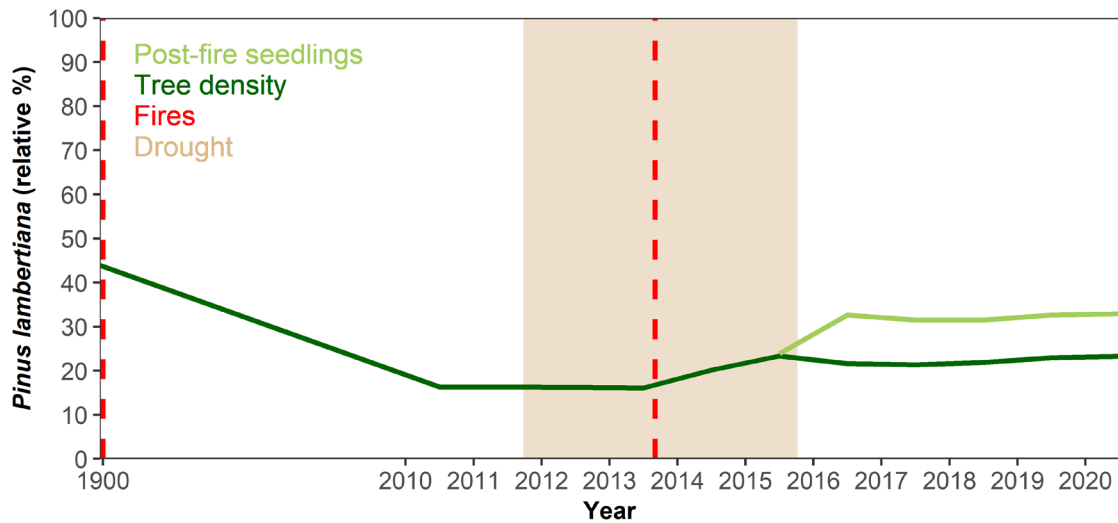
Figure 3.6. Historical (1900) and contemporary (2010–2020) relative percentage of *P. lambertiana* to *A. concolor* in the Yosemite Forest Dynamics Plot (YFDP). The Rim Fire began burning the YFDP on September 1, 2013. The YFDP had not burned since 1900. Modeled historical tree densities are from Barth et al. (2015). Contemporary tree and seedling data are resolved to the census month. Seedling data include only the 2014 and 2015 cohorts of *P. lambertiana* and *A. concolor* in the 63 quadrats. The initial seedling ratio compares germinant counts of both species for 2014 and 2015 combined; subsequent ratios are for each year. Initially, germinant ratios matched tree ratios, but the relative abundance of *P. lambertiana* then increased due to differential seedling mortality during the germination years.

CHAPTER IV

ANNUALLY RESOLVED IMPACTS OF FIRE MANAGEMENT ON CARBON

STOCKS IN YOSEMITE AND SEQUOIA & KINGS CANYON NATIONAL PARKS[1]

Abstract

Fire is a seasonal disturbance in montane forests of the Sierra Nevada that directly impacts tree species composition, forest structure, carbon storage, and carbon accumulation via tree growth. Since the 1970s, land managers in the Sierra Nevada have used prescribed fire and lightning ignitions to restore historic fire regimes after nearly a century of fire exclusion, but the impacts of fire reintroduction on forest functions, such as carbon accumulation, remain unquantified. We examined the effects of lower-severity fire on carbon allocation to tree boles by analyzing the tree-ring widths of seven mixed-conifer species: *Abies concolor* (white fir), *Abies magnifica* (red fir), *Calocedrus decurrens* (incense-cedar), *Pinus contorta* (lodgepole pine), *Pinus jeffreyi* (Jeffrey pine), *Pinus lambertiana* (sugar pine), and *Pinus ponderosa* (ponderosa pine). We used 1,619 increment cores from 888 trees collected at 105 burned and unburned sites in Yosemite and Sequoia & Kings Canyon National Parks to partition variability in post-fire growth by (1) species, (2) tree diameter, (3) fire severity, and (4) fire cause. We observed three common growth responses within five years after fire for all seven species: no change from pre-fire growth, an initial growth decrease followed by an increase, and the reverse. Post-fire growth decreases were much more common than growth increases. Proportions

---

[1]This chapter was first published as a project completion report to the National Park Service on December 31, 2014: Becker, K. M. L., and J. A. Lutz. 2014. Annually resolved impacts of fire management on carbon stocks in Yosemite and Sequoia & Kings Canyon National Parks. Report to the National Park Service

of growth decreases one year after fire ranged from 0.24 for *P. jeffreyi* to 0.43 for *P. lambertiana*, while proportions of growth increases ranged from 0.00 for *P. lambertiana* to 0.05 for *A. concolor*, *P. contorta*, and *P. ponderosa*. This pattern held when tree cores were categorized by diameter class, fire severity, and fire cause. High-severity fire was associated with the highest proportion (0.80) of growth decreases one and two years post-fire, while undifferentiated-severity fire was associated with the lowest proportions (0.11 and 0.09). Overall, post-fire growth patterns often did not differ more than one standard deviation from growth fluctuations at adjacent unburned plots. This result suggests that fire use in Yosemite and Sequoia & Kings Canyon National Parks will not adversely affect the capacity of surviving trees to attain pre-fire rates of carbon accumulation within five years after a fire event.

Introduction

Fire is a seasonal disturbance in montane forests of the Sierra Nevada that directly impacts tree species composition, vertical and horizontal forest structure, and forests' ecological functions, including hydrologic regulation, provision of wildlife habitat, above- and below-ground carbon storage in trees, and carbon accumulation via tree growth. Historically, a mean fire return interval of 2 to 20 years characterized the lower montane zone of the Sierra Nevada (van Wagtendonk et al., 2020; van Wagtendonk and Fites-Kaufman, 2006). Frequent fire interacted with species composition and structure to perpetuate a low-severity regime. Nearly a century of fire exclusion, however, has resulted in a threefold increase in tree density and ladder fuel abundance driven by fire-sensitive, shade-tolerant *Abies concolor* (white fir) and *Calocedrus decurrens* (incense-cedar; Parsons and DeBenedetti, 1979; Scholl and Taylor, 2010). The greater fuel load

has increased the likelihood of high-severity fire, precipitating a shift in the fire regime of Yosemite National Park from generally low severity to mixed severity (Thode et al., 2011). Large-diameter trees, particularly large *Pinus* individuals, have concurrently decreased in abundance, potentially due to increased susceptibility to pathogens (e.g., *Heterobasidium annosum*), bark beetles (e.g., *Dendroctonus* spp.), resource limitation induced by high tree density, or a combination of these factors (Furniss et al., 2022; Lutz et al., 2009a; Sherman and Warren, 1988).

Maintaining forests with fire-resistant and drought-tolerant constituents is an important management objective, particularly considering projections of warmer temperatures and more variable precipitation patterns that may reduce tree establishment and survivorship and increase fire size, frequency, and severity (IPCC, 2013; Kolb et al., 2007; Littell et al., 2009; Lutz et al., 2009b; Marshall et al., 2019; McDowell et al., 2008; Parks and Abatzoglou, 2020; Westerling et al., 2006). Since the 1970s, land managers in the Sierra Nevada have used prescribed fire and lightning ignitions to restore historic species composition, reduce tree density, and remove surface and ladder fuels that facilitate high-severity fire (van Wagtendonk, 2007). Effects of these management actions on the diameter distributions of individual species and on basic structural metrics, such as tree density and basal area, have been well documented (Becker and Lutz, 2016; Collins et al., 2011; Furniss et al., 2019; North et al., 2007), but the impacts of fire reintroduction on forest functions, such as carbon accumulation from tree growth, remain unquantified in many lower montane Sierra Nevada forest systems. Fire effects in upper montane forests have received even less attention. Historically, upper montane forests were characterized by median fire return intervals between 12 and 69 years (van

Wagtendonk and Fites-Kaufman, 2006). In some upper montane areas, therefore, fire and forest interactions still lie within the historic range of variability (Fulé and Laughlin, 2007).

Quantifying the effects of fire on carbon accumulation of surviving trees is necessary to inform management decisions in lower montane forests, where fire is used as a restoration tool; the same study of carbon accumulation in upper montane forests is of ecological interest because it provides an opportunity to quantify the impact of fire in systems less affected by the legacy of fire suppression.

The objective of this study was to examine the effects of lower-severity fire on carbon allocation to tree boles by analyzing the tree-ring widths of seven mixed-conifer tree species that vary in tolerance to fire and drought: *A. concolor*, *Abies magnifica* (red fir), *C. decurrens*, *Pinus contorta* (lodgepole pine), *Pinus jeffreyi* (Jeffrey pine), *Pinus lambertiana* (sugar pine), and *Pinus ponderosa* (ponderosa pine; Table C.1). We assessed differences in growth patterns at adjacent burned and unburned sites to remove climate-related trends and partitioned variability in growth response by (1) species, (2) tree diameter, (3) fire severity, and (4) fire cause.

Methods

Study area

Yosemite and Sequoia & Kings Canyon National Parks are located on the western slope of the central Sierra Nevada (Figure 4.1). Elevation in Yosemite ranges from 648 m in the foothills to 3,997 m at the crest of Mt. Lyell. Elevation in Sequoia & Kings Canyon ranges from 520 m to 4,418 m at the crest of Mt. Whitney. The climate is Mediterranean

with cool, wet winters and warm, dry summers.

Lower montane mixed-conifer forests chiefly occupy an elevational band from 1,500 m to 1,650 m (van Wagtendonk and Fites-Kaufman, 2006). Principal tree species include *A. concolor, C. decurrens, P. jeffreyi*, *P. lambertiana, P. ponderosa,* and *Quercus kelloggii* (California black oak). *Pinus ponderosa* and *Q. kelloggii* are common at lower elevations, where reduced water availability limits the abundance of *A. concolor*. *Abies concolor*–mixed-conifer forests generally occupy higher elevation sites with deeper soils. Subdominant *C. decurrens* and *P. lambertiana* are found across the full extent of the lower montane range.

Upper montane mixed-conifer stands are common between 1,950 m and 2,100 m (van Wagtendonk and Fites-Kaufman, 2006). *Abies magnifica* intersperses with *A. concolor* at lower elevations and with *P. contorta, P. jeffreyi*, *Pinus monticola* (western white pine), and *Tsuga mertensiana* (mountain hemlock) at higher elevations. *Juniperus occidentalis– Pinus jeffreyi* woodlands occupy granitic domes.

Fire suppression in these forests began in 1890 and persisted until 1968 in Sequoia & Kings Canyon and until 1972 in Yosemite, when park managers began to use prescribed fire and lightning ignitions to restore historical fire regimes (Kilgore and Briggs, 1972; van Wagtendonk, 2007). A network of forest patches has resulted, some that have burned up to five times over the past 40 years and others that have not burned since before 1890 (van Wagtendonk et al., 2012).

Site selection

Plot locations were determined a priori by geographic information system based on forest type (Keeler-Wolf et al., 2012; *Sequoia and Kings Canyon National Parks photo*

interpretation report, 2007); burn status; fire severity; slope; and distance from streams, roads, and trails. Plots were at least 50 m within the intended forest type and fire perimeter; varied in slope from 0° to 35°; and were > 100 m from streams, roads, and trails. We assessed forest type and burn status in the field and repositioned plots to better meet specifications if necessary. Balanced representation of burned and unburned forests dominated by *P. ponderosa, A. concolor, P. jeffreyi,* and *A. magnifica* was a key objective. Burned sites were prioritized over unburned sites in *P. contorta* forests due to the availability of similar data collected in 2010 from unburned stands of *P. contorta* in Sequoia & Kings Canyon.

Data collection

Between June and September of 2011, we established 105, 0.1-ha circular plots, 46 that had not burned since at least 1930 (hereafter, unburned; Yosemite: 35 plots; Sequoia & Kings Canyon: 11 plots) and 59 that had burned one to five times since 1930 (hereafter, burned; Yosemite: 32 plots; Sequoia & Kings Canyon: 27 plots; Figure 4.1). The burned plots were located within the perimeters of 47 fires (Table C.2; Eidenshink et al., 2007; Lutz et al., 2011). We used a handheld GPS set to the datum NAD83 to determine the UTM coordinates at plot center. Species and diameter at breast height (DBH) were recorded for stems ≥ 2.5 cm DBH. Two increment cores were extracted at breast height from 10 trees ≥ 8 cm DBH that represented the species and diameter complement of conifers at each plot. Cores were taken parallel to contour lines and oriented 180° from one another. Only cores from *A. concolor*, *A. magnifica*, *C. decurrens*, *P. contorta*, *P. jeffreyi*, *P. lambertiana*, and *P. ponderosa*, the most thoroughly sampled species, were included in this analysis. Diameter distributions of

each plot are available in the appendices of Becker and Lutz (2014).

We used the Relative differenced Normalized Burn Ratio (RdNBR), a Landsat-derived metric developed by Miller and Thode (2007), to characterize fire severity (Table C.3). We placed a 1-ha circular buffer around each plot and extracted RdNBR values from all 30 m × 30 m pixels with centers that fell within the buffer. The pixel values associated with each plot were averaged to obtain RdNBR values with minimal georectification error (Key and Benson, 2006).

Increment core preparation

Increment cores were air-dried, glued to wood mounts, and sanded to a high polish with increasingly smooth sandpaper (220–400 grit). Each core was examined under a microscope, and dots were penciled on the cores to mark each decade. All cores were scanned at 1200 dots per inch, and ring-widths were measured manually in WinDENDRO (version 2012a). Unusual rings were checked under a microscope to ensure correct measurement. Lists of marker years were manually generated for each core based on inspection of the scanned image. Core series from the same tree were crossdated and then compared with crossdated tree-ring series from the same site. Seventy-eight trees from burned plots and 69 trees from unburned plots were excluded from further analysis because neither increment core from the tree crossdated well (Table 4.1). Of the trees retained, 391 trees from burned plots and 340 trees from unburned plots were represented by two cores; 115 trees from burned plots and 42 trees from unburned plots were represented by single cores. Missing rings were identified and inserted in one core of 24 trees from burned plots and in one core of 5 trees from unburned plots. Missing rings were identified and inserted in both cores of 13 trees from burned plots (Table 4.1).

Analysis

Tree cores were categorized by species and geographic area. We analyzed species separately because we expected species to respond differently to fire. Degree of fire tolerance as well as the adaptations that confer fire resistance differ among species (Table C.1). Moreover, we expected fire behavior to differ depending on the species present. Species composition varies with site productivity, which can influence fire severity via the amount and type of accumulated fuel (Guarín and Taylor, 2005; Kane et al., 2015). Species, themselves, also generate unique fuel beds. Short fir needles produce a more compact layer that burns less intensely relative to pine needles (Stephens et al., 2004; van Wagtendonk and Moore, 2010). Tree cores of each species were grouped by geographic area so that tree-ring series from burned and unburned plots would share the same climate signal.

Raw ring-width data were used in this analysis. Series from the same tree were averaged together and standardized to enable comparisons of fire effects on growth among trees of different sensitivities. Ring-width indices for each tree were created by subtracting the series mean from the raw ring-width values and dividing by the series standard deviation. The influence of early growth on the ring-width indices was minimized by excluding growth rings that were within 10 years of pith.

For each species within each geographic area, the effects of climate on ring-width were removed by subtracting an unburned control chronology from growth chronologies associated with the burned sites (Peterson et al., 1994). One unburned control chronology was developed for each geographic area by averaging together the ring-width indices of trees from that set of unburned plots. Burned plots within each geographic area were

categorized by fire history. A burned chronology was developed for each set of plots with a common fire history by averaging together the ring-width indices of trees from that set of burned plots. The control chronology was subtracted from each burned chronology and the corresponding standard deviation was calculated. These results were graphically displayed over the period of known fire history (1930–2010). To verify that differences in growth could be primarily attributed to fire at the burned sites rather than irregular growth at the control sites, the unburned control indices used to generate the control chronology were categorized by plot and DBH, displayed graphically, and visually examined.

We assessed growth patterns over the five years following each fire event. The duration of post-fire study was consistent with previous work by van Mantgem et al. (2003), who demonstrated that most fire-related mortality occurs within five years after fire. By examining growth over a five-year period, we included both the immediate and delayed effects of the disturbance.

We explored variability in growth response among trees from burned plots by subtracting the unburned control chronology from individual tree indices that were categorized by DBH and plot and graphing the results. We explored variability in growth response among trees from unburned plots by repeating a similar analysis on the unburned control indices of each geographic area to establish a control for growth variability within and among series. We did this by recalculating the unburned chronology to exclude a particular control series. We then subtracted this modified control chronology from the control series we had excluded. These difference indices for unburned plots were categorized by DBH and plot and graphically displayed.

We quantified incidences of anomalous growth increases and decreases that occurred during the five-year period following each fire event. Growth increases and decreases were considered anomalous if they exceeded a threshold value. The appropriate unburned control chronology (paired by species and geographic area) was subtracted from each burned series, creating difference indices. These indices were categorized by sign. The mean and standard deviation were calculated separately for positive and negative indices. Threshold values were generated by adding the standard deviation of the positive indices to the mean of the positive indices and by subtracting the standard deviation of the negative indices from the mean of the negative indices. Five iterations of post-fire indices were compared to the threshold values, beginning with the index of the first year after fire and continuing with the mean of the indices of the first and second, first through third, first through fourth, and first through fifth years after fire. Post-fire indices were averaged because tree growth is autocorrelated, and index values associated with later post-fire years should not be regarded as independent of growth during preceding years. Threshold values were computed five times per series, each time excluding the post-fire year or years under examination from the calculation of the mean and standard deviation.

We identified the effects of species, diameter class, fire severity, and fire cause on the frequency of different types of anomalous post-fire growth. We grouped difference indices by the categories within each variable (i.e., by species, by diameter classes, by the four RdNBR categories [Table C.3], by lightning or management ignition) and calculated the proportions of series exhibiting anomalous growth increases and decreases in each group.

Results

We observed seven common growth responses during the five-year post-fire period:
(1) Post-fire growth did not deviate noticeably from pre-fire growth, (2) Post-fire growth
decreased immediately after fire, followed by an increase, (3) Post-fire growth decreased
immediately after fire, followed by a decrease, (4) Post-fire growth decreased
immediately after fire, followed by a return to pre-fire levels, (5) Post-fire growth
increased immediately after fire, followed by an increase, (6) Post-fire growth increased
immediately after fire, followed by a decrease, or (7) Post-fire growth increased
immediately after fire, followed by a return to pre-fire levels (Table 4.2). Some growth
increases extended for up to eight years post-fire, indicating that a 5-year post-fire
window may not fully capture delayed fire effects. Growth patterns at unburned sites did
not exhibit unusual fluctuations following fire years, supporting the inference that
differences between the burned and unburned chronologies reflected responses to fire at
the burned sites.

All seven species included instances of (1) no apparent fire response, (2) an initial
decrease in growth followed by an increase, and (3) an initial increase in growth followed
by a decrease (Table 4.2, Figure 4.2). The second of these three scenarios manifested
more strongly. The difference index value of zero was more than one standard deviation
from the difference indices during either the initial or the delayed post-fire response for
all species, and during both the initial and delayed response periods for *A. concolor* and
C. decurrens. All species except *P. contorta* demonstrated instances of initial growth
decreases followed by a return to pre-fire growth levels. The remaining growth patterns
of (1) an initial followed by a delayed decrease, (2) an initial followed by a delayed

increase, and (3) an initial increase followed by a return to pre-fire levels were less widespread, occurring in no more than three species each.

Neither plot nor diameter class was a reliable predictor of similar growth responses (Table 4.3, Figure 4.3). Although all species included at least one instance in which growth patterns were similar within the same plot, all species also demonstrated the reverse. Moreover, the level of within-plot variability was not consistent across plots that shared the same fire history. All species except *P. ponderosa* exhibited similar levels of variation in growth patterns among plots with the same fire history, but all seven species also included one or more instances demonstrating the opposite. Diameter class produced the same set of contradictory trends. All species included some instances where trees in the same diameter class had similar growth patterns and others where growth patterns differed. Similarly, growth patterns differed among diameter classes for all species in some but not all cases.

Post-fire growth decreases that fell below the negative threshold value were much more common than growth increases that exceeded the positive threshold value (Tables 4.4–4.7). Proportions of growth decreases one year after fire ranged from 0.24 for *P. jeffreyi* to 0.43 for *P. lambertiana*, while the proportions of growth increases ranged from 0.00 for *P. lambertiana* to 0.05 for *A. concolor*, *P. contorta*, and *P. ponderosa* (Table 4.4). This pattern resurfaced when the same data were split based on diameter class, fire severity, and fire cause (Tables 4.5–4.7). One and two years post-fire, high-severity fire was associated with the highest proportion (0.80) of growth decreases, and undifferentiated-severity fire was associated with the lowest proportions (0.11 and 0.09).

As the post-fire period under scrutiny lengthened, the proportion of series with

anomalous growth decreases tended to diminish, evidence of subsequent increases in growth. This pattern held true for all species except *A. magnifica*, all diameter class except 75.1–90.0 cm and 105.1–120.0 cm, low and moderate but not undifferentiated fire severity, and both lightning- and management-ignited fires (Tables 4.4–4.7). These exceptions to the overall pattern were not correlated (e.g., representation of *A. magnifica* in the 75.1–90.0 cm and 105.1–120.0 cm diameter classes was comparable to other species; Table C.4), suggesting that species, diameter class, and fire severity may have some merit as predictors of post-fire growth, while fire cause does not.

Discussion

The most startling result of this study was the marked lack of strong growth responses to fire relative to the background level of annual variability in growth (Tables 4.2 and 4.3). This was due, in part, to the high level of background variability. Much dendrochronological research targets trees in environments defined by specific limiting factors, such as low temperature or high drought, circumstances that homogenize growth responses. This study, in contrast, included forest-grown trees of diverse ages, diameters, and heights that were located in neighborhoods with different levels of competition, factors likely to coincide with heterogeneous responses to local climate, soil, insects, pathogens, mechanical damage, competitive processes, and fire. Interestingly, however, trees did not often exhibit greater sensitivity to fire than to other drivers of stand dynamics. In cases where growth did demonstrate a fire response, post-fire difference indices generally did not vary more than one standard deviation from the difference index value of zero and often fell within the same range as pre-fire growth (Table 4.2).

We most commonly observed growth decreases following fire, corroborating

previous research on fire and tree growth (Tables 4.4–4.7). Similarly, Slayton (2010) found that fire suppressed growth of *P. ponderosa* in the Payette National Forest of central Idaho for three years after fire, Varner et al. (2009) detected growth decreases in *Pinus palustris* (longleaf pine) one year after fire, and Mutch and Swetnam (1995) found a growth reduction in *Sequoiadendron giganteum* (giant sequoia) for one year after high-severity fire. We demonstrate this trend in six additional species: *A. concolor*, *A. magnifica*, *C. decurrens*, *P. contorta, P. jeffreyi*, and *P. lambertiana* (Table 4.4).

Delayed post-fire growth increases were more common among diameter classes < 75.0 cm DBH, suggesting that trees > 75.0 cm DBH may be sensitive to fire, despite thick bark and elevated crowns (Table 4.5, Table C.1). These results differed from Mutch and Swetnam (1995), who found that *S. giganteum* experienced prolonged growth increases following prescribed fire in the Sierra Nevada, indicating that large-diameter trees, with thick bark to minimize cambial damage, could be more likely to show growth increases during the post-fire period. In our study, the lack of post-fire growth increases in some large-diameter trees could reflect damage to stem and root systems that can occur when accumulations of bark flakes combust, increase the fire temperature near the root collar, and prolong exposure to high temperatures by smoldering (Kolb et al., 2007; Varner et al., 2009). In general, post-fire growth trends varied among trees regardless of diameter class, suggesting that (1) fire severity varied within plots, and (2) trees varied in their growth responses (Table 4.3).

Growth depressions followed by growth increases were common among series associated with low and moderate fire severity but not undifferentiated severity (Table 4.6). This suggests that fires of undifferentiated severity may hardly affect tree growth.

However, undifferentiated fire severity could, in some cases, delineate unburned patches within a fire perimeter (Kolden et al., 2012), which could explain why fewer series associated with undifferentiated severity exhibited growth responses typical of trees burned at higher severity.

Fire cause did not partition variability in post-fire growth response, indicating that the effects of prescribed versus natural fires on tree growth do not differ (Table 4.7). This is a surprising result, given that prescribed fires allegedly are more uniform, leaving behind fewer unburned patches and burning areas more consistently at undifferentiated and low severity. We suggest that fire cause did not matter because our study only included cores from trees that survived fire and were sufficiently undamaged to enable crossdating. Among this population, cause of ignition may have had minimal influence on growth because we pre-selected for trees that experienced a similar level of exposure to fire.

Overall, the scope of inference of this study was limited to fire effects on trees that were (1) long-term fire survivors and (2) sensitive to similar limiting factors and therefore possible to crossdate. The selection of cores included here may consequently represent only a fraction of the possible growth responses to fire. This is a limitation common to all post-fire studies where pre-fire demography data are unavailable (Lutz et al., 2018b).

While our study's scope was limited, our objective was broad—to examine the growth responses of seven species across their full diameter range to undifferentiated-, low-, moderate-, and high-severity fire. Due to data collection constraints, we were unable to conduct a fully balanced study. The burned and unburned series of each species that were differenced to identify the effects of fire on growth were not always located in

comparably-sized geographic areas, nor were the unburned control chronologies always generated from a consistent number of trees representing the full range of diameter classes. Our results, therefore, do not represent conclusive proportions of different fire responses within each species that a study with a balanced design and larger sample sizes could have revealed.

Although sample depth was not consistent across all species and geographic areas, this study did quantify the effect of fire on tree growth, a key step in assessing the impacts of prescribed and natural fires on carbon accumulation in forests of the Sierra Nevada. We catalogued growth responses of seven mixed-conifer species to prescribed and natural fires and examined growth sensitivity across diameter and fire severity classes. Post-fire growth patterns seldom differed noticeably from growth fluctuations that resulted from other natural disturbances. This result suggests that use of fire in Yosemite and Sequoia & Kings Canyon National Parks will not adversely affect the capacity of surviving trees to attain pre-fire rates of carbon accumulation within five years after a fire event.

References

Becker, K.M.L., Lutz, J.A., 2016. Can low-severity fire reverse compositional change in montane forests of the Sierra Nevada, California, USA? Ecosphere 7, 1–22. https://doi.org/10.1002/ecs2.1484

Becker, K.M.L., Lutz, J.A., 2014. Annually resolved impacts of fire management on carbon stocks in Yosemite and Sequoia & Kings Canyon National Parks, General Technical Report.

Collins, B.M., Everett, R.G., Stephens, S.L., 2011. Impacts of fire exclusion and recent managed fire on forest structure in old growth Sierra Nevada mixed-conifer forests. Ecosphere 2, 1–14. https://doi.org/10.1890/ES11-00026.1

Eidenshink, J., Schwind, B., Brewer, K., Zhu, Z., Quayle, B., Howard, S., 2007. A

project for monitoring trends in burn severity. Fire Ecol. 3, 3–21.

Fulé, P.Z., Laughlin, D.C., 2007. Wildland fire effects on forest structure over an altitudinal gradient, Grand Canyon National Park, USA. J. Appl. Ecol. 44, 136–146. https://doi.org/10.1111/j.1365-2664.2006.01254.x

Furniss, T.J., Das, A.J., van Mantgem, P.J., Stephenson, N.L., Lutz, J.A., 2022. Crowding, climate, and the case for social distancing among trees. Ecol. Appl. 32, 1–14. https://doi.org/10.1002/eap.2507

Furniss, T.J., Larson, A.J., Kane, V.R., Lutz, J.A., 2019. Multi-scale assessment of post-fire tree mortality models. Int. J. Wildl. Fire 28, 46–61. https://doi.org/10.1071/WF18031

Guarín, A., Taylor, A.H., 2005. Drought triggered tree mortality in mixed conifer forests in Yosemite National Park, California, USA. For. Ecol. Manage. 218, 229–244. https://doi.org/10.1016/j.foreco.2005.07.014

IPCC, 2013. Climate change 2013: the physical science basis. New York, New York, USA.

Kane, V.R., Lutz, J.A., Cansler, C.A., Povak, N.A., Churchill, D.J., Smith, D.F., Kane, J.T., North, M.P., 2015. Water balance and topography predict fire and forest structure patterns. For. Ecol. Manage. 338, 1–13. https://doi.org/10.1016/j.foreco.2014.10.038

Keeler-Wolf, T., Moore, P.E., Reyes, E.T., Menke, J.M., Johnson, D.N., Karavidas, D.L., 2012. Yosemite National Park vegetation classification and mapping project report. Natural Resource Report NPS/YOSE/NRTR-2012/598. Fort Collins, Colorado.

Key, C.H., Benson, N.C., 2006. Landscape assessment: Sampling and analysis methods, USDA Forest Service General Technical Report RMRS-GTR-164-CD.

Kilgore, B.M., Briggs, G.S., 1972. Restoring fire to high elevation forests in California. J. For. 70, 266–271.

Kolb, T.E., Agee, J.K., Fulé, P.Z., McDowell, N.G., Pearson, K., Sala, A., Waring, R.H., 2007. Perpetuating old ponderosa pine. For. Ecol. Manage. 249, 141–157. https://doi.org/10.1016/j.foreco.2007.06.002

Kolden, C.A., Lutz, J.A., Key, C.H., Kane, J.T., van Wagtendonk, J.W., 2012. Mapped versus actual burned area within wildfire perimeters: characterizing the unburned. For. Ecol. Manage. 286, 38–47. https://doi.org/10.1016/j.foreco.2012.08.020

Littell, J.S., Mckenzie, D., Peterson, D.L., Westerling, A.L., 2009. Climate and wildfire area burned in western U.S. ecoprovinces, 1916-2003. Ecol. Appl. 19, 1003–1021. https://doi.org/10.1890/07-1183.1

Lutz, J.A., Key, C.H., Kolden, C.A., Kane, J.T., van Wagtendonk, J.W., 2011. Fire frequency, area burned, and severity: A quantitative approach to defining a normal fire year. Fire Ecol. 7, 51–65. https://doi.org/10.4996/fireecology.0702051

Lutz, J.A., Larson, A.J., Swanson, M.E., 2018. Advancing fire science with large forest plots and a long-term multidisciplinary approach. Fire 1, 1–7. https://doi.org/10.3390/fire1010005

Lutz, J.A., van Wagtendonk, J.W., Franklin, J.F., 2009a. Twentieth-century decline of large-diameter trees in Yosemite National Park, California, USA. For. Ecol. Manage. 257, 2296–2307. https://doi.org/10.1016/j.foreco.2009.03.009

Lutz, J.A., van Wagtendonk, J.W., Thode, A.E., Miller, J.D., Franklin, J.F., 2009b. Climate, lightning ignitions, and fire severity in Yosemite National Park, California, USA. Int. J. Wildl. Fire 18, 765–774. https://doi.org/10.1071/WF08117

Marshall, A.M., Abatzoglou, J.T., Link, T.E., Tennant, C.J., 2019. Projected changes in interannual variability of peak snowpack amount and timing in the western United States. Geophys. Res. Lett. 46, 8882–8892. https://doi.org/10.1029/2019GL083770

McDowell, N., Pockman, W.T., Allen, C.D., David, D., Cobb, N., Kolb, T., Plaut, J., Sperry, J., West, A., Williams, D.G., Yepez, E.A., 2008. Mechanisms of plant survival and mortality during drought: why do some plants survive while others succumb to drought? New Phytol. 178, 719–739.

Miller, J.D., Thode, A.E., 2007. Quantifying burn severity in a heterogeneous landscape with a relative version of the delta Normalized Burn Ratio (dNBR). Remote Sens. Environ. 109, 66–80. https://doi.org/10.1016/j.rse.2006.12.006

Mutch, L.S., Swetnam, T.W., 1995. Effects of Fire Severity and Climate on Ring-Width Growth of Giant Sequoia After Fire. Symp. Fire Wilderness Park Manag. Past Lessons Futur. Oppor. March 30-April 1, 1993 Missoula, MT Gen Tech Rep INT-GTR-320 Ogden, UT; US Dep. Agric. For. Serv. Intermt. Res. Stn.

North, M., Innes, J., Zald, H., 2007. Comparison of thinning and prescribed fire restoration treatments to Sierran mixed-conifer historic conditions. Can. J. For. Res. 37, 331–342. https://doi.org/10.1139/X06-236

Parks, S.A., Abatzoglou, J.T., 2020. Warmer and drier fire seasons contribute to increases in area burned at high severity in western US forests from 1985 to 2017. Geophys. Res. Lett. 47, 1–10. https://doi.org/10.1029/2020GL089858

Parsons, D.J., DeBenedetti, S.H., 1979. Impact of fire suppression on a mixed-conifer forest. For. Ecol. Manage. 2, 21–33. https://doi.org/10.1016/0378-1127(79)90034-3

Peterson, D.L., Sackett, S.S., Robinson, L.J., Haase, S.M., 1994. The effects of repeated prescribed burning on pinus ponderosa growth. Int. J. Wildl. Fire 4, 239–247.

https://doi.org/10.1071/WF9940239

Scholl, A.E., Taylor, A.H., 2010. Fire regimes, forest change, and self-organization in an old-growth mixed-conifer forest, Yosemite National Park, USA. Ecol. Appl. 20, 362–380. https://doi.org/10.1890/08-2324.1

Sequoia and Kings Canyon National Parks photo interpretation report, 2007. Redlands, CA.

Sherman, R.J., Warren, R.K., 1988. Factors in Pinus ponderosa and Calocedrus decurrens mortality in Yosemite Valley, USA. Vegetatio 77, 79–85. https://doi.org/10.1007/BF00045753

Slayton, J.D., 2010. Separating the effects of wildfires from climate in growth of ponderosa pine (Pinus ponderosa Douglas ex. C. Lawson), Central Idaho, U.S.A. Master's Thesis, University of Tennessee.

Stephens, S.L., Finney, M.A., Schantz, H., 2004. Bulk density and fuel loads of ponderosa pine and white fir forest. Northwest Sceince 78, 93–100.

Thode, A.E., van Wagtendonk, J.W., Miller, J.D., Quinn, J.F., 2011. Quantifying the fire regime distributions for severity in Yosemite National Park, California, USA. Int. J. Wildl. Fire 20, 223–239. https://doi.org/10.1071/WF09060

van Mantgem, P.J., Stephenson, N.L., Mutch, L.S., Johnson, V.G., Esperanza, A.M., Parsons, D.J., 2003. Growth rate predicts mortality of Abies concolor in both burned and unburned stands 1038, 1029–1038. https://doi.org/10.1139/X03-019

van Wagtendonk, J.W., 2007. The history and evolution of wildland fire use. Fire Ecol. 3, 3–17. https://doi.org/10.4996/fireecology.0302003

van Wagtendonk, J.W., Fites-Kaufman, J.A., 2006. Sierra Nevada bioregion, in: Fire in California's Ecosystems. pp. 264–294.

van Wagtendonk, J.W., Moore, P.E., 2010. Fuel deposition rates of montane and subalpine conifers in the central Sierra Nevada, California, USA. For. Ecol. Manage. 259, 2122–2132. https://doi.org/10.1016/j.foreco.2010.02.024

van Wagtendonk, J.W., Moore, P.E., Yee, J.L., Lutz, J.A., 2020. The distribution of woody species in relation to climate and fire in Yosemite National Park, California, USA. Fire Ecol. 16, 1–23. https://doi.org/10.1186/s42408-020-00079-9

van Wagtendonk, J.W., van Wagtendonk, K.A., Thode, A.E., 2012. Factors associated with the severity of intersecting fires in Yosemite National Park, California, USA. Fire Ecol. 8, 11–31. https://doi.org/10.4996/fireecology.0801011

Varner, J.M., Putz, F.E., O'Brien, J.J., Hiers, K.J., Mitchell, R.J., Gordon, D.R., 2009.

Post-fire tree stress and growth following smoldering duff fires. For. Ecol. Manage. 258, 2467–2474. https://doi.org/10.1016/j.foreco.2009.08.028

Westerling, A.L., Hidalgo, H.G., Cayan, D.R., Swetnam, T.W., 2006. Warming and earlier spring increase western U.S. forest wildfire activity. Science (80-.). 313, 940–943. https://doi.org/10.1126/science.1128834

Tables

Table 4.1. Number of crossdated cores and trees retained for analysis and number of manipulations to those cores based on crossdating inferences. Trees remained in the analysis if at least one core could be crossdated.

Species	Burned						Unburned					
	Collected		Retained		Manipulated		Collected		Retained		Manipulated	
	Cores	Trees	Cores	Trees	Cores	Trees	Cores	Trees	Cores	Trees	Cores	Trees
Abies concolor	214	110	176	100	4	4	195	98	155	80	0	0
Abies magnifica	226	114	208	109	8	6	244	122	225	115	1	1
Calocedrus decurrens	122	63	82	48	8	6	118	60	80	43	3	3
Pinus contorta	164	82	116	71	1	1	33	17	27	15	0	0
Pinus jeffreyi	255	129	199	112	20	15	124	62	103	58	0	0
Pinus lambertiana	74	38	60	33	0	0	69	35	59	31	0	0
Pinus ponderosa	95	48	56	33	9	5	115	57	73	40	1	1
Total	1150	584	897	506	50	37	898	451	722	382	5	5

Table 4.2. Occurrence and strength of seven post-fire growth patterns by species. The initial response refers to the first or second year after fire. The delayed response is capped at five years. A weak response (W) indicates that the difference index value of zero was within one standard deviation of the difference indices. A moderate response (M) indicates that the difference index value of zero was more than one standard deviation from the difference indices either during the initial response period or the delayed response period. A strong response (S) indicates that the difference index value of zero was more than one standard deviation from the difference indices during both the initial and delayed response periods. When no initial and no delayed growth responses were observed, only weak responses were possible. When just no delayed growth response was observed, moderate responses were the strongest response possible. [†]Figure 4.2 shows a moderate example of a decrease and then an increase in growth.

Post-fire growth response	Initial: Delayed:	None None	Decrease Increase	Decrease Decrease	Decrease None	Increase Increase	Increase Decrease	Increase None
Abies concolor		W	WM[†]S	S	W	W	WM	
Abies magnifica		W	WM	W	W		W	W
Calocedrus decurrens		W	WMS		M		M	
Pinus contorta		W	M				W	
Pinus jeffreyi		W	WM		W		M	
Pinus lambertiana		W	WM		M	W	M	W
Pinus ponderosa		W	WM		W	W	W	W

Table 4.3. Variability in post-fire growth within and among plots and diameter classes by species. × indicates that a pattern was observed. [†]Figure 4.3 shows an example of trees in several plots and of several diameter classes exhibiting different growth responses.

Species	Plot				Diameter class			
	Differ within	Similar within	Differ among	Similar among	Differ within	Similar within	Differ among	Similar among
Abies concolor	×[†]	×	×	×	×	×	×	×
Abies magnifica	×	×	×	×	×	×	×	×
Calocedrus decurrens	×	×	×	×	×	×	×	×
Pinus contorta	×	×	×	×	×	×	×	×
Pinus jeffreyi	×	×	×	×	×	×	×	×
Pinus lambertiana	×	×	×	×	×	×	×	×
Pinus ponderosa	×	×	×		×	×	×	×

Table 4.4. Proportion of tree-ring series by species that demonstrated anomalous post-fire growth decreases (-) or increases (+) relative to unburned control chronologies. Values ≥ 0.2 are in bold.

Species	1 year post-fire			1–2 years post-fire			1–3 years post-fire			1–4 years post-fire			1–5 years post-fire		
	-	+	n	-	+	n	-	+	n	-	+	n	-	+	n
Abies concolor	**0.27**	0.05	165	**0.21**	0.04	154	0.16	0.02	136	0.15	0.01	131	0.15	0.02	131
Abies magnifica	**0.33**	0.02	122	**0.34**	0.02	122	**0.38**	0.03	122	**0.34**	0.04	122	**0.37**	0.04	122
Calocedrus decurrens	**0.29**	0.04	93	**0.21**	0.01	89	0.17	0.01	88	0.15	0.03	86	0.10	0.03	86
Pinus contorta	**0.29**	0.05	93	0.19	0.03	86	**0.20**	0.05	86	**0.20**	0.07	86	0.19	0.08	86
Pinus jeffreyi	**0.24**	0.03	199	0.18	0.04	199	0.08	0.03	199	0.07	0.06	199	0.07	0.05	199
Pinus lambertiana	**0.43**	0.00	46	**0.29**	0.02	41	**0.29**	0.03	35	**0.30**	0.03	33	**0.30**	0.06	33
Pinus ponderosa	**0.31**	0.05	65	0.16	0.02	61	**0.21**	0.03	61	0.16	0.03	61	0.11	0.02	61

Table 4.5. Proportion of tree-ring series by diameter class that demonstrated post-fire growth decreases (-) and increases (+) relative to unburned control chronologies. Values ≥ 0.2 are in bold.

Diameter class (cm)	1 year post-fire			1–2 years post-fire			1–3 years post-fire			1–4 years post-fire			1–5 years post-fire		
	-	+	n	-	+	n	-	+	n	-	+	n	-	+	n
8.0–15.0	**0.32**	0.05	38	0.19	0.00	36	0.14	0.00	36	0.08	0.03	36	0.06	0.03	36
15.1–30.0	**0.29**	0.02	123	**0.24**	0.03	116	0.19	0.04	113	**0.21**	0.02	111	0.18	0.02	111
30.1–45.0	**0.28**	0.06	172	**0.21**	0.06	169	0.16	0.04	161	0.15	0.07	160	0.11	0.07	160
45.1–60.0	**0.31**	0.05	131	**0.20**	0.03	122	0.16	0.03	117	0.14	0.04	115	0.15	0.04	115
60.1–75.0	**0.29**	0.03	127	**0.20**	0.02	124	**0.21**	0.03	123	0.17	0.06	122	0.18	0.05	122
75.1–90.0	0.18	0.02	49	**0.22**	0.02	46	**0.20**	0.02	45	**0.20**	0.02	45	**0.22**	0.02	45
90.1–105.0	**0.36**	0.02	61	**0.28**	0.00	58	**0.23**	0.02	56	**0.22**	0.04	55	**0.22**	0.04	55
105.1–120.0	**0.25**	0.03	36	**0.33**	0.03	36	**0.33**	0.03	33	**0.24**	0.03	33	**0.30**	0.03	33
>120	**0.28**	0.00	46	0.18	0.00	45	0.19	0.00	43	**0.22**	0.00	41	**0.20**	0.00	41

Table 4.6. Proportion of tree-ring series by fire severity that demonstrated post-fire growth decreases (-) and increases (+) relative to unburned control chronologies. Values ≥ 0.2 are in bold. RdNBR = Relative differenced Normalized Burn Ratio.

Fire severity (RdNBR)	1 year post-fire			1–2 years post-fire			1–3 years post-fire			1–4 years post-fire			1–5 years post-fire		
	-	+	n	-	+	n	-	+	n	-	+	n	-	+	n
Undifferentiated	0.11	0.03	124	0.09	0.02	124	0.09	0.03	124	0.07	0.03	115	0.07	0.04	115
Low	**0.30**	0.03	267	**0.25**	0.04	267	**0.26**	0.04	257	**0.23**	0.05	257	**0.23**	0.05	257
Moderate	**0.37**	0.01	134	**0.26**	0.03	110	0.18	0.02	100	0.16	0.06	100	0.09	0.04	100
High	**0.80**	0.00	5	**0.80**	0.00	5	—	—	0	—	—	0	—	—	0

Table 4.7. Proportion of tree-ring series by fire cause that demonstrated post-fire growth decreases (-) and increases (+) relative to unburned control chronologies. Values ≥ 0.2 are in bold.

Cause of fire	1 year post-fire			1–2 years post-fire			1–3 years post-fire			1–4 years post-fire			1–5 years post-fire		
	-	+	n	-	+	n	-	+	n	-	+	n	-	+	n
Lightning-ignited	**0.30**	0.03	337	**0.23**	0.03	330	0.18	0.02	330	0.15	0.05	321	0.14	0.04	321
Management-ignited	**0.28**	0.04	446	**0.22**	0.03	422	**0.20**	0.03	397	0.19	0.04	397	0.19	0.04	397

Figures
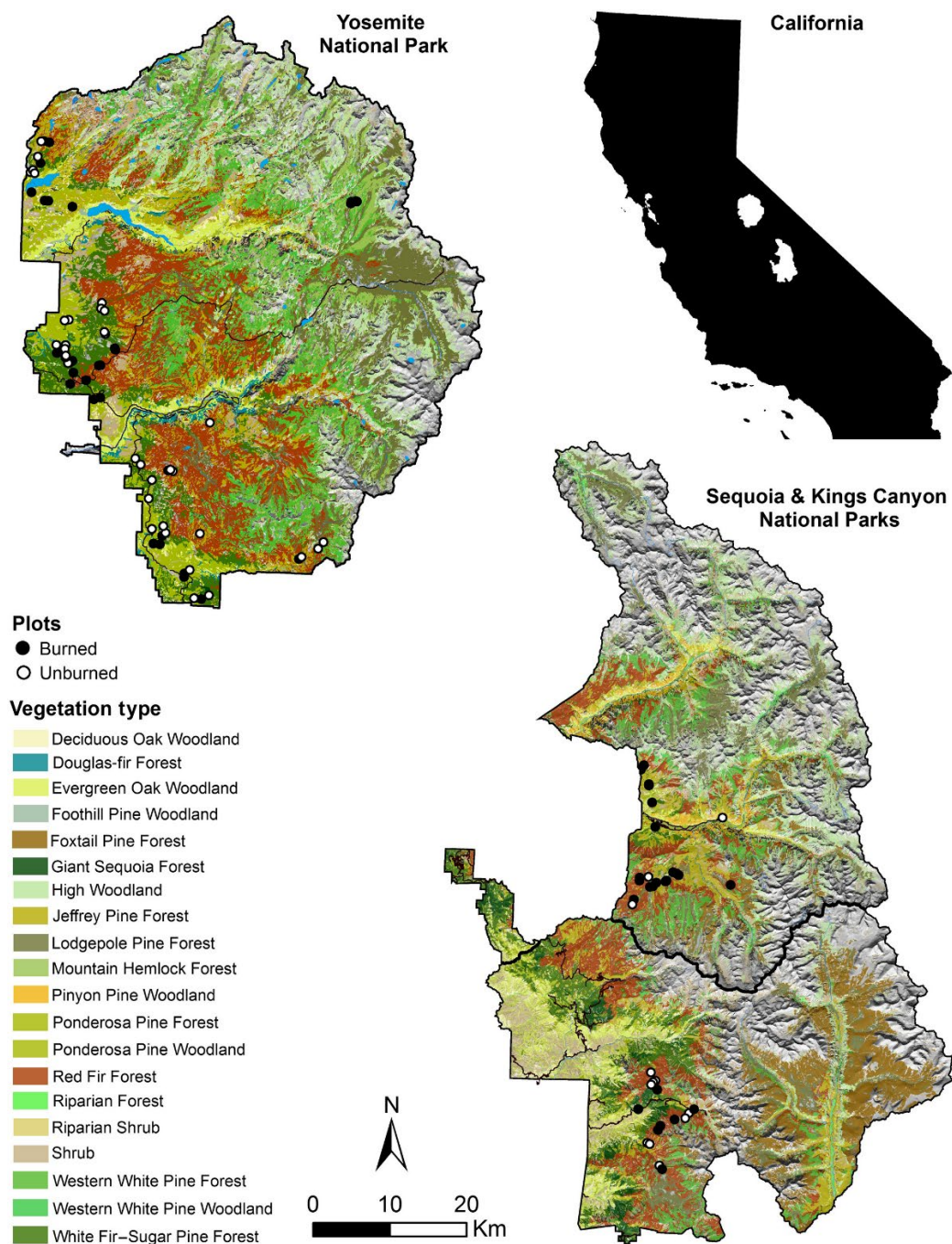
Figure 4.1. Locations of 105 study sites in Yosemite and Sequoia & Kings Canyon National Parks, California, USA, spanning lower and upper montane vegetation types (Becker and Lutz, 2016).
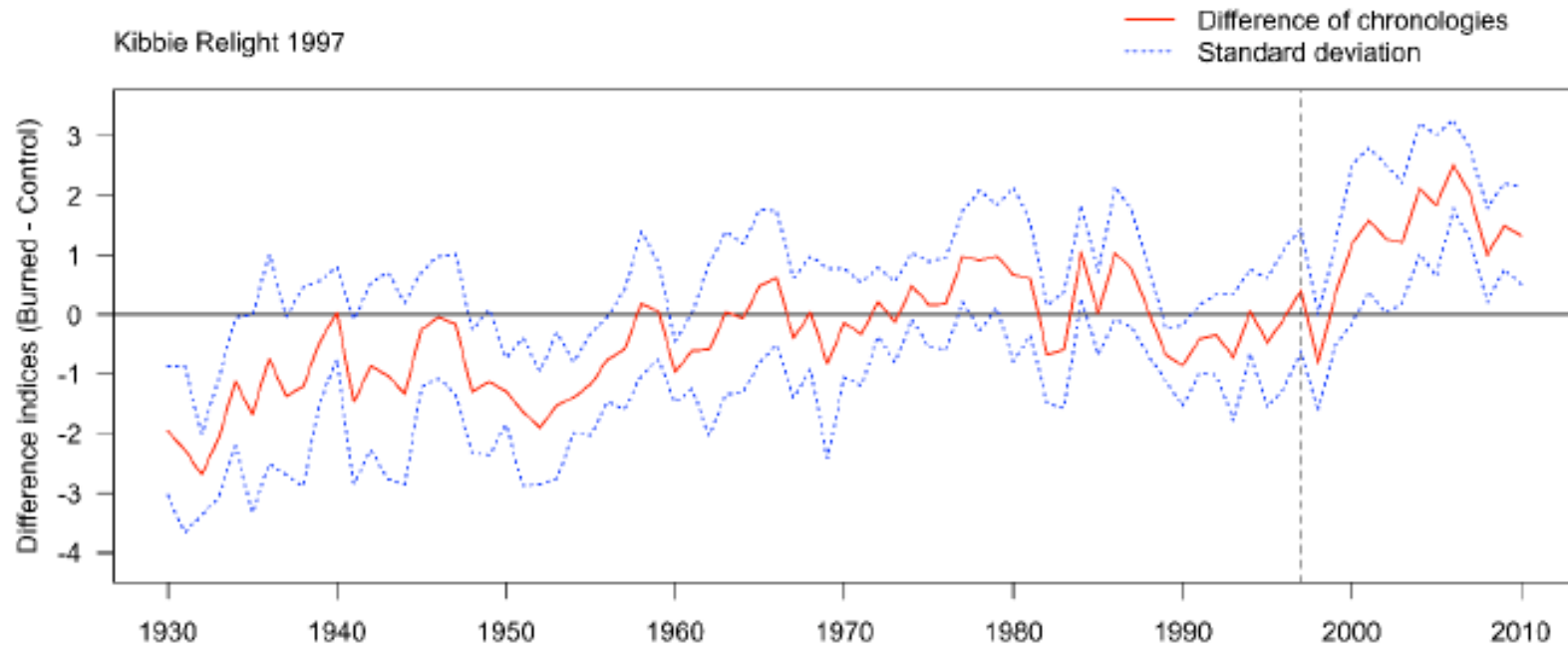
Figure 4.2. Difference indices (burned chronology minus control chronology) of *A. concolor* in the Kibbie Creek region of Yosemite National Park, demonstrating a moderate example of an initial growth decrease followed by an increase after fire. The burned chronology was developed from 6 cores representing 3 trees that occupied 1 plot within the perimeter of the 1997 management-ignited Kibbie Relight fire. The unburned chronology was developed from 12 cores representing 6 trees that occupied 2 plots in areas not burned since at least 1930.
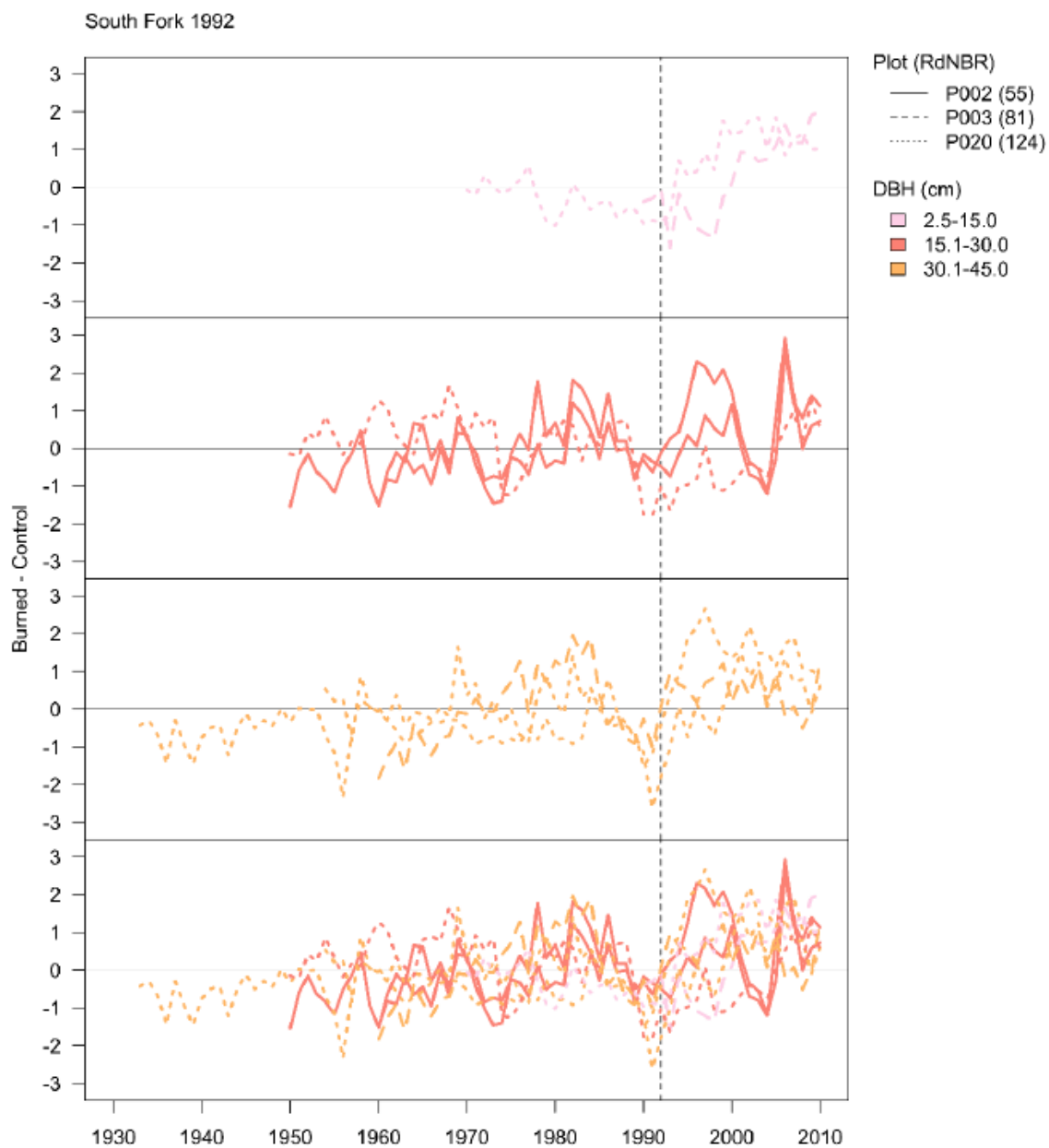
Figure 4.3. Difference indices (burned series minus control chronology) categorized by diameter class (upper panels) and shown together (bottom panel) of *A. concolor* in the Crane Flat region of Yosemite National Park, demonstrating an example of different growth responses. The burned series were developed from 15 cores representing 8 trees that occupied 3 plots within the perimeter of the 1992 management-ignited South Fork fire. The unburned chronology was developed from 78 cores representing 40 trees that occupied 9 plots in areas not burned since at least 1930.

CHAPTER V

CAUSES OF MORTALITY WITHIN TREE NEIGHBORHOODS AFFECT

GROWTH RATES OF SURVIVING TREES

Abstract

As large-diameter trees decline in abundance globally and compound disturbances

involving fire, drought, and biotic mortality agents become more common in forests,

understanding how disturbance-related changes to tree neighborhoods affect the growth

of surviving trees is increasingly important. We used a spatially explicit dataset of 34,175

trees from a study area that burned at low to moderate severity in 2013 to investigate how

post-fire changes to tree neighborhoods affected post-fire radial growth. We used

diameter measurements taken in 2014 and 2019 to estimate post-fire radial growth of

3,652 *Abies concolor* (white fir) and *Pinus lambertiana* (sugar pine) trees that survived

for at least seven years after fire. We accounted for the effects of fire injury on growth by

including measured crown injury as a covariate. To compare the relative influence of

reduced competition, which could increase radial growth, and the presence of biotic

mortality agents, which might decrease radial growth, we categorized neighboring trees

that died after the fire by mortality cause. For each focal tree, we computed crowding

metrics for each mortality cause and used these metrics to show that post-fire

neighborhood changes attributed to different causes had species-specific effects on post-

fire growth of surviving trees. Neighborhoods where competition decreased post-fire due

to fire and mechanical damage were associated with greater post-fire radial growth of

both *A. concolor* and *P. lambertiana*, and this relationship was nearly twice as strong for

P. lambertiana. In contrast, mortality of conspecific neighbors due to bark beetles did not significantly affect post-fire radial growth, suggesting that any advantage from reduced competition was counterbalanced by increased demand for defense. Tree diameter also interacted with neighborhood change for *P. lambertiana*, but this relationship was not affected by cause of mortality: small-diameter (10-cm) *P. lambertiana* exhibited a four-fold larger increase in relative growth than large-diameter (60-cm) *P. lambertiana* as neighborhood change ranged from 0 to 100% mortality. We show that the cause of mortality influences the effect of neighborhood change on growth of surviving trees in species-specific ways, allowing species differences in mortality factors to affect post-disturbance growth rates and the species composition of large-diameter tree recruitment.

Introduction

As large-diameter trees decline in abundance globally and compound disturbances involving fire, drought, and biotic mortality agents become more common in forests (Furniss et al., 2022; Lindenmayer et al., 2012; Marshall et al., 2019; Parks and Abatzoglou, 2020), understanding the effects of disturbance on the growth of surviving trees is increasingly important. Recruitment of trees into large-diameter size classes matters because large-diameter trees help maintain forest cover and seed production (Lindenmayer et al., 2012; Lutz et al., 2018a; Qiu et al., 2022). Retaining large-diameter tree populations depends on their resilience to future disturbances, making species composition of these populations an important consideration (Eidson et al., 2017; Lindenmayer et al., 2012). Post-fire mixed-conifer forests provide an opportunity to study species-specific effects of tree injury and neighborhood change on the growth of

surviving trees after disturbance.

Fire injuries compromise trees' physiological systems in ways that increase the probability of mortality and reduce growth (Furniss et al., 2019; Smith et al., 2016; Steady et al., 2019). High temperatures from fire can deform xylem cells and kill cambial and leaf tissue, reducing hydraulic efficiency and requiring trees to use carbon reserves for repair (Bär et al., 2019; Varner et al., 2021). Together, impaired hydraulic function and carbon depletion decrease resource acquisition, strain trees' capacity to defend against insects and pathogens, and reduce the amount of carbon allocated toward growth (Huang et al., 2020; Valor et al., 2018).

While fire injury can impair a tree's ability to acquire carbon, changes to the neighborhood around that tree can influence resource availability and allocation to defense (Furniss et al., 2022; Germain and Lutz, 2021). Neighboring trees compete for light, water, and nutrients. Thus, mortality of neighbors can liberate resources, increasing growth of surviving trees (Hood et al., 2016). However, mortality of neighbors could also indicate proximity of biotic mortality agents, such as genus-specific bark beetles or generalist fungal pathogens (Das et al., 2016; Raffa and Berryman, 1983). In such cases, the need for greater investment in defense (e.g., against bark beetles) or the reduction in resource acquisition from damage (e.g., from slow-acting fungal pathogens) could negate the positive effect of reduced competition on growth (Hood et al., 2016).

Despite the increasing prevalence of low- and moderate-severity fire (Parks and Abatzoglou, 2020), the relative influence of fire injury and post-fire neighborhood change on the growth of surviving trees is poorly characterized (Becker and Lutz, 2014). Nor has the relative influence of these two factors been adequately explored in mixed-

species neighborhoods, meaning that we do not know whether neighborhood changes exert species-specific effects or how species may respond differently. Species differences in post-disturbance growth rates could affect the composition of future large-diameter tree populations and thus the resilience of these populations to future climate and disturbance regimes (Lindenmayer et al., 2012).

The mixed-conifer forests of the western United States provide an opportunity to examine how compound disturbances that include fire, drought, and biotic mortality agents affect the growth of co-occurring tree species. We use a spatially explicit forest demography dataset with annual tree mortality records before and after a low- to moderate-severity fire to address two questions: 1) How do the effects of post-fire neighborhood change on radial growth vary by species or diameter of the surviving tree? 2) How do the causes of mortality within a neighborhood affect the relationship between neighborhood change and radial growth? We hypothesized that reduced competition from fire and mechanical damage would increase growth rates for smaller-diameter trees and that growth rates of these trees would not be affected by bark beetle presence because bark beetles are less likely to select smaller-diameter trees to be hosts (Koontz et al., 2021). In contrast, we expected bark beetle presence to reduce growth of larger-diameter trees because these trees are preferred hosts (Koontz et al., 2021), and we expected this effect to be stronger for species that were more commonly killed by bark beetles (e.g., *Pinus lambertiana*). These observations would support the overarching concept that the cause of neighborhood change influences the effect of neighborhood change on the growth of surviving trees, allowing species differences in mortality factors to affect post-disturbance growth rates and ultimately influence the species composition of large-

diameter tree populations.

Methods

Study area

The Yosemite Forest Dynamics Plot (YFDP; 37.77°N, 119.92°W) is a 25.6-ha study area in an unlogged, old-growth (oldest trees >500 yr) *Abies concolor–Pinus lambertiana* (white fir–sugar pine) forest in Yosemite National Park (Lutz et al., 2012; Figure 5.1). Elevation in the YFDP ranges from 1774 m to 1911 m. Between 1981 and 2010 the modeled mean January temperature ranged from -0.5 °C to 9.7 °C, and the mean July temperature ranged from 14.2 °C to 28.1 °C; mean annual precipitation was 1068 mm with the majority falling as snow (PRISM Climate Group, 2016). Principal tree species ordered by basal area are *A. concolor*, *P. lambertiana*, *Calocedrus decurrens* (incense-cedar), *Quercus kelloggii* (California black oak), and *Cornus nuttallii* (Pacific dogwood).

Prior to European settlement, the YFDP experienced low- to moderate-severity surface fires with a mean fire return interval of 30 yr (Barth et al., 2015). Although lightning-ignited spot fires have occurred within the YFDP since 1900, the area has been largely fire-excluded since the last widespread event in 1900 (Barth et al., 2015; Scholl and Taylor, 2010), leading to high tree density (Barth et al., 2015; Lutz et al., 2012) and surface fuel accumulation (Cansler et al., 2019; Gabrielson et al., 2012; Lutz et al., 2014).

On September 1st and 2nd, 2013, in the second year of a four-year drought of historic severity (Belmecheri et al., 2016), the YFDP burned in an unmanaged low- to moderate-severity fire ignited by Yosemite managers to control the spread of the Rim Fire (Blomdahl et al., 2019; Lutz et al., 2017, their Figure 1; Stavros et al., 2016). The fire

reduced aboveground live shrub biomass from 3,490 to 269 kg ha^{-1} (Lutz et al., 2017a) and consumed 79% of total surface fuel (Cansler et al., 2019).

In 2020, 4,732 trees ≥ 1 cm diameter at breast height (DBH) still survived (13.8% of the pre-fire live tree population), and tree mortality rates had returned to pre-fire levels (Table 5.1, Figure 5.2). Nearly 98% of immediate mortality of trees ≥ 10 cm DBH was associated with fire-caused crown, stem, or mechanical damage. Delayed mortality (2–4 years post-fire) was most often associated with fire damage (71%), bark beetles (46%), pathogens (34%), suppression (16%), and mechanical damage (4%) (Figure 5.3; Jeronimo et al., 2020). Agents of delayed mortality often acted in concert, with fire-caused injuries and drought predisposing larger-diameter trees to lethal outcomes from bark beetles and/or pathogens (Furniss et al., 2020b).

Data collection

The YFDP was installed in 2009 and 2010 according to the methods of the Smithsonian ForestGEO network (Davies et al., 2021). Trees ≥ 1 cm DBH were tagged, measured, identified to species, and mapped. In annual demographic surveys in 2011–2020, field technicians documented tree recruitment (i.e., trees that had newly attained ≥ 1 cm DBH) and mortality, assessing the multiple causes of mortality within one year of tree death (Lutz, 2015).

In May 2014, eight months post-fire, field crews recorded percent total crown injury (Varner et al., 2021) for every tree and remeasured DBH. DBH was remeasured again in 2019. We used the 2014 and 2019 DBH measurements to calculate post-fire mean annual basal area increment (BAI) for each tree that survived until 2020. In 2014, quality of

DBH measurement was documented as unburned at DBH, scorched at DBH, or partially

consumed at DBH. Because partial consumption at DBH affects the relationship between

BAI and DBH, we did not model post-fire growth rate for 245 trees (6.1%) that had been

partially consumed at DBH.

Measurement error, bark sloughing, bark blistering from fire damage, and reduction

of bole volume due to water loss from drought resulted in some unrealistically large

positive and negative growth rate values. We removed 35 trees (0.9%) with radial growth

rates >9 mm yr^{-1} or <-9 mm yr^{-1}, a threshold van Mantgem and Stephenson (2005) used

in a similar study in the Sierra Nevada where DBH measurements taken in 5-year

intervals were used to estimate mean annual growth. We retained both positive and

negative growth rates because we assumed all measurements were prone to error, and we

had no way of detecting which measurements were more valid than others. Negative

post-fire growth rates were relatively uncommon (5.9%).

Post-fire relative growth rate

Our objective was to investigate how the diameter of a focal tree might interact with

species and post-fire neighborhood change to influence growth rate relative to other focal

trees. However, we could not address this question with our raw data because BAI

increases with DBH, a relationship that results from larger trees having a greater ability

to acquire carbon and more bole surface area to store it. Therefore, to factor out the

influence of DBH on BAI prior to running models that included DBH as a covariate, we

fit a general linear model of BAI as a function of DBH. Because variability in post-fire

BAI increased with DBH, violating the linear model assumption of homogeneity of

variance, we added a fixed amount to all BAI values to make them > 0 and then applied a square-root transformation. We selected this transformation because it sufficiently reduced variance in growth among larger trees without changing their relative relationships. We verified that the assumption of homogeneity of variance was met by examining model residuals plotted against fitted values (Zuur et al., 2010). We extracted residuals from the model of square-root-transformed BAI and used those values as the response variable in our models of post-fire relative growth rate.

Post-fire neighborhood change metrics

We used a distance-diminished, diameter-weighted crowding (C) index to characterize the neighborhoods around focal trees (Germain and Lutz, 2021). This crowding index summarizes density, spatial pattern, and diameter information in a single metric that accounts for the diminished influence of neighbor trees, j, that are further from the focal tree, i, and the heightened influence of larger-diameter neighbor trees (Equation 5.1).

$$C_i = \sum_{j=1}^{n} \frac{DBH_j}{1+Distance_{ij}} \tag{5.1}$$

We used Equation 5.1 to quantify four types of neighborhood change (Table 5.2). By applying Equation 5.1 separately to trees that died after the fire and trees that were alive before the fire, and then assessing a ratio, we consider spatial pattern and tree size, while using the concept of mortality rate to control for differences in neighborhood density. We calculated post-fire neighborhood change metrics for circular neighborhoods with radii of 10, 15, and 20 m.

Modeling post-fire relative growth rate

Neighborhood change. We used general linear models to examine whether post-fire neighborhood change due to all causes of tree mortality (Equation 5.2) has species-specific and/or diameter-specific effects on post-fire relative growth rate of focal tree *i*. We included crown injury percent as a covariate to account for variation in post-fire growth due to fire-caused injury to the focal tree. We investigated the species-specific and diameter-specific effects of post-fire neighborhood change by considering a three-way interaction term: Neighborhood change × Species × DBH. Including this interaction term (Equation 5.6) lowered the model AIC value compared to the base model, which just included crown injury percent as a predictor (Table D.1):

$$Postfire.relative.growth.rate_i = \alpha_0 + \beta_1 Crown.injury_i$$

$$+ \beta_2 Neighborhood.change_i$$

$$+ \beta_3 Species_i + \beta_4 DBH_i + \beta_5 Neighborhood.change_i Species_i$$

$$+ \beta_6 Neighborhood.change_i DBH_i + \beta_7 Species_i DBH_i +$$

$$\beta_8 Neighborhood.change_i Species_i DBH_i \tag{5.6}$$

α_0 is an intercept term. $\beta_{1\ldots8}$ are estimated parameters for each explanatory variable. We compared the AIC values for models with neighborhood change metrics based on neighborhood radii of 10, 15, or 20 m. Because neighborhoods of radius 10 m were associated with the lowest AIC values, we reran our final model using focal trees within a 10-m buffer of the plot perimeter to maximize our sample size.

Neighborhood change by mortality cause. To determine how the cause of neighborhood mortality affects the relationship between neighborhood change, species, DBH, and post-fire relative growth rate, we fit general linear models that included three

types of post-fire neighborhood change, each due to different causes of tree mortality
(Equations 5.3–5.5). We included crown injury percent as a covariate and tested for
species-specific and diameter-specific effects of post-fire neighborhood change by
considering three-way interaction terms for each neighborhood change metric. We
performed model selection (Table D.1) and present the model with the lowest AIC
(Equation 5.7):

$$Postfire.relative.growth.rate_i = \alpha_0 + \beta_1 Crown.injury_i$$

$$+ \beta_2 Neighborhood.change.fire_i$$

$$+ \beta_3 Neighborhood.change.beetle_i + \beta_4 Species_i + \beta_5 DBH_i$$

$$+ \beta_6 Neighborhood.change.fire_i Species_i$$

$$+ \beta_7 Neighborhood.change.fire_i DBH_i$$

$$+ \beta_8 Neighborhood.change.beetle_i Species_i$$

$$+ \beta_9 Neighborhood.change.beetle_i DBH_i$$

$$+ \beta_{10} Species_i DBH_i + \beta_{11} Neighborhood.change.fire_i Species_i DBH_i$$

$$+ \beta_{12} Neighborhood.change.beetle_i Species_i DBH_i \tag{5.7}$$

α_0 is an intercept term. $\beta_{1\ldots12}$ are estimated parameters for each explanatory
variable. We compared the AIC values for models with neighborhood change metrics
based on neighborhood radii of 10, 15, or 20 m. Again, neighborhoods of radius 10 m
were associated with the lowest AIC values, so we reran our final model using focal trees
within a 10-m buffer of the plot perimeter to maximize our sample size.

Model settings. All numeric variables were standardized, so estimated coefficients
represent the relative importance of the predictors, and a one-unit change in a coefficient
represents a change of one standard deviation for that parameter. No two-way

correlations among predictors in the same model exceeded r = 0.3 (Figure D.1), and no multi-way correlations exceeded variable inflation factors of 2. Analyses were conducted in R, using the "lm" function in the "lme4" package and the "vif" function in the "car" package (R Core Team, 2020).

Results

Post-fire neighborhood change affects radial growth

Greater neighborhood change had a strong positive effect on post-fire relative radial growth of surviving trees as well as slight species- and diameter-specific effects (Figure 5.4). When neighborhood change was at its mean value, larger *P. lambertiana* exhibited greater relative growth compared with larger *A. concolor*. However, when neighborhood change was greater, relative growth of larger *P. lambertiana* decreased.

Considering mortality cause strengthens species-specific effect of neighborhood change on radial growth

Post-fire neighborhood change had stronger species-specific effects and similar diameter-specific effects on post-fire relative radial growth of surviving trees when the mortality causes driving the neighborhood change were considered (Figure 5.5). Neighborhoods where competition decreased during the post-fire period due to fire and mechanical damage were associated with greater post-fire radial growth of both *A. concolor* and *P. lambertiana*, but this relationship was nearly twice as strong for *P. lambertiana*. In contrast, mortality of conspecific neighbors due to bark beetles did not significantly affect post-fire radial growth (Figure 5.5), although including this variable and its interactions with species and diameter as covariates did improve model fit (Table

D.1). Tree diameter interacted with fire- and mechanical-caused neighborhood change for *P. lambertiana*, but the strength of this relationship was nearly identical to the result of the prior model (Equation 5.6) that did not consider mortality cause (Figures 5.4 and 5.5): as neighborhood change ranged from 0 to 100% mortality, relative growth of small-diameter (10-cm) *P. lambertiana* increased four-fold compared to large-diameter (60-cm) *P. lambertiana* (Figure 5.6).

Discussion

The recruitment of large-diameter trees after disturbance and the species composition of these populations will, in part, depend on the causes of mortality that drive the post-disturbance changes to the neighborhoods around the surviving trees. We show that different causes of post-disturbance neighborhood change have species-specific effects on the growth of surviving trees. Our results inform predictions of post-disturbance growth of surviving trees by helping us understand why the differences in post-disturbance growth are species specific and how this affects trees of different diameter classes.

Cause of mortality mediates species-specific effects of neighborhood change on growth

The causes of mortality that change neighborhoods during and after disturbances are likely to influence the species composition of large-diameter tree recruitment by impacting the effect of neighborhood change on the radial growth of surviving trees in species-specific ways. In our study area, bark beetles were a more prevalent cause of mortality among *P. lambertiana*, and these mortality events were clustered at the 10-m scale; in contrast, bark beetles were less involved in the mortality of *A. concolor*, and

these events were barely clustered (Figure 5.3; Furniss et al., 2020). This explains why we saw larger differences in how neighborhood changes affected each species when we differentiated neighborhood change by cause (Figures 5.5 and 5.6). Specifically, when neighborhood change caused by bark beetles was included as a covariate (Equation 5.7), neighborhood change due to fire and mechanical damage had a stronger positive effect on post-fire growth of *P. lambertiana* compared to the effect of neighborhood change due to all causes combined (Equation 5.6). This suggests that the mortality cause driving a neighborhood change will impact growth of surviving trees because some causes of mortality just reduce competition (e.g., mechanical damage, fire—if fire injury to the focal tree is accounted for), while others may counterbalance the benefits of reduced competition with the need for investment in defense (e.g., bark beetles; Hood et al., 2016; Raffa and Berryman, 1983). Therefore, in forests where mortality agents vary by tree species, we can expect prevalent mortality agents to affect the growth of surviving members of their associated species in predictable ways. For instance, if tree mortality is dominated by bark beetles and is spatially clustered for a species, we could expect neighborhood change around surviving members of that species to have a neutral, as opposed to a positive, effect on growth as resources liberated by bark-beetle–induced tree mortality are allocated toward defense.

Cause of mortality does not influence diameter-specific effects of neighborhood change on growth

Differentiating post-disturbance neighborhood change by mortality cause did not affect the relationship between neighborhood change and tree diameter, suggesting that mortality cause may affect the species composition of future large-diameter tree

populations but has less influence over whether large-diameter trees are recruited. Regardless of whether neighborhood change was attributed to specific mortality causes or not, relative growth of small-diameter trees increased more in response to reduced competition compared to large-diameter trees (Figures 5.5 and 5.6): small-diameter trees were released from suppression, while large-diameter trees that already occupied dominant positions and preempted the majority of resources were less sensitive (Zhang et al., 2017). Growth of large-diameter *P. lambertiana* increased the least in response to neighborhood change (Figure 5.4), but contrary to our expectation that bark beetle presence would reduce the growth of large-diameter trees because they are preferred hosts (Koontz et al., 2021), the strength of this effect hardly changed when bark beetle presence was considered (Figure 5.5). We attribute the weak relationship between neighborhood change and growth of large-diameter *P. lambertiana* to their dominant growth form and to cambial damage from smoldering duff mounds that would not have correlated with percent crown injury (Cansler et al., 2019; Nesmith et al., 2010). In contrast, we attribute the increased growth of small- and medium-diameter trees to reduced competition, indicating that the immediate and delayed effects of disturbance can facilitate the recruitment of large-diameter trees.

Study limitations and future directions

This study relates neighborhood change that resulted from a disturbance to post-disturbance growth, but artifacts of the dataset limit understanding and inference. Although tree mortality was assessed annually, growth rates are based on DBH measurements taken five years apart. Averaging over annual variation in growth

weakened our ability to detect relationships between fire injury, neighborhood change, and growth. Dendrochronological studies have shown that fire injuries can initially depress growth, which may then increase due to reduced competition (Becker and Lutz, 2014; Mutch and Swetnam, 1995), but in our dataset, these separate effects are lumped together. Moreover, because our response variable represented mean growth over a five-year period, we summarized neighborhood change over this same period, even though our annual mortality surveys would have allowed for higher temporal resolution. Future studies should use increment cores to relate annual growth to annual changes in neighborhood categorized by mortality cause.

This study also likely underestimates the influence of fungal infection on post-fire growth (Table D.1). When examining newly dead trees for factors associated with death, we removed bark near the root collar but did not fully excavate the root system. Our dataset likely underreports instances of root rot (e.g., *Armillaria* spp.) because we can only detect advanced infections. However, fungal infection is known to predispose trees to bark beetle attack through biochemical cues (Bartos and Schmitz, 1998). Therefore, when a neighborhood experienced a high degree of tree mortality due to bark beetles, which we can more readily detect, root pathogens were likely present as well, increasing the disadvantage to nearby surviving trees.

Implications and conclusions

Overall, we show that cause of mortality influences the relationship between neighborhood change and the growth of surviving trees in species-specific ways, meaning that species differences in cause of mortality could affect the species

composition of future large-diameter tree populations. This result is relevant to land
managers in the Sierra Nevada, where injury and stress from fire and drought will
continue to predispose trees to mortality by other causes (Furniss et al., 2022; Marshall et
al., 2019), and mixed-conifer species vary in tolerance to fire, drought, and biotic
mortality agents (Das et al., 2016). Our study shows that, in this region, susceptibility to
bark beetles may counterbalance the benefits of reduced competition for small- and
medium-diameter trees, but existing large-diameter trees are less sensitive to
neighborhood changes regardless of the mortality agents in their vicinity. Species
differences in post-disturbance growth among small- and medium-diameter trees could
influence the composition of large-diameter tree recruitment and thus affect the resilience
of these populations under future climate and disturbance regimes.

References

Becker, K.M.L., Lutz, J.A., 2016. Can low-severity fire reverse compositional change in
montane forests of the Sierra Nevada, California, USA? Ecosphere 7, 1–22.
https://doi.org/10.1002/ecs2.1484

Becker, K.M.L., Lutz, J.A., 2014. Annually resolved impacts of fire management on
carbon stocks in Yosemite and Sequoia & Kings Canyon National Parks, General
Technical Report.

Collins, B.M., Everett, R.G., Stephens, S.L., 2011. Impacts of fire exclusion and recent
managed fire on forest structure in old growth Sierra Nevada mixed-conifer forests.
Ecosphere 2, 1–14. https://doi.org/10.1890/ES11-00026.1

Eidenshink, J., Schwind, B., Brewer, K., Zhu, Z., Quayle, B., Howard, S., 2007. A
project for monitoring trends in burn severity. Fire Ecol. 3, 3–21.

Fulé, P.Z., Laughlin, D.C., 2007. Wildland fire effects on forest structure over an
altitudinal gradient, Grand Canyon National Park, USA. J. Appl. Ecol. 44, 136–146.
https://doi.org/10.1111/j.1365-2664.2006.01254.x

Furniss, T.J., Das, A.J., van Mantgem, P.J., Stephenson, N.L., Lutz, J.A., 2022.
Crowding, climate, and the case for social distancing among trees. Ecol. Appl. 32,

1–14. https://doi.org/10.1002/eap.2507

Furniss, T.J., Larson, A.J., Kane, V.R., Lutz, J.A., 2019. Multi-scale assessment of post-fire tree mortality models. Int. J. Wildl. Fire 28, 46–61. https://doi.org/10.1071/WF18031

Guarín, A., Taylor, A.H., 2005. Drought triggered tree mortality in mixed conifer forests in Yosemite National Park, California, USA. For. Ecol. Manage. 218, 229–244. https://doi.org/10.1016/j.foreco.2005.07.014

IPCC, 2013. Climate change 2013: the physical science basis. New York, New York, USA.

Kane, V.R., Lutz, J.A., Cansler, C.A., Povak, N.A., Churchill, D.J., Smith, D.F., Kane, J.T., North, M.P., 2015. Water balance and topography predict fire and forest structure patterns. For. Ecol. Manage. 338, 1–13. https://doi.org/10.1016/j.foreco.2014.10.038

Keeler-Wolf, T., Moore, P.E., Reyes, E.T., Menke, J.M., Johnson, D.N., Karavidas, D.L., 2012. Yosemite National Park vegetation classification and mapping project report. Natural Resource Report NPS/YOSE/NRTR-2012/598. Fort Collins, Colorado.

Key, C.H., Benson, N.C., 2006. Landscape assessment: Sampling and analysis methods, USDA Forest Service General Technical Report RMRS-GTR-164-CD.

Kilgore, B.M., Briggs, G.S., 1972. Restoring fire to high elevation forests in California. J. For. 70, 266–271.

Kolb, T.E., Agee, J.K., Fulé, P.Z., McDowell, N.G., Pearson, K., Sala, A., Waring, R.H., 2007. Perpetuating old ponderosa pine. For. Ecol. Manage. 249, 141–157. https://doi.org/10.1016/j.foreco.2007.06.002

Kolden, C.A., Lutz, J.A., Key, C.H., Kane, J.T., van Wagtendonk, J.W., 2012. Mapped versus actual burned area within wildfire perimeters: characterizing the unburned. For. Ecol. Manage. 286, 38–47. https://doi.org/10.1016/j.foreco.2012.08.020

Littell, J.S., Mckenzie, D., Peterson, D.L., Westerling, A.L., 2009. Climate and wildfire area burned in western U.S. ecoprovinces, 1916-2003. Ecol. Appl. 19, 1003–1021. https://doi.org/10.1890/07-1183.1

Lutz, J.A., Key, C.H., Kolden, C.A., Kane, J.T., van Wagtendonk, J.W., 2011. Fire frequency, area burned, and severity: A quantitative approach to defining a normal fire year. Fire Ecol. 7, 51–65. https://doi.org/10.4996/fireecology.0702051

Lutz, J.A., Larson, A.J., Swanson, M.E., 2018. Advancing fire science with large forest plots and a long-term multidisciplinary approach. Fire 1, 1–7. https://doi.org/10.3390/fire1010005

Lutz, J.A., van Wagtendonk, J.W., Franklin, J.F., 2009a. Twentieth-century decline of large-diameter trees in Yosemite National Park, California, USA. For. Ecol. Manage. 257, 2296–2307. https://doi.org/10.1016/j.foreco.2009.03.009

Lutz, J.A., van Wagtendonk, J.W., Thode, A.E., Miller, J.D., Franklin, J.F., 2009b. Climate, lightning ignitions, and fire severity in Yosemite National Park, California, USA. Int. J. Wildl. Fire 18, 765–774. https://doi.org/10.1071/WF08117

Marshall, A.M., Abatzoglou, J.T., Link, T.E., Tennant, C.J., 2019. Projected changes in interannual variability of peak snowpack amount and timing in the western United States. Geophys. Res. Lett. 46, 8882–8892. https://doi.org/10.1029/2019GL083770

McDowell, N., Pockman, W.T., Allen, C.D., David, D., Cobb, N., Kolb, T., Plaut, J., Sperry, J., West, A., Williams, D.G., Yepez, E.A., 2008. Mechanisms of plant survival and mortality during drought: why do some plants survive while others succumb to drought? New Phytol. 178, 719–739.

Miller, J.D., Thode, A.E., 2007. Quantifying burn severity in a heterogeneous landscape with a relative version of the delta Normalized Burn Ratio (dNBR). Remote Sens. Environ. 109, 66–80. https://doi.org/10.1016/j.rse.2006.12.006

Mutch, L.S., Swetnam, T.W., 1995. Effects of Fire Severity and Climate on Ring-Width Growth of Giant Sequoia After Fire. Symp. Fire Wilderness Park Manag. Past Lessons Futur. Oppor. March 30-April 1, 1993 Missoula, MT Gen Tech Rep INT-GTR-320 Ogden, UT; US Dep. Agric. For. Serv. Intermt. Res. Stn.

North, M., Innes, J., Zald, H., 2007. Comparison of thinning and prescribed fire restoration treatments to Sierran mixed-conifer historic conditions. Can. J. For. Res. 37, 331–342. https://doi.org/10.1139/X06-236

Parks, S.A., Abatzoglou, J.T., 2020. Warmer and drier fire seasons contribute to increases in area burned at high severity in western US forests from 1985 to 2017. Geophys. Res. Lett. 47, 1–10. https://doi.org/10.1029/2020GL089858

Parsons, D.J., DeBenedetti, S.H., 1979. Impact of fire suppression on a mixed-conifer forest. For. Ecol. Manage. 2, 21–33. https://doi.org/10.1016/0378-1127(79)90034-3

Peterson, D.L., Sackett, S.S., Robinson, L.J., Haase, S.M., 1994. The effects of repeated prescribed burning on pinus ponderosa growth. Int. J. Wildl. Fire 4, 239–247. https://doi.org/10.1071/WF9940239

Scholl, A.E., Taylor, A.H., 2010. Fire regimes, forest change, and self-organization in an old-growth mixed-conifer forest, Yosemite National Park, USA. Ecol. Appl. 20, 362–380. https://doi.org/10.1890/08-2324.1

Sequoia and Kings Canyon National Parks photo interpretation report, 2007. Redlands, CA.

Sherman, R.J., Warren, R.K., 1988. Factors in Pinus ponderosa and Calocedrus decurrens mortality in Yosemite Valley, USA. Vegetatio 77, 79–85. https://doi.org/10.1007/BF00045753

Slayton, J.D., 2010. Separating the effects of wildfires from climate in growth of ponderosa pine (Pinus ponderosa Douglas ex. C. Lawson), Central Idaho, U.S.A. Master's Thesis, University of Tennessee.

Stephens, S.L., Finney, M.A., Schantz, H., 2004. Bulk density and fuel loads of ponderosa pine and white fir forest. Northwest Sceince 78, 93–100.

Thode, A.E., van Wagtendonk, J.W., Miller, J.D., Quinn, J.F., 2011. Quantifying the fire regime distributions for severity in Yosemite National Park, California, USA. Int. J. Wildl. Fire 20, 223–239. https://doi.org/10.1071/WF09060

van Mantgem, P.J., Stephenson, N.L., Mutch, L.S., Johnson, V.G., Esperanza, A.M., Parsons, D.J., 2003. Growth rate predicts mortality of Abies concolor in both burned and unburned stands 1038, 1029–1038. https://doi.org/10.1139/X03-019

van Wagtendonk, J.W., 2007. The history and evolution of wildland fire use. Fire Ecol. 3, 3–17. https://doi.org/10.4996/fireecology.0302003

van Wagtendonk, J.W., Fites-Kaufman, J.A., 2006. Sierra Nevada bioregion, in: Fire in California's Ecosystems. pp. 264–294.

van Wagtendonk, J.W., Moore, P.E., 2010. Fuel deposition rates of montane and subalpine conifers in the central Sierra Nevada, California, USA. For. Ecol. Manage. 259, 2122–2132. https://doi.org/10.1016/j.foreco.2010.02.024

van Wagtendonk, J.W., Moore, P.E., Yee, J.L., Lutz, J.A., 2020. The distribution of woody species in relation to climate and fire in Yosemite National Park, California, USA. Fire Ecol. 16, 1–23. https://doi.org/10.1186/s42408-020-00079-9

van Wagtendonk, J.W., van Wagtendonk, K.A., Thode, A.E., 2012. Factors associated with the severity of intersecting fires in Yosemite National Park, California, USA. Fire Ecol. 8, 11–31. https://doi.org/10.4996/fireecology.0801011

Varner, J.M., Putz, F.E., O'Brien, J.J., Hiers, K.J., Mitchell, R.J., Gordon, D.R., 2009. Post-fire tree stress and growth following smoldering duff fires. For. Ecol. Manage. 258, 2467–2474. https://doi.org/10.1016/j.foreco.2009.08.028

Westerling, A.L., Hidalgo, H.G., Cayan, D.R., Swetnam, T.W., 2006. Warming and earlier spring increase western U.S. forest wildfire activity. Science (80-.). 313, 940–943. https://doi.org/10.1126/science.1128834

Tables

Table 5.1. Abundance of *A. concolor* and *P. lambertiana* trees in the Yosemite Forest Dynamics Plot. Trees that survived until 2020 were used to model the influence of post-fire neighborhood change on post-fire radial growth after a low- to moderate-severity fire in the fall of 2013.

Species Diameter class (cm)	Pre-fire (2013)		Seven years post-fire (2020)	
	Abundance	Basal area (m^2 ha^{-1})	Abundance	Basal area (m^2 ha^{-1})
Abies concolor				
10–30	7,372	7.43	1,095	1.54
30–60	1,853	9.55	922	5.22
≥ 60	570	12.36	409	8.61
Total (≥ 1)	**23,995**	**30.57**	**2,801**	**15.40**
Pinus lambertiana				
10–30	1,016	1.02	169	0.24
30–60	453	2.54	208	1.23
≥ 60	696	25.16	410	14.15
Total (≥ 1)	**4,616**	**28.89**	**851**	**15.63**

Table 5.2. Metrics using different types of pre-fire and post-fire neighborhood crowding (Equation 5.1) to describe four types of neighborhood change. We used these metrics to determine if cause of mortality of neighbors affected the relationship between post-fire neighborhood change and post-fire relative radial growth of surviving trees.

Description	Equation
Post-fire neighborhood change due to all causes (Equation 5.2)	$\dfrac{Crowding\ by\ trees\ that\ died\ between\ 2014\ and\ 2020}{Crowding\ by\ trees\ alive\ in\ 2013}$
Post-fire neighborhood change due to tree mortality from fire and mechanical damage, i.e., non-biotic (Equation 5.3)	$\dfrac{Crowding\ by\ trees\ that\ died\ from\ fire\ or\ mechanical\ damage\ between\ 2014\ and\ 2020}{Crowding\ by\ trees\ alive\ in\ 2013}$
Post-fire neighborhood change due to tree mortality from bark beetles (Equation 5.4)	$\dfrac{Crowding\ by\ conspecific\ trees\ that\ died\ from\ bark\ beetles\ between\ 2014\ and\ 2020}{Crowding\ by\ conspecific\ trees\ alive\ in\ 2013}$
Post-fire neighborhood change due to tree mortality from fungal pathogens (Equation 5.5)	$\dfrac{Crowding\ by\ trees\ that\ died\ from\ fungal\ pathogens\ between\ 2014\ and\ 2020}{Crowding\ by\ trees\ alive\ in\ 2013}$

Figures
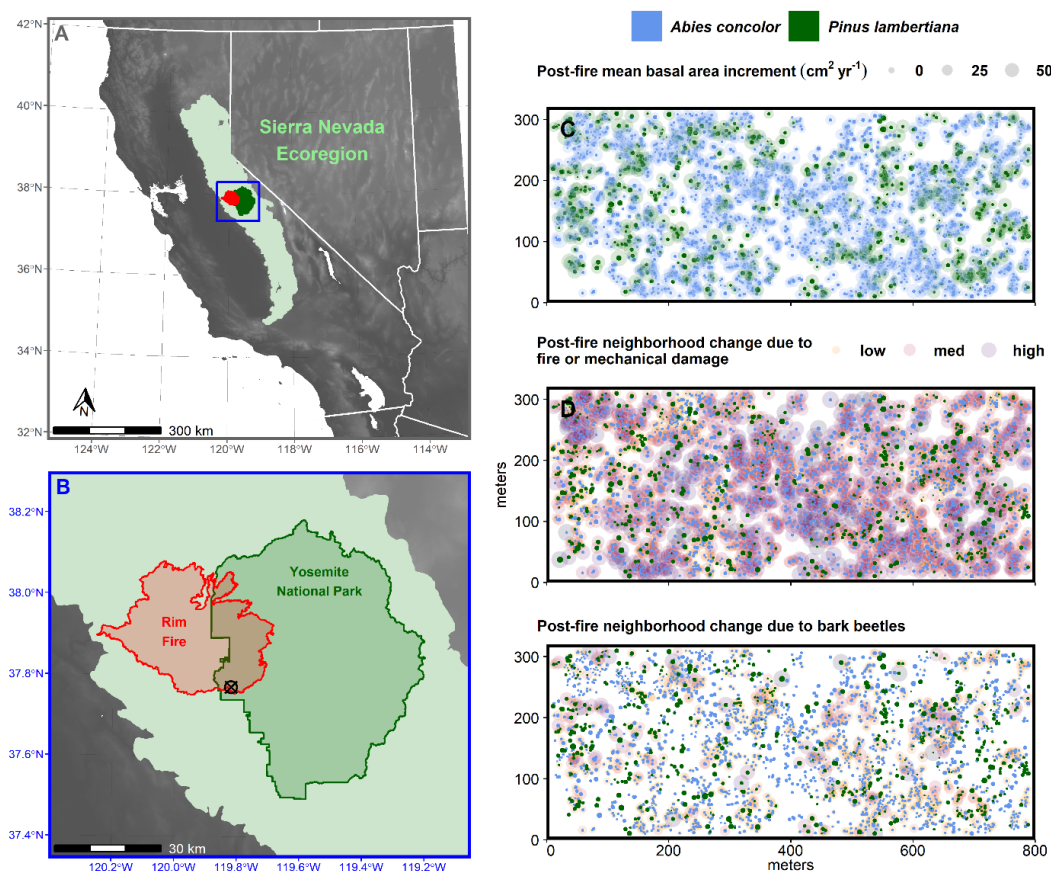
Figure 5.1. The Yosemite Forest Dynamics Plot (YFDP) is a 25.6-ha permanent study area in an old-growth *Abies concolor–Pinus lambertiana* forest in Yosemite National Park in the central Sierra Nevada, California, USA (A). The YFDP burned at low and moderate severity in the 2013 Rim Fire (B). Post-fire mean annual basal area increment was calculated for trees that survived at least until 2020 from diameter measurements taken in 2014 and 2019 (C). Low (0.2), medium (0.5), and high (0.8) values of post-fire neighborhood change due to fire or mechanical damage represent the ratio of crowding by trees that died due to fire or mechanical damage between 2014 and 2020 divided by the crowding of trees that were alive before the fire (D). Post-fire neighborhood change due to bark beetles is the ratio of crowding by conspecific trees that died due to bark beetles between 2014 and 2020 divided by the crowding of conspecific trees that were alive before the fire (Table 5.2, Equations 5.3 and 5.4). Stem diameters (solid colors) appear four times larger than their measured size.
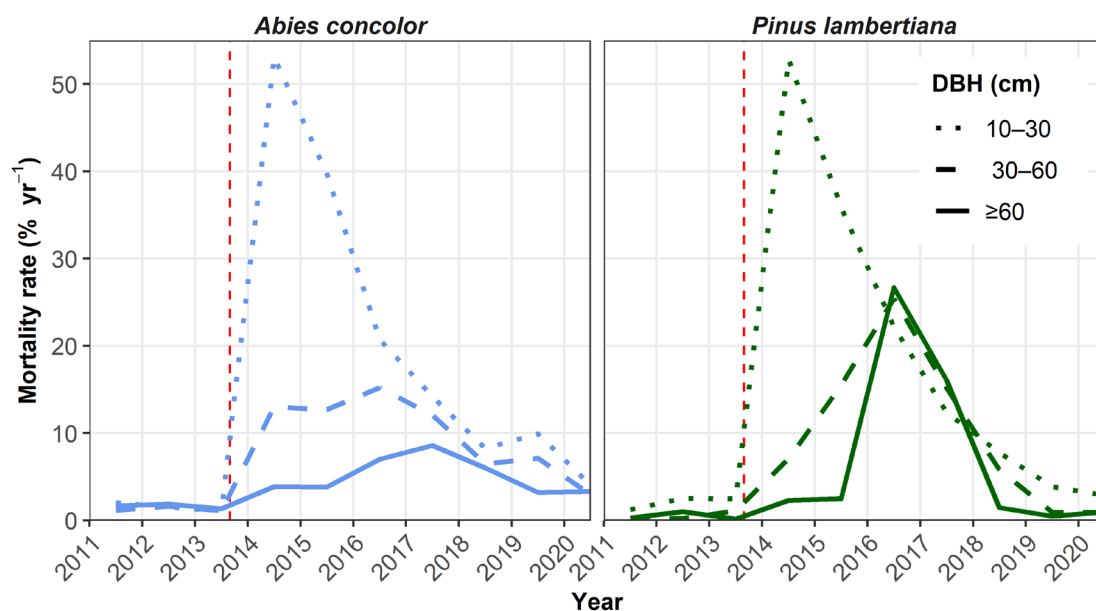
Figure 5.2. Mortality rates of trees in the Yosemite Forest Dynamics Plot before and after the Rim Fire entered the plot on August 31, 2013. Line inflection points are resolved to the month of each annual tree mortality census.
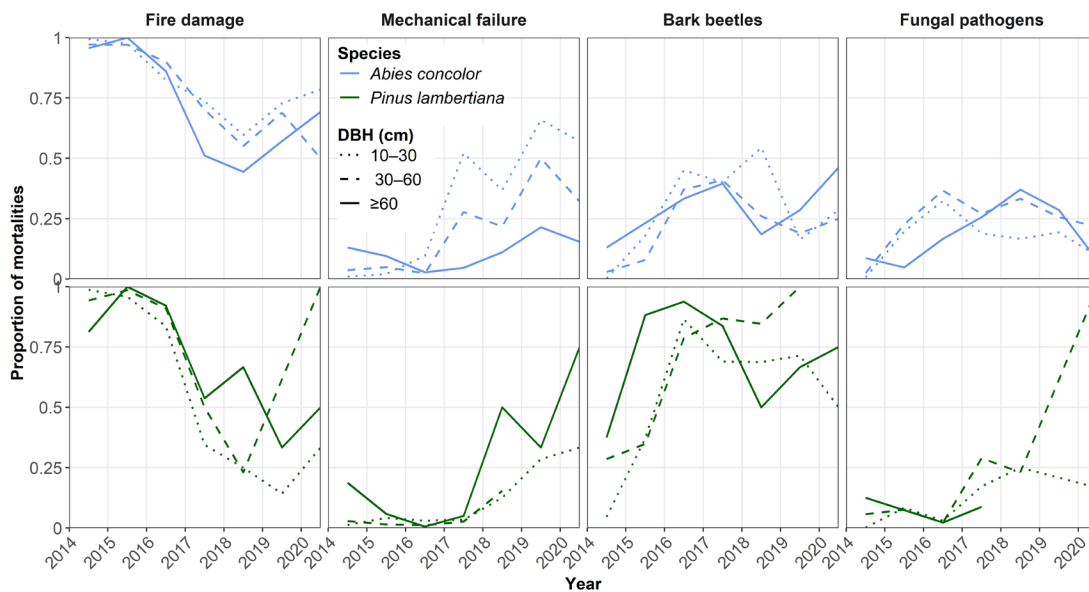
Figure 5.3. Proportion of post-fire mortalities within each conifer species partitioned by factors associated with death after the Yosemite Forest Dynamics Plot burned at low to moderate severity in the fall of 2013. Because tree death can be associated with multiple factors, the sum of proportions for a given species in a given year can exceed 1. Line inflection points are resolved to the month of each annual tree mortality census.
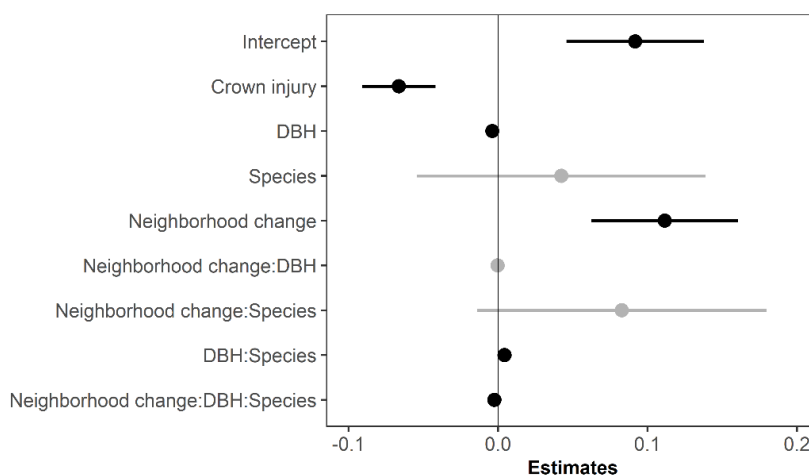
Figure 5.4. Coefficient estimates for a general linear model of relative growth of conifer trees that survived through 2020 after a low- to moderate-severity fire in 2013. Confidence intervals (CI) represent ± twice the standard error. Black symbols indicate that the CI does not overlap with zero. Neighborhood change = Equation 5.2 (Table 5.2). Estimates for species indicate the adjustment for *P. lambertiana* to the intercept value, which was associated with *A. concolor*.
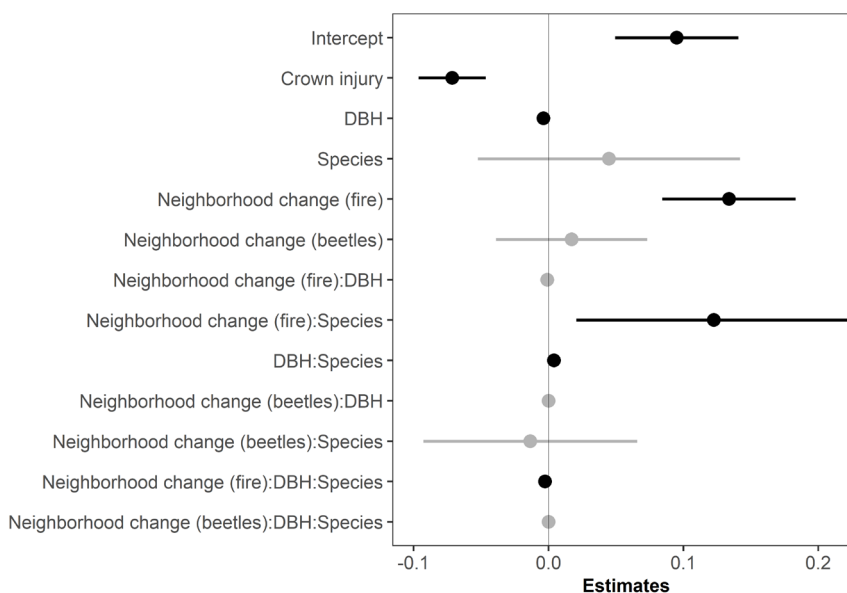
Figure 5.5. Coefficient estimates for a general linear model of relative growth of conifer trees that survived through 2020 after a low- to moderate-severity fire in 2013. Confidence intervals (CI) represent ± twice the standard error. Black symbols indicate that the CI does not overlap with zero. Neighborhood change (fire) = neighborhood change due to fire or mechanical damage (Equation 5.3; Table 5.2). Neighborhood change (beetles) = neighborhood change due to bark beetles (Equation 5.4; Table 5.2). Estimates for species indicate the adjustment for *P. lambertiana* to the intercept value, which was associated with *A. concolor*.
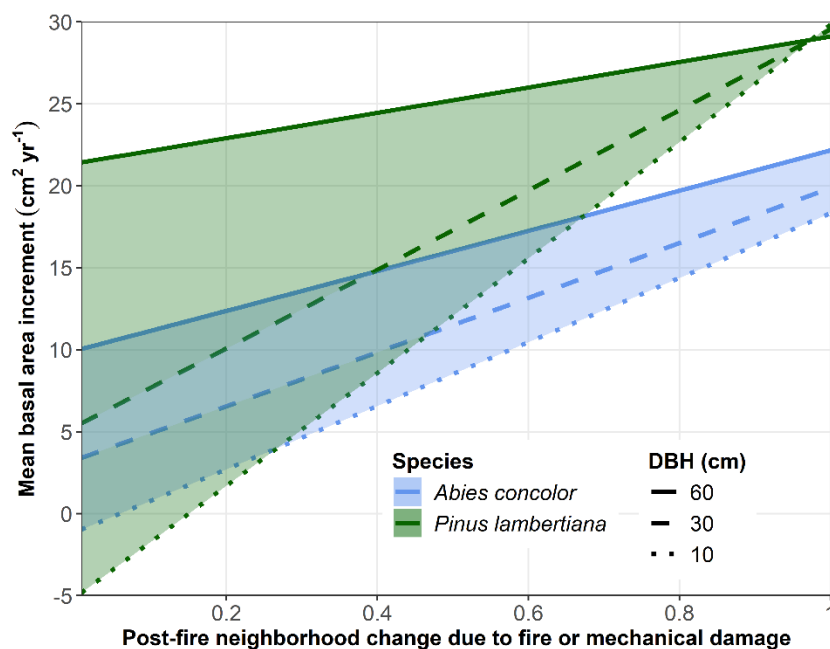
Figure 5.6. Modeled mean annual growth in basal area increment (BAI) for *A. concolor* and *P. lambertiana* from 2014 to 2019, after a low- to moderate-severity fire in 2013. This figure depicts the interaction between neighborhood change due to fire or mechanical damage and species, as well as the weaker three-way interaction between neighborhood change, species, and DBH (Figure 5.5). Shaded areas represent the modeled range of mean annual BAI for trees 10–60 cm DBH. Post-fire neighborhood change is represented as the ratio of crowding by trees that died due to fire or mechanical damage between 2014 and 2020 divided by crowding of trees that were alive in 2013, before the fire.

CHAPTER VI

SUMMARY AND CONCLUSIONS

Understanding forest ecosystems is important because forests cover approximately one-third of Earth's land area, store half of Earth's carbon, provide homes for half of Earth's species, and take up a quarter of new anthropogenic carbon emissions, slowing climate change (Davies et al., 2021; Keenan and Williams, 2018). When people spend time in forests, the setting can awaken feelings of timelessness and tranquility (Williams and Harvey, 2001). Contemporary forest research coincides with an era of unprecedented change, driven by rapid global warming from anthropogenic carbon emissions (Pörtner et al., 2022; "We must get a grip on forest science — before it's too late," 2022).

Climate change affects the frequency, severity, and extent of forest disturbances, which influence forest composition, structure, and longevity (Seidl et al., 2017). Plants have adapted to take advantage of favorable environments when they are available (Bell et al., 2014; Dobrowski et al., 2015). Thus, a change to a disturbance regime could make an environment unsuitable for the current species assemblage but could open opportunities for other species (Harsch et al., 2009). Ecosystems shift toward species composition and structure that maximize their resilience to disturbance (Hood et al., 2016; Seidl et al., 2017). In the western United States, such shifts can result in forest loss, when shrubs are better suited to the contemporary climate and fire regimes, which are and will be characterized by more frequent fires, larger patches burned at high severity, and more drought (Lauvaux et al., 2016; Marshall et al., 2019; Parks and Abatzoglou, 2020; Tepley et al., 2017). However, more subtle changes to forest composition and

structure in response to low- and moderate-severity disturbances are also happening and are important indicators of where forests will persist and what their characteristics will be. By investigating what happens to snags, seedlings, and trees in an old-growth forest after a low- to moderate-severity fire, this dissertation provides insight into future forest habitat, fuels, species composition, and structure.

Chapter II showed how low- to moderate-severity fire changes snag fall dynamics. Snags provide habitat for birds and small mammals, and after falling to the ground, they provide additional wildlife habitat and affect nutrient cycling, fuel loads, and fire behavior (Cousins et al., 2015; Harmon et al., 1986; Knapp, 2015; Thomas, 1979). Predicting how long snags will remain standing after fire is essential for managing habitat, understanding chemical cycling in forests, and modeling forest succession and fuels. Yet this analysis is, to our knowledge, the first to quantify post-fire outcomes for snags that existed pre-fire and the first to examine how local fire behavior affects snag fall rates after fire. Pre-fire snags—which tend to be preferred habitat because they include more large-diameter snags in advanced stages of decay (Thomas, 1979)—were at least twice as likely to fall as new snags within 3–5 years after fire. For pre-existing snags, diameter, height, and bole scorch height were better predictors of snag fall after fire than spatial neighborhood or local fire severity metrics. Pre-existing snags were most likely to persist five years after fire if they were > 50 cm in diameter, > 20 m tall, and charred on the bole above 3.7 m. New snags were also more likely to persist five years after fire if they were > 20 m tall. Spatial neighborhood (e.g., tree density) and local fire severity (e.g., fire-caused crown injury) within 15 m of each snag barely improved predictions of snag fall after fire. When anticipating habitat availability and fuels,

managers should expect fall rates of pre-existing snags to initially exceed fall rates of new snags. Overall, this analysis showed that fire accelerated fall rates of pre-existing snags, but case hardening of the wood from extensive bole scorch could reduce this effect.

Chapter III examined the effects of disturbance severity and microclimate on post-fire regeneration to define and compare the regeneration niches of co-occurring tree species. Climate change is altering forest composition through species-specific responses to fire and drought (Allen et al., 2010; Halofsky et al., 2020). Future forest composition depends on how the different regeneration niches of co-occurring species align with current environmental conditions, especially after fire, which can promote conifer germination by exposing mineral soil (Dobrowski et al., 2015; Zald et al., 2008). This research showed that species-specific responses to post-fire conditions can shift seedling species composition, potentially initiating changes to future overstory composition. Our results are relevant to forest management in the Sierra Nevada because we show that natural post-fire conditions can favor *P. lambertiana* seedlings while disadvantaging *A. concolor* seedlings. In the mixed-conifer forests of the Sierra Nevada, many shade-tolerant *A. concolor* have reached maturity and populated lower strata of the canopy with ladder fuels due to the past century of fire suppression (Becker and Lutz, 2016; Kilgore and Briggs, 1972). We showed that available seed, lower substrate burn severity, higher neighborhood disturbance severity, and earlier snowmelt during the germination year can naturally shift the composition of these forests away from dominance by *A. concolor* and toward *Pinus* species that are more resistant to fire and drought. By retaining *Pinus* species, natural processes may support and bolster fire use, thinning, and post-fire

planting programs that aim to increase forest resilience under climate change. Broadly, our results advance ecological theory by showing that species differences in regeneration niches will mediate how disturbance severity and microclimate influence future forest species composition.

Chapter IV examined the effects of contemporary lower-severity fire on carbon allocation to tree boles by analyzing the tree-ring widths of seven mixed-conifer species throughout the Sierra Nevada. We observed three common growth responses within five years after fire for all seven species: no change from pre-fire growth, an initial growth decrease followed by an increase, and an initial growth increase followed by a decrease. Post-fire growth decreases were much more common than growth increases, with high-severity fire associated with the highest proportion (0.80) of growth decreases one and two years post-fire, and undifferentiated-severity fire associated with the lowest proportions (< 0.12). Importantly, post-fire growth patterns often did not differ more than one standard deviation from growth fluctuations at adjacent unburned plots, suggesting that reintroducing fire in Yosemite and Sequoia & Kings Canyon National Parks will not adversely affect the capacity of surviving trees to attain pre-fire rates of carbon accumulation within five years after fire. However, because the tree cores gathered for this study were extracted from trees in plots where stems were not mapped before and after fire, we were unable to relate different post-fire growth responses to variation in local tree neighborhood and local fire severity. We addressed this shortcoming in Chapter V.

Chapter V focused on recruitment of large-diameter trees after fire, analyzing how local post-fire mortality within tree neighborhoods impacted post-fire radial growth of

surviving trees. We found that cause of mortality influenced the relationship between neighborhood change and the growth of surviving trees in species-specific ways, suggesting that species differences in cause of mortality could affect the species composition of future large-diameter tree populations. Although neighborhoods where competition decreased post-fire due to fire and mechanical damage were associated with greater post-fire radial growth for both *A. concolor* and *P. lambertiana*, this relationship was nearly twice as strong for *P. lambertiana*. In contrast, post-fire neighborhood change due to bark beetles did not affect post-fire radial growth, indicating that the need for investment in defense counterbalanced the benefits of reduced competition for small- and medium-diameter trees. Thus, post-fire mortality regimes dominated by fire and mechanical damage could accelerate large-diameter tree recruitment, especially of *Pinus* individuals, whereas post-fire mortality dominated by bark beetles would delay recruitment of large-diameter trees. This result is relevant to the management of mixed-conifer forests in the Sierra Nevada, where large-diameter tree abundance has declined (Lutz et al., 2009a); injury and stress from fire and drought will continue to predispose trees to mortality by other causes (Furniss et al., 2022; Marshall et al., 2019); and mixed-conifer species vary in tolerance to fire, drought, and biotic mortality agents (Das et al., 2016). In the Sierra Nevada, and potentially in other forests, species differences in post-disturbance growth could influence the composition of large-diameter tree recruitment and thus affect the resilience of these populations under future climate and disturbance regimes.

Collectively, these finding demonstrate that low- to moderate-severity fires can: 1) accelerate fall of pre-fire snags, which tend to be preferred habitat; 2) naturally shift the

composition of conifer seedlings toward fire- and drought-resistant *Pinus* species; and 3) stimulate the growth of small- and medium-diameter trees, especially *Pinus* species. The positive effects of low- to moderate-severity fire on *Pinus* seedlings and trees suggest that when disturbance severity is low enough to not instigate type conversion, it can instead promote species that are better adapted to the stresses of current and future disturbance and climate regimes, exemplifying the concept that ecosystems shift toward species composition and structure that maximize their resilience (Hood et al., 2016; Seidl et al., 2017).

Chapters II, III, and V of this dissertation were possible because of the existence of a long-term, spatially explicit observational old-growth forest dataset with annual resolution (Lutz, 2015; Lutz et al., 2018b). Chapter II is novel because it analyzes post-fire outcomes of a pre-fire snag population and investigated neighborhood effects on snag fall rates. These analyses were possible because the dataset spanned pre-fire and post-fire years and included spatially explicit and annual data on tree mortality (Lutz, 2015; Lutz et al., 2018b). Chapter III is novel because it analyzes annual seedling, microclimate, and spatially explicit overstory data for seven years after fire. Chapter V is novel because it analyzes the effects of spatially explicit mortality causes on growth of surviving trees. Identifying mortality causes requires annual monitoring of tree mortality (Lutz, 2015).

This dissertation is based on the first decade of data collected from the Yosemite Forest Dynamics Plot, a permanent study area in old-growth forest where trees are spatially mapped and annually monitored (Lutz et al., 2012). Publishing research during the incipient phase of a long-term study is important because it 1) serves as a comparison with future studies, and 2) helps demonstrate the immediate value of the dataset, which

can help secure funding so the long-term research effort can continue (de Lima et al.,

2022; Lutz et al., 2018b; "We must get a grip on forest science — before it's too late,"

2022). Long-term observational research in forest ecosystems is valuable because it can

reveal unknown relationships and patterns and allows researchers to examine the short-

and long-term effects of naturally occurring phenomena, such as fire and drought, on

those relationships and patterns.

References

Allen, C.D., Macalady, A.K., Chenchouni, H., Bachelet, D., McDowell, N., Vennetier, M., Kitzberger, T., Rigling, A., Breshears, D.D., Hogg, E.H. (Ted), Gonzalez, P., Fensham, R., Zhang, Z., Castro, J., Demidova, N., Lim, J.H., Allard, G., Running, S.W., Semerci, A., Cobb, N., 2010. A global overview of drought and heat-induced tree mortality reveals emerging climate change risks for forests. For. Ecol. Manage. 259, 660–684. https://doi.org/10.1016/j.foreco.2009.09.001

Becker, K.M.L., Lutz, J.A., 2016. Can low-severity fire reverse compositional change in montane forests of the Sierra Nevada, California, USA? Ecosphere 7, 1–22. https://doi.org/10.1002/ecs2.1484

Bell, D.M., Bradford, J.B., Lauenroth, W.K., 2014. Early indicators of change: Divergent climate envelopes between tree life stages imply range shifts in the western United States. Glob. Ecol. Biogeogr. 23, 168–180. https://doi.org/10.1111/geb.12109

Cousins, S.J.M., Battles, J.J., Sanders, J.E., York, R.A., 2015. Decay patterns and carbon density of standing dead trees in California mixed conifer forests. For. Ecol. Manage. 353, 136–147. https://doi.org/10.1016/j.foreco.2015.05.030

Das, A.J., Stephenson, N.L., Davis, K.P., 2016. Why do trees die? Characterizing the drivers of background tree mortality. Ecology 97, 2616–2627. https://doi.org/10.1002/ecy.1497

Davies, S.J., Abiem, I., Abu Salim, K., Aguilar, S., Allen, D., Alonso, A., Anderson-Teixeira, K., Andrade, A., Arellano, G., Ashton, P.S., Baker, P.J., Baker, M.E., Baltzer, J.L., Basset, Y., Bissiengou, P., Bohlman, S., Bourg, N.A., Brockelman, W.Y., Bunyavejchewin, S., Burslem, D.F.R.P., Cao, M., Cárdenas, D., Chang, L.W., Chang-Yang, C.H., Chao, K.J., Chao, W.C., Chapman, H., Chen, Y.Y., Chisholm, R.A., Chu, C., Chuyong, G., Clay, K., Comita, L.S., Condit, R., Cordell, S., Dattaraja, H.S., de Oliveira, A.A., den Ouden, J., Detto, M., Dick, C., Du, X., Duque, Á., Ediriweera, S., Ellis, E.C., Obiang, N.L.E., Esufali, S., Ewango, C.E.N.,

Fernando, E.S., Filip, J., Fischer, G.A., Foster, R., Giambelluca, T., Giardina, C., Gilbert, G.S., Gonzalez-Akre, E., Gunatilleke, I.A.U.N., Gunatilleke, C.V.S., Hao, Z., Hau, B.C.H., He, F., Ni, H., Howe, R.W., Hubbell, S.P., Huth, A., Inman-Narahari, F., Itoh, A., Janík, D., Jansen, P.A., Jiang, M., Johnson, D.J., Jones, F.A., Kanzaki, M., Kenfack, D., Kiratiprayoon, S., Král, K., Krizel, L., Lao, S., Larson, A.J., Li, Y., Li, X., Litton, C.M., Liu, Y., Liu, S., Lum, S.K.Y., Luskin, M.S., Lutz, J.A., Luu, H.T., Ma, K., Makana, J.R., Malhi, Y., Martin, A., McCarthy, C., McMahon, S.M., McShea, W.J., Memiaghe, H., Mi, X., Mitre, D., Mohamad, M., Monks, L., Muller-Landau, H.C., Musili, P.M., Myers, J.A., Nathalang, A., Ngo, K.M., Norden, N., Novotny, V., O'Brien, M.J., Orwig, D., Ostertag, R., Papathanassiou, K., Parker, G.G., Pérez, R., Perfecto, I., Phillips, R.P., Pongpattananurak, N., Pretzsch, H., Ren, H., Reynolds, G., Rodriguez, L.J., Russo, S.E., Sack, L., Sang, W., Shue, J., Singh, A., Song, G.Z.M., Sukumar, R., Sun, I.F., Suresh, H.S., Swenson, N.G., Tan, S., Thomas, S.C., Thomas, D., Thompson, J., Turner, B.L., Uowolo, A., Uriarte, M., Valencia, R., Vandermeer, J., Vicentini, A., Visser, M., Vrska, T., Wang, Xugao, Wang, Xihua, Weiblen, G.D., Whitfeld, T.J.S., Wolf, A., Wright, S.J., Xu, H., Yao, T.L., Yap, S.L., Ye, W., Yu, M., Zhang, M., Zhu, D., Zhu, L., Zimmerman, J.K., Zuleta, D., 2021. ForestGEO: Understanding forest diversity and dynamics through a global observatory network. Biol. Conserv. 253. https://doi.org/10.1016/j.biocon.2020.108907

de Lima, R.A.F., Phillips, O.L., Duque, A., Tello, J.S., Davies, S.J., de Oliveira, A.A., Muller, S., Honorio Coronado, E.N., Vilanova, E., Cuni-Sanchez, A., Baker, T.R., Ryan, C.M., Malizia, A., Lewis, S.L., ter Steege, H., Ferreira, J., Marimon, B.S., Luu, H.T., Imani, G., Arroyo, L., Blundo, C., Kenfack, D., Sainge, M.N., Sonké, B., Vásquez, R., 2022. Making forest data fair and open. Nat. Ecol. Evol. 6, 656–658. https://doi.org/10.1038/s41559-022-01738-7

Dobrowski, S.Z., Swanson, A.K., Abatzoglou, J.T., Holden, Z.A., Safford, H.D., Schwartz, M.K., Gavin, D.G., 2015. Forest structure and species traits mediate projected recruitment declines in western US tree species. Glob. Ecol. Biogeogr. 1–11.

Furniss, T.J., Das, A.J., van Mantgem, P.J., Stephenson, N.L., Lutz, J.A., 2022. Crowding, climate, and the case for social distancing among trees. Ecol. Appl. 32, 1–14. https://doi.org/10.1002/eap.2507

Halofsky, J.E., Peterson, D.L., Harvey, B.J., 2020. Changing wildfire, changing forests: the effects of climate change on fire regimes and vegetation in the Pacific Northwest, USA. Fire Ecol. 16. https://doi.org/10.1186/s42408-019-0062-8

Harmon, M.E., Franklin, J.F., Swanson, F.J., Sollins, P., Gregory, S. V., Lattin, J.D., Anderson, N.H., Cline, S.P., Aumen, N.G., Sedell, J.R., Lienkaemper, G.W., Cromack, K.J., Cummins, K.W., 1986. Ecology of coarse woody debris in temperate ecosystems. Adv. Ecol. Res. 15, 133–302.

Harsch, M.A., Hulme, P.E., McGlone, M.S., Duncan, R.P., 2009. Are treelines advancing? A global meta-analysis of treeline response to climate warming. Ecol. Lett. 12, 1040–1049. https://doi.org/10.1111/j.1461-0248.2009.01355.x

Hood, S.M., Baker, S., Sala, A., 2016. Fortifying the forest: thinning and burning increase resistance to a bark beetle outbreak and promote forest resilience. Ecol. Appl. 26, 1984–2000. https://doi.org/10.1002/eap.1363

Keenan, T.F., Williams, C.A., 2018. The terrestrial carbon sink. Annu. Rev. Environ. Resour. 43, 219–243. https://doi.org/10.1146/annurev-environ-102017-030204

Kilgore, B.M., Briggs, G.S., 1972. Restoring fire to high elevation forests in California. J. For. 70, 266–271.

Knapp, E.E., 2015. Long-term dead wood changes in a Sierra Nevada mixed conifer forest: Habitat and fire hazard implications. For. Ecol. Manage. 339, 87–95. https://doi.org/10.1016/j.foreco.2014.12.008

Lauvaux, C.A., Skinner, C.N., Taylor, A.H., 2016. High severity fire and mixed conifer forest-chaparral dynamics in the southern Cascade Range, USA. For. Ecol. Manage. 363, 74–85. https://doi.org/10.1016/j.foreco.2015.12.016

Lutz, J.A., 2015. The evolution of long-term data for forestry: large temperate research plots in an era of global change. Northwest Sci. 89, 255–269. https://doi.org/10.3955/046.089.0306

Lutz, J.A., Larson, A.J., Swanson, M.E., 2018. Advancing fire science with large forest plots and a long-term multidisciplinary approach. Fire 1, 1–7. https://doi.org/10.3390/fire1010005

Lutz, J.A., Larson, A.J., Swanson, M.E., Freund, J.A., 2012. Ecological importance of large-diameter trees in a temperate mixed-conifer forest. PLoS One 7, e36131. https://doi.org/10.1371/journal.pone.0036131

Lutz, J.A., van Wagtendonk, J.W., Franklin, J.F., 2009. Twentieth-century decline of large-diameter trees in Yosemite National Park, California, USA. For. Ecol. Manage. 257, 2296–2307. https://doi.org/10.1016/j.foreco.2009.03.009

Marshall, A.M., Abatzoglou, J.T., Link, T.E., Tennant, C.J., 2019. Projected changes in interannual variability of peak snowpack amount and timing in the western United States. Geophys. Res. Lett. 46, 8882–8892. https://doi.org/10.1029/2019GL083770

Parks, S.A., Abatzoglou, J.T., 2020. Warmer and drier fire seasons contribute to increases in area burned at high severity in western US forests from 1985 to 2017. Geophys. Res. Lett. 47, 1–10. https://doi.org/10.1029/2020GL089858

Pörtner, H.-O., Roberts, D.C., Tignor, M., Poloczanska, E.S., Mintenbeck, K., Alegría,

A., M. Craig, S. Langsdorf, S. Löschke, V. Möller, A. Okem, B.R., 2022. Climate change 2022: Impacts, adaptation, and vulnerability.

Seidl, R., Thom, D., Kautz, M., Martin-Benito, D., Peltoniemi, M., Vacchiano, G., Wild, J., Ascoli, D., Petr, M., Honkaniemi, J., Lexer, M.J., Trotsiuk, V., Mairota, P., Svoboda, M., Fabrika, M., Nagel, T.A., Reyer, C.P.O., 2017. Forest disturbances under climate change. Nat. Clim. Chang. 7, 395.

Stewart, J.A.E., van Mantgem, P.J., Young, D.J.N., Shive, K.L., Preisler, H.K., Das, A.J., Stephenson, N.L., Keeley, J.E., Safford, H.D., Wright, M.C., Welch, K.R., Thorne, J.H., 2021. Effects of postfire climate and seed availability on postfire conifer regeneration. Ecol. Appl. 31, 1–14. https://doi.org/10.1002/eap.2280

Tepley, A.J., Thompson, J.R., Epstein, H.E., Anderson-Teixeira, K.J., 2017. Vulnerability to forest loss through altered postfire recovery dynamics in a warming climate in the Klamath Mountains. Glob. Chang. Biol. 23, 4117–4132. https://doi.org/10.1111/gcb.13704

Thomas, J.W., 1979. Wildlife habitats in managed forests: the Blue Mountains of Oregon and Washington, Agriculture Handbook No. 553. Washington, D.C., USA. https://doi.org/10.2307/3898589

We must get a grip on forest science — before it's too late, 2022. Nature 608, 449.

Williams, K., Harvey, D., 2001. Transcendent experience in forest environments. J. Environ. Psychol. 21, 249–260. https://doi.org/10.1006/jevp.2001.0204

Zald, H.S.J., Gray, A.N., North, M., Kern, R.A., 2008. Initial tree regeneration responses to fire and thinning treatments in a Sierra Nevada mixed-conifer forest, USA. For. Ecol. Manage. 256, 168–179. https://doi.org/10.1016/j.foreco.2008.04.022

APPENDICES

APPENDIX A

SUPPLEMENTARY MATERIAL FOR CHAPTER II:

PREDICTING SNAG FALL IN AN OLD-GROWTH FOREST AFTER FIRE

Methods: Equations 2.1–2.5

We represented the influence of log consumption on snag fall by calculating the fire radiative energy (FRE) reaching each snag from the consumption of logs that were ≥ 50 cm in diameter and ≥ 1 m long and had therefore been mapped before the fire. We developed an equation based on the idea that energy radiates spherically from a piece of consumed log and that a fraction of that energy will arrive at the focal snag.

$$FRE_{focal} = \sum_{i=1}^{n} CONS.BIO_i \times 368 \times \frac{0.01}{4\pi(DIST_i - \frac{DBH_{focal}}{200})^2} \tag{2.1}$$

where FRE_{focal} is total FRE (MJ) reaching the focal snag from consumed logs within the specified annulus, i represents each 1-m^2 area with a center point within the annulus, n is the total number of 1-m^2 areas with center points within the annulus, $CONS.BIO_i$ is log biomass (Mg) consumed in the ith 1-m^2 area, 368 (MJ Mg^{-1}) is the amount of energy released in MJ from the consumption of 1 Mg of biomass (Wooster et al., 2005), 0.01 is an arbitrarily sized area (m^2) representing where energy from the consumed log makes contact with the focal snag, $DIST_i$ is the distance (m) between the rooting location of the focal snag and the center point of the ith 1-m^2 area, and DBH_{focal} is the DBH (cm) of the focal snag. DBH_{focal} is divided by 200 to convert from cm to m and to account for the radius, rather than the diameter of the tree, decreasing the distance between the log that is being consumed and the nearest part of the focal snag.

We represented the influence of neighborhood crown injury on snag fall by

developing Equations 2.2 and 2.3, which were calculated for successive annuli, and

Equation 2.4, which produced a fixed-size neighborhood metric. Equation 2.2 uses basal

area and percent crown injury as a proxy for crown injury volume within each

neighborhood annulus. Equation 2.3 is a distance-weighted version of Equation 2.2.

Equation 2.4 is a proportional metric that applies Equation 2.3 to a 15-m radius circle

around the focal snag and divides that value by the total distance-weighted basal area in

that circle. In Equations 2.3 and 2.4, distances are weighted according to the inverse-

square law:

$$Neighborhood\ crown\ scorch_{basal.area}$$

$$= \frac{\sum_{i=1}^{n} \frac{CROWN.SCORCH_i}{100} \times BA_i}{AREA\ OF\ ANNULUS} \tag{2.2}$$

$$Neighborhood\ crown\ scorch_{dist.weight}$$

$$= \frac{\sum_{i=1}^{n} \frac{CROWN.SCORCH_i}{100} \times BA_i \times \frac{1}{DIST_i^2}}{AREA\ OF\ ANNULUS} \tag{2.3}$$

$$Neighborhood\ crown\ scorch_{proportional}$$

$$= \frac{\sum_{i=1}^{n} \frac{CROWN.SCORCH_i}{100} \times BA_i \times \frac{1}{DIST_i^2}}{\sum_{i=1}^{n} BA_i \times \frac{1}{DIST_i^2}} \tag{2.4}$$

where i represents each pre-fire live tree within the specified annulus or circle, n is

the total number of pre-fire live trees within the specified annulus or circle,

$CROWN.SCORCH_i$ is percent crown injury of the ith tree, BA_i is basal area of the ith tree,

and $DIST_i$ is the distance (m) between the rooting locations of the focal snag and the ith

tree.

We represented the influence of neighborhood bole scorch on snag fall by developing a fixed-size neighborhood metric where bole scorch of stems within 15 m of the focal snag was weighted by distance from the focal snag according to the inverse-square law. To control for the density of stems around the focal snag, the sum of the distance-weighted bole scorch values was divided by the number of stems, with each stem weighted by its distance from the focal snag according to the inverse-square law:

$$Neighborhood\ bole\ scorch = \frac{\sum_{i=1}^{n} BOLE.SCORCH_i \times \frac{1}{DIST_i^2}}{\sum_{i=1}^{n} \frac{1}{DIST_i^2}} \tag{2.5}$$

where i represents each stem within 15 m of the focal snag, n is the total number of stems within 15 m of the focal snag, $BOLE.SCORCH_i$ is the maximum bole scorch height (m) of the ith stem, and $DIST_i$ is the distance (m) between the rooting locations of the focal snag and the ith stem. The FRE, basal-area–weighted, and distance-weighted crown injury metrics were included in models with post-fire neighborhood annuli. The proportional neighborhood crown injury metric, bole scorch metric, and dNBR were included as fixed-size neighborhood metrics in all post-fire neighborhood models (Table 2.2; Table A.6).

Methods: random forest models

First, we identified the lowest performing accuracy metric. For each snag population and predictor set, models were grouped based on the collinearity threshold (i.e., r = 0.7). For each model and each collinearity threshold, we extracted median values of sensitivity, specificity, and PCC from the 15 runs of that model. For each snag

population, predictor set, and accuracy metric, we generated a matrix of model (rows) by collinearity threshold (columns) that was populated by these median values. We calculated the mean of each matrix. Within each snag population and predictor set, we compared the three mean values (one associated with each accuracy metric) to select the accuracy metric that had the lowest performance.

Next, we identified the collinearity threshold that had the best performance for the lowest performing accuracy metric. For each matrix of the lowest performing accuracy metric, we calculated the column means (i.e., the mean value across models for each collinearity threshold) and selected the column with the highest value (i.e., the collinearity threshold that had the best mean performance for the lowest performing metric).

Lastly, within that selected column of the selected matrix, we identified the model with the highest value (i.e., the model that had the best median performance for the lowest performing metric). Thus, for each of the snag populations and within each of the predictor sets, a model was considered most predictive if 1) it was associated with the collinearity threshold that had the highest mean performance for the lowest performing accuracy metric, and 2) it was the best-performing model within that group.

Reference

Wooster, M.J., Roberts, G., Perry, G.L.W., Kaufman, Y.J., 2005. Retrieval of biomass combustion rates and totals from fire radiative power observations: FRP derivation and calibration relationships between biomass consumption and fire radiative energy release. J. Geophys. Res. Atmos. 110, 1–24. https://doi.org/10.1029/2005JD006318

Table A.1. Annual abundance, recruitment, and loss of pre-fire snags (i.e., died before the fire) in the 25.6-ha Yosemite Forest Dynamics Plot (YFDP). The Rim Fire burned the YFDP in the fall of 2013. Snag recruitment and loss represent changes between the year of the row they are in and the next year. Only snags ≥ 10 cm DBH were inventoried at plot establishment. Beginning in 2011, mortalities of trees ≥ 1 cm DBH were documented. Snag diameter and decay class were remeasured in 2014. Recruitment and loss due to change represent snags that had reduced in size or entered a different decay class. Stems were recorded as consumed if stem height was reduced to below 1.37 m and no piece of bole ≥ 1 m long that belonged to that stem was found nearby.

Year	Diameter class (cm)	Abundance					Recruitment from mortality / **Recruitment due to change**					Loss from fall / **Loss due to change** / *Loss from consumption*				
	Decay class	1	2	3	4	5	1	2	3	4	5	1	2	3	4	5
2010	1–<10	—	—	—	—	—	316	0	0	0	0	0	0	0	0	0
2010	10–<60	1,034	859	300	69	20	190	0	0	0	0	45	41	23	5	1
2010	≥60	67	126	123	100	20	11	0	0	0	0	0	1	0	1	1
2011	1–<10	316	0	0	0	0	298	0	0	0	0	14	0	0	0	0
2011	10–<60	1,179	818	277	64	19	163	0	0	0	0	51	46	7	1	0
2011	≥60	78	125	123	99	19	17	0	0	0	0	0	2	5	2	0
2012	1–<10	600	0	0	0	0	454	0	0	0	0	39	0	0	0	0
2012	10–>60	1,291	772	270	63	19	165	0	0	0	0	36	25	14	3	1
2012	≥60	95	123	118	97	19	9	0	0	0	0	0	2	0	1	0
2013	1–<10	1,015	0	0	0	0	**13**	**61**	**22**	**11**	**4**	85 / **84** / *463*	0 / **0** / *0*	0 / **0** / *0*	0 / **0** / *0*	0 / **0** / *0*
2013	10–<60	1,420	747	256	60	18	**53**	**319**	**247**	**144**	**16**	63 / **466** / *251*	40 / **201** / *202*	28 / **42** / *106*	4 / **13** / *34*	1 / **4** / *12*
2013	≥60	104	121	118	96	19	**8**	**38**	**46**	**63**	**7**	5 / **65** / *0*	4 / **89** / *13*	10 / **57** / *22*	6 / **24** / *40*	1 / **7** / *7*
2014	1–<10	396	61	22	11	4	—	—	—	—	—	117	21	10	1	2
2014	10–<60	693	623	327	153	17	—	—	—	—	—	5	18	5	3	0
2014	≥60	42	53	75	89	11	—	—	—	—	—	0	1	2	1	0

Year	Diameter class (cm)	Abundance					Recruitment from mortality **Recruitment due to change**					Loss from fall **Loss due to change** *Loss from consumption*				
	Decay class	1	2	3	4	5	1	2	3	4	5	1	2	3	4	5
2015	1–<10	279	40	12	10	2	—	—	—	—	—	62	11	4	1	0
	10–<60	688	605	322	150	17	—	—	—	—	—	57	34	10	4	0
	≥60	42	52	73	88	11	—	—	—	—	—	0	0	0	0	0
2016	1–<10	217	29	8	9	2	—	—	—	—	—	68	11	3	1	0
	10–<60	631	571	312	146	17	—	—	—	—	—	148	107	56	13	6
	≥60	42	52	73	88	11	—	—	—	—	—	0	0	1	1	0
2017	1–<10	149	18	5	8	2	—	—	—	—	—	49	8	0	2	0
	10–<60	483	464	256	133	11	—	—	—	—	—	201	181	87	24	8
	≥60	42	52	72	87	11	—	—	—	—	—	1	3	2	4	2
2018	1–<10	100	10	5	6	2	—	—	—	—	—	—	—	—	—	—
	10–<60	282	283	169	109	3	—	—	—	—	—	—	—	—	—	—
	≥60	41	49	70	83	9	—	—	—	—	—	—	—	—	—	—

Table A.2. Annual basal area and volume of pre-fire snags in the 25.6-ha Yosemite Forest Dynamics Plot (YFDP). The Rim Fire burned the YFDP in the fall of 2013.

Year	Diameter class (cm)	Basal area (m^2)					Volume (m^3)				
	Decay class	1	2	3	4	5	1	2	3	4	5
2010	1–<10	—	—	—	—	—	—	—	—	—	—
	10–<60	42.4	42.5	19.6	7.3	2.2	309.2	299.1	96.9	27.9	7.2
	≥60	41.6	104.8	131.3	92.9	18.5	645.1	1,550.7	1670.8	678.0	85.5
2011	1–<10	0.7	0	0	0	0	2.1	0	0	0	0
	10–<60	47.4	41.4	18.3	6.6	2.1	342.3	294.4	91.3	25.7	6.8
	≥60	50.0	103.7	131.3	92.1	17.7	766.6	1,536.0	1,670.8	673.6	81.6
2012	1–<10	1.4	0	0	0	0	3.9	0	0	0	0
	10–<60	53.3	39.4	18.1	6.6	2.1	381.7	281.2	90.6	25.6	6.8
	≥60	68.4	102.7	127	88.9	17.7	985	1518.8	1615.4	626.2	81.6
2013	1–<10	2.2	0	0	0	0	6.2	0	0	0	0
	10–<60	58.8	38.3	17.2	6.5	2.0	421.9	273.4	86.6	25.4	6.6
	≥60	74.4	101.6	127.0	88.0	17.7	1077.2	1510.7	1615.4	618.2	81.6
2014	1–<10	1.0	0.2	0.1	0.1	0	2.8	0.5	0.2	0.1	0
	10–<60	26.8	29.4	19.6	13.0	1.0	179.3	190.5	98.5	53.6	4.3
	≥60	25.9	37.3	51.6	60.1	9.2	339.3	532.9	551.9	506.9	46.2
2015	1–<10	0.7	0.1	0	0.1	0	1.9	0.3	0.1	0.1	0
	10–<60	26.8	28.9	19.5	12.7	1.0	179.0	187.8	98.1	52.7	4.3
	≥60	25.9	36.9	50.1	59.7	9.2	339.3	529.8	532.1	504.6	46.2
2016	1–<10	0.5	0.1	0	0	0	1.5	0.2	0.1	0.1	0
	10–<60	25.2	28.0	19.2	12.6	1.0	169.9	182.9	96.8	52.5	4.3
	≥60	25.9	36.9	50.1	59.7	9.2	339.3	529.8	532.1	504.6	46.2
2017	1–<10	0.4	0.1	0	0	0	1.0	0.1	0	0.1	0
	10–<60	20.4	24.9	17.5	12.2	0.8	140.7	167.1	87.7	50.4	3.7
	≥60	25.9	36.9	49.4	59.4	9.2	339.3	529.8	523.2	500.5	46.2
2018	1–<10	0.2	0	0	0	0	0.7	0.1	0	0.1	0
	10–<60	14.7	19.2	14.9	11.3	0.3	108.2	134.2	76.5	47.5	0.9
	≥60	25.6	35.5	48.2	56.4	7.9	338.1	518.4	507.6	467.8	26.4

Table A.3. Annual biomass and carbon content of pre-fire snags in the 25.6-ha Yosemite Forest Dynamics Plot (YFDP). The Rim Fire burned the YFDP in the fall of 2013.

Year	Diameter class (cm)	Biomass (Mg)					Carbon content (Mg)				
	Decay class	1	2	3	4	5	1	2	3	4	5
2010	1–<10	—	—	—	—	—	—	—	—	—	—
	10–<60	113.8	99.6	28.3	6.5	1.6	58.2	50.9	14.4	3.4	0.8
	≥60	236.5	477.7	445.9	172.5	16.9	120.9	245.5	230.8	89.8	8.8
2011	1–<10	0.8	0	0	0	0	0.4	0	0	0	0
	10–<60	126.1	98.0	26.6	6.0	1.5	64.4	50.1	13.6	3.1	0.8
	≥60	280.3	472.6	445.9	171.5	16.2	143.4	242.9	230.8	89.3	8.5
2012	1–<10	1.4	0	0	0	0	0.7	0	0	0	0
	10–<60	141.5	93.4	26.4	5.9	1.5	72.2	47.8	13.5	3.1	0.8
	≥60	359.2	467.2	430.4	159.4	16.2	183.9	240.1	222.9	83	8.5
2013	1–<10	2.3	0	0	0	0	1.2	0	0	0	0
	10–<60	157.7	90.9	25.2	5.9	1.4	80.5	46.5	12.9	3.1	0.8
	≥60	393.8	464.3	430.4	157.5	16.2	201.5	238.7	222.9	82.1	8.5
2014	1–<10	1.0	0.2	0.1	0	0	0.5	0.1	0	0	0
	10–<60	67.5	65.0	28.1	12.7	0.7	34.4	33.2	14.4	6.7	0.4
	≥60	123.2	167.3	150.6	126.8	8.3	63.1	85.9	77.6	66.2	4.4
2015	1–<10	0.7	0.1	0	0	0	0.4	0	0	0	0
	10–<60	67.4	64.1	27.9	12.5	0.7	34.4	32.7	14.3	6.6	0.4
	≥60	123.2	166.5	145.4	126.2	8.3	63.1	85.4	74.9	65.9	4.4
2016	1–<10	0.6	0.1	0	0	0	0.3	0	0	0	0
	10–<60	64.0	62.4	27.6	12.5	0.7	32.7	31.9	14.1	6.6	0.4
	≥60	123.2	166.5	145.4	126.2	8.3	63.1	85.4	74.9	65.9	4.4
2017	1–<10	0.4	0	0	0	0	0.2	0	0	0	0
	10–<60	53.2	57.1	25.0	12.0	0.6	27.1	29.1	12.8	6.3	0.3
	≥60	123.2	166.5	143.1	125.4	8.3	63.1	85.4	73.7	65.5	4.4

2018	1–<10	0.3	0	0	0	0	0.1	0	0	0	0
	10–<60	41.2	45.9	21.6	11.3	0.2	21.0	23.5	11.1	5.9	0.1
	≥60	122.8	162.8	139.0	116.8	4.9	62.9	83.6	71.6	61.0	2.6

Table A.4. Annual abundance, recruitment, and loss of post-fire snags in the 25.6-ha Yosemite Forest Dynamics Plot (YFDP). The Rim Fire burned the YFDP in the fall of 2013. Counts of snag recruitment and loss represent changes between the year of the row they are in and the next year. Dynamics of pre-fire snags are reported in Tables A.1–A.3.

Year	Diameter class (cm)	Abundance					Recruitment from mortality					Loss from fall				
	Decay class	1	2	3	4	5	1	2	3	4	5	1	2	3	4	5
2013	1–<10	0	0	0	0	0	15,554	231	44	9	4	0	0	0	0	0
	10–<60	0	0	0	0	0	5,406	50	10	5	1	0	0	0	0	0
	≥60	0	0	0	0	0	44	0	0	0	0	0	0	0	0	0
2014	1–<10	15,554	231	44	9	4	630	0	0	0	0	638	53	10	3	3
	10–<60	5,406	50	10	5	1	1,911	2	0	0	0	6	0	0	0	0
	≥60	44	0	0	0	0	43	0	0	0	0	0	0	0	0	0
2015	1–<10	15,546	178	34	6	1	104	1	0	0	0	1,908	30	5	0	0
	10–<60	7,311	52	10	5	1	832	0	0	0	0	265	2	1	0	0
	≥60	87	0	0	0	0	217	0	0	0	0	0	0	0	0	0
2016	1–<10	13,742	149	29	6	1	69	0	0	0	0	3,741	36	5	1	0
	10–<60	7,878	50	9	5	1	417	0	0	0	0	741	6	2	2	0
	≥60	304	0	0	0	0	119	0	0	0	0	4	0	0	0	0
2017	1–<10	10,070	113	24	5	1	47	0	0	0	0	3,350	37	6	1	0
	10–<60	7,554	44	7	3	1	196	0	0	0	0	1,486	8	4	0	1
	≥60	419	0	0	0	0	32	0	0	0	0	3	0	0	0	0
2018	1–<10	6,720	76	18	4	1	—	—	—	—	—	—	—	—	—	—
	10–<60	6,068	36	3	3	0	—	—	—	—	—	—	—	—	—	—
	≥60	416	0	0	0	0	—	—	—	—	—	—	—	—	—	—

Table A.5. Annual basal area, volume, biomass, and carbon content of post-fire snags in the 25.6-ha Yosemite Forest Dynamics Plot (YFDP). The Rim Fire burned the YFDP in the fall of 2013. Decay class 5 values were < 0.1 for every metric and are not reported. Dynamics of pre-fire snags are reported in Tables A.1–A.3.

Year	Diameter class (cm)	Basal area (m^2)				Volume (m^3)				Biomass (Mg)				Carbon content (Mg)			
	Decay class	1	2	3	4	1	2	3	4	1	2	3	4	1	2	3	4
2014	1–<10	33.4	0.4	0.1	0	96	1.1	0.2	0	36.5	0.4	0.1	0	18.6	0.2	0	0
2014	10–<60	139.9	1	0.2	0.1	791.2	4.4	1.1	0.6	305.7	1.6	0.3	0.1	155.7	0.8	0.2	0.1
2014	≥60	39.9	0	0	0	479.5	0	0	0	175.9	0	0	0	90.1	0	0	0
2015	1–<10	34.8	0.3	0.1	0	100.2	0.9	0.2	0	38.2	0.3	0.1	0	19.5	0.2	0	0
2015	10–<60	218.6	1.1	0.2	0.1	1,317.6	5.4	1.1	0.6	499.8	1.9	0.3	0.1	254.9	1	0.2	0.1
2015	≥60	67.9	0	0	0	866.5	0	0	0	314	0	0	0	161.1	0	0	0
2016	1–<10	31.3	0.3	0.1	0	90.2	0.8	0.2	0	34.5	0.3	0	0	17.6	0.1	0	0
2016	10–<60	272.4	1	0.1	0.1	1,777.7	4.3	0.6	0.6	667.3	1.6	0.2	0.1	340.8	0.8	0.1	0.1
2016	≥60	263	0	0	0	4,000.3	0	0	0	1391	0	0	0	719.8	0	0	0
2017	1–<10	23.1	0.3	0.1	0	66.5	0.7	0.2	0	25.6	0.2	0	0	13	0.1	0	0
2017	10–<60	290.8	0.9	0.1	0.1	1,969.7	3.7	0.4	0.4	736.7	1.4	0.1	0.1	376.4	0.7	0.1	0
2017	≥60	357.4	0	0	0	5,610.9	0	0	0	1,947.9	0	0	0	1,008.2	0	0	0
2018	1–<10	16.5	0.2	0.1	0	47.9	0.5	0.1	0	18.6	0.2	0	0	9.4	0.1	0	0
2018	10–<60	258	0.8	0.1	0.1	1,790.1	3.4	0.2	0.4	669.7	1.3	0.1	0.1	342.2	0.6	0	0
2018	≥60	355	0	0	0	5,592.6	0	0	0	1,941.7	0	0	0	18.6	0.2	0	0

Table A.6. All predictor variables initially considered for modeling snag fall. Diameter class thresholds based on crown injury represent the 0–20th percentile (least scorched; 1–9 cm DBH), 20–40th percentile (10–14 cm DBH), 40–60th percentile (15–20 cm DBH), 60–80th percentile (20–27 cm DBH), and > 80th percentile (≥ 28 cm DBH). Snag diameter class thresholds were $1 \leq DBH < 10$ cm, $10 \leq DBH < 60$ cm, and DBH ≥ 60 cm. Pre-fire Neighborhood and Neighborhood Fire Severity metrics were calculated within annuli of radii 0–3, 3–6, 6–9, 9–12, and 12–15 m surrounding each focal snag. [†]Only applies to post-fire snag populations.

Variable	Name in Table A.7	Variable description	Units	Source
Fixed snag attributes				
Species	SPECIES	Snag species	—	Field data
Slope	slope	Computed from the focal cell and the surrounding 8, 10×10 m² cells	Degrees	1-m DEM
Transformed aspect	aspect.mod	Computed from the focal cell and the surrounding 8, 10×10 m² cells	Cosine transformed (1 = NE; -1 = SW)	1-m DEM
Topographic position	tpi	The elevation difference between a focal cell and the mean of surrounding 8, 10×10 m² cells	m	1-m DEM
Terrain ruggedness	tri	The mean of the absolute elevation difference of a focal cell and the surrounding 8, 10×10 m² cells	m	1-m DEM
Roughness	roughness	The largest elevation difference between a focal cell and the surrounding 8, 10×10 m² cells	m	1-m DEM
[†]Time of death	TIME_DEATH	Time after the fire until the tree died	Years	Field data
Pre-fire snag attributes				
DBH	DBH_C1	Pre-fire DBH	cm	Field data
Height	SNAG_HEIGHT_C1int.2	Pre-fire snag height	m	Field data
Decay	SC_C1.fills	Pre-fire decay class	1 (least decayed) through 5	Field data
Post-fire snag attributes				
DBH	DBH	Post-fire DBH	cm	Field data

Variable	Name in Table A.7	Variable description	Units	Source
Height	SNAG_HEIGHT.fills	Post-fire snag height	m	Field data
Decay	SC	Post-fire decay class	1 (least decayed) through 5	Field data
Bole scorch	BOLE_SCORCH.fills	Highest point of flame scorch on stem bole	m	Field data
Unburned	UNBURNED	Located within an unburned patch ≥ 1 m^2	—	Field data
†Crown injury	CROWN_SCORCH.fills	Tree needle death attributed to fire	Percentage	Field data

Pre-fire snag isolation

Variable	Name in Table A.7	Variable description	Units	Source
Pre-fire isolation from trees	PRE_TREE_ISO	Distance to nearest tree pre-fire	m	Field data
Pre-fire isolation from mortality	PRE_MORT_ISO	Distance to nearest 2013 mortality pre-fire	m	Field data
Pre-fire isolation from snags	PRE_SNAG_ISO	Distance to nearest snag pre-fire	m	Field data
Pre-fire isolation from stem fall	PRE_FALL_ISO	Distance to nearest stem that fell in 2013	m	Field data

Variable	Name in Table A.7	Variable description	Units	Source
Pre-fire isolation from logs	PRE_LOG_ISO	Distance to nearest stem that fell after plot establishment through 2013	m	Field data
Pre-fire isolation from coarse woody debris	PRE_CWD_ISO_.0 PRE_CWD_ISO_.025 PRE_CWD_ISO_.05 PRE_CWD_ISO_.1	Distance to nearest 1-m^2 area where > 0, ≥ 0.025, ≥ 0.05, or ≥ 0.1 Mg of pre-fire logs ≥ 50 cm diameter were present before the fire. Each mass threshold was associated with a distance variable.	m	Field data
Pre-fire neighborhood annuli	*=outer annulus radius			
Tree density	live_den.2013_* live_den_80.2013_* live_den_60.2013_* live_den_40.2013_* live_den_20.2013_* live_den_0.2013_*	Trees ≥ 1 cm DBH alive in 2013; total and separated into five diameter classes based on crown injury	Trees ha^{-1}	Field data
Tree basal area	live_ba.2013_*	Trees ≥ 1 cm DBH alive in 2013	m^2 ha^{-1}	Field data
Mortality density	new_mort_den.2013_* new_mort_den_80.2013_* new_mort_den_60.2013_* new_mort_den_40.2013_* new_mort_den_20.2013_* new_mort_den_0.2013_*	Tree mortalities detected in 2013; total and separated into five diameter classes based on crown injury	Trees ha^{-1}	Field data
Mortality basal area	new_mort_ba.2013_*	Tree mortalities detected in 2013	m^2 ha^{-1}	Field data

Variable	Name in Table A.7	Variable description	Units	Source
Snag density	snag_den.2013_* snag_den_60.2013_* snag_den_10.2013_* snag_den_1.2013_*	Snags ≥ 1 cm DBH in 2013; total and separated into three snag diameter classes	Snags ha^{-1}	Field data
Snag basal area	snag_ba.2013_*	Snags ≥ 1 cm DBH in 2013	m^2 ha^{-1}	
Fall density	new_fall_den.2013_* new_fall_den_80.2013_* new_fall_den_60.2013_* new_fall_den_40.2013_* new_fall_den_20.2013_* new_fall_den_0.2013_*	Stem falls detected in 2013; total and separated into five diameter classes based on crown injury	Stems ha^{-1}	Field data
Fall basal area	new_fall_ba.2013_*	Stem falls detected in 2013	m^2 ha^{-1}	Field data
Log density	log_den.2013_* log_den_80.2013_* log_den_60.2013_* log_den_40.2013_* log_den_20.2013_* log_den_0.2013_*	Stems ≥ 1 cm DBH that had fallen by 2013; total and separated into five diameter classes based on crown injury	Stems ha^{-1}	Field data
Log basal area	log_ba.2013_*	Stems ≥ 1 cm DBH that had fallen by 2013	m^2 ha^{-1}	Field data
Coarse woody debris volume	PRE_CWD_VOL_*	Pre-fire logs ≥ 50 cm diameter and ≥ 1 m long	m^3 ha^{-1}	Field data
Coarse woody debris biomass	PRE_CWD_BIO_*	Pre-fire logs ≥ 50 cm diameter and ≥ 1 m long	Mg ha^{-1}	Field data
Post-fire fixed-size neighborhood				

Variable	Name in Table A.7	Variable description	Units	Source
Crown injury proportion	CROWN_SCORCH_PRO	Absolute local crown injury was divided by the sum of the basal area of each tree scaled by the inverse-square law to represent proportional neighborhood crown injury within 15 m of each focal snag.	—	Field data
Neighborhood bole scorch	BOLE_SCORCH_COMP	The inverse-square law was used to calculate the influence on each focal snag of the bole scorch of each stem within a radius of 15 m of the focal snag. The sum of these values was divided by the number of stems within 15 m of the focal snag scaled by the inverse-square law.	—	Field data
dNBR	dNBR	Satellite-derived index for 30-m pixels of environmental change caused by fire	Relative index	Landsat
Post-fire snag isolation				
Post-fire isolation from trees	POST_TREE_ISO	Distance to nearest tree post-fire	m	Field data
Post-fire isolation from tree mortality	POST_MORT_ISO	Distance to nearest stem that died in the fire	m	Field data

Variable	Name in Table A.7	Variable description	Units	Source
Post-fire isolation from snags	POST_SNAG_ISO	Distance to nearest snag post-fire	m	Field data
Post-fire isolation from stem fall	POST_FALL_ISO	Distance to nearest stem that fell in the fire	m	Field data
Post-fire isolation from logs	POST_LOG_ISO	Distance to nearest stem that fell after plot establishment through the fire year	m	Field data
Post-fire isolation from consumed trees	POST_TCONS_ISO	Distance to nearest tree that was consumed in the fire	m	Field data
Post-fire isolation from consumed snags	POST_SCONS_ISO	Distance to nearest snag that was consumed in the fire	m	Field data
Post-fire isolation from coarse woody debris consumption	CONS_ISO_.0 CONS_ISO_.025 CONS_ISO_.05 CONS_ISO_.1	Distance to nearest 1-m^2 area where > 0, ≥ 0.025, ≥ 0.05, or ≥ 0.1 Mg of pre-fire logs ≥ 50 cm diameter were consumed in the fire. Each consumption threshold was associated with a distance variable.	m	Field data

Post-fire neighborhood annuli   *=outer annulus radius

Variable	Name in Table A.7	Variable description	Units	Source
Tree density	live_den.2014_* live_den_80.2014_* live_den_60.2014_* live_den_40.2014_* live_den_20.2014_* live_den_0.2014_*	Trees ≥ 1 cm DBH alive in 2014; total and separated into five diameter classes based on crown injury	Trees ha^{-1}	Field data
Tree basal area	live_ba.2014_*	Trees ≥ 1 cm DBH alive in 2014	m^2 ha^{-1}	Field data
Mortality density	new_mort_den.2014_* new_mort_den_80.2014_* new_mort_den_60.2014_* new_mort_den_40.2014_* new_mort_den_20.2014_* new_mort_den_0.2014_*	Tree mortalities detected in 2014; total and separated into five diameter classes based on crown injury	Trees ha^{-1}	Field data
Mortality basal area	new_mort_ba.2014_*	Tree mortalities detected in 2014	m^2 ha^{-1}	Field data
Snag density	snag_den.2014_* snag_den_60.2014_* snag_den_10.2014_* snag_den_1.2014_*	Snags ≥ 1 cm DBH in 2014; total and separated into three snag diameter classes	Snags ha^{-1}	Field data
Snag basal area	snag_ba.2014_*	Snags ≥ 1 cm DBH in 2014	m^2 ha^{-1}	
Fall density	new_fall_den.2014_* new_fall_den_80.2014_* new_fall_den_60.2014_* new_fall_den_40.2014_* new_fall_den_20.2014_* new_fall_den_0.2014_*	Stem falls detected in 2014; total and separated into five diameter classes based on crown injury	Stems ha^{-1}	Field data

Variable	Name in Table A.7	Variable description	Units	Source
Fall basal area	new_fall_ba.2014_*	Stem falls detected in 2014	m^2 ha^{-1}	Field data
Log density	log_den.2014_* log_den_80.2014_* log_den_60.2014_* log_den_40.2014_* log_den_20.2014_* log_den_0.2014_*	Stems ≥ 1 cm DBH that had fallen by 2014; total and separated into five diameter classes based on crown injury	Stems ha^{-1}	Field data
Log basal area	log_ba.2014_*	Stems ≥ 1 cm DBH that had fallen by 2014	Stems ha^{-1}	Field data
Tree consumption density	new_cons_live_den.2014_* new_cons_live_den_80.2014_* new_cons_live_den_60.2014_* new_cons_live_den_40.2014_* new_cons_live_den_20.2014_* new_cons_live_den_0.2014_*	Tree consumption detected in 2014; total and separated into five diameter classes based on crown injury	Trees ha^{-1}	Field data
Tree consumption basal area	new_cons_live_ba.2014_*	Tree consumption detected in 2014	m^2 ha^{-1}	Field data
Snag consumption density	new_cons_snag_den.2014_* new_cons_snag_den_60.2014_* new_cons_snag_den_10.2014_* new_cons_snag_den_1.2014_*	Snag consumption detected in 2014; total and separated into five diameter classes based on crown injury	Trees ha^{-1}	Field data
Snag consumption basal area	new_cons_snag_ba.2014_*	Snag consumption detected in 2014	m^2 ha^{-1}	Field data

Variable	Name in Table A.7	Variable description	Units	Source
Coarse woody debris volume consumed	POST_CWD_VOL_*	Difference between pre-fire logs ≥ 50 cm diameter and ≥ 1 m long and the same logs post-fire; logs were spatially adjusted back to their pre-fire location if they moved during the fire	$m^3\ ha^{-1}$	Field data
Coarse woody debris biomass consumed	POST_CWD_BIO_*	Difference between pre-fire logs ≥ 50 cm diameter and ≥ 1 m long and the same logs post-fire; logs were spatially adjusted back to their pre-fire location if they moved during the fire	$Mg\ ha^{-1}$	Field data
Distance-weighted fire radiative energy	FRE_DW_*	Fire radiative energy (FRE) from consumed logs ≥ 50 cm diameter was calculated for each 1-m^2 area using (Wooster et al., 2005); the inverse-square law was used to calculate FRE arriving at each focal snag from within each annulus	MJ	Field data
Distance-weighted crown injury	CROWN_SCORCH_DW_*	Crown injury percentage was multiplied by basal area for each tree within each annulus; the inverse-square law was used to scale the contribution of each tree to neighborhood crown injury	—	Field data
Crown injury basal area	CROWN_SCORCH_BA_*	Crown injury percentage was multiplied by basal area for each tree within each annulus and divided by the area of the annulus	$m^2\ ha^{-1}$	Field data

Table A.7. Model inputs for four selected models. ***Bold, italicized blue text*** indicates variables that were confirmed by Boruta, were retained after collinear variables were removed, and were run as inputs to random forest. **Bold text** indicates variables that were confirmed by Boruta but were removed because they exceeded the collinearity threshold for that model and were not selected to be kept. Numbers in parentheses are mean importance values averaged across 15 runs of random forest.

Response variable: Pre-fire snags DBH ≥ 10 cm	Model: Post-fire predictors, r = 0.7, 0–3 m neighborhood

DBH (67.1), SNAG_HEIGHT.fills (38.1), BOLE_SCORCH.fills (21.2), CROWN_SCORCH_DW_3 (14.2), SC (14), snag_ba.2014_3 (12), CROWN_SCORCH_BA_3 (12), snag_den_10.2014_3 (11.5), live_ba.2014_3 (10.8), BOLE_SCORCH_COMP (10.1), snag_den.2014_3 (9.4), slope (8.8), live_den_0.2014_3 (8.5), CROWN_SCORCH_PRO (6.7), SPECIES (6.1); **tri, roughness, new_mort_den.2014_3, new_mort_ba.2014_3, snag_den_60.2014_3**

Response variable: Pre-fire snags DBH ≥ 10 cm	Model: Pre-fire predictors, r = 0.7, 0–15 m neighborhood

DBH_C1 (64.4), SNAG_HEIGHT_C1.int.2 (27.5), SPECIES (10.8), live_den_0.2013_3 (10.3), live_ba.2013_3 (8.8), PRE_CWD_VOL_12 (7.5), tri (6.9), SC_C1.fills (6.7), live_den.2013_6 (6.5), live_den_80.2013_9 (5.8), new_mort_ba.2013_15 (5.6), live_den_60.2013_12 (4.9); **slope, live_den_80.2013_6, live_den.2013_9, PRE_CWD_VOL_9, PRE_CWD_VOL_15, PRE_CWD_BIO_9, PRE_CWD_BIO_12, PRE_CWD_BIO_15**

Response variable: Post-fire snags DBH ≥ 10 cm	Model: Post-fire predictors, r = 0.7, 0–6 m neighborhood

SPECIES (61.5), SNAG_HEIGHT.fills (55.7), TIME_DEATH (32), BOLE_SCORCH.fills (27.9), tpi (23.6), dNBR (20.8), new_mort_ba.2014_3 (20.2), slope (18.4), CROWN_SCORCH_PRO (17.8), BOLE_SCORCH_COMP (17.7), snag_ba.2014_3 (17.5), CROWN_SCORCH_BA_6 (16.7), aspect.mod (15.6), live_den.2014_6 (15.5), snag_ba.2014_6 (15.4), live_ba.2014_6 (15.2), CROWN_SCORCH_DW_3 (15.1), live_ba.2014_3 (14.7), new_mort_den_80.2014_3 (14.7), new_mort_den_80.2014_6 (14.3), snag_den_10.2014_6 (13.4), new_cons_live_ba.2014_3 (12.8), new_cons_live_ba.2014_6 (12.7), live_den_40.2014_6 (12.3), FRE_DW_6 (11.8), live_den_60.2014_3 (11.7), live_den_80.2014_6 (11), live_den_0.2014_6 (10.8), POST_CWD_VOL_6 (10.6), live_den.2014_3 (10.5), live_den_60.2014_6 (10.4), new_cons_live_den_80.2014_6 (10.2), live_den_20.2014_6 (10), snag_den_10.2014_3 (9.6), live_den_40.2014_3 (9.3), new_cons_live_den_80.2014_3 (9.1), log_ba.2014_6 (7.7), log_ba.2014_3 (7.5); **tri, roughness, DBH, CROWN_SCORCH.fills, CROWN_SCORCH_BA_3, CROWN_SCORCH_DW_6, new_mort_den.2014_3, snag_den.2014_3, snag_den_60.2014_3, new_cons_live_den.2014_3, new_mort_den.2014_6, new_mort_ba.2014_6, new_mort_den_60.2014_6, snag_den.2014_6, snag_den_60.2014_6, new_cons_live_den.2014_6, POST_CWD_VOL_3, POST_CWD_BIO_3, POST_CWD_BIO_6**

Response variable: Post-fire snags DBH ≥ 10 cm	Model: Pre-fire predictors, r = 0.5, 0–3 m neighborhood

SPECIES (81.6), TIME_DEATH (58.3), tpi (46.6), slope (41.1), aspect.mod (38.7), live_den.2013_3 (33.8), live_ba.2013_3 (28.1), snag_ba.2013_3 (22.2), PRE_CWD_BIO_3 (17.1), snag_den.2013_3 (16.3), live_den_40.2013_3 (13.9), live_den_20.2013_3 (11.6); **tri, roughness, live_den_80.2013_3, live_den_60.2013_3, live_den_0.2013_3, snag_den_60.2013_3, snag_den_10.2013_3, PRE_CWD_VOL_3**
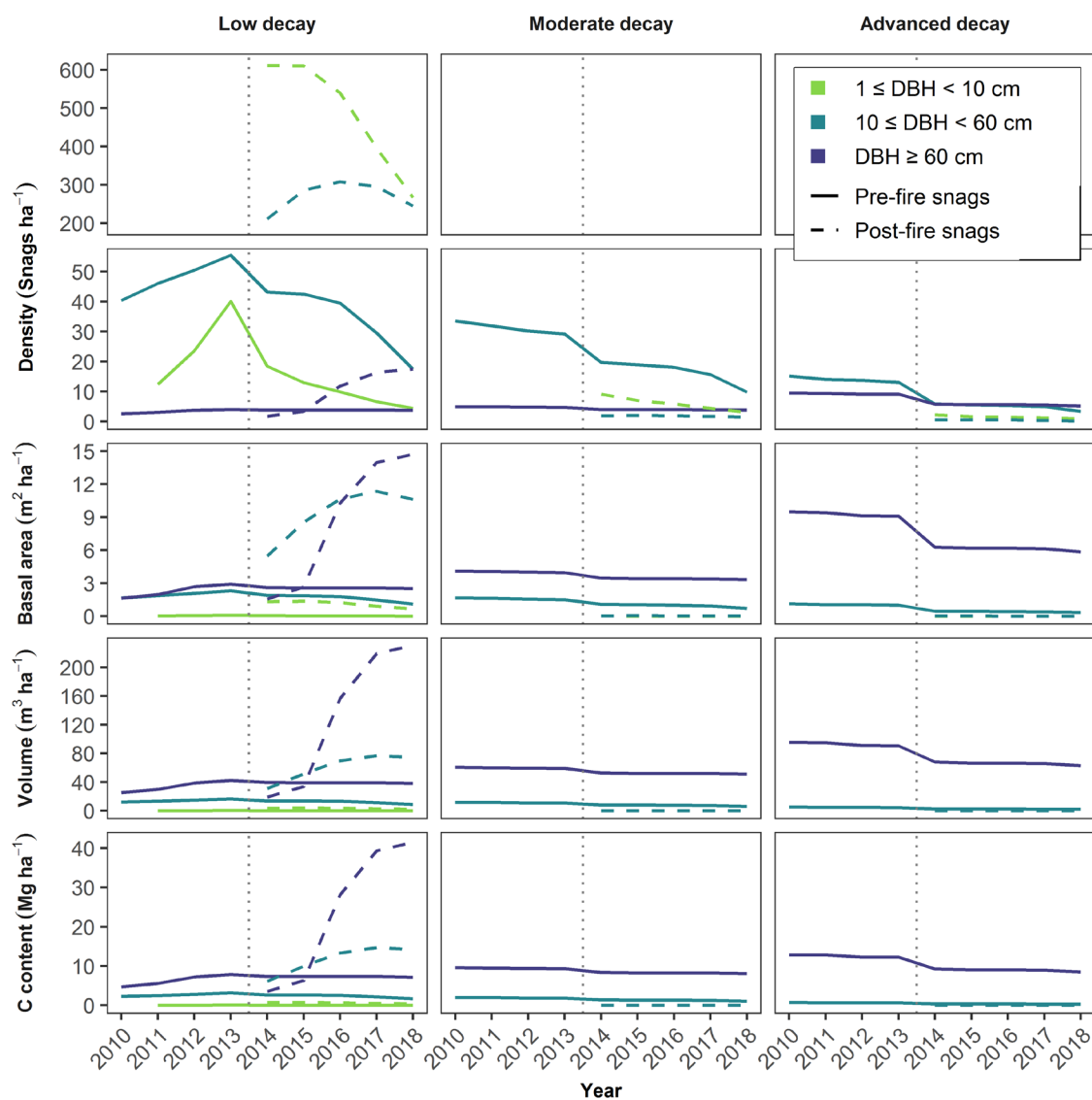
Figure A.1. Snag dynamics in the Yosemite Forest Dynamics Plot from 2011 to 2018 by density, basal area, volume, and carbon (C) content. The vertical dotted line represents the fire event in the fall of 2013. Because snags $1 \leq DBH < 10$ cm were not included in the dataset at plot establishment, all snags $1 \leq DBH < 10$ cm are trees that died after 2010. Low Decay: decay class 1; Moderate Decay: decay classes 2 or 3; Advanced Decay: decay classes 4 or 5.
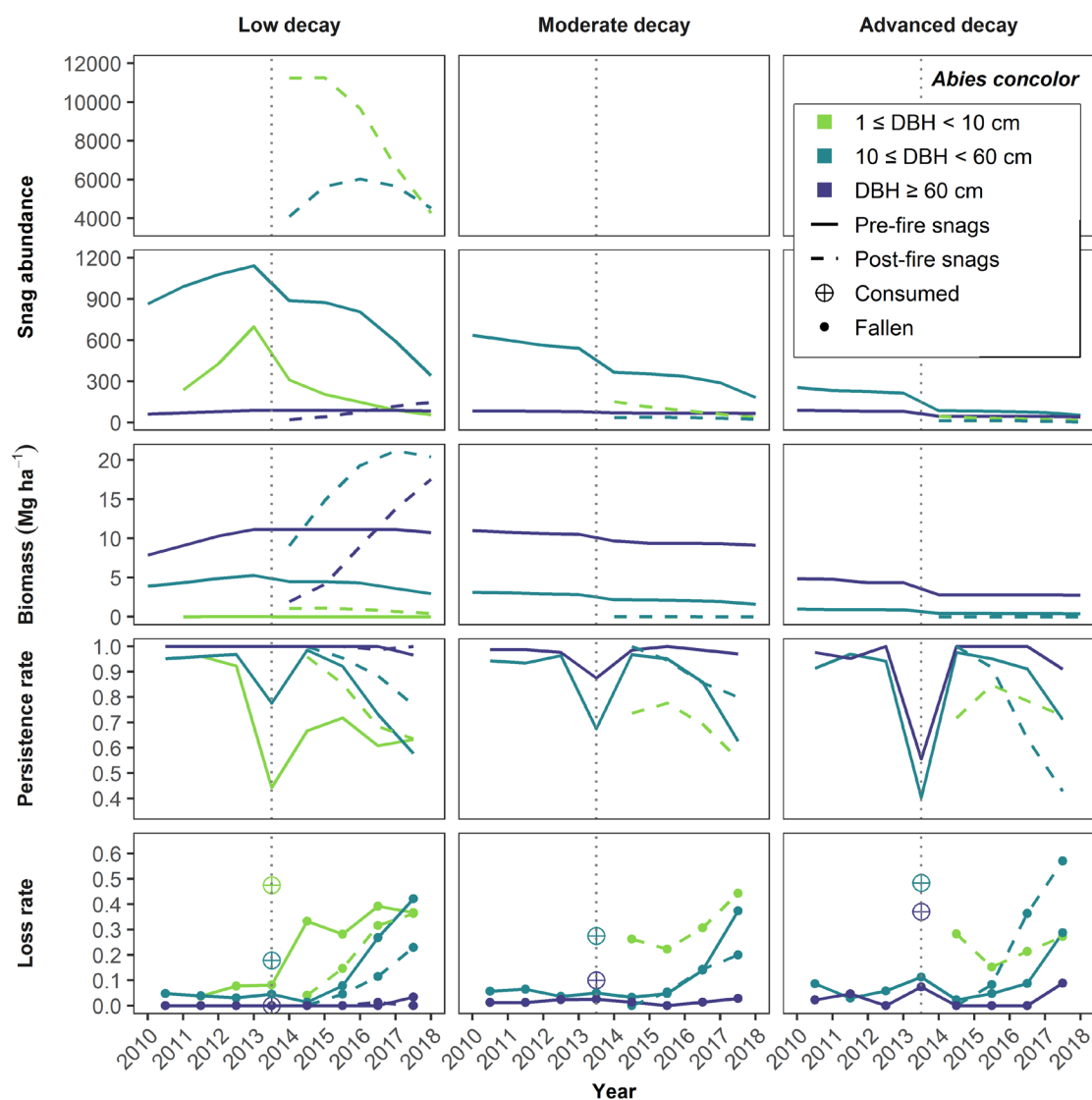
Figure A.2. Snag dynamics for *Abies concolor* (white fir) in the Yosemite Forest Dynamics Plot from 2011 to 2018. Snag persistence and fall rates were calculated as changes in the snag population between summer field seasons. The vertical dotted line represents the fire event in the fall of 2013. Because snags $1 \leq DBH < 10$ cm were not included in the dataset at plot establishment, all snags $1 \leq DBH < 10$ cm are trees that died after 2010. Low Decay: decay class 1; Moderate Decay: decay classes 2 or 3; Advanced Decay: decay classes 4 or 5.
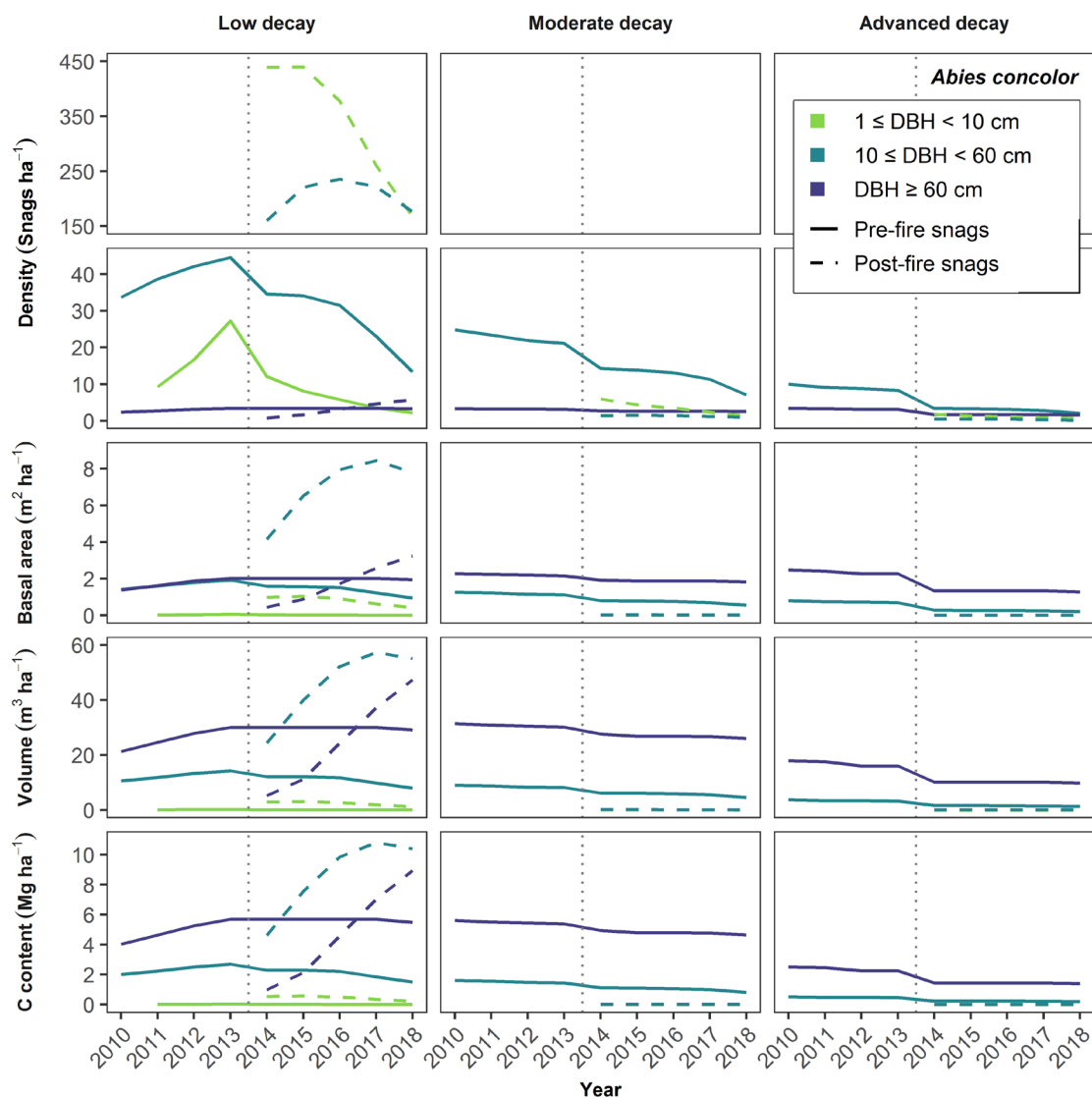
Figure A.3. Snag dynamics for *Abies concolor* in the Yosemite Forest Dynamics Plot from 2011 to 2018 by density, basal area, volume, and carbon (C) content. The vertical dotted line represents the fire event in the fall of 2013. Because snags $1 \leq$ DBH < 10 cm were not included in the dataset at plot establishment, all snags $1 \leq$ DBH < 10 cm are trees that died after 2010. Low Decay: decay class 1; Moderate Decay: decay classes 2 or 3; Advanced Decay: decay classes 4 or 5.
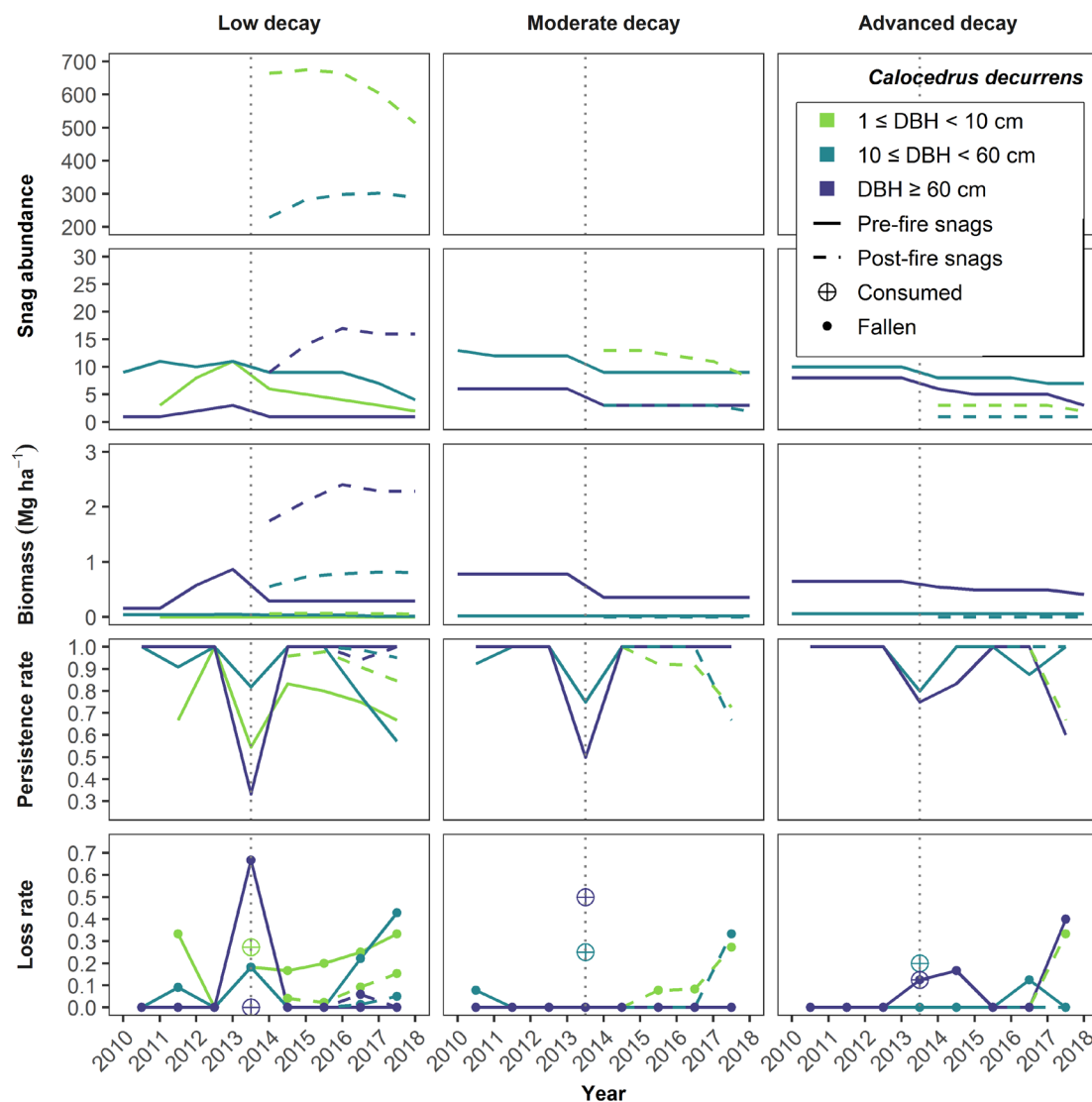
Figure A.4. Snag dynamics for *Calocedrus decurrens* (incense-cedar) in the Yosemite Forest Dynamics Plot from 2011 to 2018. Snag persistence and fall rates were calculated as changes in the snag population between summer field seasons. The vertical dotted line represents the fire event in the fall of 2013. Because snags $1 \leq DBH < 10$ cm were not included in the dataset at plot establishment, all snags $1 \leq DBH < 10$ cm are trees that died after 2010. Low Decay: decay class 1; Moderate Decay: decay classes 2 or 3; Advanced Decay: decay classes 4 or 5.
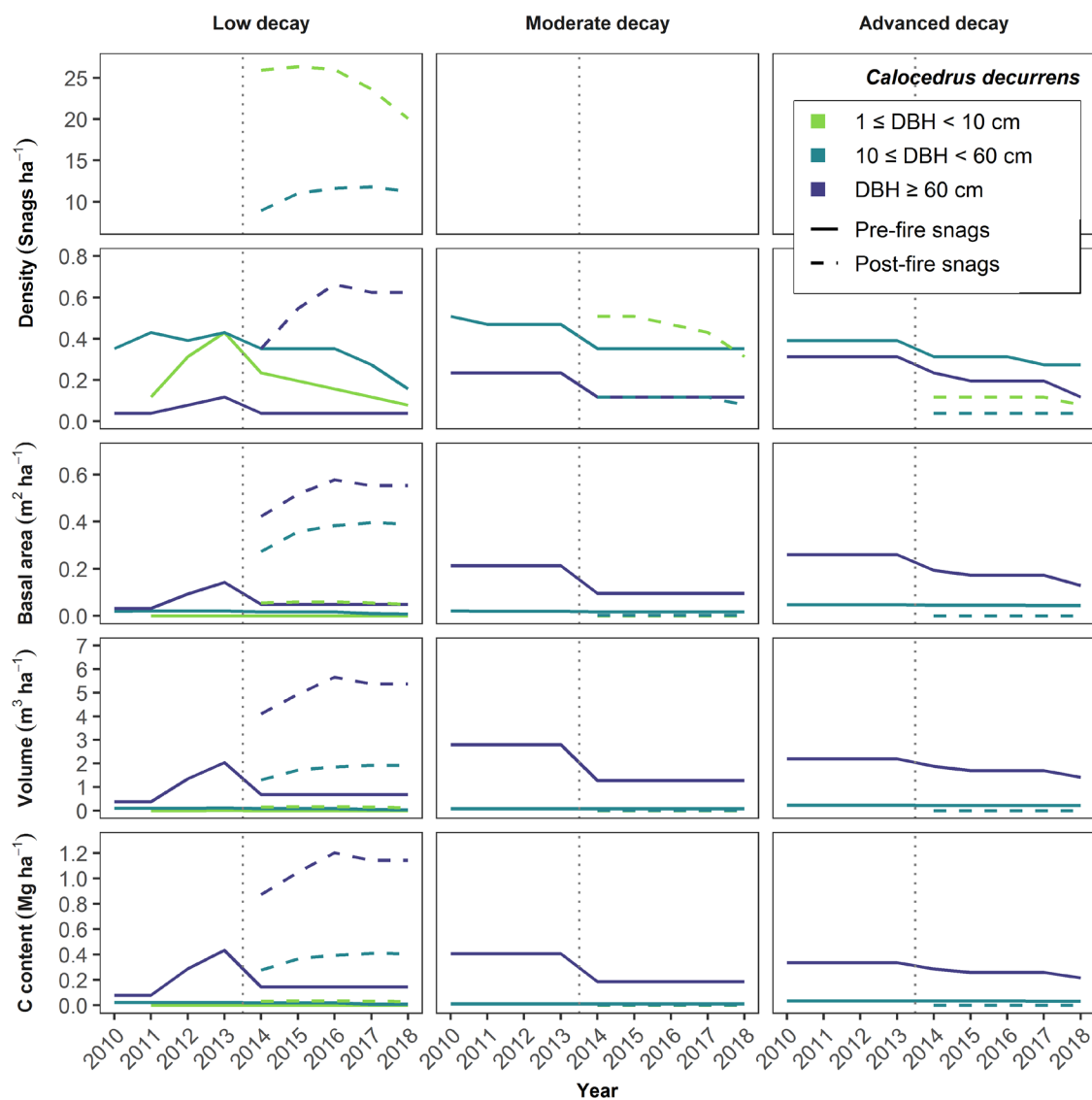
Figure A.5. Snag dynamics for *Calocedrus decurrens* in the Yosemite Forest Dynamics Plot from 2011 to 2018 by density, basal area, volume, and carbon (C) content. The vertical dotted line represents the fire event in the fall of 2013. Because snags $1 \leq$ DBH < 10 cm were not included in the dataset at plot establishment, all snags $1 \leq$ DBH < 10 cm are trees that died after 2010. Low Decay: decay class 1; Moderate Decay: decay classes 2 or 3; Advanced Decay: decay classes 4 or 5.
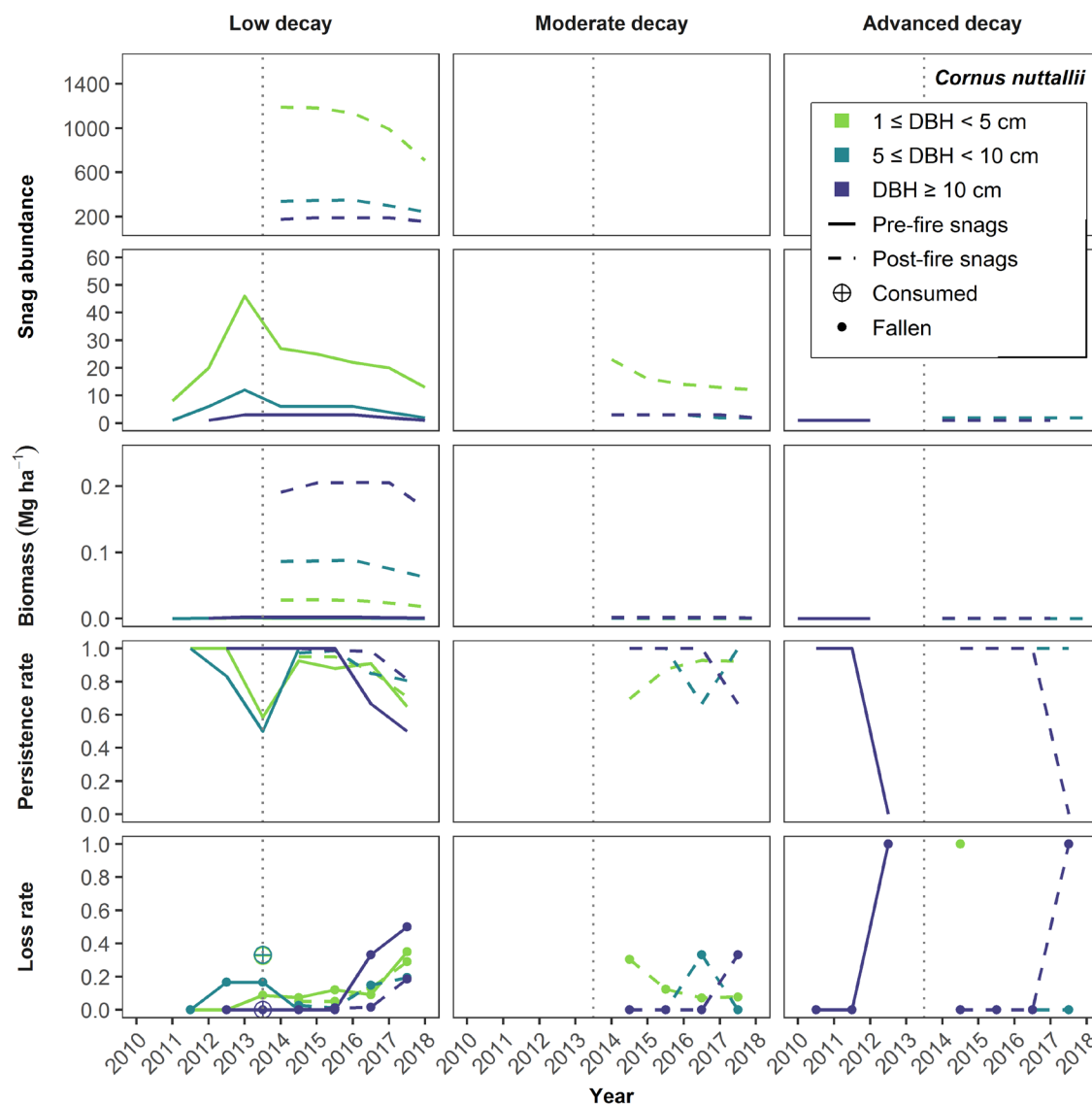
Figure A.6. Snag dynamics for *Cornus nuttallii* (Pacific dogwood) in the Yosemite Forest Dynamics Plot from 2011 to 2018. Snag persistence and fall rates were calculated as changes in the snag population between summer field seasons. The vertical dotted line represents the fire event in the fall of 2013. Because snags $1 \leq DBH < 10$ cm were not included in the dataset at plot establishment, all snags $1 \leq DBH < 10$ cm are trees that died after 2010. Low Decay: decay class 1; Moderate Decay: decay classes 2 or 3; Advanced Decay: decay classes 4 or 5.
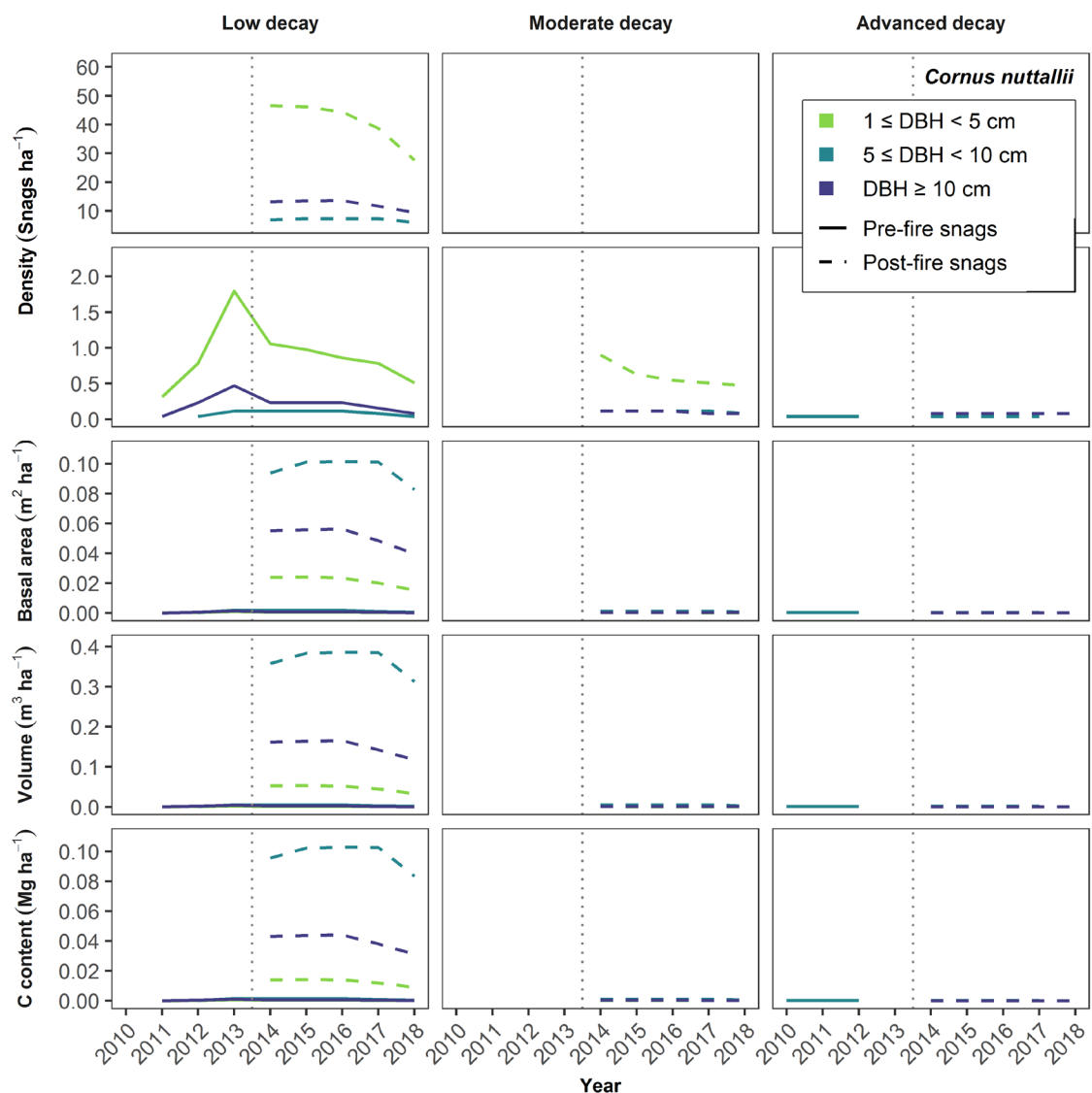
Figure A.7. Snag dynamics for *Cornus nuttallii* in the Yosemite Forest Dynamics Plot from 2011 to 2018 by density, basal area, volume, and carbon (C) content. The vertical dotted line represents the fire event in the fall of 2013. Because snags $1 \leq DBH < 10$ cm were not included in the dataset at plot establishment, all snags $1 \leq DBH < 10$ cm are trees that died after 2010. Low Decay: decay class 1; Moderate Decay: decay classes 2 or 3; Advanced Decay: decay classes 4 or 5.
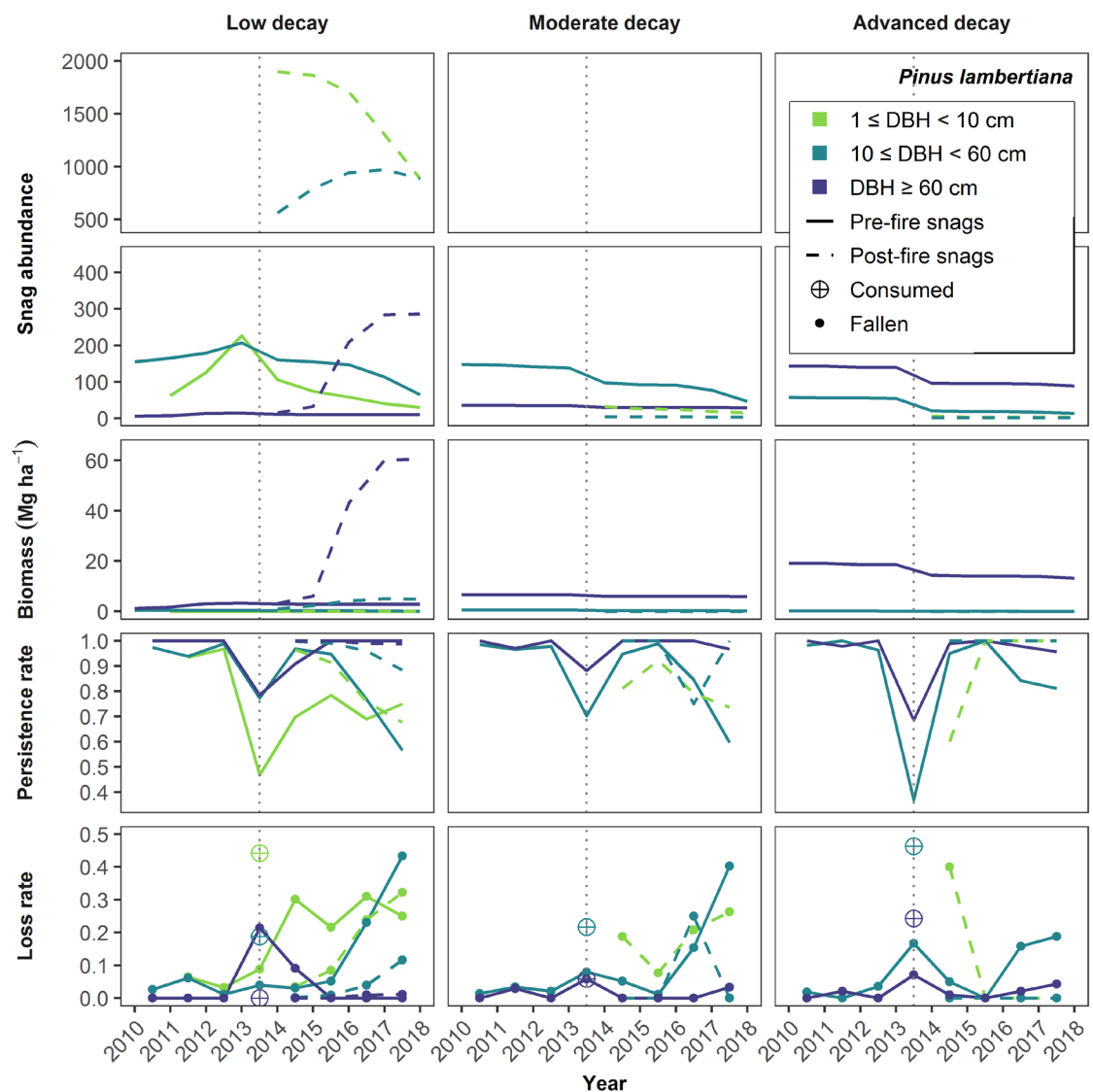
Figure A.8. Snag dynamics for *Pinus lambertiana* (sugar pine) in the Yosemite Forest Dynamics Plot from 2011 to 2018. Snag persistence and fall rates were calculated as changes in the snag population between summer field seasons. The vertical dotted line represents the fire event in the fall of 2013. Because snags $1 \leq DBH < 10$ cm were not included in the dataset at plot establishment, all snags $1 \leq DBH < 10$ cm are trees that died after 2010. Low Decay: decay class 1; Moderate Decay: decay classes 2 or 3; Advanced Decay: decay classes 4 or 5.

Figure A.9. Snag dynamics for *Pinus lambertiana* in the Yosemite Forest Dynamics Plot from 2011 to 2018 by density, basal area, volume, and carbon (C) content. The vertical dotted line represents the fire event in the fall of 2013. Because snags $1 \leq DBH < 10$ cm were not included in the dataset at plot establishment, all snags $1 \leq DBH < 10$ cm are trees that died after 2010. Low Decay: decay class 1; Moderate Decay: decay classes 2 or 3; Advanced Decay: decay classes 4 or 5.
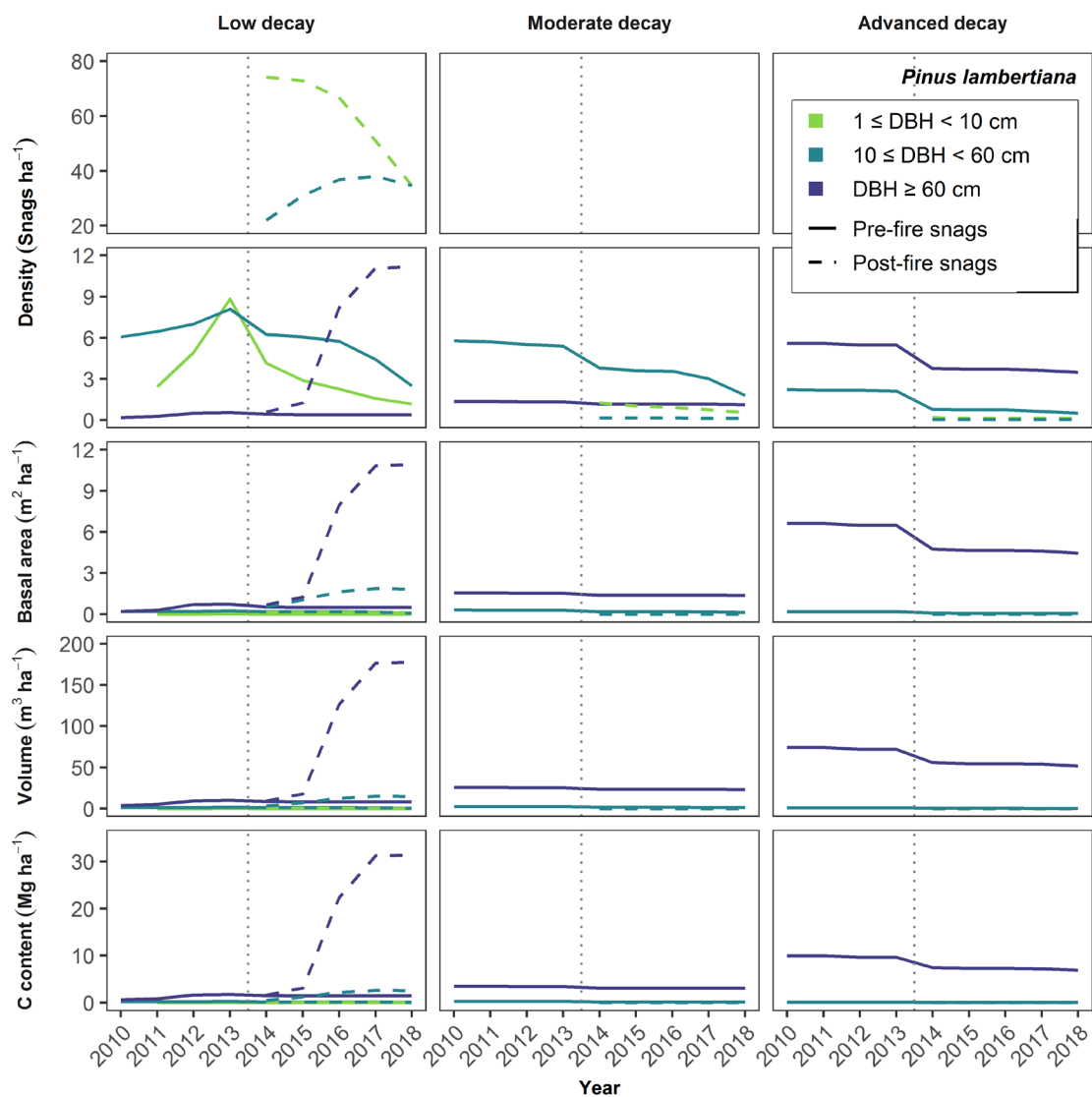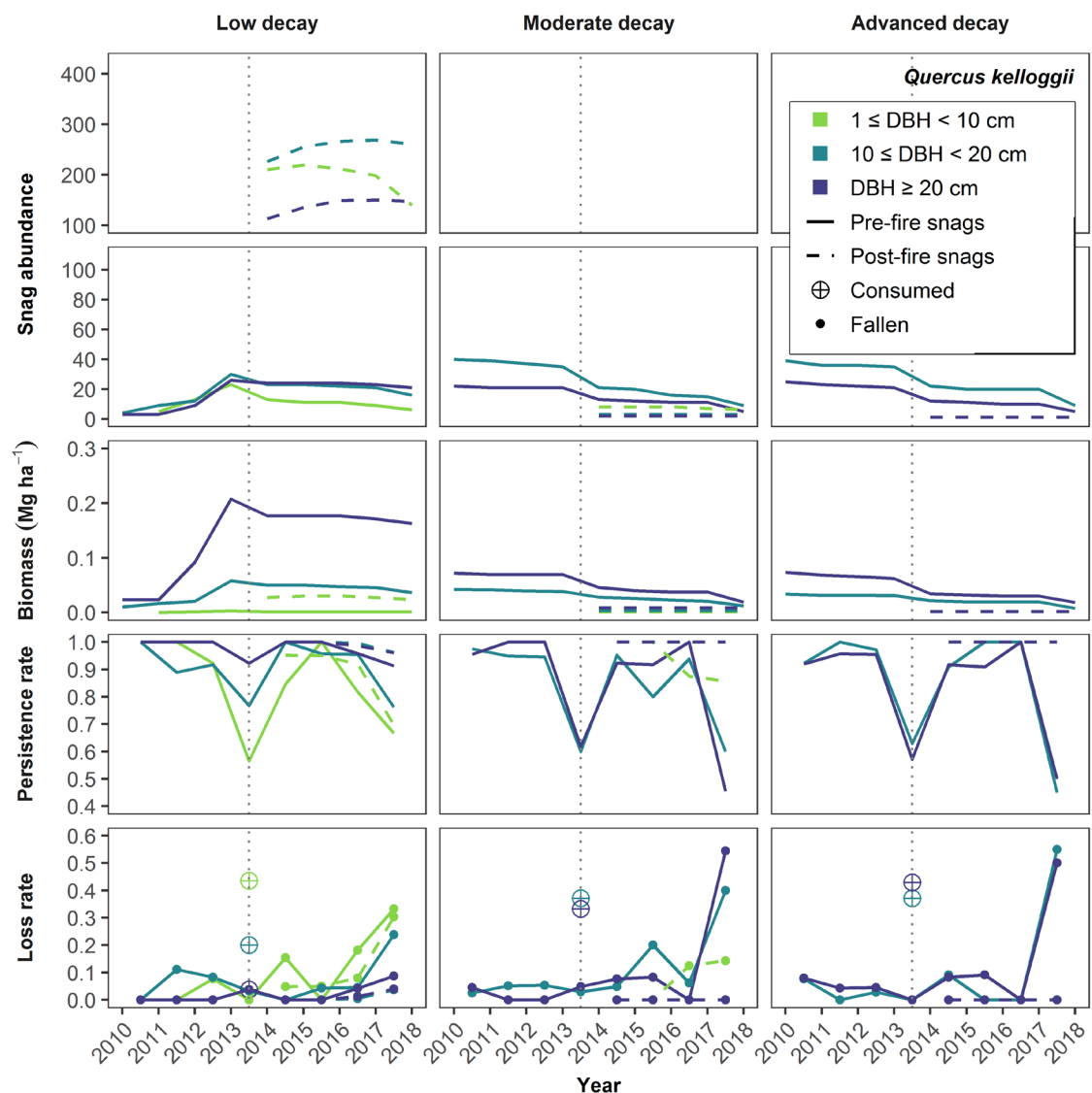
Figure A.10. Snag dynamics for *Quercus kelloggii* (California black oak) in the Yosemite Forest Dynamics Plot from 2011 to 2018. Snag persistence and fall rates were calculated as changes in the snag population between summer field seasons. The vertical dotted line represents the fire event in the fall of 2013. Because snags 1 ≤ DBH < 10 cm were not included in the dataset at plot establishment, all snags 1 ≤ DBH < 10 cm are trees that died after 2010. Low Decay: decay class 1; Moderate Decay: decay classes 2 or 3; Advanced Decay: decay classes 4 or 5.

Figure A.11. Snag dynamics for *Quercus kelloggii* in the Yosemite Forest Dynamics Plot from 2011 to 2018 by density, basal area, volume, and carbon (C) content. The vertical dotted line represents the fire event in the fall of 2013. Because snags $1 \leq DBH < 10$ cm were not included in the dataset at plot establishment, all snags $1 \leq DBH < 10$ cm are trees that died after 2010. Low Decay: decay class 1; Moderate Decay: decay classes 2 or 3; Advanced Decay: decay classes 4 or 5.
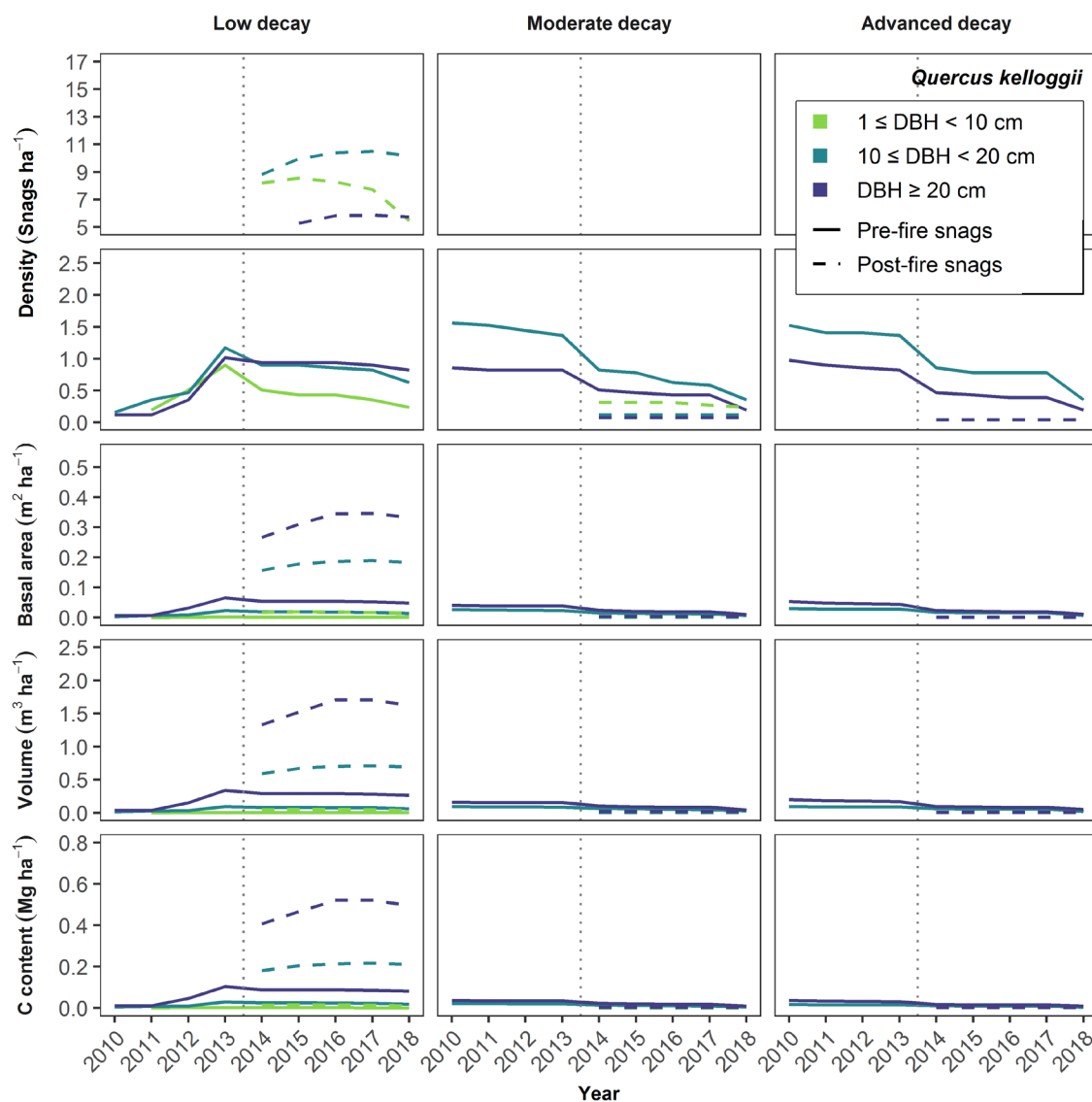
Figure A.12. Random forest model accuracy metrics for models of the fall of pre-fire snags ≥ 10 cm DBH. Model accuracy was determined by 10-fold cross validation. Panel rows indicate whether the models were constrained to pre-fire or post-fire predictor variables. Within each panel, seven models occupy seven rows (see Table 2.2); the accuracy of each model is represented by the three boxplots that occupy that row. The boxplots represent the distribution of the model accuracy of 15 random forest analyses, each run with a different seed. The r-values indicate the maximum level of collinearity between predictor variables.
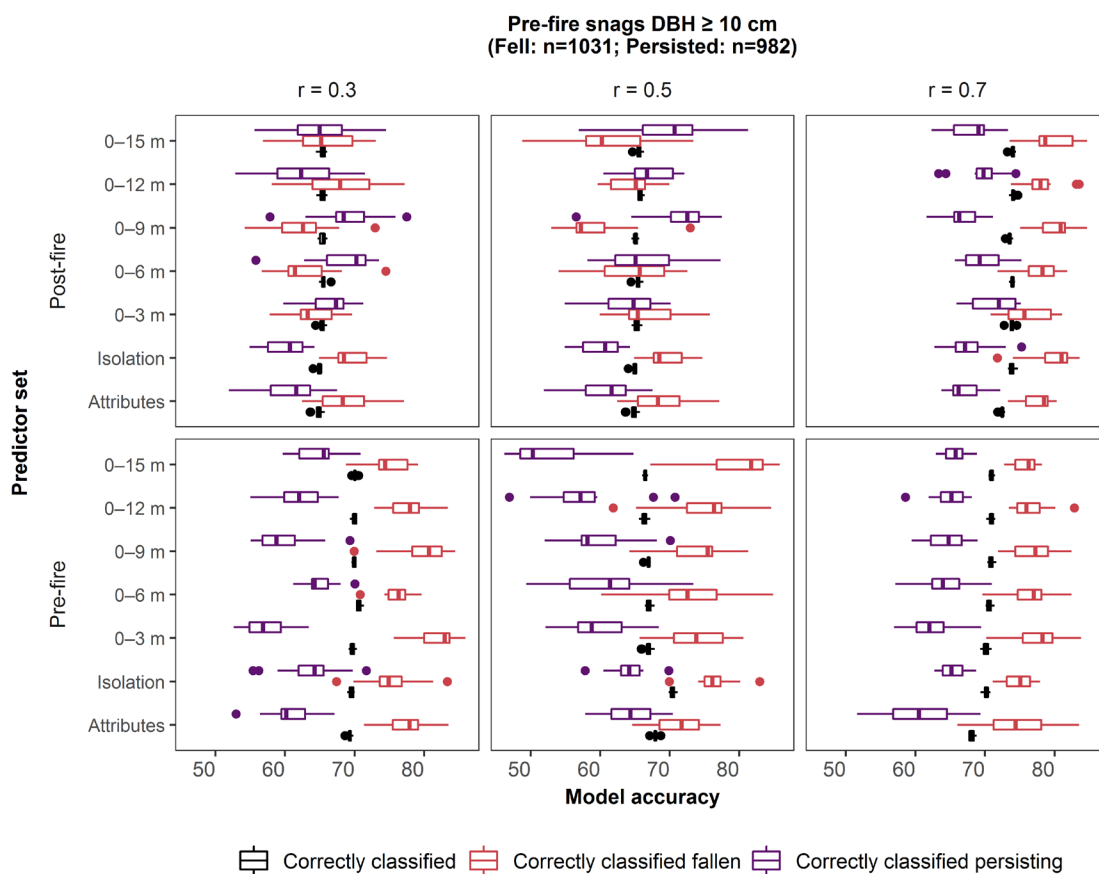
Figure A.13. Random forest metrics for models of the fall of post-fire snags ≥ 10 cm DBH. Model accuracy was determined by 10-fold cross validation. Panel rows indicate whether the models were constrained to pre-fire or post-fire predictor variables. Within each panel, models occupy six or seven rows (see Table 2.2); the accuracy of each model is represented by the three boxplots that occupy that row. The boxplots represent the distribution of the model accuracy of 15 random forest analyses, each run with a different seed. The r-values indicate the maximum level of collinearity between predictor variables.
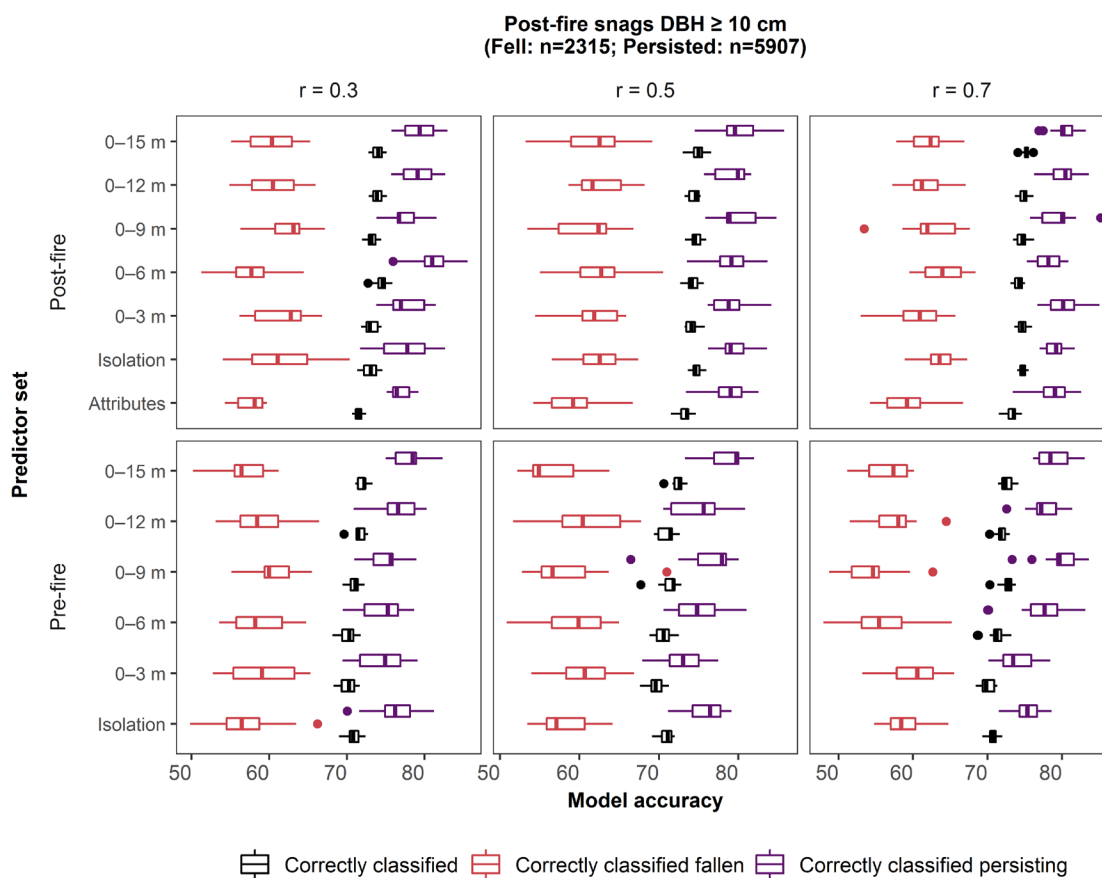
Post-fire snags DBH ≥ 10 cm
(Fell: n=2315; Persisted: n=2315)
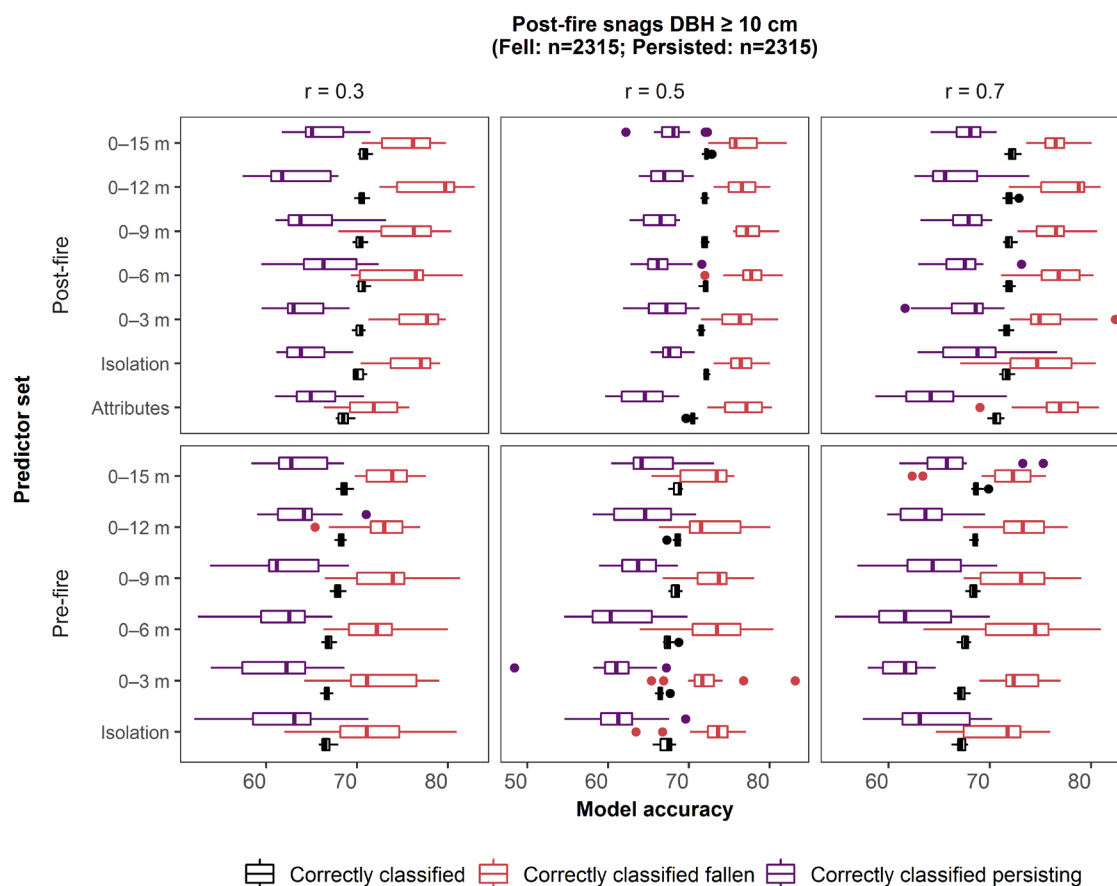
Figure A.14. Random forest metrics for models of the fall of post-fire snags ≥ 10 cm DBH run with balanced data. To verify whether an imbalance in snag outcomes was driving the difference in sensitivity and specificity for the post-fire snag population, which is slightly imbalanced, we randomly selected subsets of the more common outcome to generate a balanced dataset: 2,315 snags were randomly selected without replacement from the 5,907 snags that persisted. Five random draws were run on each of three seeds. When we reran the random forest models with balanced data, the results resembled the pre-fire snag population models: sensitivity tended to be the higher metric and, for each model, the difference between sensitivity and specificity was reduced. Model accuracy was determined by 10-fold cross validation. Panel rows indicate whether the models were constrained to pre-fire or post-fire predictor variables. Within each panel, models occupy six or seven rows (see Table 2.2); the accuracy of each model is represented by the three boxplots that occupy that row. The boxplots represent the distribution of the model accuracy of those 15 random forest analyses. The r-values indicate the maximum level of collinearity between predictor variables.

Figure A.15. Correlation matrix of important continuous variables in the most predictive model (i.e., 0–3 m neighborhood, r = 0.7) that used just post-fire variables to predict fall of pre-fire snags ≥ 10 cm DBH (see Table 2.2). Variables that correlated with at least one other variable at $r^2 > |0.15|$ were selected for display. See Table A.6 for predictor variable definitions.
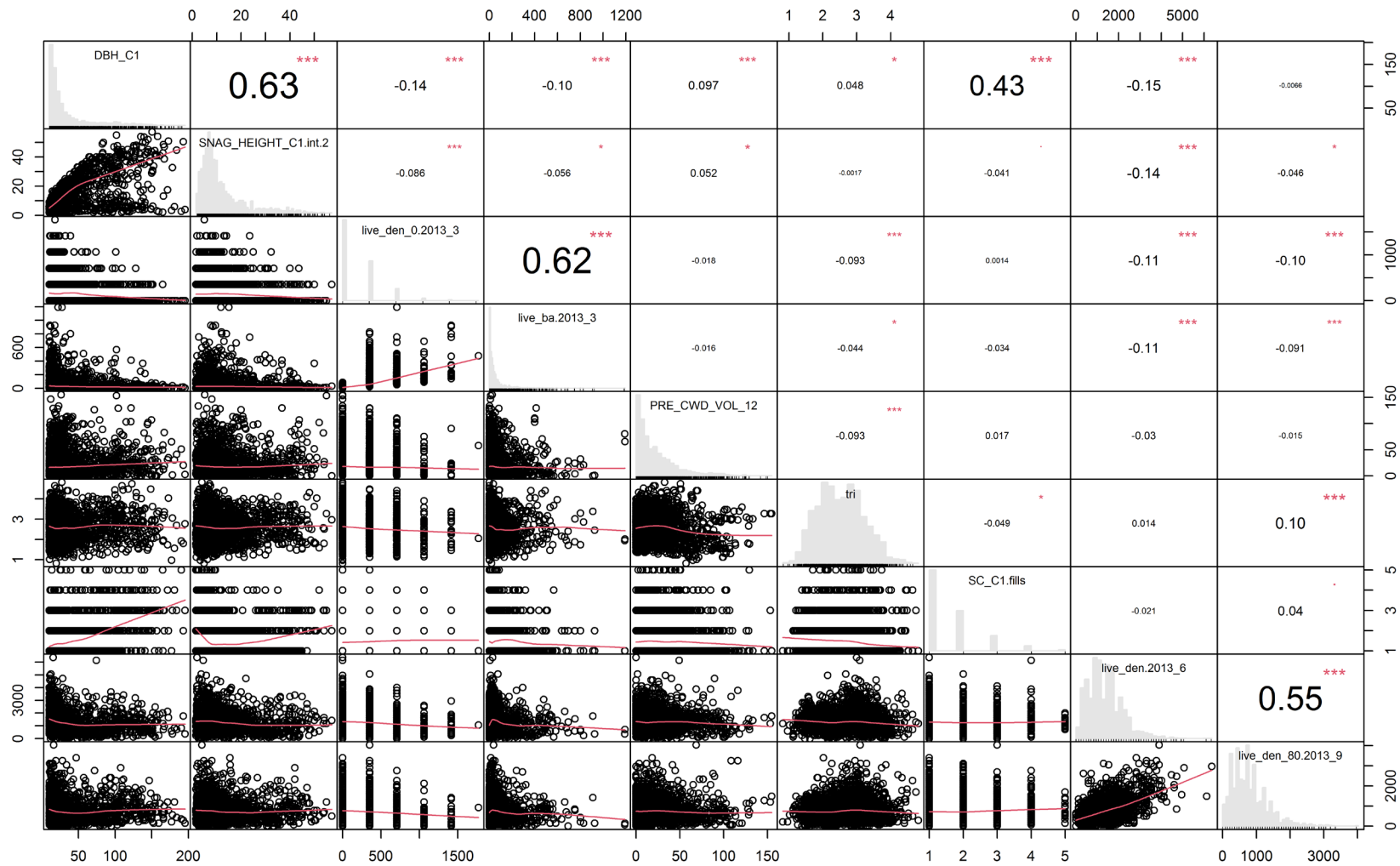
Figure A.16. Correlation matrix of important continuous variables in the most predictive model (i.e., 0–15 m neighborhood, r = 0.7) that used just pre-fire variables to predict fall of pre-fire snags ≥ 10 cm DBH (see Table 2.2). See Table A.6 for predictor variable definitions.
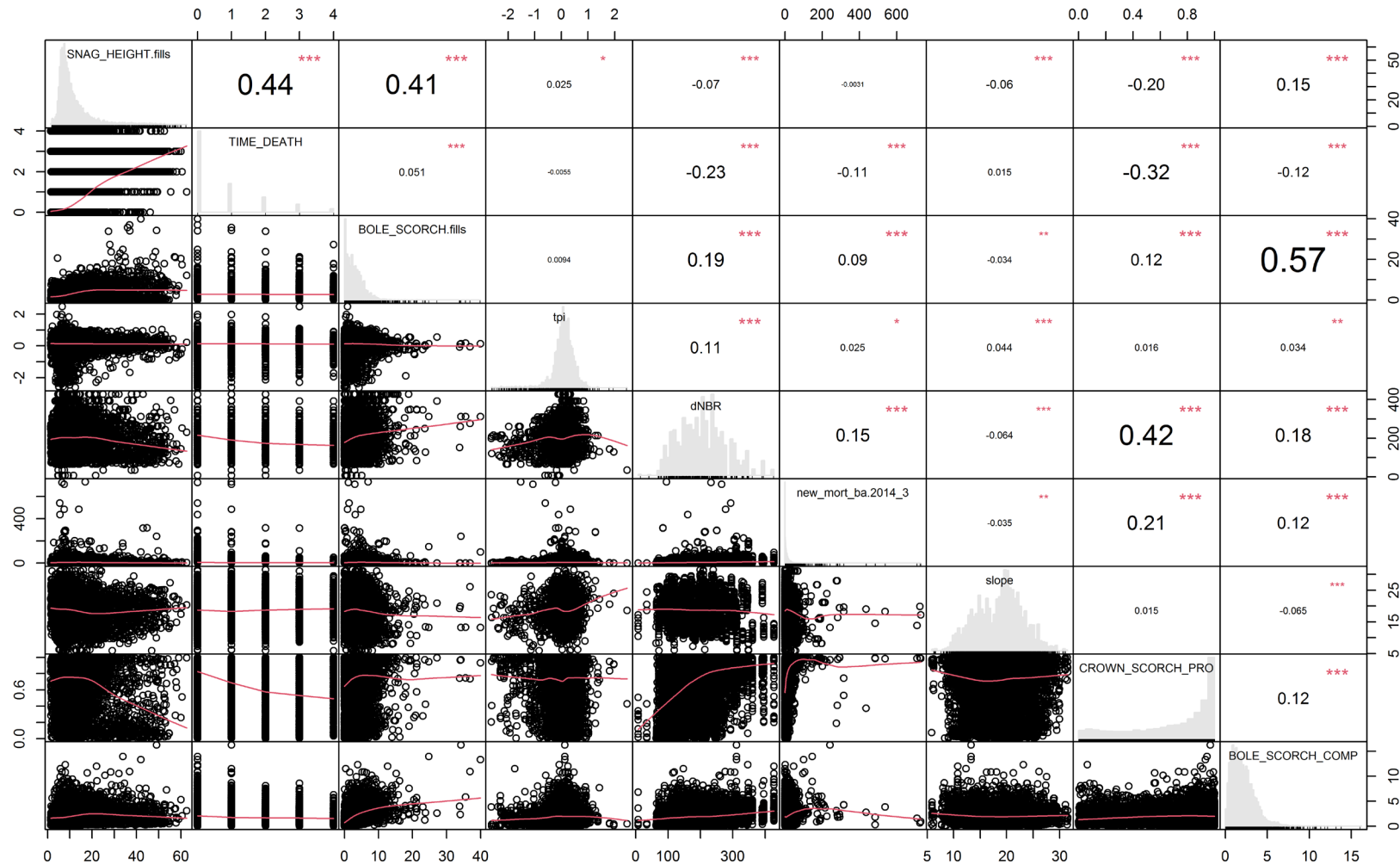
Figure A.17. Correlation matrix of important continuous variables in the most predictive model that used just post-fire variables (i.e., 0–6 m neighborhood, r = 0.7) to predict fall of post-fire snags ≥ 10 cm DBH (see Table 2.2). See Table A.6 for predictor variable definitions.

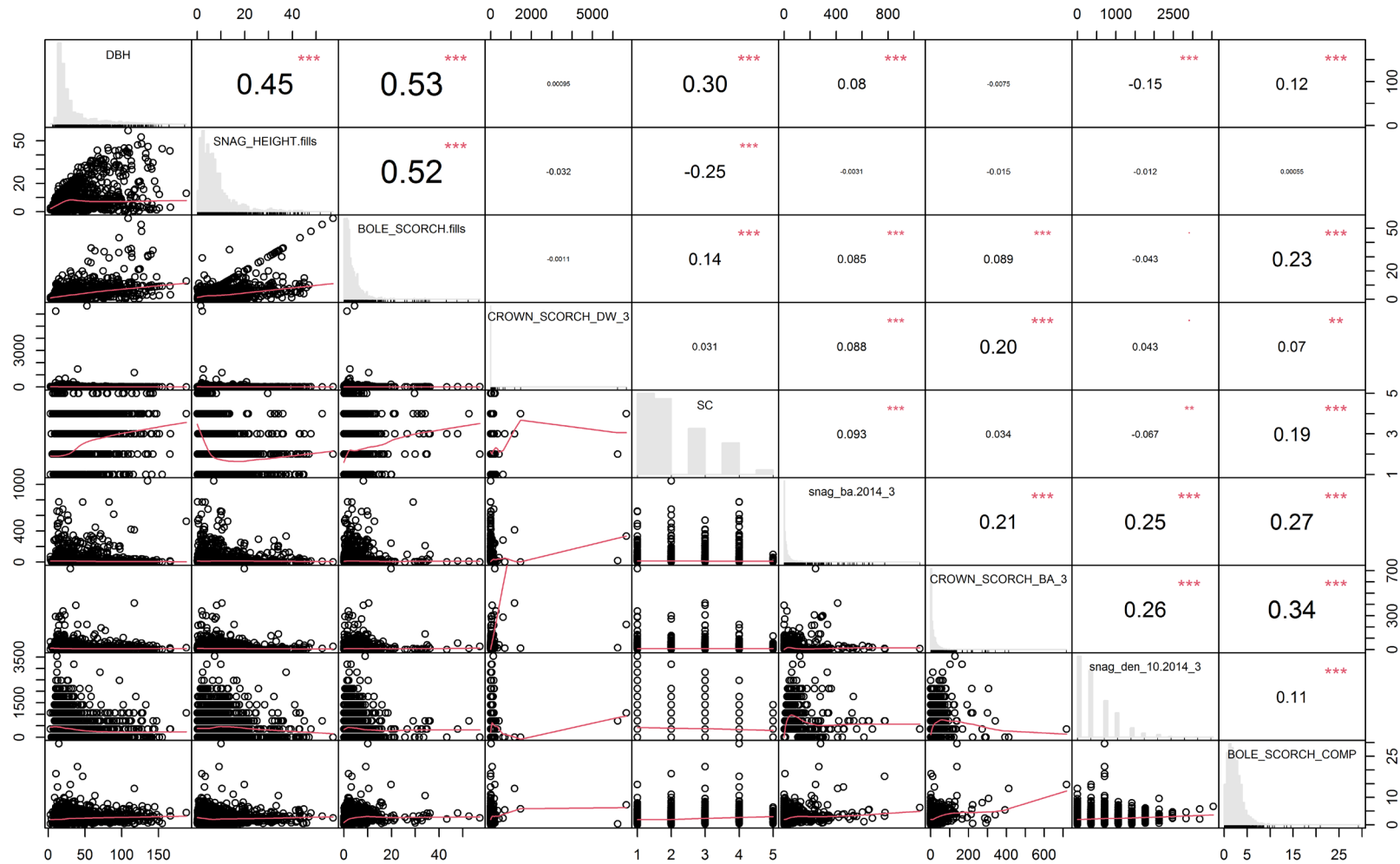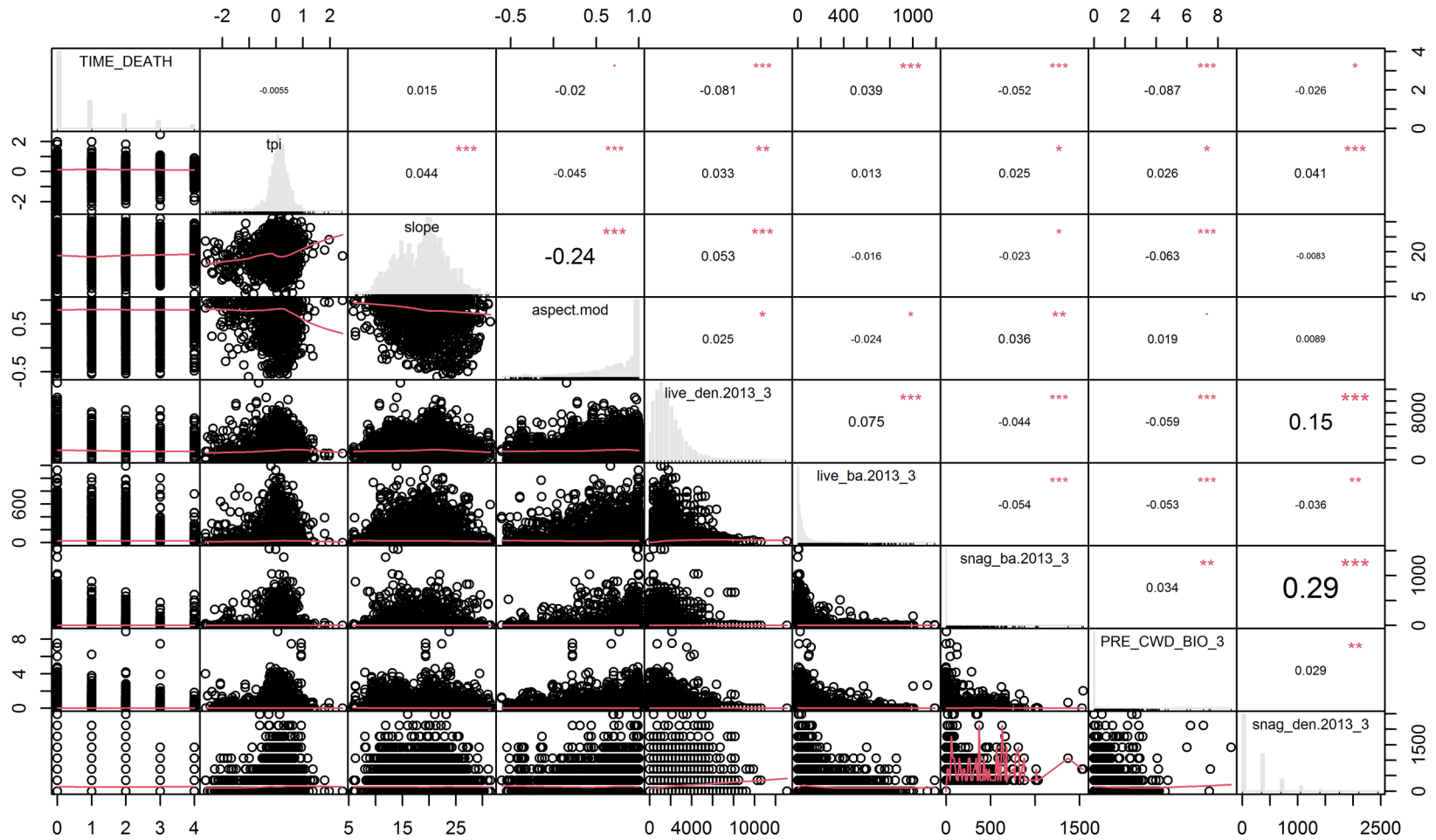Figure A.18. Correlation matrix of important continuous variables in the most predictive model (i.e., 0–3 m neighborhood, r = 0.5) that used just pre-fire variables to predict fall of post-fire snags ≥ 10 cm DBH (see Table 2.2). See Table A.6 for predictor variable definitions.

Figure A.19. Partial dependence plots of the nine most important continuous pre-fire predictor variables in random forest models of the fall of pre-fire snags ≥ 10 cm DBH. Solid lines represent mean partial dependence values from 15 model runs. Gray dotted lines represent minimum and maximum partial dependence values from the 15 model runs. Density units are trees ha^{-1}. Basal area units are m^2 ha^{-1}. Volume units are m^3 ha^{-1}.

Figure A.20. Partial dependence plots of the nine most important continuous post-fire predictor variables in random forest models of the fall of pre-fire snags ≥ 10 cm DBH. Vertical red dashed lines and the corresponding values indicate thresholds that were used to categorize snags in multi-variate partial dependence plots (Figure 2.4). Solid lines represent mean partial dependence values from 15 model runs. Gray dotted lines represent minimum and maximum partial dependence values from the 15 model runs. Density units are trees ha^{-1}. Basal area units are m^2 ha^{-1}.
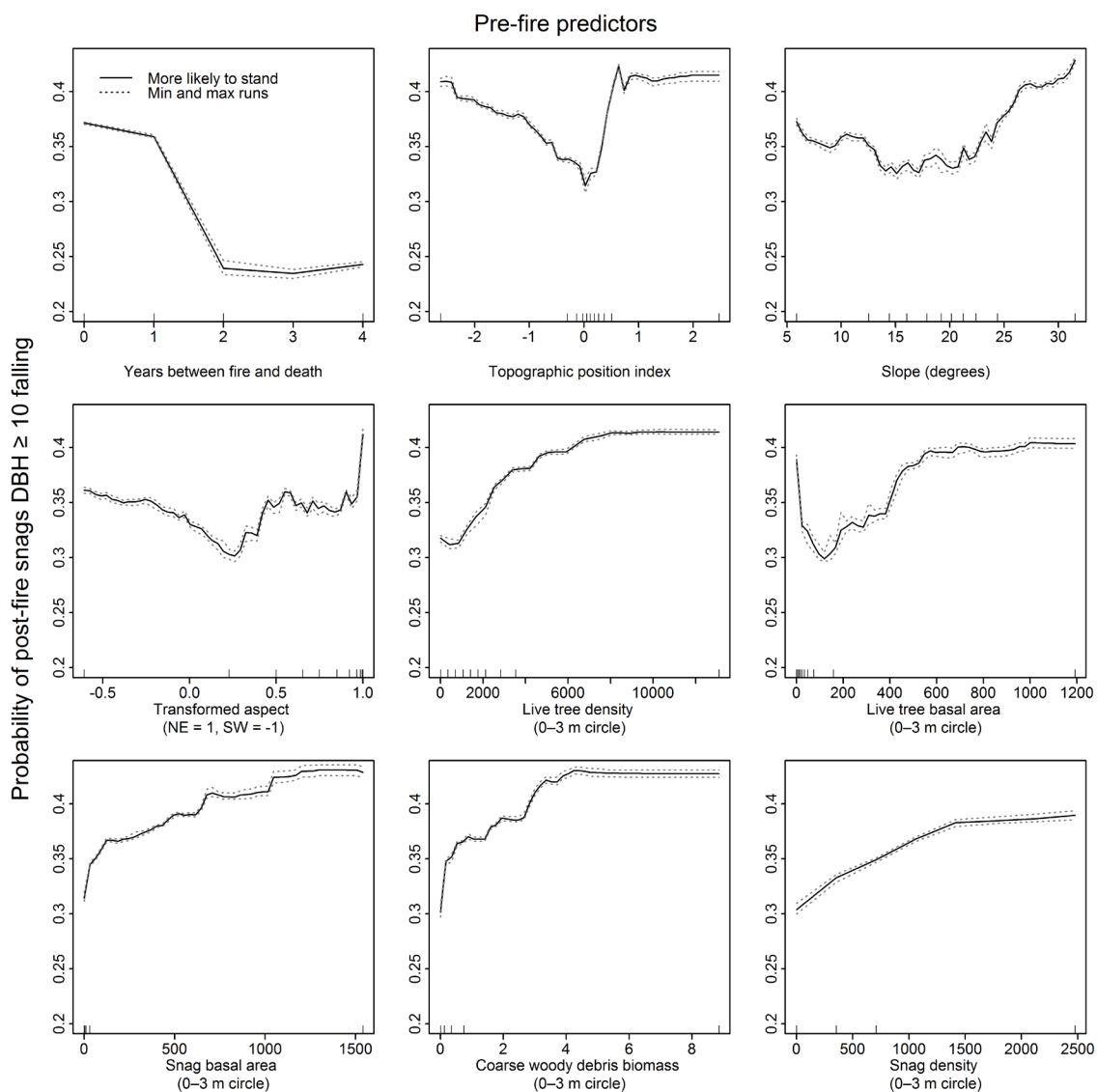
Figure A.21. Partial dependence plots of the nine most important continuous pre-fire predictor variables in random forest models of the fall of post-fire snags ≥ 10 cm DBH. Solid lines represent mean partial dependence values from 15 model runs. Gray dotted lines represent minimum and maximum partial dependence values from the 15 model runs. Density units are trees ha^{-1}. Basal area units are m^2 ha^{-1}. Biomass units are Mg ha^{-1}.

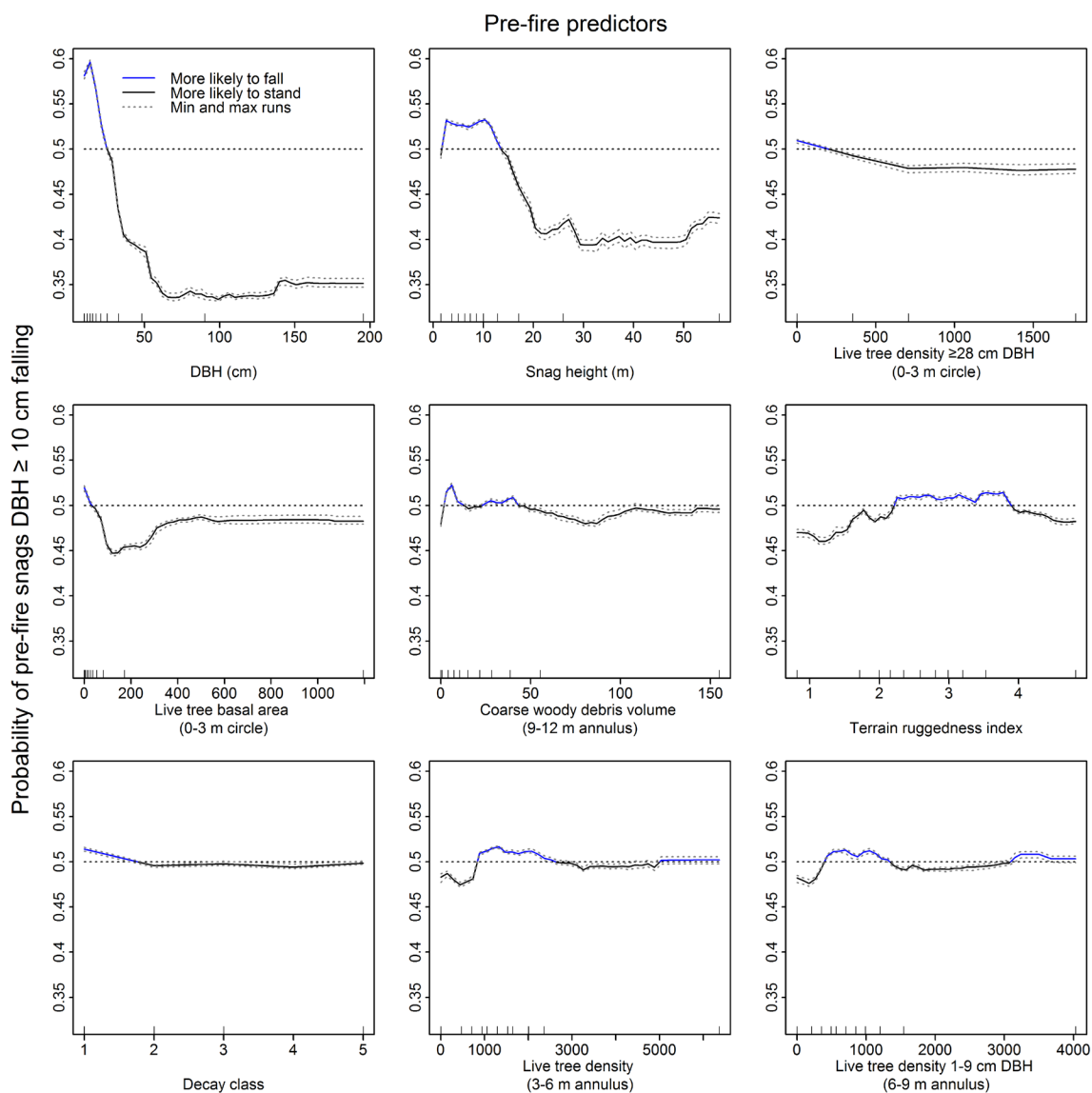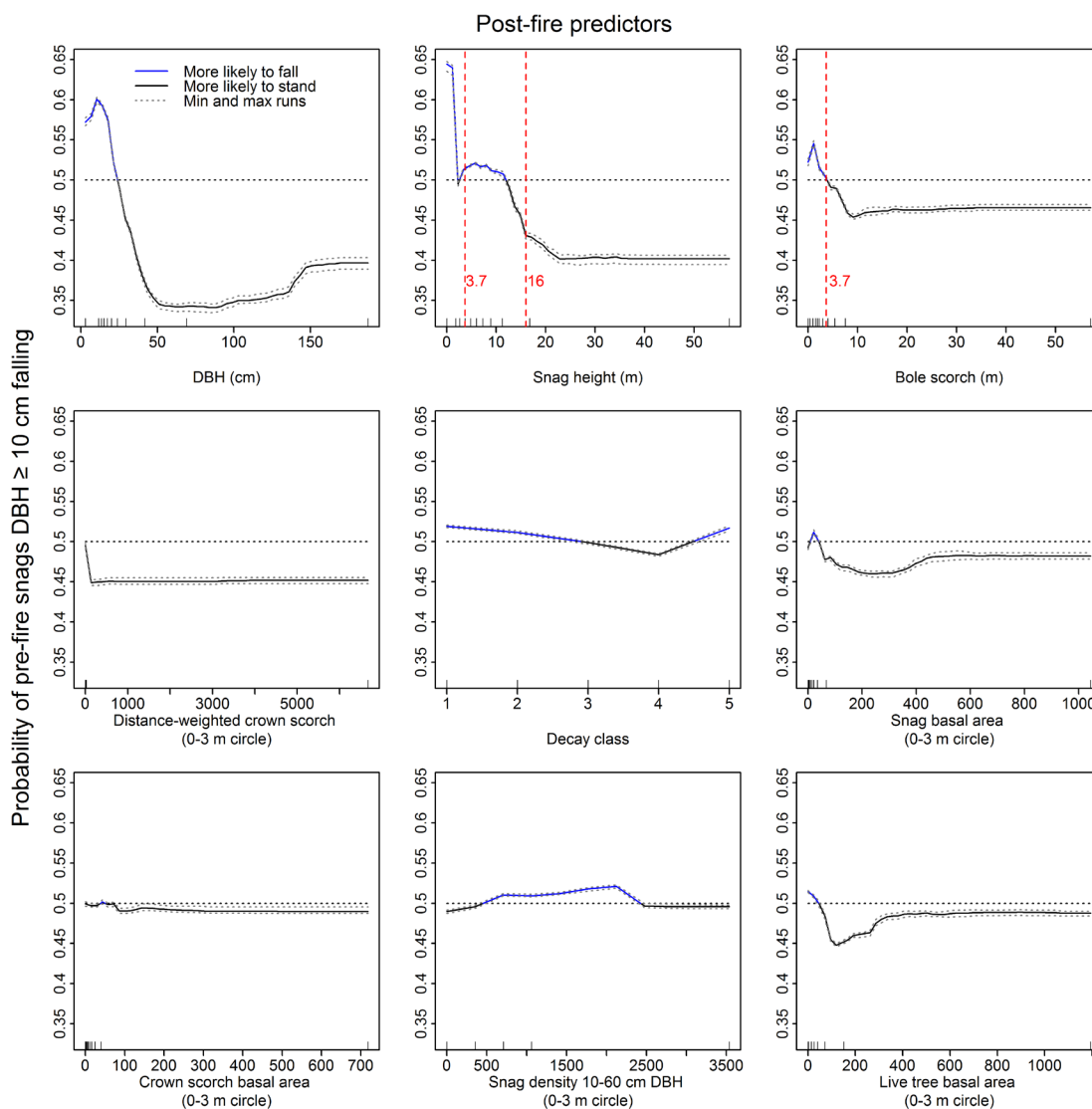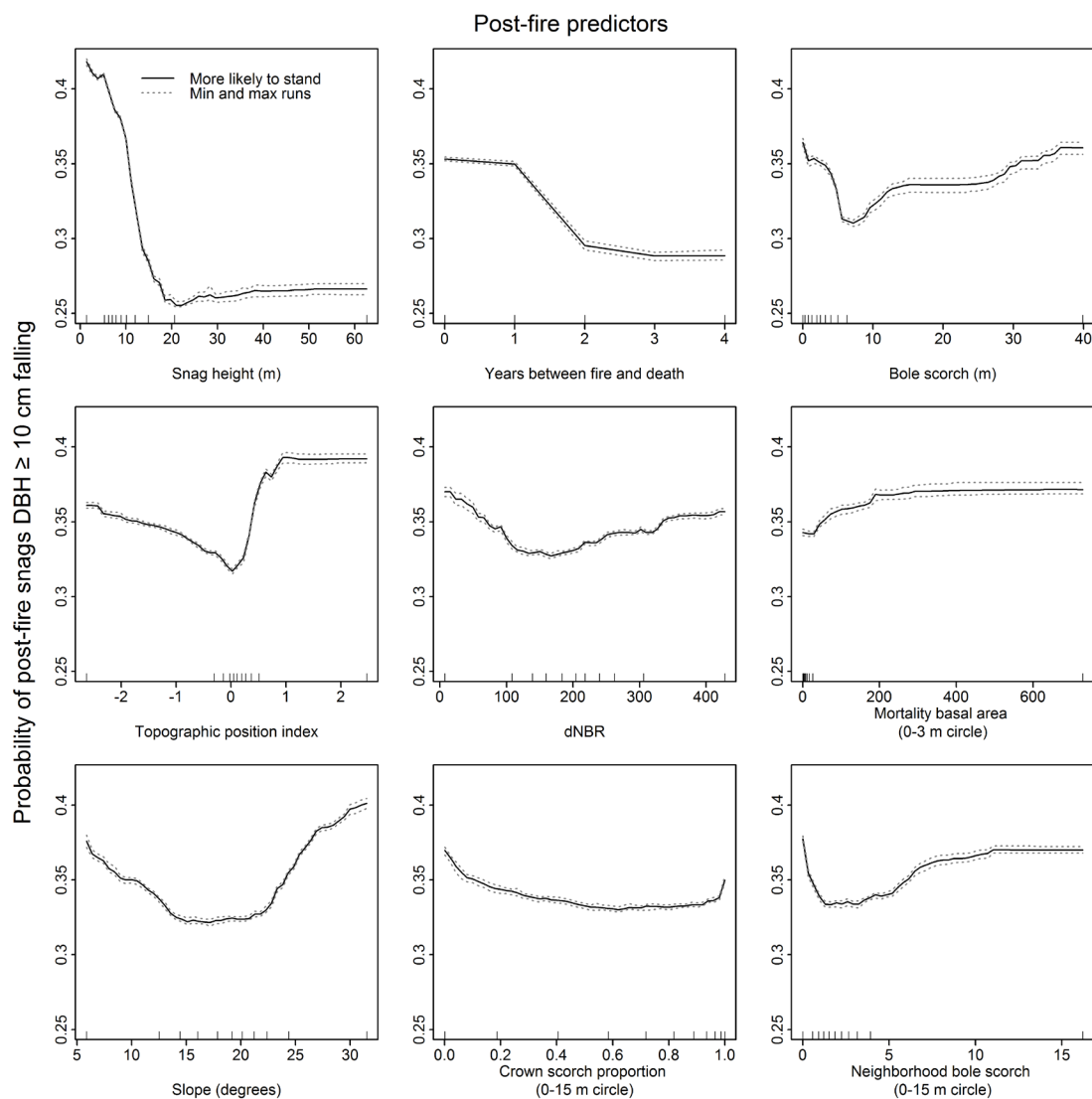Figure A.22. Partial dependence plots of the nine most important continuous post-fire predictor variables in random forest models of the fall of post-fire snags ≥ 10 cm DBH. Solid lines represent mean partial dependence values from 15 model runs. Gray dotted lines represent minimum and maximum partial dependence values from the 15 model runs. Basal area units are $m^2\,ha^{-1}$.

APPENDIX B

SUPPLEMENTARY MATERIAL FOR CHAPTER III:

DIFFERENCES IN REGENERATION NICHE MEDIATE HOW DISTURBANCE

SEVERITY AND MICROCLIMATE AFFECT FOREST SPECIES COMPOSITION

Table B.1. Conifer germination rate and annual number of germinants in 63, 1-m^2 quadrats in the Yosemite Forest Dynamics Plot after a low-severity fire in the fall of 2013. Seedling inventories began in 2014. Two 0.3-m^2 seed traps were installed adjacent to each seedling quadrat in the summer of 2015 and were emptied in May or June of 2016–2020. Seed trap contents were used to calculate germination rate by providing an estimate of total annual seed rain that fell within the total area of the seedling quadrats.

Species	*Abies concolor*		*Pinus lambertiana*	
Year	Germination rate	Germinants	Germination rate	Germinants
2014	—	507	—	0
2015	—	49	—	174
2016	0	0	0.119	3
2017	0	0	0	0
2018	0.010	34	0.023	6
2019	0	0	0	0
2020	0	0	0.037	5

Table B.2. Climate metrics influencing annual mortality of seedlings as determined by AIC model selection of explanatory variables representing snow duration and high temperature during summer or fall. We asked how fire severity, annual snow duration, and annual high temperature interacted with species (*A. concolor* vs. *P. lambertiana*) to influence annual seedling survival. We compared different metrics representing snow duration and high temperature extremes and selected the metrics for our **final model** that produced the lowest AIC. ΔAIC = AIC – min(AIC).

Snow duration metric	High temperature metric		AIC	ΔAIC
	Season	Days of maximum temperature period		
		1	**769.36**	**0.00**
	June–	3	769.43	0.07
	August	5	769.61	0.25
		7	769.47	0.11
Final snow disappearance date		1	769.89	0.53
	September	3	770.48	1.12
		5	771.00	1.64
		7	770.97	1.61
		1	773.87	4.51
	June–	3	773.92	4.56
	August	5	774.01	4.65
		7	773.92	4.56
Snow disappearance date after period of longest continuous snow cover		1	773.39	4.03
	September	3	773.65	4.29
		5	774.25	4.89
		7	774.06	4.70
		1	779.59	10.23
	June–	3	779.43	10.07
	August	5	779.44	10.08
		7	779.31	9.95
Days of longest continuous snow cover		1	784.48	15.12
	September	3	784.73	15.37
		5	784.92	15.56
		7	784.93	15.57
		1	778.71	9.35
	June–	3	778.60	9.24
	August	5	778.65	9.29
		7	778.52	9.16
Total days of snow cover		1	782.88	13.52
	September	3	783.20	13.84
		5	783.45	14.09
		7	783.47	14.11

Table B.3. Model selection process for factors influencing overall seedling survival and seedling survival during different life stages. We asked how species and fire severity interact to influence seedling survival. The most parsimonious model is in bold text; models within 2 AIC units were considered equally parsimonious. ΔAIC = AIC – min(AIC).

Response variable	Model	AIC	ΔAIC
Seedling survival: both life stages	Null (random effects only)	777.77	32.13
	Species	758.94	13.30
	Substrate burn severity	776.84	31.20
	Neighborhood fire severity (30 m)	772.52	26.88
	Species + Substrate burn severity + Neighborhood fire severity (30 m)	749.14	3.05
	Species × Substrate burn severity	752.78	7.14
	Species × Substrate burn severity + Neighborhood fire severity (30 m)	**745.64**	**0**
Seedling survival: first-year	Null (random effects only)	849.78	41.42
	Species	828.38	20.02
	Substrate burn severity	850.81	42.45
	Neighborhood fire severity (30 m)	832.82	24.46
	Species + Substrate burn severity + Neighborhood fire severity (30 m)	**808.36**	**0**
	Species × Substrate burn severity	829.42	21.06
	Species × Substrate burn severity + Neighborhood fire severity (30 m)	810.35	1.99
Seedling survival: second-year and older	Null (random effects only)	410.10	9.5
	Species	408.87	8.27
	Substrate burn severity	409.79	9.19
	Neighborhood fire severity (30 m)	412.08	11.48
	Species + Substrate burn severity + Neighborhood fire severity (30 m)	409.59	8.99
	Species × Substrate burn severity	**400.60**	**0**
	Species × Substrate burn severity + Neighborhood fire severity (30 m)	402.38	1.78

Table B.4. Model selection process for factors influencing seedling survival during the germination year. We asked how the effect of species, fire severity, and their interaction on seedling survival during the germination year compared to the effect of species, snow duration, and their interaction on seedling survival during the germination year. The most parsimonious model is in bold text; models within 2 AIC units were considered equally parsimonious. ΔAIC = AIC – min(AIC).

Response variable	Model	AIC	ΔAIC
	Null (Random effects only)	273.33	28.04
	Species	267.96	22.67
	Substrate burn severity	272.51	27.22
	Neighborhood fire severity (30 m)	255.93	10.64
	Final snow disappearance	270.79	25.50
	Species + Substrate burn severity + Neighborhood fire severity (30 m) + Final snow disappearance	248.12	2.83
	Species × Neighborhood fire severity (30 m)	249.84	4.55
	Species × Final snow disappearance	263.18	17.89
Seedling survival during the germination year	Species × Neighborhood fire severity (30 m) + Substrate burn severity	250.95	5.66
	Species × Neighborhood fire severity (30 m) + Final snow disappearance	248.64	3.35
	Species × Final snow disappearance + Substrate burn severity	262.91	17.62
	Species × Final snow disappearance + Neighborhood fire severity (30 m)	**245.29**	**0**
	Species × Neighborhood fire severity (30 m) + Species × Final snow disappearance	247.28	1.99
	Species × Neighborhood fire severity (30 m) + Species × Final snow disappearance + Substrate burn severity	248.49	3.20

Table B.5. Model selection process for factors influencing annual seedling survival after the germination year. We asked how the effect of species, fire severity, and their interaction on annual seedling survival compared to the effect of species, snow duration, and their interaction on annual seedling survival. The most parsimonious model is in bold text; models within 2 AIC units were considered equally parsimonious. ΔAIC = AIC – min(AIC).

Response variable	Model	AIC	ΔAIC
	Null (Random effects only)	778.03	11.21
	Basic (Seedling age + random effects only)	781.89	15.07
	Species	783.20	16.38
	Substrate burn severity	782.00	15.18
	Neighborhood fire severity (30 m)	783.86	17.04
	Final snow disappearance	770.65	3.83
	Species + Substrate burn severity + Neighborhood fire severity (30 m) + Final snow disappearance	773.31	6.49
	Species × Substrate burn severity	778.16	11.34
Annual seedling survival after germination year	Species × Final snow disappearance	773.13	6.31
	Species × Substrate burn severity + Neighborhood fire severity (30 m)	779.70	12.88
	Species × Substrate burn severity + Final snow disappearance	**766.82**	**0**
	Species × Final snow disappearance + Substrate burn severity	772.79	5.97
	Species × Final snow disappearance + Neighborhood fire severity (30 m)	775.07	8.25
	Species × Substrate burn severity + Species × Final snow disappearance	768.09	1.27
	Species × Substrate burn severity + Species × Final snow disappearance + Neighborhood fire severity (30 m)	769.59	2.77

Table B.6. Coefficient estimates for generalized linear mixed models of survival of *P. lambertiana* and *A. concolor* seedlings that germinated in 2014 or 2015. To compare the effects of fire severity and species on survival during different life stages, we fit three models: 1) seedling survival from germination until 2020 (Both stages combined), 2) seedling survival during the first year of life (First-year), and 3) seedling survival after the first year of life until 2020 (Second-year and older). See Table B.3 for AIC model selection results. Predictors were standardized, so a one-unit change in the estimate represents a change of one standard deviation for numeric quantities. **** = $p < 0.001$; *** = $p < 0.01$; ** = $p < 0.05$; * = $p < 0.1$.

Predictor variable	Estimate	Standard error	z-value	*p*-value
Model: Both stages combined				
Intercept (Species = *A. concolor*)	0.5735	0.1286	4.461	****
Species = *P. lambertiana*	-0.7426	0.1577	-4.708	****
Substrate burn severity	-0.4004	0.1325	-3.023	***
Fire severity (30 m)	-0.3842	0.1182	-3.249	***
Substrate burn severity : Species = *P. lambertiana*	0.3592	0.1554	2.311	**
Model: First-year				
Intercept (Species = *A. concolor*)	-0.08926	0.13483	-0.662	
Species = *P. lambertiana*	-0.92929	0.18886	-4.921	****
Substrate burn severity	-0.10076	0.13889	-0.725	
Fire severity (30 m)	-0.67001	0.13848	-4.838	****
Substrate burn severity : Species = *P. lambertiana*	-0.01179	0.17926	-0.066	
Model: Second-year and older				
Intercept (Species = *A. concolor*)	-0.6888	0.2225	-3.096	***
Species = *P. lambertiana*	-0.4283	0.2685	-1.595	
Substrate burn severity	-0.7560	0.2377	-3.180	***
Fire severity (30 m)	-0.0919	0.1944	-0.473	
Substrate burn severity : Species = *P. lambertiana*	0.8139	0.2793	2.914	***

Table B.7. Coefficient estimates for a generalized linear mixed model of first-year survival for seedlings that germinated in 2015 to compare the relative importance of fire severity and snow duration; coefficient estimates for a generalized linear mixed model of annual survival of *P. lambertiana* and *A. concolor* second-year and older seedlings that germinated in 2014 or 2015. We asked how fire severity, annual snow duration, and annual high temperature interacted with species to influence annual seedling survival. We compared AIC values to choose the metrics representing snow duration and high temperature (Table B.2). We report the results for the best-fit models according to AIC model selection (Tables B.4 and B.5). Predictors were standardized, so a one-unit change in the estimate represents a change of one standard deviation for numeric quantities. **** $= p < 0.001$; *** $= p < 0.01$; ** $= p < 0.05$; * $= p < 0.1$.

Predictor variable	Estimate	Standard error	z-value	*p*-value
Model: First-year seedling survival (germinated in 2015)				
Intercept (Species = *A. concolor*)	0.1925	0.2804	0.686	
Species = *P. lambertiana*	-1.1628	0.3065	-3.794	****
Fire severity (30 m)	-0.7161	0.1413	-5.068	****
Annual snow disappearance date	-0.7450	0.3255	-2.289	**
Annual snow disappearance date : Species = *P. lambertiana*	0.6166	0.3551	1.736	*
Model: Annualized second-year and older seedling survival				
Intercept (Age = 2, Species = *A. concolor*)	-2.4073	0.2640	-9.118	****
Age = 3	-0.3809	0.2620	-1.454	
Age = 4	0.1231	0.2735	0.450	
Age = 5	0.2055	0.3125	0.658	
Age = 6	0.1785	0.5307	0.336	
Species = *P. lambertiana*	-0.1664	0.2599	-0.640	
Substrate burn severity	-0.5486	0.2043	-2.686	***
Annual snow disappearance date	-0.5438	0.1548	-3.513	****
Substrate burn severity : Species = *P. lambertiana*	0.6145	0.2464	2.494	**
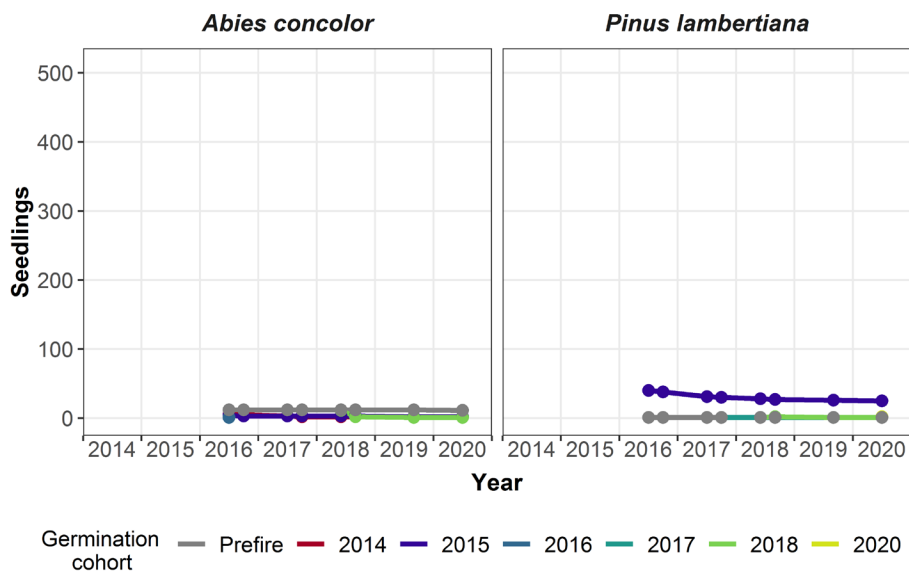
Figure B.1. Conifer seedling abundance by germination cohort in 40 additional 1-m^2 quadrats placed in unburned patches in the Yosemite Forest Dynamics Plot in summer of 2016, after a low- to moderate-severity fire in the fall of 2013. All unburned patches ≥ 1 m^2 had been delineated in the summer of 2014 by field technicians (Blomdahl et al., 2019). Each patch was examined in ArcMap 10.4 and seedling quadrats were positioned a priori (ESRI, 2011). Patches were assessed in the field, and an alternate was selected if evidence of fire was detected or the patch occupied a streambed. Seedling quadrats were installed in unburned patches that ranged from 16 m^2 to 40 m^2. Within the unburned quadrats, seedling age of post-fire germinants was assigned based on morphological similarity to seedlings of known age in previously installed quadrats. Seedlings recruited before the fire were designated as "pre-fire" but not given a specific age.
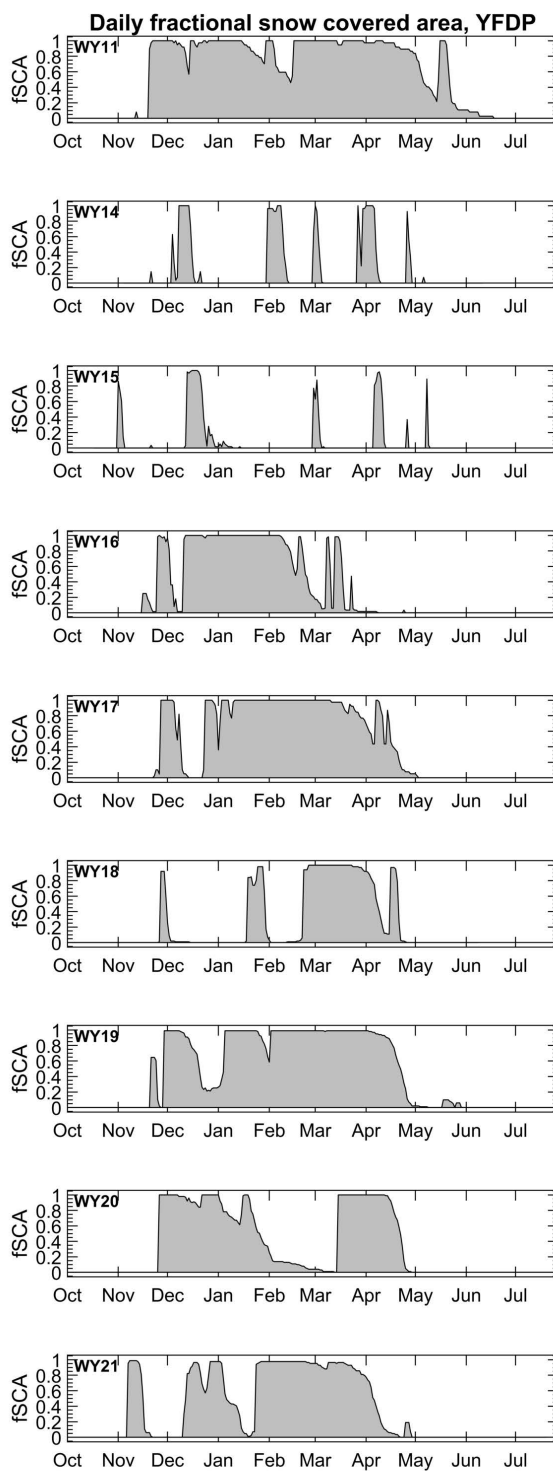
Figure B.2. Daily fractional snow-covered area in the Yosemite Forest Dynamics Plot based on up to 103 HOBO data loggers. Figure created by Dr. Mark Raleigh of Oregon State University.
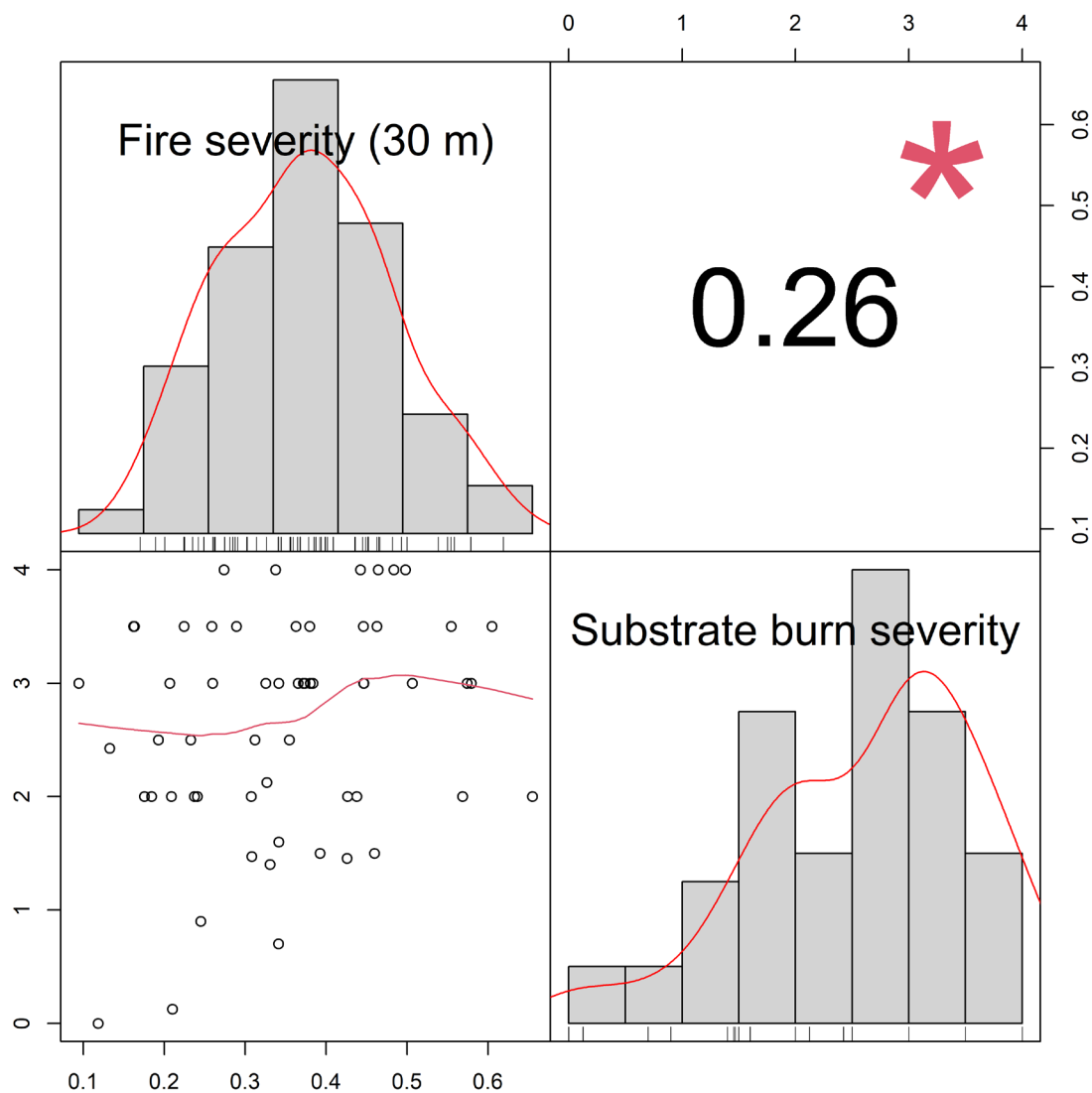
Figure B.3. Correlations of fire severity ratio and substrate burn severity metrics for the 59, 1-m² quadrats where *A. concolor* and/or *P. lambertiana* seedlings germinated in 2014 or 2015. Higher values indicate higher severity.
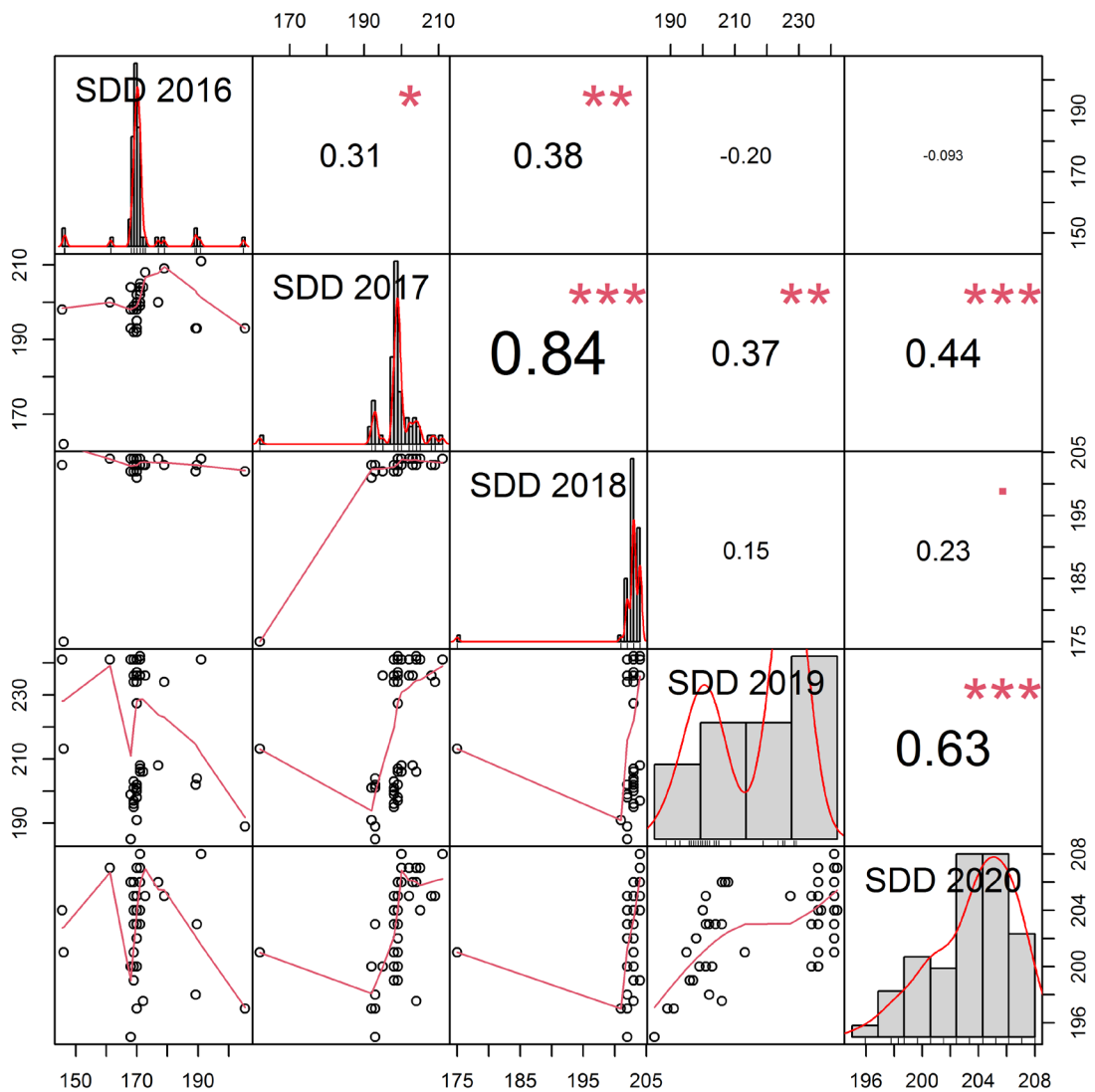
Figure B.4. Correlations of snow disappearance Julian date (SDD) reported by HOBO data loggers in the 59, 1-m^2 quadrats where *A. concolor* and/or *P. lambertiana* seedlings germinated in 2014 or 2015.
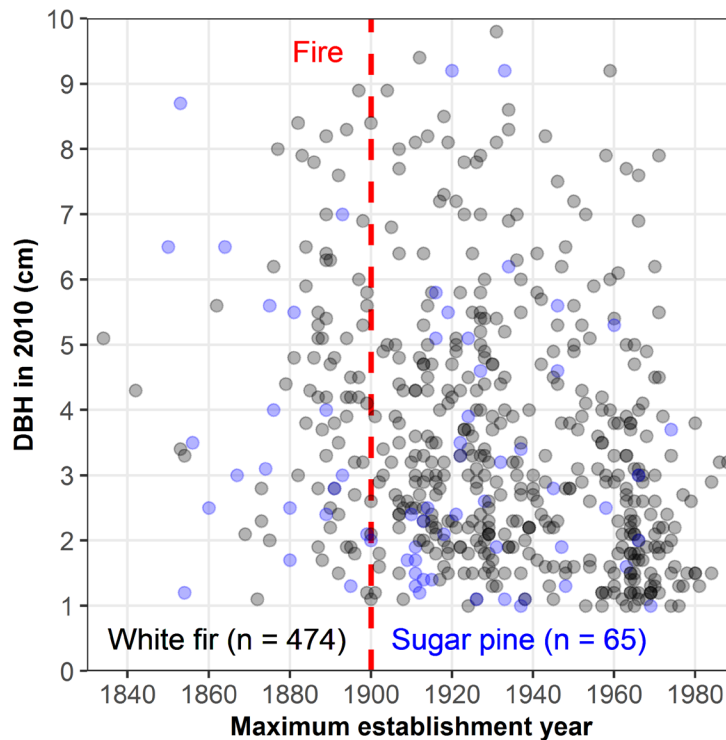
Figure B.5. Pith years of basal cookies of *A. concolor* and *P. lambertiana* stems < 10 cm DBH that had fallen by September 2016, three years after a fire burned the Yosemite Forest Dynamics Plot. The last widespread fire had occurred in 1900. Basal cookies were collected between 0 and 30 cm from the root collar. Pith year represents the most recent possible establishment year.

References

Blomdahl, E.M., Kolden, C.A., Meddens, A.J.H., Lutz, J.A., 2019. The importance of small fire refugia in the central Sierra Nevada, California, USA. For. Ecol. Manage. 432, 1041–1052. https://doi.org/10.1016/j.foreco.2018.10.038

ESRI, 2011. ArcGIS Desktop: Release 10. Environmental Systems Research Institute, Redlands.

APPENDIX C

SUPPLEMENTARY MATERIAL FOR CHAPTER IV:

ANNUALLY RESOLVED IMPACTS OF FIRE MANAGEMENT ON CARBON STOCKS

IN YOSEMITE AND SEQUOIA & KINGS CANYON NATIONAL PARKS

Table C.1. Relative tolerances and adaptations to fire of seven mixed-conifer species in lower and upper montane forests (Fites-Kaufman et al., 2007; van Wagtendonk and Fites-Kaufman, 2006).

Tree species	Fire resistance	Fire adaptations	Drought tolerance	Shade tolerance
Abies concolor	low (young) moderate (mature)	thick bark (mature)	low	high
Abies magnifica	low (young) moderate (mature)	thick bark (mature)	high	high (seedling) moderate (sapling)
Calocedrus decurrens	low (young) moderate (mature)	thick bark (mature)	high	high
Pinus contorta	low/moderate	thin bark (mature)	high, also high tolerance for poor drainage	—
Pinus jeffreyi	high	thick bark (young); elevated crown (mature); protected buds	high	low
Pinus lambertiana	low (young) moderate (mature)	thick bark (mature); elevated crown	moderate	low (dense shade) high (moderate shade)

Tree species	Fire resistance	Fire adaptations	Drought tolerance	Shade tolerance
Pinus ponderosa	high	thick bark (young); elevated crown (mature); protected buds	high	low

Table C.2. Fire attributes and sample depth for 29 fires in Yosemite National Park and 18 fires in Sequoia & Kings Canyon National Park (Eidenshink et al., 2007; Lutz et al., 2011).

Fire name	Start date	Cause	Size (ha)	Species sampled	No. of plots	No. of trees
Yosemite National Park						
Wawona	1970	MI	178.9	CADE, PIPO	2	14
Wawona	1971	MI	61.2	CADE, PIPO	1	7
Wawona	1973	MI	36.1	CADE, PIPO	1	7
Wawona	1975	MI	18.7	CADE, PIPO	1	7
PW27	9/27/1978	MI	2074.3	CADE, PIJE, PIPO	2	17
PW09	1979	MI	1932.5	ABCO, PILA	1	9
YNP-111	1980	MI	830.4	ABCO, PILA	1	9
So. Wawona	4/15/1985	MI	36.9	CADE, PIPO	1	7
Eleanor	1986	LTG	583.6	ABCO, CADE, PIPO	1	8
Elbow	8/10/1988	LTG	182.3	ABMA, PICO	4	37
Pw3	10/16/1989	MI	688.4	ABCO, ABMA, PIJE, PILA	4	38
M Grove	1990	MI	9.4	ABCO, PILA	1	10
South Fork	10/15/1992	MI	209.6	ABCO, CADE, PILA, PIPO	3	23
YNP-0065	9/14/1993	MI	37.4	ABCO, CADE	1	6
Studhorse	6/7/1994	MI	56.5	CADE, PIPO	1	7
Ackerson	8/14/1996	LTG	23938.7	ABCO, CADE, PIJE, PILA, PIPO	5	46
Mg #9	9/17/1997	MI	17.3	ABCO, PILA	1	10
Kibbie Relight	9/18/1997	MI	993.4	ABCO, ABMA, PIJE, PILA	2	19
Eleanor	8/10/1999	LTG	1042.3	ABCO, CADE, PIPO	1	8
Studhorse 4	5/13/2002	MI	21.3	CADE, PIPO	1	7
YI Burn	9/27/2002	MI	31.4	ABCO, CADE	1	6
PW-3 Gin Flat	10/3/2002	MI	1360.3	ABCO, ABMA, PIJE, PILA	4	38
Soupbowl	6/1/2005	MI	57.4	CADE, PIPO	1	7
PW5-AD	6/27/2005	MI	104.3	ABCO, CADE, PILA	1	9
PW3-23	8/28/2005	MI	699.0	ABCO, CADE, PILA	2	19
Jack WF	11/8/2007	LTG	447.9	ABCO, CADE, PILA	1	9
Mariposa	9/30/2008	MI	53.5	ABCO, PILA	1	10
Wawona NW	10/14/2008	MI	249.5	ABCO, CADE, PILA	2	15
Big Meadow	8/26/2009	MI	3058.7	ABCO, CADE, PILA, PIPO	3	24

Sequoia & Kings Canyon National Park						
Atwell Mil	6/20/1946	MI	90.0	ABCO, ABMA	1	10
Castle Gro	9/15/1947	MI	149.6	ABMA	1	7
Comanche	7/22/1974	LTG	1218.4	ABCO, ABMA, PICO, PIJE	8	70
Ferguson	6/26/1977	LTG	4216.3	ABMA, PICO, PIJE	1	10
Lewis Crk	9/30/1980	MI	3368.8	PIJE, PIPO	3	16
Sugarloaf	7/28/1985	LTG	1152.2	ABCO, ABMA, PICO, PIJE	8	70
Paradise	1/14/1994	MI	55.7	ABCO, CADE, PILA	1	5
Mineral I	10/11/1995	MI	843.1	ABCO, CADE, PILA	1	5
Shee Cree	10/27/1997	MI	149.7	ABCO, PIPO	1	7
Lewis Cree	10/13/1998	MI	645.2	PIJE, PIPO	3	16
Tar Gap	8/17/1999	MI	248.3	ABMA	1	9
Tar Gap RX	10/10/2002	MI	489.4	ABCO, ABMA	2	19
Atwood	6/25/2003	MI	1098.4	ABCO, ABMA, CADE, PILA	3	24
Williams	7/28/2003	LTG	1404.8	ABCO, ABMA, PICO, PIJE	5	49
Comb	7/22/2005	LTG	3947.3	ABMA, PIJE	4	30
Highbrid E	10/24/2005	MI	344.6	PIJE	1	10
Horse	7/19/2009	LTG	268.7	PICO	1	7
Sheep	7/16/2010	LTG	3650.1	ABCO, PIPO	1	7

Table C.3. Fire severity thresholds for the Relative differenced Normalized Burn Ratio (RdNBR; Miller and Thode, 2007). Landsat-undifferentiated fire severity refers to areas within fire perimeters with RdNBR values that do not differ from adjacent unburned areas (Kolden et al., 2012).

Fire severity	RdNBR	No. of plots	No. of cores
Undifferentiated	<69	14	125
Low	69-	30	136
Moderate	316-	16	274
High	>640	1	5

Table C.4. Examination of collinearity between species and fire severity and fire cause. LTG = Lightning; MI = Management ignited.

Species	Fire severity				Fire cause	
	Undiff.	Low	Mod.	High	LTG	MI
Abies concolor	32	64	23	2	29	140
Abies magnifica	14	76	6	0	43	85
Calocedrus decurrens	12	18	16	0	17	78
Pinus contorta	14	44	3	0	93	0
Pinus jeffreyi	36	47	64	0	148	58
Pinus lambertiana	11	13	10	3	7	39
Pinus ponderosa	6	12	14	0	14	53

References

Eidenshink, J., Schwind, B., Brewer, K., Zhu, Z., Quayle, B., Howard, S., 2007. A project for monitoring trends in burn severity. Fire Ecol. 3, 3–21.

Fites-Kaufman, J., Rundel, P., Stephenson, N., Weixelman, D.A., 2007. Montane and subalpine vegetation of the Sierra Nevada and Cascade ranges, in: Terrestrial Vegetation of California. pp. 456–501.

Kolden, C.A., Lutz, J.A., Key, C.H., Kane, J.T., van Wagtendonk, J.W., 2012. Mapped versus actual burned area within wildfire perimeters: characterizing the unburned. For. Ecol. Manage. 286, 38–47. https://doi.org/10.1016/j.foreco.2012.08.020

Lutz, J.A., Key, C.H., Kolden, C.A., Kane, J.T., van Wagtendonk, J.W., 2011. Fire frequency, area burned, and severity: A quantitative approach to defining a normal fire year. Fire Ecol. 7, 51–65. https://doi.org/10.4996/fireecology.0702051

Miller, J.D., Thode, A.E., 2007. Quantifying burn severity in a heterogeneous landscape with a relative version of the delta Normalized Burn Ratio (dNBR). Remote Sens. Environ. 109, 66–80. https://doi.org/10.1016/j.rse.2006.12.006

van Wagtendonk, J.W., Fites-Kaufman, J.A., 2006. Sierra Nevada bioregion, in: Fire in California's Ecosystems. pp. 264–294.

APPENDIX D

SUPPLEMENTARY MATERIAL FOR CHAPTER V:

CAUSES OF MORTALITY WITHIN TREE NEIGHBORHOODS AFFECT GROWTH

RATES OF SURVIVING TREES

Table D.1. Model selection process for factors influencing relative post-fire radial growth of trees that survived for seven years after a low- to moderate-severity fire. We asked how post-fire neighborhood change differently affects the relative radial growth of *A. concolor* and *P. lambertiana*, while accounting for the degree of fire injury. We also examine whether the cause of mortality that drove the neighborhood change affects the relationship between neighborhood change and relative radial growth. We report AIC for models that used crowding metrics based on 10-m radius neighborhoods, which had lower AIC than 15- or 20-m neighborhoods. Change = (crowding of trees that died between 2014 and 2020)/(crowding of trees alive in 2013); Other = (crowding of trees that died from fire or mechanical damage between 2014 and 2020)/(crowding of trees alive in 2013); Beetle = (crowding of trees that died from bark beetle attack between 2014 and 2020)/(crowding of conspecific trees alive in 2013); Fungus = (crowding of trees that died from fungal pathogens between 2014 and 2020)/(crowding of trees alive in 2013). The most parsimonious model is in bold text; models within 2 AIC units were considered equally parsimonious. $\Delta AIC = AIC - \min(AIC)$.

| Model	AIC	ΔAIC
Base model (Crown injury)	5995.89	254.66
Base + Change × Species × DBH	5851.23	110.01
Base + Other × Species × DBH	5854.22	112.99
Base + Beetle × Species × DBH	5821.33	80.10
Base + Fungus × Species × DBH	5925.47	184.24
Base + Other × Species × DBH + Beetle × Species × DBH	**5741.22**	**0.00**
Base + Other × Species × DBH + Fungus × Species × DBH	5858.57	117.34
Base + Beetle × Species × DBH + Fungus × Species × DBH	5827.06	85.83
Base + Other × Species × DBH + Beetle × Species × DBH + Fungus × Species × DBH	5746.13	4.90
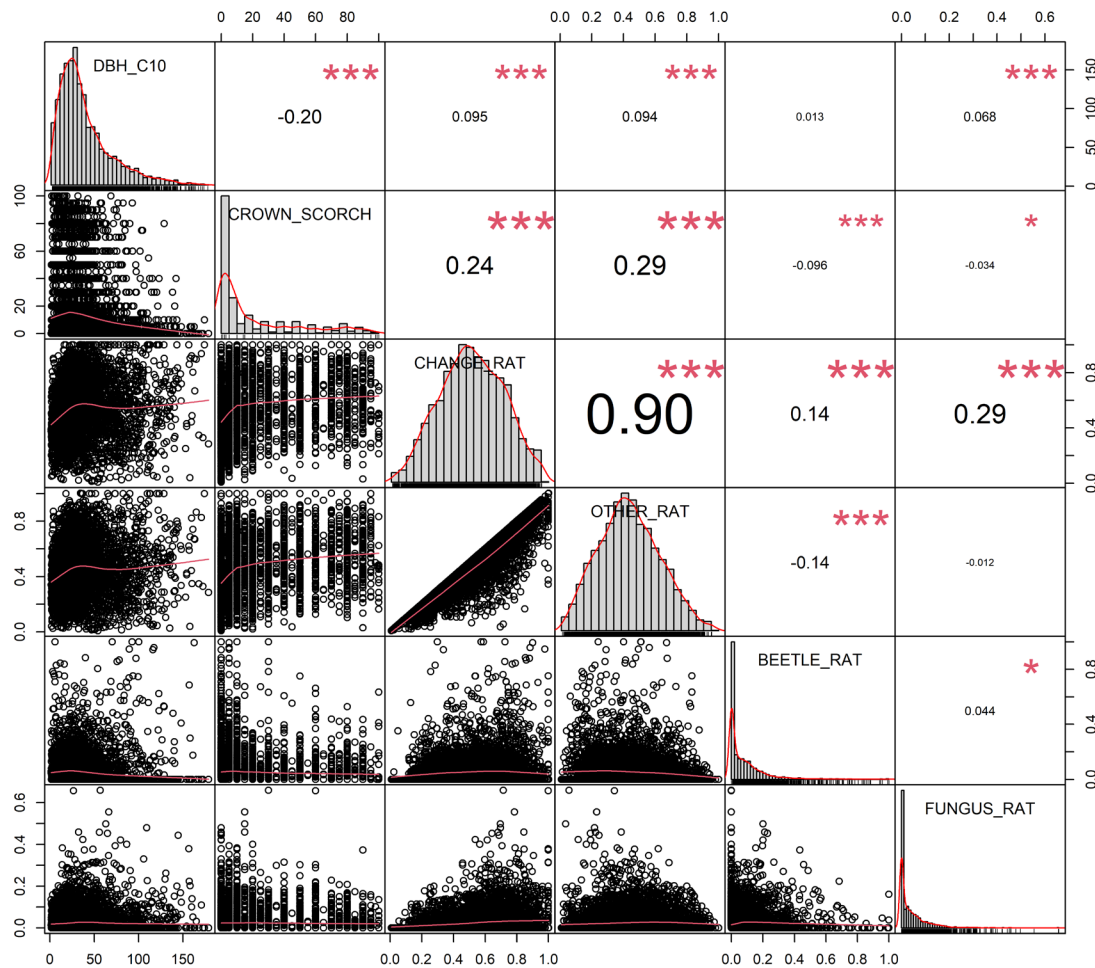
Figure D.1. Correlations of variables used to model post-fire relative radial growth as a function of fire injury and post-fire neighborhood change after a low- to moderate-severity fire in fall of 2013. DBH_C10 = DBH in 2019; CROWN_SCORCH = crown injury (%); CHANGE_RAT = (crowding of trees that died between 2014 and 2020)/(crowding of trees alive in 2013); OTHER_RAT = (crowding of trees that died from fire or mechanical damage between 2014 and 2020)/(crowding of trees alive in 2013); BEELTE_RAT = (crowding of conspecific trees that died from bark beetle attack between 2014 and 2020)/(crowding of conspecific trees alive in 2013); FUNGUS_RAT = (crowding of trees that died from fungal pathogens between 2014 and 2020)/(crowding of trees alive in 2013).
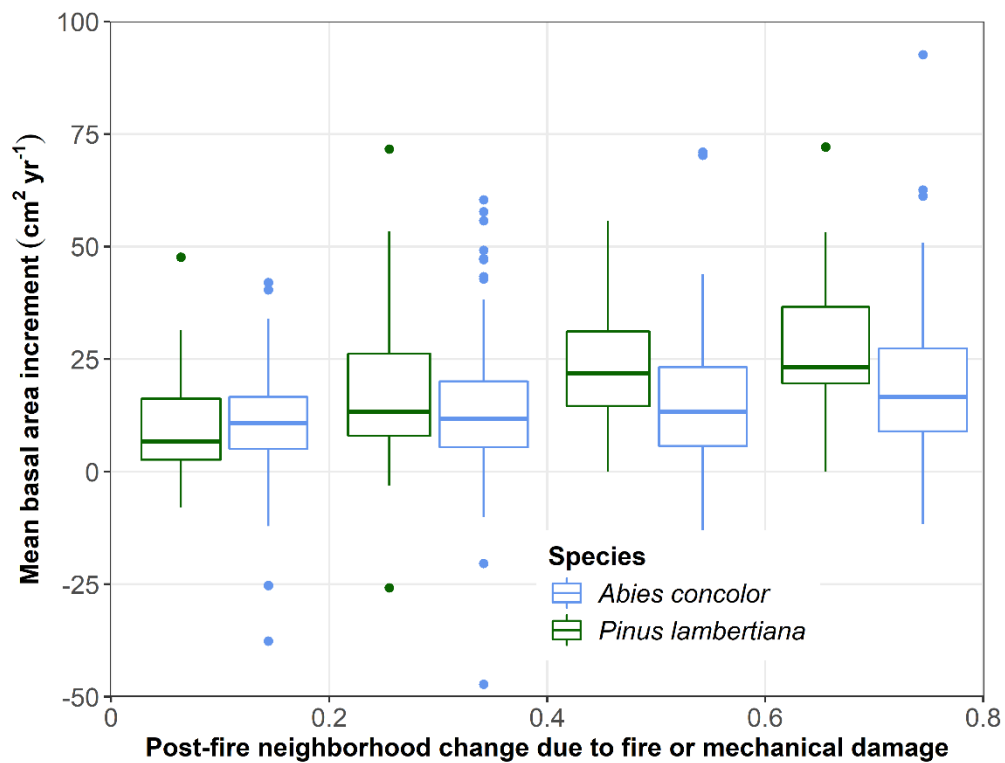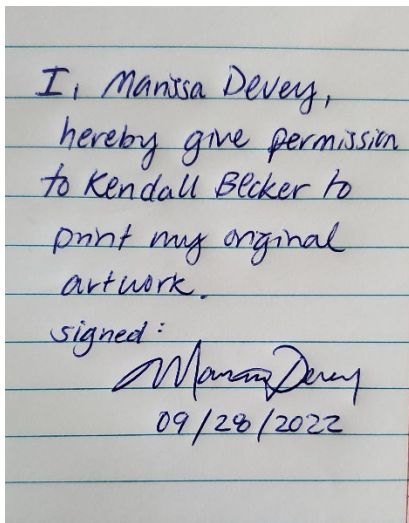
Figure D.2. Mean annual growth in basal area increment (BAI) of 30–60 cm DBH *A. concolor* and *P. lambertiana* from 2014 to 2019, after a low- to moderate-severity fire in 2013. This figure depicts the interaction between species and post-fire neighborhood change due to fire or mechanical damage, defined as the ratio of crowding by trees that died due to fire or mechanical damage between 2014 and 2020 divided by crowding of trees that were alive before the fire. Boxplots represent the distribution of mean basal area increment for four levels of neighborhood change: 0.0–0.2, 0.2–0.4, 0.4–0.6, and 0.6–0.8. One negative outlier data point is not pictured.

APPENDIX E

PERMISSION-TO-USE LETTER

Permission to use from Marissa Devey (Frontispiece):

CURRICULUM VITAE

KENDALL M. L. BECKER
Email: kendall.becker@usu.edu

EDUCATION

Institution	Degree	Program	Year	GPA
Utah State University	Ph.D.	Ecology	2022	4.0

"Old-growth forest dynamics after fire and drought in the Sierra Nevada, California, USA"
Defense Date: December 16, 2021
Committee Chair: James A. Lutz

University of Washington	M.S.	Ecosystem Analysis	2014	3.92

"Effects of low-severity fire on species composition and structure in montane forests of the Sierra Nevada"
Defense Date: May 13, 2014
Committee Chair: Gregory J. Ettl

Yale University	B.S.	Applied Physics	2008	3.47

"Ice Growth Dynamics and Thermodynamics"
Chair: John S. Wettlaufer

PROFESSIONAL EXPERIENCE

2017–2022 **Science Writing Center Assistant Director.** Utah State University, Logan, UT.
> I developed relationships with departments and professors in all science-related colleges across campus to increase instructor awareness and student use of the Science Writing Center. I organized grant-writing and personal statement workshops for undergraduate and graduate students. I recruited, trained, and mentored scientific writing tutors. I tutored undergraduates, graduate students, and postdoctoral researchers in scientific writing. I worked closely with Writing Center professionals and faculty in the humanities to strengthen connections across disciplines.

2014–2017 **Doctoral fellow.** Utah State University, Logan, UT.
> I conducted forest demography research in the field and laboratory. I assisted with field logistics, and trained and mentored technicians, staff, and undergraduate and graduate researchers in field techniques, computer programming, and scientific writing.

2011–2014   **Research assistant.** University of Washington, Seattle, WA.
I conducted forest research in the field and laboratory. I trained and mentored technicians, staff, and undergraduate researchers in field techniques, dendroecological techniques, data analysis, and scientific writing.

PUBLICATIONS

Google scholar statistics (as of 2022/October/12)   **Citations:** 349   **h-index:** 5

PEER-REVIEWED PUBLICATIONS

[5] Teich, M., **K. M. L. Becker**, M. S. Raleigh, and J. A. Lutz. 2022. Large-diameter trees affect snow duration in post-fire old-growth forests. Ecohydrology 15(3): e2414. https://doi.org/10.1002/eco.2414

[4] Lutz, J. A., T. J. Furniss, D. J. Johnson, S. J. Davies, D. Allen, A. Alonso, K. Anderson-Teixeira, A. Andrade, J. Baltzer, **K. M. L. Becker**, E. M. Blomdahl, N. A. Bourg, S. Bunyavejchewin, D. F. R. P. Burslem, C. A. Cansler, K. Cao, M. Cao, D. Cárdenas, L-W. Chang, K-J Chao, W-C. Chao, J-M. Chiang, C. Chu, G. B. Chuyong, K. Clay, R. Condit, S. Cordell, H. S. Dattaraja, A. Duque, C. E. N. Ewango, G. A. Fisher, C. Fletcher, J. A. Fruend, C. Giardina, S. J. Germain, G. S. Gilbert, Z. Hao, T. Hart, B. C. H. Hau, F. He, A. Hector, R. W. Howe, C-F. Hsieh, Y-H. Hu, S. P. Hubbell, F. M. Inman-Narahari, A. Itoh, D. Janik, A. R. Kassim, D. Kenfack, L. Korte, K. Král, A. J. Larson, Y-D. Li, Y. Lin, S. Liu, S. Lum, K. Ma, J-R. Makana, Y. Malhi, S. M. McMahon, W. J. McShea, H. R. Memiaghe, X. Mi, M. Morecroft, P. M. Musili, J. A. Myers, V. Novotny, A. de Oliveira, P. Ong, D. A. Orwig, R. Osterag, G. G. Parker, R. Patankar, R. P. Phillips, G. Reynolds, L. Sack, G-Z. M. Song, S-H. Su, R. Sukumar, I-F. Sun, H. S. Suresh, M. E. Swanson, S. Tan, D. W. Thomas, J. Thompson, M. Uriarte, R. Valencia, A. Vicentini, T. Vrška, X. Wang, G. D. Weiblen, A. Wolf, S-H. Wu, H. Xu, T. Yamakura, S. Yap, and J. K. Zimmerman. 2018. Global importance of large-diameter trees. Global Ecology and Biogeography. doi: http://dx.doi.org/10.1111/geb.12747

[3] Lutz, J. A., T. J. Furniss, S. J. Germain, **K. M. L. Becker**, E. M. Blomdahl, S. M. A. Jeronimo, C. A. Cansler, J. A. Freund, M. E. Swanson, and A. J. Larson. 2017. Shrub communities, spatial patterns, and shrub-mediated tree mortality following reintroduced fire in Yosemite National Park, California, USA. Fire Ecology 13(1): 104–126. doi: http://dx.doi.org/10.4996/fireecology.1301104

[2] Lutz, J. A., J. R. Matchett, L. W. Tarnay, D. F. Smith, **K. M. L. Becker**, T. J. Furniss, and M. L. Brooks. 2017. Fire and the distribution and uncertainty of carbon sequestered as aboveground tree biomass in Yosemite and Sequoia & Kings Canyon National Parks. Land 6(10): 1–24. doi: http://dx.doi.org/10.3390/land6010010

[1] **Becker, K. M. L.**, and J. A. Lutz. 2016. Can low-severity fire reverse compositional change in montane forests of the Sierra Nevada, California, USA? Ecosphere 7:e01484 doi: http://dx.doi.org/10.1002/ecs2.1484

NON-REFEREED PUBLICATIONS

[5] Lutz, J. A., A. J. Larson, **K. M. L. Becker**, T. J. Furniss, E. Blomdahl, S. J. Germain, and M. E. Swanson. 2016. Post Rim Fire assessment of fuel consumption and mortality in the Yosemite Forest Dynamics Plot. Final Report to the National Park Service.

[4] Matchett, J. R., J. A. Lutz, L. W. Tarnay, D. G. Smith, **K. M. L. Becker**, and M. L. Brooks. 2015. Wildfires impact carbon storage differently across Sierra Nevada forest types. USGS WERC Publication Brief.

[3] Matchett, J. R., J. A. Lutz, L. W. Tarnay, D. G. Smith, **K. M. L. Becker**, and M. L. Brooks. 2015. Impacts of fire management on aboveground tree carbon stocks in Yosemite and Sequoia & Kings Canyon National Parks. Natural Resources Report NPS/SIEN/NRR-2015/910. National Park Service, Fort Collins, Colorado. Referreed by NPS and USGS Scientists.

[2] **Becker, K. M. L.**, and J. A. Lutz. 2014. Annually resolved impacts of fire management on carbon stocks in Yosemite and Sequoia & Kings Canyon National Parks. Report to the National Park Service.

[1] **Becker, K. M. L.** 2014. Effects of low-severity fire on species composition and structure in montane forests of the Sierra Nevada. Master's Thesis. University of Washington, School of Environmental and Forest Sciences. Seattle, Washington, USA. 153 p.

PRESENTATIONS

INVITED

[6] **Becker, K. M. L.** Predicting snag fall in an old-growth forest after fire. *Intermountain Society of American Foresters Spring Meeting*, Logan, UT. April 22, 2022.

[5] **Becker, K. M. L.** USU Writing Lab—Science/Math. *Cache County School District Professional Development Day*, Logan, UT. October 11, 2019.

[4] **Becker, K. M. L.** The Writing Process: Tips for Manuscript Writing. *Department of Animal, Dairy, and Veterinary Sciences Graduate Research Symposium*, Logan, UT. August 12, 2020.

[3] **Becker, K. M. L.** Low-severity fire impacts snag dynamics in an old-growth forest: Does tree neighborhood matter? *Restoring The West Conference*, Logan, UT. October 18, 2017.

[2] **Becker, K. M. L.** Snag demography before and after fire in an old-growth forest Sierra Nevada, California. *Intermountain Society of American Foresters Spring Meeting*, Logan, UT. April 22, 2016.

[1] **Becker, K. M. L.** Effects of lower-severity fire on species composition and structure of montane forests in the Sierra Nevada. *Intermountain Society of American Foresters Spring Meeting*, Logan, UT. April 11, 2014.

CONTRIBUTED

[11] Holdrege, M. C., and **K. M. L. Becker.** Communicating and Interpreting Common Statistical Output. *Utah State University Ecology Center Ecolunch*, Logan, UT. March 31, 2022.

[10] **K. M. L. Becker.** Old-growth forest dynamics after fire and drought in the Sierra Nevada, California, USA. *Department of Wildland Resource Graduate Research Seminar*, Logan, UT. December 6, 2021.

[9] Andersen, S. B., **K. M. L. Becker**, and J. Heaps. A Writing Community: Writing Center Directors Teach Effective Peer Review for the (Equitable) Classroom. *Compositionist Conference*, Logan, UT. August 24, 2021.

[8] Andersen, S. B., **K. M. L. Becker**, and J. Heaps. A Writing Community: Writing Center Directors Teach Effective Peer Review for the Classroom. *Empowering Teaching Excellence Conference*, Logan, UT. August 18, 2021.

[7] **K. M. L. Becker.** Writing for Learning in Science Courses. *Empowering Teaching Excellence Conference*, Logan, UT. August 14, 2019.

[6] Allred, J., A. Ensign, and **K. M. L. Becker**. Applying Mathematics in Writing Center Research. *Rocky Mountain Writing Centers Association Mini-Regional Conference*, Salt Lake City, UT. March 30, 2018.

[5] **Becker, K. M. L.** Low-severity fire impacts snag dynamics in an old-growth forest: Does tree neighborhood matter? Sierra Nevada, California. *Annual Meeting of the Ecological Society of America*, Portland, OR. August 10, 2017.

[4] **Becker, K. M. L.** Reconstructing historical post-fire recruitment in the Yosemite Forest Dynamics Plot. *Department of Wildland Resources Graduate Symposium*, Logan, UT. April 15, 2016.

[3] **Becker, K. M. L.** Assessing the effects of climate and fire on forest species composition: A comparison of controls on post-fire seedling recruitment in the Yosemite Forest Dynamics Plot. *Department of Wildland Resources Graduate Symposium*, Logan, UT. April 17, 2015.

[2] **Becker, K. M. L.** Effects of lower-severity fire on species composition and structure in montane forests of the Sierra Nevada, California, USA. *School of Environment and Forest Sciences Graduate Research Seminar*, Seattle, WA. May 13, 2014.

[1] **Becker, K. M. L.** Effects of lower-severity fire on structure of montane forests in the Sierra Nevada. *85th Annual Meeting of the Northwest Scientific Association*, Missoula, MT. March 28, 2014.

ACCESSIONED DATASETS

[2] Lutz, J. A., J. A. Freund, A. J. Larson, M. E. Swanson, T. J. Furniss, **K. M. L. Becker**, E. M. Blomdahl, C. A. Cansler, S. J. Germain, and S. M. A. Jeronimo. 2017. Data for allometric equations of *Chrysolepis sempervirens*, *Cornus sericea*, *Corylus cornuta* ssp. *californica*, and *Leucothoe davisiae*. Utah State University Dataset 72. https://doi.org/10.15142/T3WK55

[1] Lutz, J. A., T. J. Furniss, S. J. Germain, **K. M. L. Becker**, E. M. Blomdahl, S. M. A. Jeronimo, C. A. Cansler, J. A. Freund, M. E. Swanson, and A. J. Larson. 2017. Shrub consumption and immediate community change by reintroduced fire in Yosemite National Park, California, USA; Supplemental Information. Utah State University. http://doi.org/10.15142/T3HP4D

AWARDS

Source	Timespan	Amount
USU Ecology Center Research Award	2017	$5 000
CTFS–ForestGEO Research Award	2016	$3 500
USU Ecology Center Research Award	2015	$3 500
USU Ecology Center Student Travel Grant	2014	$300
National Science Foundation Graduate Fellowship	2014–2017	$138 000
Byron and Alice Lockwood Fellowship	2011–2012	$36 500
Total	2011–2017	$186 800

TEACHING

2019–2022   **Instructor.** *WILD 4100/6100: Scientific Communication for Natural Resource Professionals*. 4 semesters: face-to-face; 2 semesters: online. I developed curriculum for a communication-intensive course that taught scientific reading, writing, and oral presentation skills. Utah State University.

2018–2021   **Co-instructor.** *NSF GRFP Workshop Series.* Elective course. I co-developed an annual grant-writing workshop series with a volunteer-based mentorship framework. Utah State University.

2018–2021   **Co-instructor.** *ENGL 4910: Tutoring Practicum*. I co-developed lecture, discussion, and activity materials to train incoming undergraduate peer writing tutors. Utah State University.

2019–2021   **Guest lecturer.** *WILD 2200: Ecology of Our World.* "Scientific Writing Structure and Principles." I developed an interactive lecture and class activity and adapted it for online instruction. Utah State University.

2019 & 2021   **Guest lecturer.** *WILD 3810: Plant and Animal Populations.* "Wildlife Management Scientific Writing Structure and Principles." I developed an interactive lecture and class activity and adapted it for online instruction. Utah State University.

2019 & 2020   **Guest lecturer.** *CHEM 1215: Chemical Principles Laboratory I.* "Scientific Lab Report Writing Structure and Principles." I developed an interactive lecture and class activity. Utah State University.

2019   **Guest lecturer.** *BIOL 4750/6750 Behavioral Neurobiology.* "Scientific Writing Principles Applied to Peer Review." I developed an interactive class activity. Utah State University.

2019	**Coordinator.** I initiated a collaboration between the Utah State University Writing Center and the Cache County School District to provide a three-session workshop series to help middle school and high school teachers prepare their students for the writing demands of college. Utah State University.
2017	**Teaching assistant.** *WILD 3820: Forest Plants: Identification, Biology, and Function.* I developed writing assignments to help students learn course content and expanded and maintained the course's herbarium. Utah State University.
2015 & 2017	**Guest lecturer.** *WILD 6730: Forest Community Ecology.* "Plant Ecophysiology." I developed an interactive lecture and class activity. Utah State University.
2015 & 2017	**Guest lecturer.** *WILD 6730: Forest Community Ecology.* "Introduction to Ordination." I developed an interactive lecture and computer-programming–based class activity. Utah State University.
2016	**Guest lecturer.** *WILD 5710: Forest Vegetation Disturbance Ecology and Management.* "Conducting pathology exams and identifying agents of tree mortality." I co-designed a field-based lecture and activity. Utah State University.
2014	**Guest lecturer.** *WILD 5710: Forest Vegetation Disturbance Ecology and Management.* "Field methods and long-term forest dynamics plots." I co-designed a field-based lecture and activity. Utah State University.
2013	**Undergraduate senior research project mentor.** University of Washington.
2011	**Elementary school math tutor.** Sylvan Learning, Seattle, WA.
2010	**Physics, math & Spanish tutor.** North Seattle Community College, Seattle, WA.
2008–2009	**Science and math outreach educator.** Pacific Science Center, Seattle, WA.

SERVICE

Manuscript reviewer: *Ecosphere* 1, *Empowering Teaching Excellence* 4, *Fire Ecology* 1

2022	**Mentor.** NSF Graduate Research Fellowship Program Workshop Series.
2017–2021	**Mentor.** QCNR Undergraduate Student Mentorship Program.
2017	**Member.** Restoring the West Conference Planning Committee.
2017	**Student Representative.** Wildland Resources Faculty Search Committee.
2016–2017	**Graduate Student Liaison.** Wildland Resources Department.
2016–2017	**Co-Chair.** Ecology Center Seminar Committee.
2016	**Volunteer Educator.** Natural Resources Field Days.
2016	**Officer.** USU Graduate Student Council.
2015	**Judge.** Hillcrest Elementary Science Fair.
2014–2015	**Member.** Ecology Center Seminar Committee.
2012	**Officer.** Forestry Honor Society: Xi Sigma Pi.

RELATED QUALIFICATIONS

CERTIFICATIONS: Desert Mountain Medicine: Wilderness first responder, Wilderness anaphylaxis training, CPR, AED; American Institute for Avalanche Research and Education: Avalanche I Training Course.

SOFTWARE PROFICIENCIES: R, ArcMap, WinDENDRO, Microsoft Excel, Mendeley Reference Manager, Zoom, Slack.

TECHNICAL SKILLS: Forest inventory and stand analysis (species identification, height and diameter measurements); Tree pathology surveys (identification of bark beetle and fungal species, assessment of tree vigor and causes of stress); 4-season backcountry travel (alpine touring skis, cross country skis, snow shoes, shoes); Navigation (compass, map, GPS), Dendroecological techniques (tree core extraction and processing, ring-width measurement, detrending, cross-dating); Herbarium specimen preparation (plant collection, pressing, mounting); Carpentry (drill, saw, hatchet, hammer, staple gun, belt sander).